Equity Options and Stochastic Interest Rates[1]:

Errors in Black-Scholes Prices and Hedges for European- and American-style equity options when short rates are Ornstein-Uhlenbeck

A dissertation submitted to
the Department of Mathematics and Applied Mathematics
in the Faculty of Science at the University of Cape Town
as partial fulfillment of the requirements of the degree of
Master of Science.

David M Acott

November 24, 2006

[1]The financial assistance of the Department of Labour (DoL) towards this research is hereby acknowledged. Opinions expressed and conclusions arrived at are those of the author and are not necessarily to be attributed to the DoL.

Abstract

This dissertation considers the errors when using Black-Scholes prices and hedges for European equity options (Black&Scholes (1973), Merton (1973)) and American equity options (Karatzas (1988)) in an economy with stochastic interest rates. In particular, we consider an economy with Vasicek (1977) type interest rates.

Analytic investigation shows the direction of European equity option pricing errors to be dependent only on the level of correlation between the stock price and the short rate The direction of European equity option hedge errors is dependent jointly on this correlation and the extent to which the option is in the money. While American equity option prices permit a Markovian representation, analytic comparison of these prices is not feasible.

Numerical investigations are carried out in a model calibrated to the South African market in early 2005. For all prices and hedges considered, proportional errors grow as the option moves out-of-the-money, but only become material very deep out-of-the-money.

Total errors for European option prices and hedges are largest when the option is at-the-money. Price errors reflect mis-estimation of uncertainty and display no systematic bias towards either hedge instrument.

The Black-Scholes model consistently exercises all American equity options earlier than its stochastic interest rate counterpart. This induces, together with the errors associated with European options, an under-estimation of option prices around the Black-Scholes Optimal Exercise Boundary.

The technique of ρ-hedging, despite its theoretical contradictions, proves remarkably accurate at hedging the interest rate risk of equity options except around the Optimal Exercise Boundary of American options, but displays enhanced convexity (i.e. 'Gamma'-type risks) over the stochastic interest rate model.

Acknowledgements

Every epic has a grand cast playing assorted roles. This dissertation is no exception. My sincere thanks are extended to:

- My parents, Michael and Heather Acott, for support - both literal and emotional - throughout my academic career and for never (openly) doubting that I would complete this degree.
- My supervisor, Dr. Peter Ouwehand, whose inspirational coursework laid the foundation for this research, for his valuable input to the later stages of this document.
- The Department of Mathematics of Finance at the University of the Witwatersrand, for welcome, inclusion and support above and beyond the call of duty while resided in Johannesburg - particular thanks to Uncle Dave, Hardy Hulley and Dr. Grimbola, but also Grant, Tombola, Happy Harris, Jack, Nadia, Nevena and the ever-efficient Zahn.
- Chaggy, for emotional and physical support, and for never confusing moral character with academic progress.
- Friends in industry, who kindly provided insight (and occasionally data too), and the menagerie of friends who agreed to proof read various portions of this document.
- The many foreign academics who were prepared to give invaluable snippets of knowledge in the field of their expertise to this complete stranger.
- All those friends who attempted to keep me sane through the many months I immersed myself in research

Funding from the Department of Labour is gratefully acknowledged.

List of Abbreviations

Abbreviation	Expansion	Definition / First Instance
ACC	American Contingent Claim	p.35
ECC	European Contingent Claim	p.18
EEP	Early Exercise Premium	p.42
EMM	Equivalent Martingale Measure	p.20
FRA	Forward Rate Agreement	p.75
HJM	Heath, Jarrow and Morton model	p.3
MPC	Monetary Policy Committee	p.74
OEB	Optimal Exercise Boundary	p.42
OBS	Original Black-Scholes model	p.9
PDE	Partial Differential Equation	p.2
PSOR	Projected Successive Over-Relaxation	p.60
RCLL	Right-Continuous, Left Limits	p.10
RNM	Risk-Neutral Measure	p.20
SDE	Stochastic Differential Equation	p.9
VBS	Vasicek-augmented Black-Scholes model	p.12
ZAR	South African Rand	p.69

List of Symbols

Symbol	Description	Definition / First Instance
$[\,]$	Square parentheses indicate a function, e.g. $\mu_S[t,\omega] : [0,\mathcal{H}] \times \Omega \mapsto \mathbb{R}$	–
$(\,)$	Round parentheses indicate multiplication, e.g. $a[z]\big(b[z] + c[z]\big) = \big(a[z]b[z]\big) + a[z]\big(a[z]c[z]\big)$	–
$\langle\,\rangle$	Quadratic variation process	p.11
	Parentheses retain their standard interpretation in interval and set notation, e.g. $(0,\mathcal{H}) = [0,\mathcal{H}]\backslash\{0,\mathcal{H}\}$.	
$a_{(\cdot)}$	Limit of integration of standard normal distribution in pricing OBS European equity options $c^{\mathcal{O}}$ and $p^{\mathcal{O}}$.	p.24
A	American contingent claim (ACC). The function $A[t,\omega]$ is a random variable representing the ACC's payoff upon exercise at t.	p.35
$\mathbf{A}^C$	Matrix of coefficients for $\hat{C}^{\mathcal{O}}$ in the linear complimentarity problem resulting from the discretisation of the relevant variational inequality.	p.61, p.142
$\mathbf{A}^P$	Matrix of coefficients for $\hat{P}^{\mathcal{O}}$ in the linear complimentarity problem resulting from the discretisation of the relevant variational inequality.	p.143
α	Constant mean reversion rate of the short rate r.	p.13
$b_{(\cdot)}$	Limit of integration of standard normal distribution for pricing VBS European equity options $c^{\mathcal{V}}$ and $p^{\mathcal{V}}$	p. 28
$B^{\mathcal{O}}[t,T]$	Discount bond pricing function under OBS model	p.22
$B^{\mathcal{V}}[t,T,r]$	Discount bond pricing function under VBS model	p.23
$\mathcal{B}[t,\omega]$	Value of the bank account $\mathcal{B}$ at time t in state ω	p.10, p.13
c	European equity call option	p.24

$c^{\mathcal{O}}[t,S]$	OBS price function for an European equity call option	p.24
$c^{\mathcal{V}}[t,S.r]$	VBS price function for an European equity call option	p.28
C	American equity call option	p.38
$C^{\mathcal{O}}[t,S]$	OBS price function for an American equity call option	p.41
$C^{\mathcal{V}}[t,S,r]$	VBS price function for an American equity call option	p.44
$\widetilde{C}^{\mathcal{O}}[t,y]$	Transformed version of $C^{\mathcal{O}}$ for ease of approximation.	p.61
$\widetilde{C}^{\mathcal{V}}[t,z_1,z_2]$	Transformed version of $C^{\mathcal{V}}$ for ease of approximation.	p.64
$\hat{C}^{\mathcal{O}}_{i,j}$	Estimate of $\widetilde{C}^{\mathcal{O}}$ at $(t,y)=(t_i,y_l)$.	p.61
$\hat{C}^{\mathcal{V}}_{i,j,k}$	Estimate of $\widetilde{C}^{\mathcal{V}}[t_i,z_{1,j},z_{2,k}]$.	p.65
$\check{\mathbf{C}}^{\mathcal{O}(l)}_{i,j}$	Vector of approximations to $\hat{C}^{\mathcal{O}}_{i,j}$ at l^{th} iteration of PSOR cycle.	p.62
$\check{C}^{\mathcal{V}}_{i,j,k}$	Intermediate estimate of the value of $\widetilde{C}^{\mathcal{V}}_{i,j,k}$.	p.65
$\mathcal{C}^{(1)}_{(2)}$	Continuation Area. Sub-set of the domain of the claim (2), when priced under the model (1), where immediate exercise is sub-optimal.	p.41
χ	Instantaneous correlation between the Brownian motions W and V	p.12
$\chi_c[t,T]$	Critical correlation for time t such that a European equity option maturing at T is priced identically under OBS and VBS models.	p.29
$\mathcal{D}^{(\cdot)}_{(\cdot)}$	Domain of inputs to the Markovian pricing function for the claim in the subscript, when priced under the model in the superscript.	p.41
δ	Constant dividend yield on the risky asset S	p.10, p.13
$\Delta_{(\cdot)}$	Constant step size for the variable in the subscript in the relevant approximation scheme	p.65, p.140
e	Base of the natural logarithm (i.e. Napier's constant)	p.13
E	European contingent claim (ECC). The function $E[\omega]$ is a random variable representing the ECC's payoff at maturity.	p.18

$\mathbb{E}^{(\cdot)}[\,]$	Expectation operator. Superscript indicates the relevant probability measure.	p.12
$g^{(\cdot)}_{(\cdot)}$	Limit of integration of standard normal distribution when valuing the early exercise premium of the the contingent claim in the superscript	p. 42
$\mathcal{F}$	The base sigma-algebra on the probability space within which we price securities.	p.9, p.12
$\mathcal{F}_t$	Sigma-algebra generated by the realisations of $W^{\mathbb{P}}_s$ and $V^{\mathbb{P}}_s$ up to t - an element of $\mathbb{F}$	p.9, p.12
$\mathbb{F}$	Filtration on the probability space $(\Omega, \mathbb{P}, \mathcal{F})$ generated by the Brownian motions $W^{\mathbb{P}}$ and $V^{\mathbb{P}}$.	p.9, p.12
$\phi^{(\cdot)}_{(\cdot)}[t,\omega]$	Integrand of the integrator in the superscript for the martingale representation of the random variable in the subscript.	p.20
$\Phi[\cdot]$	Cumulative standard normal distribution function.	p.24
$\gamma[t,T]$	Instantaneous volatility of the fraction $\frac{S[t]}{B^{\mathcal{V}}[t,T,r]}$	p.26
$\Gamma[t,T]$	Total volatility of the forward price $\frac{S[u]}{B^{\mathcal{V}}[u,T,r]}$ over $[t,T]$	p.26
$h[Y]$	Reward function used in the theorems 4.2.3 and 4.2.4	p.35, p.35
$h_n[Y]$	Sequence of functions converging pointwise to h from below.	p.35, p.35
$H^{(\cdot)}_{(\cdot);(\cdot)}$	Holdings of the in-model hedging portfolio for the contingent claim in the first subscript, held in the second subscript, when priced under the model in the superscript	p.24
$\tilde{H}^{(\cdot)}_{(\cdot);(\cdot)}$	Holdings of the out-of-model hedging portfolio (i.e. ρ-heging portfolio) for the contingent claim in the first subscript, held in the second subscript, when priced under the model in the superscript	p.54
$\mathcal{H}$	Finite horizon to which the security market models extend	p.9, p.12
i	Time index for $\hat{C}^{\mathcal{O}}$ and $\hat{C}^{\mathcal{V}}$	p.61, p.65
$\mathbb{1}_{\{(\cdot)\}}$	The indicator function of the statement in the subscript	p.18
$\eta^{(\cdot)}_{(\cdot)}$	Optimal stopping time for the problem in the superscript, starting at the time in the subscript.	p.34

j	S index for $\hat{C}^{\mathcal{O}}$; z_1 index for $\hat{C}^{\mathcal{V}}$.	p.61, p.65
k	Arbitrary constant used for boundedness of functions; also z_2 index for $\hat{C}^{\mathcal{V}}$.	p.11, p.65
K	Strike price - the price at which the call (put) option allows the risk asset to be bought (sold).	p.24
κ	Roots of the S-quadratic (C-5).	p.142
L	Local time of the process in the argument spent at zero.	p.137
$\mathcal{L}^2$	Space of square-integrable functions	p.18
$\lambda_{(\cdot)}$	Market price of risk associated with the Brownian motion indicated in the subscript.	p.12, p.15
Λ	Lebesgue measure on the interval $[0, \mathcal{H}]$	p.9, p.12
M	Martingale portion of the Doob-Meyer decomposition of a supermartingale	p.34
$\mathcal{M}^{(\cdot)}_{(\cdot)}$	Martingale portion of the early exercise premium $\mathcal{P}^{(\cdot)}_{(\cdot)}$ of the contingent claim in the subscript when priced under the model in the superscript.	p.137
$\mu_{(\cdot)}[t, \omega]$	Real-world drift of the process indicated in the subscript	–
$n_{(\cdot)}$	Number of steps in the discretisation of the variable in the subscript.	p.61
N	Finite variation portion of the Doob-Meyer decomposition of a supermartingale	p.34
$\mathcal{N}^{(\cdot)}_{(\cdot)}$	Finite variation portion of the early exercise premium $\mathcal{P}^{(\cdot)}_{(\cdot)}$ of the contingent claim in the subscript when priced under the model in the superscript.	p.137
$\nu^{(\cdot)}_{(\cdot)}$	Linear coefficients of the drifts of z_1 and z_2 in terms of the short rate r. per (C-9a).	p.67, p.144
$\mathcal{O}$	The Original Black-Scholes Model	p.9
p	European equity put option	p.28
$p^{\mathcal{O}}[t, S]$	OBS price function for an European equity put option	p.28
$p^{\mathcal{V}}[t, S, r]$	VBS price function for an European equity put option	p.29

P	American equity put option	p.47
$P^{\mathcal{O}}[t,S]$	OBS price function for an American equity put option	p.48
$P^{\mathcal{V}}[t,S,r]$	VBS price function for an American equity put option	p.49
$\mathcal{P}^{(\cdot)}_{(\cdot)}$	Early exercise premium (excess of American price over European price). Subscript indicates the contingent claim, superscript indicates the model under which the claim is priced.	p.42
$\mathbb{P}$	Real-world measure on the measurable space $(\Omega,\mathcal{F})$	p9, p.12
$\Pi[t,\omega]$	Trading strategy	p.11, p.14
$\Pi_{(\cdot)}[t,\omega]$	Element of a trading strategy. Represents unit holdings in the security indicated in the subscript.	p.11, p.14
$q_{(\cdot)}{}^{(\cdot)}$	Probabilities of the discrete movements of z_1 and z_2 to approximate their risk-neutral process.	p.66, p.147
$\mathbb{Q}$	Risk-neutral measure on the measurable space $(\Omega,\mathcal{F})$	p.19, p.19
$\mathbb{Q}^S$	Equivalent martingale measure on the measure on the measurable space $(\Omega,\mathcal{F})$	p.25
$\mathbb{Q}^T_B$	Equivalent martingale measure on the measure on the measurable space $(\Omega,\mathcal{F})$	p.25
θ	Risk-neutral ($\mathbb{Q}$) mean of the short rate r	p.16, p.20
$\bar{\theta}$	Real-world ($\mathbb{P}$) mean of the short rate r	p.13
$r[t,\omega]$	The short rate in the VBS model. Often abbreviated to r	p.13
$\tilde{r}^{(\cdot)}_{(\cdot)}$	Spot rate level determining the Optimal Exercise Boundary for the American contingent claim in the subscript when priced under VBS model.	p.46
R	Constant instantaneous return on the riskless asset β in the OBS model	p.10
$R[t,T,r]$	Spot rate for maturity T implied by the short rate $r[t]$	p.23
$R^{-1}[t,T,R]$	Short rate implied by a spot rate R for maturity t	p.23
$\rho^{\mathcal{O}}_{(\cdot)}$	Sensitivity to the OBS price of the contingent claim in the subscript to changes in the interest rate R	p.51

$S[t,\omega]$	Price of the risky asset S (aka stock price) at time t.	p.9, p.12
$S^{*}_{(\cdot)}[t,T,B]$	Critical stock price level at which VBS and OBS hedges at time t for a European option expiring at time T agree. Subscript equals 1 for stock hedge and 2 for bond hedge.	p.31, p.31
$\tilde{S}^{(\cdot)}_{(\cdot)}$	Stock price level determining the Optimal Exercise Boundary for the American contingent claim in the subscript, priced under the model in the superscript.	p.42
$\mathcal{S}$	Stopping Area. Sub-set of the domain of the claim in the subscript, when priced under the model in the superscript, where immediate exercise is optimal.	p.41
$\sigma_{(\cdot)}[t,\omega]$	Instantaneous volatility of the process indicated in the subscript. Often, but not always, constant.	–
ς	Intermediate variable used in PSOR iterations	p.62
t	Current time / Time at which contingent claim is valued	–
T	Exipry time of the contingent claim considered (if appropriate).	–
τ	Any stopping time.	p.34
$\mathcal{T}_{t,T}$	The collection of all stopping times taking values in $[t,T]$.	p.34
u	Time-related integrator	–
$\mathcal{V}$	The Vasicek-augmented Black-Scholes Model	p.12
$V^{(\cdot)}_t$	Noise process affecting the short rate r. Superscript indicates the measure under which V is Brownian.	p.9, 12, 20
$W^{(\cdot)}_t$	Noise process affecting the stock price S. Superscript indicates the measure under which W is Brownian.	p.9, 12, 20
$x[t,\omega]$	A payoff stream, reflecting total receipts (payments) until time t	p.10, p.14
$x_0[t,\omega]$	Consensus optimal payoff stream of the contingent claim X_0.	p.15
$x_{(\cdot)}$	A payoff set: any set of payoff streams. Subscript indicates correspondence with contingent claims.	p.10, p.14
$X_{(\cdot)}[t,\omega]$	(Price of) a contingent claim. Subscript indicates correspondence with underlying payoff set.	p.10, p.14

$\tilde{X}_{(\cdot)}[t,\omega]$	Our proposed price of a contingent claim. Subscript indicates correspondence with underlying payoff set. Used only in pricing theorems.	p.10, p.14
$X_0[t,\omega]$	The primary contingent claim, which determines the market price of interest rate risk.	p.15
$\mathbb{X}$	The set of all contingent claims trading in the modelled economy.	p.10, p.14
ξ	Time variable.	p.27
ξ_t	(Appendix A only) $\mathbb{P}$-expectation at tine t of the Radon-Nikodym derivative $\frac{d\mathbb{Q}}{d\mathbb{P}}$.	p.135
y	Natural logarithm of the stick price S, used in OBS approximation schemes.	p.61
Y	$\mathbb{Q}$-Markovian vector	p.39, p.44
z_1, z_2	Orthogonal variables used in the approximation of $C^{\mathcal{V}}$.	p.64
$Z_t^{(\cdot)}$	Aggregate noise process affecting the forward price $\frac{S[t]}{B^{\mathcal{V}}[t,T,r]}$. Superscript indicates the measure under which Z is Brownian.	p.27
ω	Single state of the world, representing one realisation of all Brownian paths.	p.9, p.12
Ω	Set of all possible events ω	p.9, p.12

List of Tables

3.1 Comparison of hedge portfolio bond short sales for European equity call options. 31
3.2 Comparison of hedge portfolio stock purchases for European equity call options. 32
3.3 Comparison of hedge portfolio bond purchases for European equity put options. 32
3.4 Comparison of hedge portfolio stock short sales for European equity put options. 33

7.1 At-the-money SAFEX ALSI volatilities, 15 February 2005 70
7.2 Dividend Yields implied by Closing Futures Prices, 3 January 2005 72

8.1 $S_1^*[t, t+1, B]$ for various correlations and three year spot rates 91

List of Figures

7.1 Observed value and historical volatility of ZAR, 2001-2004 69
7.2 Observed historical ALSI 40 volatility , 2 July 2001 to 3 January 2005 71
7.3 Observed dividend yields on the ALSI 40, 1 October 2002 to 3 January 2005 72
7.4 South African Yield Curve on 15 February 2005 73
7.5 Fitted and Observed Yield Curves, 15 February 2005 74
7.6 Observed 3×6 FRA volatility, 2 July 2001 to 3 January 2005 75
7.7 Relationship between Short and Spot Rates 76
7.8 Observed FRA-ALSI correlation, 2 July 2001 to 3 January 2005 77

8.1 Critical Correlation Path 82
8.2 Total Forward Price Variance 83
8.3 OBS Call and Put prices at $T-t=1$ 84
8.4 Total Pricing Error at $T-t=1$ for $\chi=-25\%$ 84
8.5 Proportional Pricing Error at $T-t=1$ for $\chi=-25\%$ 85
8.6 Total Pricing Error at $T-t=1$ for $\chi=0$ 85
8.7 Total Pricing Error at $T-t=1$ for $\chi=25\%$ 86
8.8 OBS Call and Put Prices at $T-t=3$ 86
8.9 Total Price Errors at $T-t=3$ for $\chi=-25\%$ 87
8.10 Proportional Price Errors at $T-t=3$ for $\chi=-25\%$ 88
8.11 Total Price Errors at $T-t=3$ for $\chi=0$ 88
8.12 Proportional Price Errors at $T-t=3$ for $\chi=0$ 89
8.13 Total Price Errors at $T-t=3$ for $\chi=25\%$ 89
8.14 Proportional Price Errors at $T-t=3$ for $\chi=25\%$ 90
8.15 Critical stock prices one year from expiry for $\chi=\chi_c[t,t+1]$ 91
8.16 OBS hedge purchases of stock at $T-t=1$ 92
8.17 OBS hedge purchases of discount bonds at $T-t=1$ 92
8.18 Total Hedging Error at $T-t=1$ for $\chi=-25\%$ 93
8.19 Proportional Hedging Errors at $T-t=1$ for $\chi=-25\%$ 93
8.20 Total Hedging Errors at $T-t=1$ for $\chi=25\%$ 94
8.21 Critical stock prices three years from expiry for $\chi=\chi_c[t,t+3]$ 95
8.22 OBS Hedge Stock Purchases at $T-t=3$ 95
8.23 OBS Hedge Discount Bond Purchases at $T-t=3$ 96
8.24 Total Hedge Errors at $T-t=3$ for $\chi=-25\%$. 96
8.25 Total Hedge Errors at $T-t=3$ for $\chi=25\%$. 97

9.1 Optimal Exercise Boundary $\tilde{S}_C^{\mathcal{O}}[t]$ for $R\in[3\%,15\%]$ 99
9.2 Errors in OEB estimation: $\tilde{S}_C^{\mathcal{O}}$ - $\tilde{S}_C^{\mathcal{V}}$ for $\chi=0$ 101

9.3 Early Exercise Premium $\mathcal{P}_C^{\mathcal{O}}$ for $T-t=1$ and $T-t=3$ . . . 102
9.4 Errors in EEP estimation: $\mathcal{P}_C^{\mathcal{O}} - \mathcal{P}_C^{\mathcal{V}}$ for $\chi=0$ . . . 102
9.5 Total pricing errors at $T-t=1$ for $\chi=-25\%$ and $\chi=25\%$ . . . 103
9.6 Total pricing errors at $T-t=3$ for $\chi=-25\%$ and $\chi=25\%$ . . . 104
9.7 Relative pricing errors for $\chi=-25\%$ . . . 104
9.8 OBS Stock Hedges for $T-t=1$ and $T-t=3$ . . . 105
9.9 Total Stock Hedge Errors at $T-t=1$ . . . 106
9.10 Proportional Stock Hedge Errors at $T-t=1$ . . . 106
9.11 Total Stock Hedge Errors at $T-t=3$ for $\chi=0$ . . . 107
9.12 OBS Fixed Income Hedge Values at $T-t=1$ and $T-t=3$ . . . 108
9.13 Fixed Income Hedge errors at $T-t=1$ . . . 108
9.14 OBS ρ-hedge bond purchases for $T-t=1$ and $T-t=3$ . . . 109
9.15 Comparison of bond purchases for OBS ρ-hedge and VBS hedge at $T-t=3$ for $S[t]=200$ . . . 110
9.16 Total errors in ρ-hedge bond purchases for $\chi=25\%$ and $\chi=-25\%$ . . . 111

10.1 Optimal Exercise Boundary $\tilde{S}_P^{\mathcal{O}}[t]$ for $R\in[3\%,15\%]$ . . . 113
10.2 Optimal Exercise Boundary $\tilde{S}_P^{\mathcal{V}}[t,R^{-1}R]$ for $\chi=0$ . . . 114
10.3 Errors in OEB estimation: $\tilde{S}_P^{\mathcal{O}}$ - $\tilde{S}_P^{\mathcal{V}}$ for $\chi=0$ . . . 114
10.4 OBS Early Exercise Premium $\mathcal{P}_P^{\mathcal{O}}$ at $T-t=1$ and $T-t=3$ . . . 115
10.5 OEBs $\tilde{S}_P^{\mathcal{O}}$ and $\tilde{S}_P^{\mathcal{V}}$ at $T-t=3$ against contours of $p^{\mathcal{O}}-p^{\mathcal{V}}$, all for $\chi=0$ . . . 116
10.6 Total EEP error $\mathcal{P}_P^{\mathcal{O}} - \mathcal{P}_P^{\mathcal{V}}$ at $T-t=3$ for $\chi=0$ . . . 117
10.7 OBS Prices at $T-t=1$ and $T-t=3$ . . . 118
10.8 Total pricing error at $T-t=1$ . . . 118
10.9 Total pricing error at $T-t=3$ . . . 119
10.10 Exaggerated illustration of the 'convexity paradox' . . . 119
10.11 Proportional pricing error for $\chi=-25\%$ for $T-t=1$ and $T-t=3$ . . . 120
10.12 OBS Stock Hedges for $T-t=1$ and $T-t=3$ . . . 121
10.13 Total stock hedge error at $T-t=3$ for $\chi=25\%$ . . . 121
10.14 Proportional stock hedge error at $T-t=3$ for $\chi=25\%$ . . . 122
10.15 OBS Fixed Income Hedge Purchases at $T-t=1$ and $T-t=3$. . . . 122
10.16 Total Error in Fixed Income Hedge Purchases at $T-t=3$. . . . 123
10.17 Proportional Error in Fixed Income Hedge Purchases at $T-t=3$. . . . 124
10.18 OBS ρ-hedge bond purchases for $T-t=1$ and $T-t=3$ . . . 125
10.19 Total error in ρ-hedge bond purchases at $T-t=1$ and 3 . . . 126
10.20 OEBs $\tilde{S}_P^{\mathcal{O}}$ and $\tilde{S}_P^{\mathcal{V}}$ against contours of $(\mathcal{P}_P^{\mathcal{O}}/P^{\mathcal{O}})$ at $T-t=3$ for $\chi=0$. . . . 127

C-1 Explicit determination of $\check{C}^{\mathcal{V}}$ from $\hat{C}^{\mathcal{V}}$. . . . 149
C-2 Cross-section through $\mathcal{D}_C^{\mathcal{V}}$ at fixed time . . . 150
C-3 Domains of interest and concern in (z_1,z_2)-space . . . 151
C-4 Cross-sectional extension of terminal condition . . . 152
C-5 Location of nodes within Domain of Calculation . . . 153
C-6 Domain of Calculation . . . 154
C-7 Spatial cross-section of the domain of calculation through QAES . . . 156

Contents

List of Abbreviations ii

List of Symbols iii

List of Tables x

List of Figures xi

1 Introduction 1
- 1.1 Aim and Purpose . . . 1
- 1.2 Literature Review . . . 1
  - 1.2.1 Equity Option Pricing . . . 1
  - 1.2.2 Stochastic Interest Rates . . . 2
  - 1.2.3 Equity Options with Stochastic Rates . . . 3
- 1.3 Outline . . . 4

I Theory 7

2 Security Market Models 9
- 2.1 The Black-Scholes Model . . . 9
- 2.2 The Vasicek-augmented Black-Scholes Model . . . 12

3 European Options 18
- 3.1 Pricing and Hedging . . . 18
  - 3.1.1 General Theory . . . 19
  - 3.1.2 Discount Bonds . . . 22
  - 3.1.3 European Equity Options . . . 24
- 3.2 Model Comparison . . . 29
  - 3.2.1 Prices . . . 29
  - 3.2.2 Hedges . . . 30

4 American Options 34
- 4.1 Some Optimal Stopping Theory . . . 34
- 4.2 American Contingent Claim Pricing . . . 35
- 4.3 American Equity Option Pricing . . . 38
  - 4.3.1 American Equity Call Option Pricing . . . 38

4.3.2 American Equity Put Option Pricing . . . 47

5 Critique of ρ-hedging 50
5.1 Theoretical Disadvantages . . . 51
5.1.1 Stochastic Calibration Switching . . . 51
5.1.2 Flat Yield Curve Arbitrage . . . 52
5.1.3 Intermediate Portfolio Cashflows . . . 53
5.2 Practical Advantages . . . 54

II Implementation 56

6 Approximation Schemes 58
6.1 Overview of Approximation Schemes . . . 58
6.2 Approximating American Options with Constant Rates . . . 60
6.3 Approximating American Options with Vasicek Rates . . . 63

7 Calibrations 68
7.1 Stock Price Parameters . . . 69
7.1.1 Stock Price Volatility σ_S . . . 70
7.1.2 Stock Dividend Yields δ . . . 71
7.2 Short Rate Parameters . . . 73
7.2.1 Yield Curve Fitting . . . 73
7.2.2 Spot Rate Volatility σ_r . . . 75
7.2.3 Comparison of Spot Rates and Short Rates . . . 76
7.3 Correlation . . . 76

III Numerical Results 79

8 Numerical Results I: European Options 81
8.0.1 Difference Symmetry . . . 81
8.0.2 Correlation and Forward Price Variance . . . 82
8.1 Option Prices . . . 83
8.1.1 Shorter-term options: $T-t=1$ . . . 83
8.1.2 Longer-term options: $T-t=3$ . . . 86
8.2 Hedge Parameters . . . 90
8.2.1 Shorter-term options: $T-t=1$ . . . 91
8.2.2 Longer-term options: $T-t=3$ . . . 94

9 Numerical Results II: American Call Options 98
9.0.3 Approximation Scheme Details . . . 98
9.1 Optimal Exercise Boundaries . . . 99
9.2 Premia and Prices . . . 101
9.2.1 Early Exercise Premia . . . 101
9.2.2 Call Option Prices . . . 103
9.3 Call Hedge Parameters . . . 105
9.3.1 In-Model Hedges . . . 105

9.3.2 Out-of-Model ρ-hedges . . . 108

10 Numerical Results III: American Put Options **112**
10.0.3 Approximation Scheme Details . . . 112
10.1 Optimal Exercise Boundaries . . . 112
10.2 Premia and Prices . . . 115
10.2.1 Early Exercise Premia . . . 115
10.2.2 Put Option Prices . . . 117
10.3 Put Hedge Parameters . . . 120
10.3.1 In-Model Hedges . . . 120
10.3.2 Out-of-Model ρ-hedges . . . 124

11 Conclusions **128**
11.1 Pricing and Hedging Theory . . . 128
11.1.1 European Option Prices . . . 128
11.1.2 American Option Prices . . . 129
11.1.3 ρ-Hedging . . . 129
11.2 Approximation . . . 130
11.3 Numerical Investigations . . . 130
11.3.1 European Options . . . 130
11.3.2 American Call Options . . . 131
11.3.3 American Put Options . . . 132
11.4 Further Research . . . 133

IV Appendices **134**

A Girsanov's Theorem for Correlated Brownian Motions **135**

B Early Exercise Premia **137**
B.1 OBS Early Exercise Premia . . . 137
B.2 VBS Early Exercise Premia . . . 139

C Approximation Schemes: Derivations **140**
C.1 American Options with Constant Short Rate . . . 140
C.2 American Options with Vasicek Short Rate . . . 144

D Matlab Code **157**
D.1 Code for OBS American Call $C^{\mathcal{O}}$ . . . 157
D.1.1 AmCallMaster.m . . . 157
D.1.2 AmCall.m . . . 157
D.1.3 SolveCallPSOR.m . . . 160
D.1.4 BScall.m . . . 161
D.1.5 LocateOBSCallOEB.m . . . 161
D.1.6 InterpolateCall.m . . . 161
D.1.7 PerpCallOEB . . . 162
D.2 Code for OBS American Put $P^{\mathcal{O}}$ . . . 162
D.2.1 AmPutMaster.m . . . 162

D.2.2 AmPut.m 162
D.2.3 SolvePutPSOR.m 165
D.2.4 BSput.m 166
D.2.5 LocateOBSPutOEB.m 166
D.2.6 InterpolatePut.m 166
D.2.7 PerpPutOEB 167
D.3 Code for VBS American Call $C^{\mathcal{V}}$ 167
D.3.1 AmCallVBS.m 167
D.3.2 LocateVBSCallOEB.m 173
D.4 Code for VBS American Put $P^{\mathcal{V}}$ 174
D.4.1 AmPutVBS.m 174
D.4.2 LocateVBSPutOEB.m 181

Chapter 1

Introduction

1.1 Aim and Purpose

The seminal work of Black and Scholes (1973) regarding equity option pricing has become a foundation of modern finance. This work is also the *de facto* standard framework for pricing, hedging and otherwise analysing equity-based contingent claims.

As with most models, this framework makes necessary simplifying assumptions. These simplifications include, amongst others, a constant interest rate. This dissertation aims to provide an initial consideration, analysis and enumeration of the errors in equity option pricing and hedging created by this constant interest rate assumption. We consider the effects thereof for both puts and calls, of both European and American types.

To examine Black Scholes option pricing errors we need to compare these prices to those under a 'better' model. This requires postulating a stochastic form for interest rates. There is a plethora of competing interest rate models from which to chose, each with their pro's and con's.

From the variety of models this dissertation selects the Vasicek (1977) model. This model is often criticised as being an excessively simple model of interest rates. However, this dissertation is only an initial step in analysing errors from the constant interest rate assumption. For our purposes the Vasicek model provides an appropriate tradeoff between analytic tractability and accurate, appropriate yield curve modelling.

In particular, the Vasicek model is often criticised for not correctly pricing even an initial yield curve. Paradoxically, we embrace this error. Extensions to price an initial yield curve require an infinite vector of additional inputs. Such inputs are themselves highly likely to affect equity option prices, and hence the apparent error. By excluding this input vector we deliberately limit the parameters which could possibly affect option pricing and hedging errors. This simplifies the analysis of error causation, and is appropriate for this initial investigation.

1.2 Literature Review

1.2.1 Equity Option Pricing

Equity option pricing has a long history, with literature dating back to Bachelier (1900). However, most modern option pricing starts with the work of Black and Scholes (1973).

By hedging an option with positions in the underlying stock, Black and Scholes create

an instantaneously risk-free portfolio. Using arbitrage arguments, they arrive at a partial differential equation (PDE) which the option price solved. Merton (1973) relaxes some of the assumptions Black and Scholes used. He also takes their analysis further, demonstrating that appropriate holdings of stock and cash will perfectly replicate the option payoff.

Harrison and Pliska (1981), extending work by Harrison and Krepps (1979) and Cox, Ross and Rubinstein (1979), apply Merton's replicating arguments to the pricing of a very general class of contingent claims. Harrison and Pliska's arguments use martingale theory, and can be shown as equivalent to the PDE approach (subject to regularity conditions) using the Feynman-Kač Theorem (see e.g. Duffie (1996)). Indeed, there are now a variety of recognised congruent pricing methodologies - see Andreasen, Jensen and Poulson (1998) for a discussion.

Under the replicating pricing paradigm, European options - exercisable only on expiry date - are priced easily. The resultant closed-form solution is known famously as the Black-Scholes equation.

American options - exercisable at any time up to expiry - pose a more difficult problem. Merton (1973) shows that American call options on assets without cashflows before maturity will never be optimally exercised before maturity (while interest rates remain positive), and are hence equivalent to European options. Beyond this special case, no tractable solution has yet been proposed for valuing American options: current valuation methods are reliant on numerical approximations.

Within a slightly different pricing regime, McKean (1965) recognised the American option as the solution to a free boundary PDE. Early approximation schemes include tree methods (Cox, Ross and Rubinstein (1979) and Boyle (1986)) and finite difference schemes (Schwartz (1977), Brennan and Schwartz (1978) and Courtadon (1982)).

Bensoussan (1984) introduces the notion of an American option as an optimal stopping problem; this notion is extended in Karatzas (1988).

As the standard equity model has Markovian dynamics, the optimal stopping problem simplifies to a hitting time problem, or equivalently a free boundary PDE. Dividing the domain across the hitting boundary into continuation and stopping regions provides further insight into the valuation problem. This hitting boundary is commonly referred to as the Optimal Exercise Boundary (OEB).

Jaillet, Lamberton and Lapeyre (1990) use the division of the domain to formulate the American problem as a variational inequality. Applying Cryer's (1971) Projected Successive Over-Relaxation scheme to the variational inequality corrects errors in earlier finite difference schemes.

Using three different approaches, Kim (1990), Jacka (1991) and Carr, Jarrow and Myneni (1992) use this division to decompose the American option into a European option and an Early Exercise Premium. The resultant integral equation suggests alternative methods of locating the OEB, as documented in Huang, Subrahmanyam and Yu(1996). Peskir (2002) confirms the uniqueness of the OEB, and hence the validity of such methods.

Myneni (1992) provides an accessible overview of the main results in the pricing of American options.

1.2.2 Stochastic Interest Rates

Merton (1973) models discount bond prices using Geometric Brownian Motion with deterministic volatility and stochastic drift. He fails, however, to specify the stochastic drift or to describe effectively the relationship between the dynamics of bonds of different maturities.

In a one-factor setting, Vasicek (1977) uses any two interest rate-sensitive securities to show that a common market price of interest rate risk must exist between all interest rate-sensitive securities. He prices bonds using only this market price of risk (MPR) and the assumed dynamics for the instantaneous interest rate. As an example, he solves the case where the instantaneous interest rate follows a mean-reverting Brownian motion - the model which has taken his name, and will be used in this dissertation. Alternative one-factor models have been presented by Dothan (1978), Ball and Torous (1983) and Cox, Intersoll and Ross (1985A,B) (hereafter CIR).

Time-homogenous one-factor models inherently imply perfect instantaneous correlation between bonds, and struggle to fit most shapes of yield curves. Brennan and Schwartz (1979, 1982), Schaefer and Schwartz (1984), Fong and Vasicek (1991), Longstaff and Schwartz (1992A,B) and Langetieg (1980) have all addressed these drawbacks by adding factors to the model. More popular corrections through time inhomogeneity have been initiated by Ho and Lee (1986), Hull and White (1990B), Black, Derman and Toy (1990) and Black and Karasinski (1993). Hull and White (1994B) introduce a time inhomonogeous two-factor model, while Brigo and Mercurico (2001) suggest an arbitrary multiplicative coefficient to calibrate any model to observed yield curve.

Somewhat analogously to the Black-Scholes model, Heath, Jarrow and Morton (1992) (hereafter HJM) show that specification of the volatility of instantaneous forward rates, together with the existing yield curve, is sufficient to fully determine an interest rate model. This provides a broad framework which nests all major diffusion models. Recent attention has focused on subsets of HJM which model observable market rates - so-called market models - as pioneered by Brace, Gatarek and Musiela (1997), Miltersen, Sandmann and Sonderman (1997) and Jamshidian (1997).

Many one-factor models admit closed-form solutions for European options on discount bonds - see Cox, Ingersoll and Ross (1985B) and Jamshidian (1989). Jamshidian (1989) also describes the decomposition of European options on coupon bonds into a portfolio of options on the strips, applicable to all monotonic one-factor models.

Jamshidian (1991,1993) examines American options on coupon-bearing bonds in one-factor Gaussian interest rate models, while Chesney, Elliott and Gibson (1993) do so for discount bonds within the CIR model, and Jorgensen(1996) extends this to all (monotonic) one-factor models. Other than that, and in contrast to equity options, there is very little theoretical material pricing American options on bonds and other interest rate instruments. This may be attributable to the ubiquity of tree methods such as Hull and White (1990A, 1993, 1994A), Black and Karasinski (1992) or even Li, Ritchken and Sankarasubrahmanian (1995) in interest rate pricing and the ease with which such methods handle American options.

1.2.3 Equity Options with Stochastic Rates

The author has found a dearth of literature covering the influence of stochastic interest rates on equity options.

Rabinovitch (1989) considers European equity options when the short rate is Ornstein-Uhlenbeck. He derives a closed-form solution, and makes a limited numerical comparison under some extreme assumptions for stock-short rate correlation.

Amin and Jarrow (1992) generalise the framework of Heath, Jarrow and Morton (1992) by imbedding their stochastic interest rate economy into one containing an arbitrary number of additional risky assets. They extend the American option price of Karatzas (1988) to this

generalised HJM economy.

Ho, Stapleton and Subrahmanyam (1997B) extend the Richardson extrapolation of Geske and Johnson (1984) to value American equity options when interest rates are stochastic. They extrapolate from compound option prices obtained in a multivariate binomial approximation of the joint process of stock and bond prices. Numerical comparisons show the effect of stochastic interest rates to be largest when stock volatility is low, time to option expiry is large and stock-bond correlation is positive.

Menkveld and Vorst (2000) consider American equity options when the short rate follows a Hull-White (1990B) process. They use numerical integration of a compound option formula to arrive at a faster Richardson extrapolation. Their analysis of American put options show that stochastic intersest rates do not significantly affect option prices. They find (numerically) that increasing stock-rate correlation increases the option price, and that differing initial shapes of the term structure can have counter-intuitive influences on optimal exercise strategies.

1.3 Outline

We proceed as follows. Part I discusses the theory of option pricing. Here. Chapter 2 lays the foundation by presenting the two security market models in which we price equity options.

First presented is the well-studied Black-Scholes model, into which we introduce a novel definition of contingent claims that facilitates probabilistic no-arbitrage pricing of both European and American contingent claims under the same framework. For purposes of clarity this is referred to as the Original Black-Scholes (OBS) model. Thereafter we introduce a model which augments this framework with a Vasicek-type (i.e Ornstein-Uhlenbeck) short rate, together with a contingent claim which prices short rate risk. This second model is referred to as the Vasicek-augmented Black-Scholes (VBS) model.

European contingent claims, exercisable only at option expiry, are considered in Chapter 3. We use classical hedging arguments to arrive at well-known risk-neutral pricing functions. This is used to price discount bonds and, together with a change of numéraire technique, price European equity options.

In comparing model results for prices and also hedges we control for stock price and spot rate to option expiry (hereafter 'spot rate'). We show how model differences in European option prices depend only on correlation between stock price and short rate, but that model difference in hedge parameters depend jointly on this correlation and also the extent to which the option is in-the-money.

We can implement a Doob-Meyer decomposition on the Snell envelope an on American Contingent Claim's (ACC) payoff. Thus ACCs, which may be exercised any time up to expiry, may also be priced using the classical hedging arguments - as shown in Chapter 4. OBS prices for American equity options are Markovian functions of stock price and time to expiry, and the optimal exercise strategy is the first hitting time of a curve of critical stock prices called the Optimal Exercise Boundary.

We then show that VBS prices for American equity options are also Markovian, this time in stock price, short rate and time to expiry. Accordingly the optimal exercise strategy for the option is the first hitting time of an OEB in one more dimension.

Though OBS prices permit an elegant and intuitive analytic early exercise representation, VBS prices do not. Thus we do not possess analytic American formulae for both models, and hence cannot make analytic price and hedge comparisons. Comparison can only be done by

numerical example, conducted in Part III.

Finally, Chapter 5 covers the technique of ρ-hedging. We discuss its many theoretical weaknesses and explain the circumstances under which these out-of-model hedges may coincide with in-model hedges.

Part II addresses the implementation of the model prices derived in Part I, in order to arrive at the numerical results in Part III.

European option prices are easily calculated with tables of the standard cumulative normal distribution. American option prices, being optimal stopping problems, require detailed numerical approximation schemes. Chapter 6 describes the numerical techniques used to approximate American option prices.

For both OBS and VBS models, American option prices are converted from optimal stopping problems into variational inequalities, via free boundary partial differential equations. OBS prices are calculated using Crank-Nicolson approximations to the partial differential equation, with a Projected Successive Over-Relaxation scheme to solve the resulting constrained matrix problem.

Chapter 6 then discusses why we require our own scheme for approximating VBS option prices, derives a scheme meeting our requirements and shows the stability requirements of this scheme. This scheme uses explicit finite difference approximations in two orthogonal variables.

Chapter 7 briefly covers the calibration of our VBS model to the South African market in early 2005 using both ruling market data as well as four years of market price history. The calibration intends to make this dissertation's numerical findings plausibly applicable to the South African market.

The results from our numerical investigations appear in Part III, and are divided over three chapters.

Put-call parity implies that total errors in European call and European put option pricing are identical. This allows us to combine all our numerical analysis of European options into Chapter 8.

First addressing total European option pricing error, we show this to be greatest when options are at-the-money, and increasing in magnitude with increasing time to expiry. However, as a proportion of option price such errors are generally immaterial (<5%), becoming material only when the option is deep out-of-the-money.

Following this we analyse European option hedging errors, which exhibit interesting patterns, but whose proportional error is remarkably similar to those of prices. This similarity suggests that European option pricing error reflects not a systematic bias towards either hedge instrument, but rather a mis-estimation of total model uncertainty.

Our analysis of Americans is split over chapters 9 and 10. We start with American equity call options in Chapter 9. First considering optimal exercise boundaries (OEBs), we show these to be consistently under-estimated by the Black-Scholes model - implying that this model always exercises options sub-optimally early. This effect carries into our price analysis as an under-estimate of option price near to Black-Scholes early exercise.

However our calibration's relatively large size of costs of early exercise, in comparison to

the corresponding benefits, makes optimal early exercise extremely unlikely. Consequently the American equity call option bears strong resemblance to its European counterpart, thus so too do the price and hedge comparisons of Chapter 9.

Chapter 10 presents the last of our numerical analysis - American equity put options. Beginning once more with OEBs, we again find Black-Scholes estimates consistently exercising excessively early, implying price under-estimates around the OEB. In this case the OEBs are highly accessible, indicating a large probability of optimal exercise before option expiry.

We investigate pricing and also hedging errors for American equity put options, both of which exhibit European effects at-the-money and early exercise effects around the Black-Scholes OEB. Neither effect is material in relation to the true parameter value - except deep out-of-the-money. Lastly, a consideration of ρ-hedging of American equity put options reveals surprising accuracy (given our theoretical concerns), except around Black-Scholes 'optimal' exercise.

We present the conclusion of our analysis, as well as scope for further research, in Chapter 11. Appendices are included in Part IV.

This dissertation assumes that the reader has a basic knowledge of partial differential equations and their numerical estimation, probability theory and arbitrage pricing theory.

Part I

Theory

The following four chapters consider the theory of pricing and hedging equity options in the two models of interest to us. Chapter 2 presents separately both models of interest to us.

We begin our pricing analysis in chapter 3, considering European contingent claims. This chapter describes the standard replication arguments, and applies these to get pricing formulae for discount bonds and European equity options. Finally it considers the difference both in pricing of and hedging of European equity options across our two models.

We turn our attention in chapter 4 to American equity options. We demonstrate how to apply replicating arguments to these more complicated claims, show the Markovian nature of American equity option prices, and consider the properties of the optimal exercise strategy.

Lastly chapter 5 explores the theoretical and practical issues around the technique of ρ-hedging a technique which uses the sensitivity of Black-Scholes option prices to interest rates in order to hedge the option price risk stemming from interest rate stochasticity.

Chapter 2

Security Market Models

This chapter develops and describes the two comparative models for the market within which equities trade - one with constant interest rates, the other with stochastic interest rates. Both models are presented in a probability theoretic-environment, with a minimal assumption set.

The first section presents the famous Black-Scholes model, where interest rates are constant. In the second section we augment this model with the so-called Vasicek model for interest rates, where the instantaneous cost of borrowing follows a mean-reverting Brownian motion. The first model will be referred to as the Original Black-Scholes (OBS) model, in contra-distinction to the Vasicek-augmented Black-Scholes (VBS) model presented in the second section.

2.1 The Black-Scholes Model

This section presents the Black-Scholes model for derivative security pricing which should be familiar to most readers of this dissertation. The market modelled contains a single risky asset S, which typically represents the price of a single equity stock or perhaps a stock index, but which could also be a traded currency or commodity. Most of this theory results from the seminal papers of Black and Scholes (1973) and Merton (1973), as well as the associated application of martingale theory pioneered by Harrison and Kreps (1979) and Harrison and Pliska (1981).

Let us model uncertainty with a one-dimensional Brownian motion $\{W_t^{\mathbb{P}}\}_{t\in[0,\mathcal{H}]}$ restricted to the finite horizon $[0,\mathcal{H}]$ on a filtered probability space $(\Omega,\mathbb{P},\mathcal{F},\mathbb{F})$. The filtration $\mathbb{F} = \{\mathcal{F}_t\}_{t\in[0,\mathcal{H}]}$ is that generated by $W^{\mathbb{P}}$, with $\mathcal{F}_{\mathcal{H}} = \mathcal{F}$, augmented by the usual conditions. (See Duffie (1996) Appendix F for elaboration of the usual conditions). Let Λ be the Lebesgue measure on $[0,\mathcal{H}]$.

We construct a simple security market based on the following seven assumptions. These are divided into assumptions regarding market structure (2.1.A1 to 2.1.A3), market efficiency (2.1.A4 to 2.1.A6) and technical requirements for mathematical constructs and for investor agreement (2.1.A7).

Assumption 2.1.A1 *The dynamics of the risky asset S are governed by the Stochastic Differential Equation (SDE)*

$$dS[t,\omega] = \mu_S[t,\omega]\cdot S[t,\omega]\cdot dt + \sigma_S\cdot S[t,\omega]\cdot dW_t^{\mathbb{P}} \tag{2.1a}$$

where σ_S is a constant.

Assumption 2.1.A2 *The risky asset S pays dividends continuously, maintaining a constant dividend yield δ.*

Assumption 2.1.A3 *There is a second, riskless asset β (which we will call the bank account) with dynamics*

$$d\beta[t] = R \cdot \beta[t] \cdot dt \tag{2.1b}$$

where R is constant.

Assumption 2.1.A4 *Both assets are infinitely divisible, and trade continuously through time in any amount.*

Note that the equations in assumptions 2.1.A1 and 2.1.A3 are solved respectively by

$$S[t,\omega] = S[0,\omega] \cdot \exp\left[\int_0^t \mu_S[s,\omega]ds - \frac{1}{2}\sigma_S^2 t + \sigma_S \cdot W_t^{\mathbb{P}}\right] \tag{2.2a}$$

$$\beta[t] = \beta[0]\exp[R \cdot t] \tag{2.2b}$$

Most variables considered are state-dependent. For most of this dissertation we will suppress this state dependency for ease of notation, unless explicit expression of state dependency enhances clarity or avoids confusion.

Definition 2.1.1 *A* **payoff stream** *$x[t,\omega]$ is a RCLL[1] semimartingale $x : [0,\mathcal{H}] \times \Omega \mapsto \mathbb{R}$ progressively measurable with respect to the filtration $\mathbb{F}$.*

The payoff stream $x[t,\omega]$ represents for each path ω the cumulative (undiscounted) cash receipts (or payments) over $(0,t]$.

Many financial derivative contracts, including the option contracts studied in this dissertation, give the buyer the right to choose between two or more payoff streams. It is useful to collect the alternatives into one grouping:

Definition 2.1.2 *A* **payoff set** *$\boldsymbol{x}$ is any collection of payoff streams x.*

Our interest is in the valuation of a payoff streams x within a payoff set $\boldsymbol{x}$.

Definition 2.1.3 *For any payoff set $\boldsymbol{x}_i$ a* **contingent claim** *$X_i[t,\omega]$ is a RCLL semimartingale $X_i : [0,\mathcal{H}] \times \Omega \mapsto \mathbb{R}$ progressively measurable with respect to the filtration $\mathbb{F}$ representing the price of the right to all the remaining cashflows over $(t,\mathcal{H}]$ from any one payoff stream x chosen from $\boldsymbol{x}_i$ by the buyer of the claim.*

For examples of the link between payoff streams, payoff sets and contingent claims see Definition 3.1.9 of European call options and Definition 4.3.1 of American equity call options.

Let $\mathbb{X}$ represent all the contingent claims trading in our economy. The pricing action is essentially the specification of these semi-martingale processes; hedging is addressed during the action of pricing. Note that at $\mathcal{H}$, any claim X_i must have zero value as it has zero further entitlements or obligations.

Assumption 2.1.A5 *There are no taxes or transaction costs relating to the assets S, β or any of the claims in $\mathbb{X}$.*

[1] Right Continuous with Left Limits. See Duffie (1996) Appendix F for details

Assumptions 2.1.A5 and 2.1.A4 imply that short sales are permitted in any finite amount and at no charge.

The constant R in assumption 2.1.A3 represents the instantaneous reward of risk-free investing. As short sales are permitted, R also represents the instantaneous cost of borrowing. This cost is constant for all times and maturities. Later this dissertation will relax the assumption of deterministic interest rates.

Our pricing techniques require the notions of portfolios and of arbitrage:

Definition 2.1.4 *For any $X_i \in \mathbb{X}$ and for any $x_i \in x_i$, an* **admissable self-financing trading strategy** $\Pi[t,\omega] = \big(\Pi_S[t,\omega], \Pi_\beta[t,\omega], \Pi_X[t,\omega]\big)$ *is an $\mathcal{F}_t$-previsible process* $\Pi : [0,\mathcal{H}] \times \Omega \mapsto \mathbb{R}^3$ *satisfying*

1. The integrability constraint

$$\int_0^{\mathcal{H}} \Big(\big|\Pi_S[s](\mu[s]+\delta)S[s]\big|ds + \Pi_S^2[s]\cdot\sigma_S^2\cdot S^2[s]ds + \big|\Pi_\beta[s]\cdot R\cdot\beta[s]\big|ds - \big|\Pi_X[s]d\big(X_i[s]+x_i[s]\big)\big| + \Pi_X^2[s]\cdot d\langle X_i[s]+x_i[s]\rangle \Big) < \infty \quad \mathbb{P}-a.s. \tag{2.3a}$$

   which guarantees the existence of the integral in 2 below;

2. The self-financing constraint

$$\Pi_S[t]\cdot S[t] + \Pi_\beta[t]\cdot\beta[t] + \Pi_X[t]\cdot X_i[t] = \int_0^t \Big(\Pi_S[s]\big(dS[s]+\delta S[s]ds\big) + \Pi_\beta[s]d\beta[s] + \Pi_X[s]d\big(X_i[s]+x_i[s]\big)\Big) + \Pi_S[0]\cdot S[0] + \Pi_\beta[0]\cdot\beta[0] + \Pi_X[0]\cdot X_i[0] \tag{2.3b}$$

   and

3. The admissability constraint that there exists a k such that:

$$\Pi_S[t]\cdot S[t] + \Pi_\beta[t]\cdot\beta[t] + \Pi_X[t]\cdot X_i[t] > k \quad \Lambda\times\mathbb{P}-a.s. \tag{2.3c}$$

   which precludes pathological arbitrage opportunities such as those built on the 'suicide strategy' of Harrison and Pliska (1981).

Unlike many textbook definitions of portfolios, it is necessary to consider the dynamics of the sum of the contingent claim X_i and the payoff stream x_i - $d\big(X_i[s]+x_i[s]\big)$ - so that the notion of self-financing extends to include any cashflows from the contingent claim. In particular, American options can be exercised by the holder - generating a cashflow - at any time during the life of the option. For pricing purposes our definition of self-financing must cover the entire life of the option, catering for exercise at random times during the option's life.

In practice portfolios may contain multiple contingent claims. Our portfolio definition only includes one contingent claim, as this is sufficient for the pricing and hedging analysis in following chapters. Extending our definition to include more contingent claims would not change this analysis, but only complicate the definition.

Definition 2.1.5 *An* **arbitrage opportunity** *is an admissable self-financing trading strategy satisfying:*

$$\Pi_S[0] \cdot S[0] + \Pi_\beta[0] \cdot \beta[0] + \Pi_X[0] \cdot X[0] = 0 \tag{2.4a}$$

$$\Pi_S[\mathcal{H}] \cdot S[\mathcal{H}] + \Pi_\beta[\mathcal{H}] \cdot \beta[\mathcal{H}] \geq 0 \quad \mathbb{P} - a.s. \tag{2.4b}$$

$$\mathbb{P}\Big[\Pi_S[\mathcal{H}] \cdot S[\mathcal{H}] + \Pi_\beta[\mathcal{H}] \cdot \beta[\mathcal{H}] > 0\Big] > 0 \tag{2.4c}$$

(Note that $X[\mathcal{H}] = 0$ by construction). In order to price contingent claims we will rely heavily on

Assumption 2.1.A6 *There are no arbitrage opportunities.*

We conclude construction of the Black-Scholes model with

Assumption 2.1.A7 *Investors agree on the values of the three constants σ_S, δ and R. They also agree that the function $\lambda_W[t,\omega] : [0,\mathcal{H}] \times \Omega \mapsto \mathbb{R}$ defined by $\lambda_W[t,\omega] = \frac{\mu_S[t,\omega] - R}{\sigma_S}$ is $\mathcal{F}_t^W$-previsible and satisfies the Novikov condition, i.e.*

$$\mathbb{E}^{\mathbb{P}}\left[\exp\left[\frac{1}{2}\int_0^{\mathcal{H}} \lambda_W^2[s,\omega]ds\right]\right] < \infty$$

.

We will refer to the model described by assumptions 2.1.A1-2.1.A6 as the Original Black-Scholes (OBS) model, in contradistinction to the Vasicek augmented Black-Scholes (VBS) model presented next.

2.2 The Vasicek-augmented Black-Scholes Model

The previous section presented the well-studied Black-Scholes Model for contingent claim pricing. This section extends that model to include interest rate stochasticity. We chose a particularly simple form of interest rate dynamics - the so-called Vasicek model, first considered in Vasicek (1977).

As noted in chapter 1, such simplicity is appropriate given the scope of this investigation. The chosen model provides tractability, and is often used as an introduction to term structure modelling. Simplicity and tractability result in this model being well understood. Finally, the simplicity limits the number of factors which could affecting equity option pricing.

The author has only seen the proposed model considered in Rabinovitch (1989), although it nests naturally within the models of Amin and Jarrow (1992) and Ritchken and Sankarasubrahmanian (1995) amongst others. Consider the filtered probability space $(\Omega, \mathbb{P}, \mathcal{F}, \mathbb{F})$ supporting the Brownian motions $\{W_t^{\mathbb{P}}\}_{t\in[0,\mathcal{H}]}$ and $\{V_t^{\mathbb{P}}\}_{t\in[0,\mathcal{H}]}$, both restricted to a horizon $[0,\mathcal{H}]$ and with constant correlation $\chi \in [-1,1]$. Let the filtration $\mathbb{F} = \{\mathcal{F}_t\}_{t\in[0,\mathcal{H}]}$ be that generated by the Brownian motions $W_t^{\mathbb{P}}$ and $V_t^{\mathbb{P}}$ and satisfying the usual conditions, with $\mathcal{F}_{\mathcal{H}} = \mathcal{F}$. Again set Λ to be the Lebesgue measure on $[0,\mathcal{H}]$.

We build a securities market model on top of this probability space with:

Assumption 2.2.A1 *There is a risky asset S governed by the S.D.E.*

$$dS[t,\omega] = \mu_S[t,\omega] \cdot S[t,\omega]dt + \sigma_S \cdot S[t,\omega]dW_t^{\mathbb{P}} \tag{2.5a}$$

where σ_S is constant.

Assumption 2.2.A2 *The risky asset S makes continuous dividend payments at a constant yield δ.*

Assumption 2.2.A3 *There is a process r, which we will call the* **short rate**, *satisfying Ornstein-Uhlenbeck dynamics:*

$$dr[t,\omega] = \alpha(\bar{\theta} - r[t,\omega]) + \sigma_r dV_t^{\mathbb{P}} \tag{2.5b}$$

where α, $\bar{\theta}$ and σ_r are constants.

Assumption 2.2.A4 *There is an instantaneously riskless asset β, called the bank account, satisfying*

$$d\beta[t,\omega] = r[t,\omega] \cdot \beta[t,\omega]dt \tag{2.5c}$$

The equations 2.5a - 2.5c are solved respectively by:

$$S[t,\omega] = S[0,\omega] \cdot \exp\left[\int_0^t \mu_S[s,\omega]ds - \tfrac{1}{2}\sigma_S^2 t + \sigma_S W_t^{\mathbb{P}}\right\} \tag{2.6a}$$

$$r[t,\omega] = \bar{\theta} + (r[0,\omega] - \bar{\theta})e^{-\alpha t} + \sigma_r \int_0^t e^{-\alpha(t-s)} dV_s^{\mathbb{P}} \tag{2.6b}$$

$$\beta[t,\omega] = \beta[0,\omega] \cdot \exp\left[\int_0^t r[s,\omega]ds\right] \tag{2.6c}$$

As in the previous section, we will often dispense with explicit state-dependence of the variables. Other than σ_S, σ_r, α and $\bar{\theta}$ the remaining variables are not constant other than by accident.

The stochastic process r is not assumed to be traded directly. Rather, it exhibits itself through the dynamics of the traded asset β, the bank account. β represents an (instantaneously) riskless investment. Thus the short rate r is the instantaneous risk-free rate of return.

Remark 2.2.1 *From equation (2.6b) it follows that, conditional on any sigma field $\mathcal{F}_t^V \in \mathbb{F}^V$ and for any $s \in (t, \mathcal{H}]$, $r[s]$ is a Gaussian process. This allows a strictly positive probability that any future short rate will be negative. Opponents of this model argue that such probabilities are unrealistic representations of reality; Rogers (1996) shows how this can distort security pricing. Proponents counter that, for most plausible calibrations, such probabilities are so low as to be negligible; also that negative overnight rates were observed in Switzerland in the 1960s and negative forward rates were implied by the Japanese yield curve in the late 1990s (Brown (2001)).*

Remark 2.2.2 *The parameter χ represents the correlation between unanticipated stock returns and unanticipated changes in the short rate. Most methods of fundamental stock analysis discount future cash flows at rates in excess of the default-free spot rates (defined later in later in chapter 3). As short (and hence spot) rates rise, the fundamental stock price should thus fall. This suggests a negative value of χ.*

Central bank overnight rates are the closest available proxy to our theoretical riskless instantaneous rate. In practice, changes in central bank overnight rates also impact on growth and inflation forecasts, and hence on the cashflows to be discounted. The correlation coefficient, while often observed as negative, is not always so.

As with the OBS model, we define contingent claims through their dependence on payoff streams and payoff sets:

Definition 2.2.3 *A* **payoff stream** $x[t,\omega]$ *is a RCLL* $\mathcal{F}_t$*-measurable map* $x : [0,\mathcal{H}]\times\Omega \mapsto \mathbb{R}$.

Definition 2.2.4 *A* **payoff set** $\boldsymbol{x}$ *is any collection of payoff streams.*

Definition 2.2.5 *For any payoff set* $\boldsymbol{x}_i$ *a* **contingent claim** $X_i[t,\omega]$ *is a RCLL* $\mathcal{F}_t$*-measurable map* $X_i : [0,\mathcal{H}]\times\Omega \mapsto \mathbb{R}$ *representing the value of the right to all the remaining cashflows over* $(t,\mathcal{H}]$ *from any one payoff stream* x *chosen from* $\boldsymbol{x}_i$ *by the buyer of the claim.*

Let $\mathbb{X}$ represent the set of all contingent claims trading in this economy.

Assumption 2.2.A5 *There are no taxes or transaction costs relating to trading in either the contingent claims* $\mathbb{X}$ *or the assets* S *and* β.

Definition 2.2.6 *For any* $X_i, X_j \in \mathbb{X}$, *an* **admissable self-financing trading strategy** $\Pi[s] = (\Pi_S[s], \Pi_\beta[s]. \Pi_i[s], \Pi_j[s])$ *is an* $\mathcal{F}_t$*-previsible process* $\Pi : [0,\mathcal{H}]\times\Omega \mapsto \mathbb{R}^4$ *safisfying*

1. *The integrability constraint*

$$\int_0^{\mathcal{H}} \Big(\big|\Pi_S[s](\mu_S[s]+\delta)S[s]\big|ds + \Pi_S^2[s]\cdot\sigma_S^2\cdot S^2[s]ds + \big|\Pi_i[s]d(X_i[s]+x_i[s])\big|ds + \Pi_i^2[s]d\langle X_i[s]+x_i[s]\rangle + \big|\Pi_j[s]d(X_j[s]+x_j[s])\big|ds + \Pi_j^2[s]d\langle X_j[s]+x_j[s]\rangle + \big|\Pi_\beta[s]\cdot r[s]\cdot\beta[s]\big|ds\Big) < \infty \quad \mathbb{P}-a.s. \tag{2.7a}$$

2. *The self-financing constraint that* $\forall t \subset [0,\mathcal{H}]$ *and with* $\mathbb{P}=1$,

$$\begin{aligned}\Pi_S[t]\cdot S[t] + \Pi_\beta[t]\cdot\beta[t] + \Pi_i[t]\cdot X_i[t] + \Pi_j[t]\cdot X_j[t] &= \Pi_S[0]\cdot S[0] + \Pi_\beta[0]\cdot\beta[0] + \Pi_i[0]\cdot X_i[0] + \Pi_j[0]\cdot X_j[0] \\ &+ \int_0^t \Big(\Pi_i[s]d\big(X_i[s]+x_i[s]\big) + \Pi_j[s]d\big(X_j[s]+x_j[s]\big) \\ &+ \Pi_S[s]\big(dS[s]+\delta S[s]ds\big) + \Pi_\beta[s]d\beta[s]\Big)\end{aligned} \tag{2.7b}$$

3. *The admissability constraint that there exists a* k *such that*

$$\Pi_S[t]\cdot S[t] + \Pi_\beta[t]\cdot\beta[t] + \Pi_i[t]\cdot X_i[t] + \Pi_j[t]\cdot X_j[t] > k \quad \Lambda\times\mathbb{P}-a.s. \tag{2.7c}$$

Once more our portfolio definition contains the minumum number of contingent claims required for the pricing and hedging process. Expanding this definition, while possible, would not change our later analysis.

The notion of portfolios allows the vital construction of arbitrage opportunities:

Definition 2.2.7 *An* **arbitrage possibility** *is a self-financing trading strategy satisfying*

$$\Pi_S[0]\cdot S[0] + \Pi_\beta[0]\cdot\beta[0] + \Pi_i[0]\cdot X_i[0] + \Pi_j[0]\cdot X_j[0] = 0 \tag{2.8a}$$

$$\Pi_S[\mathcal{H}]\cdot S[\mathcal{H}] + \Pi_\beta[\mathcal{H}]\cdot\beta[\mathcal{H}] \geq 0 \quad \mathbb{P}-a.s. \tag{2.8b}$$

$$\mathbb{P}\big[\Pi_S[\mathcal{H}]\cdot S[\mathcal{H}] + \Pi_\beta[\mathcal{H}]\cdot\beta[\mathcal{H}] > 0\big] > 0 \tag{2.8c}$$

The use of arbitrage, or rather its absence, will drive our pricing techniques:

Assumption 2.2.A6 *There are no arbitrage opportunities.*

Remark 2.2.8 *Unlike the Black-Scholes case, our assumptions thus far are insufficient to provide a unique price for every traded security. This price ambiguity stems from the lack of specification of the market price of interest rate risk. As we have not specified any markets for assets exhibiting interest rate risk, no price is assigned for such risk. In financial parlance, the model is incomplete. This is rectified by:*

Assumption 2.2.A7 *Investors agree on the identity of a 'primary' contingent claim X_0, the identity of the optimal cashflow x_0 supporting X_0 and that the dynamics of X_0 are*

$$dX_0[t] = \mu_0[t] \cdot X_0[t] \cdot dt + \sigma_0^W[t] \cdot X_0[t] \cdot dW_t^{\mathbb{P}} + \sigma_0^V[t] \cdot X_0[t] \cdot dV_t^{\mathbb{P}} - dx_0[t,\omega] \tag{2.9}$$

where $\mu_0[t]$, $\sigma_0^W[t]$ and $\sigma_0^V[t]$ are agreed $\mathcal{F}_t$-previsible functions, and $\sigma_0^V[t]$ is $\mathbb{P}$-a.s. non-zero.

By assuming that σ_0^V is non-zero we ensure that X_0 displays interest-rate sensitivity, and thus that its dynamics implicitly price interest rate risk.

The dynamics of the traded assets S and X_0 allow us to define the parameters

$$\lambda_W[t] = \frac{\mu_S[t] - r[t]}{\sigma_S} \tag{2.10a}$$

$$\lambda_V[t] = \frac{\mu_0[t] - r[t]}{\sigma_0^V[t]} - \lambda_W[t] \cdot \frac{\sigma_0^W[t]}{\sigma_0^V[t]} \tag{2.10b}$$

It follows from these definitions that

$$\mu_S[t] = r[t] + \lambda_W[t] \cdot \sigma_S$$
$$\mu_0[t] = r[t] + \lambda_W[t] \cdot \sigma_0^W[t] + \lambda_V[t] \cdot \sigma_0^V[t]$$

and it is obvious that λ_W represents the return in excess of the short rate received by the holder of the assets S and X_0, and similarly with λ_V. It will transpire that the arbitrage-free price of all contingent claims also yield excess returns of λ_W and λ_V per unit of sensitivity to $W^{\mathbb{P}}$ and $V^{\mathbb{P}}$ respectively. Consequently λ_W and λ_V are called the market price of stock price and interest rate risk respectively.

Assumption 2.2.A8 *The market price of interest rate risk is constant, i.e. $\lambda_V[t,\omega] = \lambda_V$.*

Remark 2.2.9 *The primary contingent claim X_0 serves to set the market price of interest rate risk, λ_V, for the purposes of obtaining a risk-neutral measure and hence for arbirage-free pricing — as discussed in the next two chapters. X_0 may be a simple contingent claim such as a discount bond (see Definition 3.1.4), but Assumption 2.2.A7 allows for more complex contingent claims to serve this function.*

Assumption 2.2.A9 *Investors agree on the values of the constants σ_S, σ_r, α, $\bar{\theta}$ and λ_V, and that λ_W satisfies the Novikov condition (see Assumption 2.1.A7).*

In the following chapters we will be particularly interested in a process strongly resembling

$$\begin{aligned} r[t] - \frac{\sigma_r \lambda_V}{\alpha}\left[1 - e^{-\alpha t}\right] \\ = \theta + \big(r[0] - \theta\big)e^{-\alpha t} + \sigma_r \int_0^t e^{-\alpha(t-s)} dV_t^P \end{aligned} \tag{2.11}$$

where $\theta = \bar{\theta} - \frac{\sigma_r \lambda_V}{\alpha}$.

By assumption 2.2.A8 the process in (2.11) will also have Ornstein-Uhlenbeck dynamics - see equation 2.6b. This indeed is the rationale for including assumption 2.2.A8.

Remark 2.2.10 *Assumption 2.2.A8 ensures that the dynamics of the process in (2.11) retain an Ornstein-Uhlenbeck form. As pointed out by Hull and White (1990B), this can be relaxed to assuming that $\lambda_V[t,\omega]$ is linear in r, i.e. $\lambda_V[t,\omega] = \lambda_V^{(1)} + \lambda_V^{(2)} \cdot r[t,\omega]$, where $\lambda_V^{(1)}$ and $\lambda_V^{(2)}$ are consensus constants.*

Remark 2.2.11 *As the Vasicek model makes assumptions regarding the market price of interest rate risk, it is termed a partial equilibrium model. Equilibrium is only partial, as there is no guarantee that the form of λ_V is consistent with investors' utility functions.*

Contrasting approaches to the market price of interest risk include general equilibrium models which model investor preferences and determine the market price of interest rate risk at aggregate equilibrium (such as Cox, Ingersoll and Ross (1985A,B)) and no-arbitrage models which directly model the process in 2.11- ignoring the form of λ_V - pioneered in Hull and White (1990B).

Cox, Ingersoll and Ross (1985B) show how a mis-specified form of λ_V in a partial equilibrium framework may lead to inconsistencies between pricing and utility maximisation. However, simple representative utility functions can be constructed to be consistent with a very broad class of forms of λ_V. Such utility functions generate general equilibrium frameworks which are consistent with partial equilibrium assumptions - see Duffie (1996) Exercise 10.3 for details.

Remark 2.2.12 *As it turns out, only the dynamics of 2.11 influence security pricing. Assumptions 2.2.A3, 2.2.A7, 2.2.A8 and 2.2.A9 can be collectively relaxed to assuming that investors agree*

- *on the existence of a primary claim satisfying (2.9)*
- *that the process in (2.11) is Ornstein-Uhlenbeck*
- *that the market price of interest rate risk $\lambda_V[t]$ satisfies the Novikov condition (see Assumption 2.1.A7), and*
- *on the values of the constants of the σ_S, δ, α, θ σ.*

The primary asset may be differently specified between different investors, and also be stochastic for any investor. Importantly, this allows discount bonds (defined in the following chapter) maturing before the model horizon $\mathcal{H}$, or any other claim displaying V-risk (and which hence prices V-risk) to be used as the primary claim.

As the assets β, S and X_0 will be used in the following chapters to hedge other contingent claims, we conclude the construction of our VBS economy with

Assumption 2.2.A10 *The assets S, β and X_0 trade continuously through time in any amount, and are infinitely divisible.*

We will refer to the model generated by assumptions 2.2.A1 through 2.2.A10 as the Vasicek-Black-Scholes (VBS) model. The assumptions made are sufficient to price a very broad class of contingent claims.

Trivially, setting $\sigma_r = \alpha = 0$ and $r[0] = R$ (or $\sigma_r = 0$, $r[0] = \theta = R$) returns us to the original Black-Scholes setting of constant interest rates. In this case the VBS and OBS results will concur.

Chapter 3

European Options

European call options - unlike their American counterparts - may only be exercised on their expiry date. This restriction on exercise timing greatly simplifies the analysis of option prices and hedges.

This chapter considers and compares the prices and hedges of European equity options under both the OBS and VBS models. The first section derives these prices and hedges. At very little marginal cost we develop theory to price all European contingent claims, then apply this to discount bonds (which are used extensively throughout this dissertation) and then equity options. The second section compares the VBS and OBS formulae, addressing first prices and then hedges.

Recall we are comparing the two securities market models described in the previous chapter. The dynamics of the securities S and B (and, in the VBS model, the security X_0 and the short rate r) are described under the real-world measure $\mathbb{P}$. This, together with the assumptions in chapter 2 regarding market structure, prove sufficient to price European contingent claims.

European equity call options are a specific case of a European contingent claim, which makes a random payment (determinable by the payment date) on a known payment date. Mathematically, we define this as

Definition 3.0.1 *A* **European contingent claim***(ECC) X_E with expiry time T is the contingent claim supported by the payoff set $\boldsymbol{x}_E$ containing the single payoff stream*

$$x_E[t,\omega] = E[\omega] \cdot \mathbb{I}_{\{t \geq T\}} \tag{3.1}$$

for any $T \in [0, \mathcal{H}]$ where E is any $\mathcal{F}_T$-measurable random variable with $E \in \mathcal{L}^2[\Omega, \mathcal{F}_T, \mathbb{Q}]$, and $\mathbb{Q}$ is the risk-neutral measure defined by (3.2a) and (3.5).

3.1 Pricing and Hedging

Both the models presented in the previous chapter are complete (see Harrison and Pliska (1981)) in the sense that there are as many non-linear risky assets with determined dynamics as there are sources of noise. This allows us to perfectly hedge any ECC using a dynamic portfolio of these risky assets, augmented with the bank account. As this portfolio perfectly replicates the ECC cashflows (by construction) it is known as the replicating portfolio, or alternately as the hedging portfolio.

To prevent arbitrage possibilities the ECC value and the value of the replicating portfolio must agree at all times. This key insight leads to the celebrated Black-Scholes option prices for European equity option prices, as well as their VBS counterparts.

We will present results for both models, but only include proofs for the VBS model. OBS proofs are simpler, but follow otherwise identical logic.

3.1.1 General Theory

On page 12 we defined λ_W, the market price of W-risk in the OBS model, by

$$\lambda_W[t,\omega] = \frac{\mu_S[t,\omega] - r[t]}{\sigma_S}$$

which represents the instantaneous drift of the risky asset in excess of the interest rate R per unit of volatility σ_S. Using this variable we can define the new measure $\mathbb{Q}$ through the Radon-Nikodym derivative

$$\frac{d\mathbb{Q}}{d\mathbb{P}} = \exp\left[\int_{t=0}^{\mathcal{H}} -\lambda_W[t,\omega]dW_t^{\mathbb{P}} - \frac{1}{2}\int_{t=0}^{\mathcal{H}} \lambda_W^2[t,\omega]dt\right] \tag{3.2a}$$

λ_W was assumed in 2.1.A7 to satisfy the Novikov condition, so it follows from Girsanov's Theorem (see any stochastic calculus textbook, e.g. Øksendal (1998), Karatzas and Shreve (1991), Protter (1990)) that

$$W_t^{\mathbb{Q}} = W_t^{\mathbb{P}} + \int_0^t \lambda_W[s,\omega]ds \tag{3.2b}$$

is a standard Brownian motion with respect to the the measure $\mathbb{Q}$ and the filtration $\mathcal{F}_t$.

The measure $\mathbb{Q}$ is equivalent to $\mathbb{P}$, and plays an important role in pricing European contingent claims:

Theorem 3.1.1 *For all $t \in [0,\mathcal{H}]$ the OBS price of a European contingent claim is $\mathbb{P}$-almost surely*

$$X_E[t,\omega] = e^{-R(T-t)} \cdot \mathbb{E}^{\mathbb{Q}}\left[E[\omega]\middle|\mathcal{F}_t\right] \cdot \mathbb{1}_{\{t<T\}} \tag{3.3}$$

where $E[\omega]$ is the $\mathcal{L}^2[\mathcal{F}_T,\mathbb{Q}]$ random variable from which the sole payoff stream is created (see definition 3.0.1).

The proof of 3.1.1 follows the lines of 3.1.3 but is simpler and so omitted for parsimony.

The VBS model contains two sources of noise, W and V, priced in the market at

$$\lambda_W[t] = \frac{\mu_S[t] - r[t]}{\sigma_S}$$

and

$$\lambda_V[t] = \frac{\mu_0[t] - r[t]}{\sigma_0^V[t]} - \lambda_W[t]\cdot\frac{\sigma_0^W[t]}{\sigma_0^V[t]}$$

respectively. Using both these market prices of risk we can create the new measure $\mathbb{Q}$ through

$$\frac{d\mathbb{Q}}{d\mathbb{P}} = \exp\left[-\int_0^{\mathcal{H}} \frac{\lambda_W[t] - \chi\cdot\lambda_V}{1-\chi^2}dW_t^{\mathbb{P}} - \int_0^{\mathcal{H}} \frac{\lambda_V - \chi\cdot\lambda_W[t]}{1-\chi^2}dV_t^{\mathbb{P}} - \frac{1}{2}\int_0^{\mathcal{H}} \frac{\lambda_W^2[t] - 2\chi\cdot\lambda_W[t]\cdot\lambda_V + \lambda_V^2}{1-\chi^2}\right] \tag{3.5}$$

From Assumptions 2.2.A9 and 2.2.A8 we have

$$\mathbb{E}^{\mathbb{P}}\left[\exp\left[\frac{1}{2}\int_0^{\mathcal{H}} \lambda_W[t]^2 - 2\chi\lambda_W[t]\lambda_V + \lambda_V^2\, dt\right]\right] < \infty$$

and can invoke Girsanov's Theorem, defining the processes

$$W_t^{\mathbb{Q}} = W_t^{\mathbb{P}} + \int_0^t \lambda_W[s]ds \tag{3.6a}$$

$$V_t^{\mathbb{Q}} = V_t^{\mathbb{P}} + \lambda_V \cdot t \tag{3.6b}$$

both of which are Brownian motions under the measure $\mathbb{Q}$, still with constant correlation χ, shown in appendix A.

Setting $\theta = \bar{\theta} - \frac{\lambda_V \cdot \sigma_r}{\alpha}$, the short rate dynamics under $\mathbb{Q}$ are

$$dr[t] = \alpha\left(\theta - r[t]\right)dt + \sigma_r dV_t^{\mathbb{Q}} \tag{3.7a}$$

and are solved by

$$r[t,\omega] = \theta + (r[0,\omega] - \theta)e^{-\alpha t} + \sigma_r \int_0^t e^{-\alpha(t-s)} dV_s^{\mathbb{Q}} \tag{3.7b}$$

and retain their Ornstein-Uhlenbeck nature. This is the reason behind assumption 2.2.A8 - see remark 2.2.10. The $\mathbb{Q}$-dynamics of r are the process alluded to through equation (2.11).

Recall that X_0 is the primary contingent claim which prices interest rate risk, and has agreed optimal cashflow x_0. Both X_0 and S have a drift rate $r[t]$ under $\mathbb{Q}$ (before cash distributions - i.e before payments from the optimal payoff stream x_0 or from dividends $\delta\, S[t]$):

$$dS[t] = r[t] \cdot S[t] \cdot dt + \sigma_S \cdot S[t]\, dW_t^{\mathbb{Q}} - \delta \cdot S[t]\, dt \tag{3.7c}$$

$$dX_0[t] = r[t] \cdot X_0[t]\, dt + \sigma_0^W[t] \cdot X_0[t]\, dW_t^{\mathbb{Q}} + \sigma_0^V[t] \cdot X_0[t]\, dV_t^{\mathbb{Q}} - dx_0[t] \tag{3.7d}$$

As the discounted values $\frac{S}{\beta}$ and $\frac{X_0}{\beta}$ (and also most discounted contingent claim values) have zero drift under $\mathbb{Q}$ (still before cash distributions), $\mathbb{Q}$ is often called the equivalent martingale measure (EMM). Alternatively, as assets yield no return in excess of the short rate regardless of risk carried - implying that investors in a world with measure $\mathbb{Q}$ have risk-neutral utility functions - $\mathbb{Q}$ is also referred to as the risk-neutral measure (RNM).

As will become apparent in the remainder of this chapter, contingent claim prices are obtained under the measure $\mathbb{Q}$. Hence agreement on the parameters of the $\mathbb{Q}$-dynamics of S and r, combined with the observed market values of S and r implicit in 2.2.A5, are sufficient to ensure agreement on the unique prices of all elements of $\mathbb{X}$. See remark 2.2.12 for an indication of how our assumptions may be relaxed.

In order to prove our European contingent claim pricing formulae we will require

Theorem 3.1.2 Martingale Representation Theorem
For any $\mathcal{F}_T$-measurable random variable $E[\omega] \in \mathcal{L}^2[\Omega, \mathcal{F}_T, \mathbb{Q}]$ there exists a unique $\mathcal{F}_t$-previsible pair $(\phi^W[t], \phi^V[t])$ such that

$$E[\omega] = \mathbb{E}^{\mathbb{Q}}[E] + \int_0^T \phi_E^W[t] dW_t^{\mathbb{Q}} + \int_0^T \phi_E^V[t] dV_t^{\mathbb{Q}}$$

Proof. see Øksendal (1998) page 53.

We have only presented the Martingale Representation Theorem in two dimensions, which is the case of immediate interest to us. It holds in general for n dimensions, in which case the pre-visible vector has n components.

As discussed earlier the security market models we consider are complete. Thus for every ECC there exists a portfolio which replicates the claim cashflows exactly. We derive our ECC price by showing that, if values of the ECC and its replicating portfolio do not always coincide, then arbitrage is possible.

Theorem 3.1.3 *For all $t \in [0, \mathcal{H}]$ and the VBS price of a European contingent claim is $\mathbb{P}$-almost surely*

$$X_E[t,\omega] = \mathbb{E}^{\mathbb{Q}}\left[\exp\left[-\int_t^T r[s]ds\right] \cdot E[\omega]\middle|\mathcal{F}_t\right] \cdot \mathbb{I}_{\{t<T\}} \tag{3.8}$$

Proof.
Let $\tilde{X}_E[t,\omega] = \mathbb{E}^{\mathbb{Q}}\left[\exp\left[-\int_t^T r[s]ds\right] \cdot E[\omega]|\mathcal{F}_t\right] \cdot \mathbb{I}_{\{t<T\}}$ be our proposed ECC price, and set $\bar{E}[\omega] = \frac{E[\omega]}{\beta[T,\omega]}$ to be the ECC payoff discounted by the bank account at ECC expiry. Since the $\mathbb{Q}$-distribution of r is Gaussian, $\beta^{-1}[T.\omega]$ has a lognormal distribution and is hence in $\mathcal{L}^2[\mathcal{F}_T, \mathbb{Q}]$; by the Cauchy-Schwarz inequality $\bar{E}$ is also in $\mathcal{L}^2[\mathcal{F}_T, \mathbb{Q}]$. We can use theorem 3.1.2 to express $\bar{E}$ as

$$\bar{E}[\omega] = \mathbb{E}^{\mathbb{Q}}\left[\bar{E}\right] + \int_0^T \phi_{\bar{E}}^W[s,\omega]\, dW_s^{\mathbb{Q}} + \int_0^T \phi_{\bar{E}}^V[s,\omega]\, dV_s^{\mathbb{Q}}$$

Suppose that there is a $(t.\omega)$ where the ECC price X_E is less than our proposed price $\tilde{X}_E$, i.e. $X_E[t,\omega] < \tilde{X}_E[t,\omega]$. Noting that $\tilde{X}_E[T,\omega] = \beta[T,\omega] \cdot \bar{E}[\omega]$ it is easily shown that the portfolio

$$\begin{aligned}
\Pi_E[s] =& \mathbb{I}_{\{t\le s\le\mathcal{H}\}} \\
\Pi_0[s] =& \frac{-\beta[s]\phi_{\bar{E}}^V[s]}{\sigma_0^V[s]\cdot X_0[s]} \cdot \mathbb{I}_{\{t\le s<T\}} \\
\Pi_S[s] =& \left(\frac{\beta[s]\cdot\sigma_{\bar{E}}^V[s]\cdot\sigma_0^W[s]}{\sigma_0^V[s]\cdot\sigma_S\cdot S[s]} - \frac{\beta[s]\cdot\phi_{\bar{E}}^W[s]}{\sigma_S\cdot S[s]}\right)\cdot\mathbb{I}_{\{t\le s<T\}} \\
\Pi_\beta[s] =& \left(\tilde{X}_E[s] - \Pi_S[s]\cdot S[s] - \Pi_0[s]\cdot X_0[s]\right)\tfrac{1}{\beta[s]}\cdot\mathbb{I}_{\{t\le s<T\}} \\
&+ \left(\tilde{X}_E[t] - X_E[t]\right)\cdot\tfrac{1}{\beta[t]}\cdot\mathbb{I}_{\{t<s\le\mathcal{H}\}}
\end{aligned}$$

represents an arbitrage strategy unless $\mathbb{P}[\exists t : X_E[t.\omega] < \tilde{X}_E[t,\omega]] = 0$. Symmetrical arguments yield $\mathbb{P}[\exists t : X_E[t,\omega] > \tilde{X}_E[t.\omega]] = 0$.

□

The proof above relies on the ability to replicate the ECC payoff using holdings the risky asset, the primary contingent claim and the bank account. Should the ECC price be less than that of the replicating portfolio, arbitrage opportunities exist through purchasing the ECC and selling the replicating portfolio. The reverse strategy exploits the arbitrage opportunities present when the ECC price exceeds that of its replicating portfolio.

3.1.2 Discount Bonds

Definition 3.1.4 *A* **discount bond** $X_{B[T]}$ *maturing at time* T *is the ECC created by the payoff set with the sole payoff stream* $x_{B[T]} = \mathbb{I}_{\{t \geq T\}}$.

Discount bonds (a.k.a. zero coupon bonds) are a simple but particularly useful contingent claim. They represent the right to receive a payment of 1 at time T for certain, and are the obvious vehicle for discounting future payments of known size and timing.

Applying theorem 3.1.1 to price discount bonds within the OBS assumptions leads to the price

$$X_{B[T]} = e^{-R(T-t)} \tag{3.9a}$$

We introduce the notation $B^{\mathcal{O}}[t,T]$ to denote this price, i.e.

$$B^{\mathcal{O}}[t,T] = X_{B[t]} = e^{-R(T-t)} \tag{3.9b}$$

As interest rates are assumed here to be deterministic, the discount bond is perfectly replicated by holding e^{-RT} units of the bank account. As such, discount bonds and the bank account are perfect substitutes.

VBS prices for discount bonds provide a more interesting study. Using 2.6c in our application of theorem 3.1.3 we get the VBS price to be

$$X_{B[T]}[t,\omega] = \mathbb{E}^{\mathbb{Q}}\left[\exp\left[-\int_t^T r[s]ds\right]\middle|\mathcal{F}_t^V\right]$$

$$X_{B[T]}[t,\omega] = \mathbb{E}^{\mathbb{Q}}\left[\exp\left[-(r[t]-\theta)\int_t^T e^{-\alpha(s-t)}ds - \theta(T-t) - \int_{s=t}^T\int_{u=t}^s \sigma_r e^{-\alpha(s-u)}dV_u^{\mathbb{Q}}\,ds\right]\middle|\mathcal{F}_t^V\right]$$

$$X_{B[T]}[t,\omega] = \exp\left[-\theta(T-t) - \left(\frac{1-e^{-\alpha(T-t)}}{\alpha}\right)(r[t]-\theta)\right] \times \mathbb{E}^{\mathbb{Q}}\left[\exp\left[-\sigma_r\int_{u=t}^T\int_{s=u}^T e^{-\alpha(s-u)}ds\,dV_u^{\mathbb{Q}}\right]\middle|\mathcal{F}_t^V\right]$$

Conditional on $\mathcal{F}_t^V$, the integral $\int_t^T \left(1-e^{-\alpha(T-u)}\right)dV_u^{\mathbb{Q}}$ has a normal distribution under $\mathbb{Q}$ with variance $\frac{1}{2\alpha}\left(2\alpha(T-t) - 3 + 4e^{-\alpha(T-t)} - e^{-2\alpha(T-t)}\right)$ and zero mean. Following on this, the exponential of this integral has a lognormal distribution. Using the known mean of a lognormal random variable (see Rice (1995) p.146 Example D) we reduce $X_{B[T]}$ to:

$$X_{B[T]}[t,\omega] = \exp\left[-\theta(T-t) - (r[t]-\theta)\left(\frac{1-e^{-\alpha(T-t)}}{\alpha}\right) + \frac{\sigma_r^2}{4\alpha^3}\left(2\alpha(T-t) - 3 + 4e^{-\alpha(T-t)} - e^{-2\alpha(T-t)}\right)\middle|\mathcal{F}_t^V\right]$$

Setting $D[\tau] = \dfrac{1 - e^{-\alpha\tau}}{\alpha}$:

$$X_{B[T]}[t,\omega] = \exp\left[-r[t]D[T-t] - \left(\theta - \frac{\sigma_r^2}{2\alpha^2}\right)(T - t - D[T-t]) - \frac{\sigma_r^2}{4\alpha}(D[T-t])^2\right]$$

As the bond price $X_{B[T]}$ is dependent only on current time, maturity and current short rate, we introduce the function

$$B^{\mathcal{V}}[t,T,r] = \exp\left[-rD[T-t] - \left(\theta - \frac{\sigma_r^2}{2\alpha^2}\right)(T - t - D[T-t]) - \frac{\sigma_r^2}{4\alpha}(D[T-t])^2\right] \quad (3.10)$$

which captures the dependency of the discount bond price $X_{B[t]}$ on the variables θ, σ_r, α, r.

Remark 3.1.5 *$D[T-t]$ represents the instantaneous proportional sensitivity of the discount bond price $B^{\mathcal{V}}[t,T,r]$ to drops in the short rate $r[t]$. For this reason it is often called the modified duration of the bond. This is in contradistinction to the (unmodified) duration of any bond - the instantaneous proportional sensitivity of the bond price to drops in the gross continuous yield to maturity. For discount bonds duration is trivially time to maturity.*

In this model discount bond prices are stochastic through their dependence on the level of the short rate. Application of Itô's Lemma yields

$$dB^{\mathcal{V}}[t,T,r] = \left(\frac{\partial B^{\mathcal{V}}[t,T,r]}{\partial t} + \frac{\partial B^{\mathcal{V}}[t,T,r]}{\partial r}\alpha(\theta - r) + \frac{1}{2}\frac{\partial^2 B^{\mathcal{V}}[t,T,r]}{\partial r^2}\sigma_r^2\right) - \sigma_r \cdot D[T-t]B^{\mathcal{V}}[t,T,r] \cdot dV_t^{\mathbb{Q}} \quad (3.11)$$

Remark 3.1.6 *The dynamics in (3.11) imply that all discount bonds have perfect instantaneous correlation. In real bond markets such correlation is less than perfect. This shortcoming is not unique to the Vasicek model, but common between all one-factor models. It can be corrected by adding noise sources, at the cost of model parsimony.*

In the remainer of this dissertation we will frequently implicitly assume that discount bonds are available to hedge other, more exotic, contingent claims. This requires either that discount bonds trade continuously, or - in the VBS model - that the discount bonds concerned *are* the primary contingent claim X_0, in which case its dynamics determine - and are not determined by - the EMM $\mathbb{Q}$.

The bond pricing formula (3.10) gives varying yields-to-maturity (y-t-m's) for every maturity $T \in [t, \mathcal{H}]$.

Definition 3.1.7 *The* **spot rate** *$R[t,T,r[t]]$ is the continuous yield to maturity at time t for the discount bond maturing at time T, i.e.*

$$\begin{aligned} R[t,T,r] &= \frac{-\ln B^{\mathcal{V}}[t,T,r]}{T-t} \\ &= r\frac{D[T-t]}{T-t} + \left(\theta - \frac{\sigma_r^2}{2\alpha^2}\right)\left(1 - \frac{D[T-t]}{T-t}\right) + \frac{\sigma_r^2}{4\alpha}\frac{D^2[T-t]}{T-t} \end{aligned} \quad (3.12)$$

As the spot rate R is a one-to-one function mapping the short rate r into the spot rate R, we can define the inverse function R^{-1} from R to r by

$$R^{-1}[t,T,R] = R\frac{T-t}{D[T-t]} + \left(\theta - \frac{\sigma_r^2}{2\alpha^2}\right)\left(\frac{T-t}{D[T-t]} - 1\right) - \frac{\sigma_r^2}{4\alpha}D[T-t] \quad (3.13)$$

Remark 3.1.8 *Given a short rate, only three further parameters (α, θ and σ_r) completely determine the spot rate curve. Bar some exceptions, three parameters provide insufficient freedom to fit an observed curve of market spot rates. Humped spot curves prove particularly hard to fit.*

The Vasicek model is often criticised for this failure to calibrate to observed yield curves. Pricing of complicated derivative securities is questionable if even the simplest securities (discount bonds) are mis-priced. This drawback is shared with all time-homogenous interest rate models.

Miscalibration is partially alleviated by introducing further factors (i.e. sources of noise) into the model. It can be fully alleviated by making one (or more) of the model parameters time-dependent - see Hull and White (1990, 1994B).

We will use discount bonds extensively in our pricing of European equity options.

3.1.3 European Equity Options

European equity options represent the right (but not the obligation) to transact in the risky asset S at a fixed price on a fixed date. They are divided into call options, being the right to purchase, and put options, the right to sell. We will spend most of our time deriving results for call options; results for put options follow similarly.

Definition 3.1.9 *A* **European equity call option** $X_c[t,\omega]$, *is the contingent claim created by a payoff set containing the single payoff stream* $x_c[t,\omega] = \big[S[T] - K\big]^+ \cdot \mathbb{I}_{\{t \geq T\}}$.

The ECC X_c represents the right (but not the obligation) to buy the asset S at expiry time T for the strike price K. We consider first European equity call option pricing under the OBS model. It follows from Theorem 3.1.1, with substitutions of equations (2.2) and (3.2b) and some algebraic manipulation that prior to expiry,

$$X_c^{\mathcal{O}}[t,\omega] = S[t] \cdot e^{-\delta(T-t)} \cdot \Phi[a_1] - K \cdot e^{-R(T-t)} \cdot \Phi[a_2] \tag{3.14a}$$

where

$$a_1 = \frac{\ln S[t] - \ln K + (R - \delta - \frac{1}{2}\sigma_S^2)(T-t)}{\sigma\sqrt{T-t}}$$

$$a_2 = a_1 - \sigma\sqrt{T-t}$$

$\Phi[\,]$ is the standard cumulative normal distribution function.

Notice that the European equity call option price is Markovian, dependent only on the two variables t and $S[t]$. We define the function $c^{\mathcal{O}}\big[t, S[t]\big]$ to represent this relationship on t and $S[t]$, i.e.

$$c^{\mathcal{O}}\big[t,S\big] = S \cdot e^{-\delta(T-t)} \cdot \Phi[a_1] - K \cdot e^{-R(T-t)} \cdot \Phi[a_2] \tag{3.14b}$$

with a_1, a_2 and Φ as defined above. This is the celebrated Black-Scholes call option pricing formula, first published in Black & Scholes (1972). The replicating portfolio comprises $H_{c;S}^{\mathcal{O}}[t,S] = e^{-\delta(T-t)} \cdot \Phi[a_1]$ units of the stock $S[t]$ and $H_{c;B[T]}^{\mathcal{O}}[t,S] = -K \cdot \Phi[a_2]$ units of the bond $B^{\mathcal{O}}[t,T]$.

The pricing of European equity call options under the VBS assumptions is more intricate, but leads to greater insight. Theorem 3.1.3 yields

$$\begin{aligned} X_c[t,\omega] =& \mathbb{E}^{\mathbb{Q}}\left[\exp\left[-\int_t^T r[s]ds\right]\cdot[S[T]-K]^+\middle|\mathcal{F}_t\right] \\ =& \mathbb{E}^{\mathbb{Q}}\left[\exp\left[-\int_t^T \theta+(r[t]-\theta)e^{-\alpha(s-t)}+\left(\int_t^s \sigma_r\, e^{-\alpha(s-u)}dV_u^{\mathbb{Q}}\right)ds\right]\times\right. \\ & \left.\left[S[t]\times\exp\left[\int_t^T r[s]ds-\left(\delta+\tfrac{\sigma_S^2}{2}\right)(T-t)+\sigma_S\left(W_T^{\mathbb{Q}}-W_t^{\mathbb{Q}}\right)\right]-K\right]^+\middle|\mathcal{F}_t\right] \end{aligned} \tag{3.15}$$

While analytical solution of 3.15 is technically feasible, this requires manipulation of bivariate cumulative Gaussian distribution function. We take a more parsimonious route involving only univariate cumulative Gaussian distributions. Our methodology uses the change of numéraire technique documented by Geman, el Karoui & Rochet (1995), and which traces its roots to Jamshidian (1987).

We can rewrite 3.15 as

$$\begin{aligned} X_c[t,\omega] =& \beta[t]\cdot\mathbb{E}^{\mathbb{Q}}\left[\left[\frac{S[T]-K}{\beta[T]}\right]^+|\mathcal{F}_t\right] \\ =& \beta[t]\cdot\mathbb{E}^{\mathbb{Q}}\left[\frac{S[T]}{\beta[T]}\cdot\mathbb{I}_{\{S[T]>K\}}|\mathcal{F}_t\right] \\ & -\beta[t]\cdot\mathbb{E}^{\mathbb{Q}}\left[\frac{K}{\beta[T]}\cdot\mathbb{I}_{\{S[T]>K\}}|\mathcal{F}_t\right] \end{aligned} \tag{3.16}$$

Define the new measures $\mathbb{Q}^S$ and $\mathbb{Q}_B^T$ by

$$\begin{aligned} \frac{d\mathbb{Q}^S}{d\mathbb{Q}} =& e^{\delta\mathcal{H}}\frac{S[\mathcal{H}]}{S[0]}\frac{\beta[0]}{\beta[\mathcal{H}]} \\ & \exp\left[\sigma_S W_{\mathcal{H}}^{\mathbb{Q}}-\frac{\sigma_S^2}{2}\mathcal{H}\right] \end{aligned} \tag{3.17a}$$

$$\begin{aligned} \frac{d\mathbb{Q}_B^T}{d\mathbb{Q}} =& \lim_{t\uparrow T}\frac{B^{\mathcal{V}}[t,T,r[t]]}{B^{\mathcal{V}}[0,T,r[0]]}\frac{\beta[0]}{\beta[T]} \\ =& \exp\left[-\int_0^T D[T-s]\sigma_r dV_s^{\mathbb{Q}}-\tfrac{1}{2}\int_0^T(D[T-s]\cdot\sigma_r)^2 ds\right\} \end{aligned} \tag{3.17b}$$

Again invoking Girsanov's Theorem, the processes $W^{\mathbb{Q}^S}$ and $V^{\mathbb{Q}^S}$ defined by

$$W_t^{\mathbb{Q}^S} = W_t^{\mathbb{Q}} - \sigma_S t \tag{3.18a}$$

$$V_t^{\mathbb{Q}^S} = V_t^{\mathbb{Q}} - \chi\sigma_S t \tag{3.18b}$$

are Brownian motions with correlation χ under $\mathbb{Q}^S$, as shown in appendix A. Similarly,

$$W_t^{\mathbb{Q}_B^T} = W_t^{\mathbb{Q}} + \lambda\int_0^{t\wedge T}\sigma_r D[T-s]ds \tag{3.19a}$$

$$V_t^{\mathbb{Q}_B^T} = V_t^{\mathbb{Q}} + \int_0^{t\wedge T}\sigma_r D[T-s]ds \tag{3.19b}$$

are Brownian motions with correlation χ under $\mathbb{Q}_B^T$.

While the dynamics of β are consistent across the measures $\mathbb{P}$, $\mathbb{Q}$, $\mathbb{Q}^S$ and $\mathbb{Q}_B^T$, those of $B^{\mathcal{V}}$ and S are not:

$$d\beta[t] = \beta[t]r[t]dt \tag{3.20a}$$

$$dS[t] = S[t]\left(\left(r[t] + \sigma_S^2\right)dt + \sigma_S dW_t^{\mathbb{Q}^S} - \delta dt\right) \tag{3.20b}$$

$$dS[t] = S[t]\left(\left(r[t] - \chi\sigma_S D[T-t]\sigma_r \mathbb{I}_{\{t\leq T\}}\right)dt + \sigma_S dW_t^{\mathbb{Q}_B^T} - \delta dt\right) \tag{3.20c}$$

$$dB^{\mathcal{V}}[t,T,r] = B^{\mathcal{V}}[t,T,r]\left(\left(r[t] - D[T-t]\sigma_S\chi\sigma_r\right)dt - D[T-t]\sigma_r dV_t^{\mathbb{Q}^S}\right) \tag{3.20d}$$

$$dB^{\mathcal{V}}[t,T,r] = B^{\mathcal{V}}[t,T,r]\left(\left(r[t] + D^2[T-t]\sigma_r^2\right)dt - D[T-t]\sigma_r dV_t^{\mathbb{Q}_B^T}\right) \tag{3.20e}$$

We can then use Itô's Lemma to determine the dynamics of the quotients $\frac{\beta}{S}$, $\frac{B}{S}$ and $\frac{S}{B}$:

$$d\left(\frac{\beta[t]}{S[t]}\right) = \frac{\beta[t]}{S[t]}\left(\delta dt - \sigma_S dW_t^{\mathbb{Q}^S}\right) \tag{3.21a}$$

$$d\left(\frac{B^{\mathcal{V}}[t,T,r]}{S[t]}\right) = \frac{B^{\mathcal{V}}[t,T,r]}{S[t]}\left(\delta dt - D[T-t]\sigma_r dV_t^{\mathbb{Q}^S} - \sigma_S dW_t^{\mathbb{Q}^S}\right) \tag{3.21b}$$

$$d\left(\frac{S[t]}{B^{\mathcal{V}}[t,T,r]}\right) = \frac{S[t]}{B^{\mathcal{V}}[t,T,r]}\left(-\delta dt + \sigma_S dW_t^{\mathbb{Q}_B^T} + \sigma_r D[T-t]dV_t^{\mathbb{Q}_B^T}\right)\mathbb{I}_{\{t<T\}} \tag{3.21c}$$

Returning to simplification of (3.16):

$$\begin{aligned}
&\beta[t]\cdot\mathbb{E}^{\mathbb{Q}}\left[\frac{S[T]}{\beta[T]}\cdot\mathbb{I}_{\{S[T]>K\}}|\mathcal{F}_t\right]\\
&=\beta[t]\cdot\mathbb{E}^{\mathbb{Q}}\left[\frac{S[T]}{\beta[T]}\cdot\frac{\beta[\mathcal{H}]}{\beta[0]}\cdot\frac{S[0]}{S[\mathcal{H}]}\cdot e^{-\delta\mathcal{H}}\cdot\frac{d\mathbb{Q}^S}{d\mathbb{Q}}\cdot\mathbb{I}_{\{S[T]>K\}}|\mathcal{F}_t\right]\\
&=\beta[t]\cdot\frac{S[0]}{\beta[0]}\cdot\mathbb{E}^{\mathbb{Q}^S}\left[\frac{S[T]}{\beta[T]}\cdot\mathbb{E}^{\mathbb{Q}^S}\left[\frac{\beta[\mathcal{H}]}{S[\mathcal{H}]}|\mathcal{F}_T\right]\cdot\mathbb{I}_{\{S[T]>K\}}|\mathcal{F}_t\right]e^{-\delta\mathcal{H}}\times\mathbb{E}^{\mathbb{Q}}\left[\frac{d\mathbb{Q}^S}{d\mathbb{Q}}|\mathcal{F}_t\right] \qquad (3.22a)\\
&=\beta[t]\cdot\mathbb{E}^{\mathbb{Q}^S}\left[\frac{S[T]}{\beta[T]}\cdot\frac{\beta[T]}{S[T]}\cdot e^{\delta(\mathcal{H}-T)}\cdot\mathbb{I}_{\{S[T]>K\}}|\mathcal{F}_t\right]\times e^{-\delta\mathcal{H}}e^{\delta t}\cdot\frac{S[t]}{B[t]}\\
&=S[t]\cdot e^{-\delta(T-t)}\cdot\mathbb{Q}^S[S[T]>K|\mathcal{F}_t]
\end{aligned}$$

The second step requires application of both Bayes' Law and the Tower Property of Conditional Expectation; the third relies on the martingale property of $e^{-\delta t}\frac{\beta[t]}{S[t]}$ under $\mathbb{Q}^S$, which follows from 3.21a, and of $e^{\delta t}\frac{S[t]}{\beta[t]}$ under $\mathbb{Q}$, which follows from 3.7c, as well as cancellation of $\frac{\beta[0]}{S[0]}$. Similar manipulation yields

$$\beta[t]\cdot\mathbb{E}^{\mathbb{Q}}\left[\frac{K}{\beta[T]}\cdot\mathbb{I}_{\{S[T]>K\}}|\mathcal{F}_t\right] = B^{\mathcal{V}}[t,T,r[t]]\cdot K\cdot\mathbb{Q}_B^T[S[T]>K|\mathcal{F}_t] \tag{3.22b}$$

Setting

$$\gamma[t,T] = \sqrt{(\sigma_r D[T-t])^2 + 2\sigma_r D[T-t]\sigma_S\cdot\chi + \sigma_S^2} \tag{3.23a}$$

$$\begin{aligned}
\Gamma[t,T] &= \int_t^T \gamma^2[u,T]du \qquad (3.23b)\\
&= \frac{\sigma_r^2}{\alpha^2}\left((T-t) - 2D[T-t] + \tfrac{1}{2}D[2(T-t)]\right)\\
&\quad + \frac{2\sigma_r\sigma_S\chi}{\alpha}\left((T-t) - D[T-t]\right) + \sigma_S^2(T-t)
\end{aligned}$$

then by Lèvy's characterisation of Brownian motion,

$$Z_t^{\mathbb{Q}^S} = \int_0^t \frac{\sigma_S}{\gamma[u,T]} dW_u^{\mathbb{Q}^S} + \int_0^t \frac{\sigma_r D[T-u]}{\gamma[u,T]} dV_u^{\mathbb{Q}^S} \tag{3.24a}$$

and

$$Z_t^{\mathbb{Q}_B^T} = \int_0^t \frac{\sigma_S}{\gamma[u,T]} dW_u^{\mathbb{Q}_B^T} + \int_0^t \frac{\sigma_r D[T-u]}{\gamma[u,T]} dV_u^{\mathbb{Q}_B^T} \tag{3.24b}$$

are $\mathbb{Q}^S$ and $\mathbb{Q}_B^T$ Brownian motions over $[0.T]$ respectively, and (3.21b) becomes

$$d\left(\frac{B^{\mathcal{V}}[t.T,t[t]]}{S[t]}\right) = \frac{B^{\mathcal{V}}[t,T.r[t]]}{S[t]}\left(\delta dt - \gamma[t,T] dZ_t^{\mathbb{Q}^S}\right)$$

This S.D.E. is solved by

$$\lim_{\xi \uparrow T} \ln\left[\frac{B^{\mathcal{V}}[\xi,T.r[\xi]]}{S[T]}\right] = \ln\left[\frac{B^{\mathcal{V}}[t,T,r[t]]}{S[t]}\right] + \delta(T-t) - \tfrac{1}{2}\Gamma[t,T] - \int_t^T \gamma[u,T] dZ_u^{\mathbb{Q}^S}$$

(Limits are necessary as the discount bond price $B^{\mathcal{V}}$, being a RCLL process, takes a value of 0 at T, but has a left-hand limit of 1 at T.)

And so under the measure $\mathbb{Q}^S$, conditional on $\mathcal{F}_t$, the limit

$$\ln\left[\lim_{\xi \uparrow T} \frac{B^{\mathcal{V}}[\xi,T,r[\xi]]}{S[t]}\right]$$

has a Gaussian distribution with mean

$$\left(\frac{B^{\mathcal{V}}[t,T,r[t]]}{S[t]} + \delta(T-t) - \tfrac{1}{2}\Gamma[t,T]\right)$$

and variance $\Gamma[t,T]$.

Using

$$\lim_{t \uparrow T} B^{\mathcal{V}}[t.T.r[t]]$$

and invoking the standard limit theorems of integration theory, we get

$$\begin{aligned}\mathbb{Q}^S[S[T] > K|\mathcal{F}_t] &= \mathbb{Q}^S\left[\tfrac{1}{S[T]} < \tfrac{1}{K}|\mathcal{F}_t\right] = \mathbb{Q}^S\left[\lim_{\xi \uparrow T} \tfrac{B^{\mathcal{V}}[\xi,T,r[\xi]]}{S[T]} < \tfrac{1}{K}|\mathcal{F}_t\right] \\ &= \Phi\left[\frac{\ln S[T] - \ln B^{\mathcal{V}}[t,T,r[t]] - \ln K - \delta(T-t) + \frac{1}{2}\Gamma[t,T]}{\sqrt{\Gamma[t,T]}}\right]\end{aligned} \tag{3.25a}$$

where Φ still represents the Gaussian cumulative density function. The same techniques simplify (3.22b) to

$$\mathbb{Q}_B^T[S[T] > K|\mathcal{F}_t] = \Phi\left[\frac{\ln S[t] - \ln B^{\mathcal{V}}[t,T.r[t]] - \ln K - \delta(T-t) - \frac{1}{2}\Gamma[t,T]}{\sqrt{\Gamma[t.T]}}\right] \tag{3.25b}$$

with Γ as defined in (3.23b).

Putting it all together simplifies (3.15) into a Markovian formulation dependent only on time, the stock price and the short rate. From here on we will replace the random variable X_c by its Markovian fomulation $c^{\mathcal{V}}$, with

$$X_c[t,\omega] = c^{\mathcal{V}}[t, S[t], r[t]] = S[t] \cdot e^{-\delta(T-t)} \cdot \Phi[b_1] - K \cdot B^{\mathcal{V}}[t, T, r[t]] \cdot \Phi[b_2] \tag{3.26}$$

$$\text{where } b_1 = \frac{\ln S[t] - \ln B^{\mathcal{V}}[t,T,r[t]] - \ln K - \delta(T-t) + \frac{1}{2}\Gamma[t,T]}{\sqrt{\Gamma[t,T]}}$$

$$\text{and } b_2 = b_1 - \sqrt{\Gamma[t,T]}$$

This formula is a specific version of the option pricing result (40) in Merton (1973). Geman, El Karoui and Rochet (1995) show that Black-Scholes-type formulae hold if the volatility of the forward price $\frac{S[t]}{B[t,T]}$ is deterministic. Our result is similar to Rabinovitch (1989) eq. (8) (differing only between our volatility term 3.23b and his term (7); ours is correct)

The European equity call price in (3.26) is dependent on the short rate r only through its influence on the discount bond price $B^{\mathcal{V}}[t,T,r[t]]$. Given the price of this discount bond, our formula is identical to eq. (3.10) in Ritchken and Sankarasubrahmaniam (1995) derived in the Hull-White (1990B) no-arbitrage model of interest rates.

Remark 3.1.10 *All of our comparisons will be made controlling for the spot rate R (and implicitly the bond price $B[t,T]$). As our formula agrees with that in Ritchken and Sankarasubrahmanian (1995), our analysis for European equity options applies equally to Hull-White (1990B) term structure dynamics.*

The claim c can be perfectly replicated with a self-financing portfolio containing $H^{\mathcal{V}}_{c;S} = e^{\delta(T-t)}\Phi[b_1]$ units of the stock $S[t]$ and $H^{\mathcal{V}}_{c;B[t]} = -K\Phi[b_2]$ units of the discount bond $B^{\mathcal{V}}[t,T,r]$. It is interesting to note that this portfolio has no holdings of cash. Intuitively, as any cash transfers are fixed in units at time T, the ideal hedging instrument has a fixed cash value at time T - i.e. the discount bond.

Should this bond not trade actively, such discount bond holdings can be synthesized using the risky asset S, the primary contingent claim X_0 and the bank account $\mathcal{B}[t]$. These results extend to most diffusion models of interest rates.

We now turn our attention to European equity put options, which represent the right to sell the risky asset S at expiry T for the fixed strike price K.

Definition 3.1.11 *A* **European equity put option** *$X_p[t,\omega]$ with expiry $T \in (0,\mathcal{H}]$ is the contingent claim created by the payoff set with the sole element*

$$x_p[t,\omega] = [K - S[T]]^+ \cdot \mathbb{I}_{\{t \geq T\}}$$

Using either put-call parity, or a full analysis along the lines used to support our call formulae, it follows that under the OBS assumptions the European equity put option $X^{\mathcal{O}}_p$ takes the Markovian form

$$p^{\mathcal{O}}[t,S] = K \cdot e^{-R(T-t)} \cdot \Phi[-a_2] - S[t] \cdot e^{-\delta(T-t)} \cdot \Phi[-a_1] \tag{3.27}$$

where a_1 and a_2 are as defined for equation (3.14a).

The European equity put option is replicated by a portfolio holding $H^{\mathcal{O}}_{p;S}[t,S] = -e^{-\delta(T-t)}\Phi[-a_1]$ units of the risky asset S and $H^{\mathcal{O}}_{p;B[T]}[t,S] = K\Phi[-a_2]$ units of the discount bond $B^{\mathcal{O}}[t,T]$.

Likewise, under the VBS model the price European equity put option X_p takes the Markovian form

$$\begin{aligned} X_p[t,\omega] &= p^{\mathcal{V}}\left[t, S[t,\omega], r[t,\omega]\right] \\ &= KB^{\mathcal{V}}\left[t,T,r[t,\omega]\right]\Phi[-b_2] - S[t,\omega]e^{-\delta(T-t)}\Phi[-b_1] \end{aligned} \tag{3.28}$$

where b_1 and b_2 are those defined for (3.26).

The VBS replicating portfolio for p contains $H^{\mathcal{V}}_{p;S} = -e^{\ \delta(T-t)}\Phi[-b_1]$ units of the risky asset S and $H^{\mathcal{V}}_{p;B[T]}[t,S] = K\cdot\Phi[-b_2]$ units of the discount bond maturing at option expiry.

Having established closed-form solutions both prices and hedges of $c^{\mathcal{O}}$ and $c^{\mathcal{V}}$, we are in a position make explicit comparisons.

3.2 Model Comparison

3.2.1 Prices

The OBS price $C^{\mathcal{O}}$ can be nested within the VBS price $C^{\mathcal{V}}$ by setting $\sigma_r = 0$ and $r = \theta = R$. Thus our model comparison boils down to examining the effect on the option price of an change in σ_r.

The derivation leading to (3.26) highlights that it is not the volatility σ_S of the risky asset which influences option prices, but rather the volatility of the quotient $\frac{S[t]}{B^{\mathcal{V}}[t,T,r]}$ (as well as the volatility of the inverse of this quotient, which is the same as the volatility of the quotient itself). This volatility is unaffected by the changes of measure we use.

Our parameter $\Gamma[t,T]$ represents the total variance of the natural logarithm of this quotient at option expiry, and is an aggregate measure of the volatility of $\frac{S}{B}$ over the life of the option from pricing time t to expiry T.

It is straightforward to show that while the correlation χ is less than a time-dependent critical value $\chi_c[t,T]$, defined by

$$\chi_c[t,T] = \frac{\sigma_r(2D[T-t] - (T-t) - \frac{1}{2}D[2(T-t)])}{2\alpha\sigma_S(T-t-D[T-t])} \tag{3.29}$$

that the VBS model will exhibit lower volatility of $\frac{S}{B}$, and vice-versa.

Intuitively, with more volatility in the system the option to exercise (or not to exercise) a call contract carries more value. Some quick calculus confirms that for $\chi < \chi_c[t,T]$ we have $c^{\mathcal{V}}[t,S[t],r[t]] < c^{\mathcal{O}}[t,S[t]]$ (with $c^{\mathcal{O}}$ evaluated at $R = R[t,T,r[t]]$), and vice-versa. This is consistent with the results in Rabinovitch (1989), after correction for his previous error (see page 28).

The same result holds true for European equity put options, i.e. that if and only if $\chi < \chi_c[t,T]$ then $p^{\mathcal{V}}\left[t,S[t],r[t]\right] < p^{\mathcal{O}}\left[t,S[t]\right]$ (with $p^{\mathcal{O}}$ evaluated at $R = R\left[t,T,r[t]\right]$).

3.2.2 Hedges

Comparison of hedge parameters under different models requires more work, but rewards with more understanding. For ease of development, this analysis starts with the fixed income hedge $H^{\mathcal{V}}_{c;B[t]}[t,S,r] = K\Phi[b_2]$.

As $H^{\mathcal{O}}_{c;B[T]}[t,S] = K\Phi[a_2]$ and $H^{\mathcal{V}}_{c;B[T]}[t,S,r] = K\Phi[b_2]$, it follows from the monotonicity of $\Phi[\cdot]$ that $H^{\mathcal{O}}_{c;B[T]}[t,S]\Big|_{R[t,T,r]} > H^{\mathcal{V}}_{c;B[T]}[t,S,r] \Leftrightarrow a_2 > b_2$:

$$\begin{aligned} & a_2 > b_2 \\ \iff & \frac{\ln S[t] - \ln K - \ln B[t,T,r] - (\delta + \frac{1}{2}\sigma_S)(T-t)}{\sigma_S\sqrt{(T-t)}} > \frac{\ln S[t] - \ln K - \ln B[t,T,r] - \delta(T-t) - \Gamma[t,T]}{\sqrt{\Gamma[t,T]}} \\ \iff & \left(\ln S[t] - \ln K - \ln B[t,T] - \delta(T-t) + \tfrac{1}{2}\sigma_S\sqrt{(T-t)\Gamma[t,T]}\right) \\ & \quad \times \left(\sqrt{\Gamma[t,T]} - \sigma_S\sqrt{T-t}\right) > 0 \end{aligned} \tag{3.30}$$

Two factors work jointly in determining the relative size of OBS and VBS hedges. We consider these separately.

The first factor concerns uncertainty over the life of the option. The total variance of the fraction $\frac{S}{B}$ is larger than the total volatility of the numerator S only if the additional variance introduced by the denominator B is not counter-balanced by negative covariance between S and B. So long as S and B are sufficiently negatively correlated (i.e. $V^{\mathbb{Q}^T_B}$ and $V^{\mathbb{Q}^T_B}$ have sufficiently large correlation), we have $\Gamma[t,T] > \sigma_S^2(T-t)$. This threshold correlation is the critical correlation defined in (3.29).

We are also aware that, under the forward measure $\mathbb{Q}^T_B$ the distribution of $\ln S[T]$ is Gaussian, with mean $\ln S[t] - \ln B[t,T] - \delta(T-t) - \frac{1}{2}\Gamma[t,T]$ and variance $\Gamma[t,T]$.

Now any increase in the parameter $\Gamma[t,T]$ will simultaneously increase the variance and decrease the mean of $\ln S[T]$ under the measure $\mathbb{Q}^T_B$. Our immediate concern is the effect of Γ increases on the $\mathbb{Q}^T_B$ probability of exercise, i.e. $\mathbb{Q}^T_B[S[T] > K|\mathcal{F}_t]$:

While K is below the $\mathbb{Q}^T_B$ mean of $S[T]$, both the effects of increasing Γ will decrease the $\mathbb{Q}^T_B$-probability that c ends in-the-money. While K is above the $\mathbb{Q}^T_B$ mean of $S[T]$, the effects on the $\mathbb{Q}^T_B$-exercise probability of Γ increases operate in different directions. While

$$K > \frac{S[t]}{B[t,T]} \cdot \exp\left[\tfrac{1}{2}\Gamma[t,T] - \delta(T-t)\right] \tag{3.31a}$$

the mean effect dominates, and the $\mathbb{Q}^T_B$ probability of exercise rises. Likewise when (3.31a) fails to hold then the variance effect dominates, and the $\mathbb{Q}^T_B$ probability of exercise falls. We can express the inequality (3.31a) in a more usable form as

$$S[t] < K \cdot B[t,T]\exp\left[\delta(T-t) - \tfrac{1}{2}\Gamma[t,T]\right] \tag{3.31b}$$

Now, the OBS model can be nested within the VBS model with $\sigma_r = 0$. Comparison of the OBS and VBS hedges simplifies to measuring the effect of moving σ_r from 0 to its calibration value (while keeping all other variables *including the discount bond price* constant).

The second factor in the final line of inequality (3.30) concerns the effect on total variance of the forward price until option expiry of introducing a stochastic interest rate. Specifically, it evaluates the direction of such effect.

Table 3.1: Comparison of hedge portfolio bond short sales for European equity call options.

	$\chi < \chi_c$ (i.e. stochastic interest rate decreases S/B volatility)	$\chi > \chi_c$ (i.e. stochastic interest rate increases S/B volatility)
$S[t] < S_2^*[t,T,B[t,T]]$ (i.e positive sensitivity to S/B vol changes)	$a_2 > b_2$ (OBS hedge short sales exceed VBS hedge short sales)	$a_2 < b_2$ (VBS hedge short sales exceed OBS hedge short sales)
$S[t] > S_2^*[t,T,B[t,T]]$ (i.e. negative sensitivity to S/B vol changes)	$a_2 < b_2$ (VBS hedge short sales exceed OBS hedge short sales)	$a_2 > b_2$ (OBS hedge short sales exceed VBS hedge short sales)

See (3.31c) for a definition of S_2^*.

The first factor of (3.30) evaluates the sensitivity of the Gaussian limit of integration to the total[1] change in forward price total volatility. Only while the option is sufficiently out-of-the-money, i.e. while $S[t] < S_2^*[t,T,B[t,T]]$ where

$$S_2^*[t,T,B[t,T]] = K \cdot B[t,T] \exp\left[\delta(T-t) - \tfrac{1}{2}\sigma_S\sqrt{(T-t)\Gamma[t,T]}\right] \tag{3.31c}$$

will the change in total volatility induce a change of the same direction in the $\mathbb{Q}_B^T$ probability of exercise.

Put simply, we are concerned jointly with the direction of change in forward price total volatility, and the way this will increase the relevant exercise probability. These conclusions are summarised in Table 3.1.

Examination of the hedge portfolio purchases of the risky asset follows a similar route. Again, the hedge parameter is related to an exercise probability. We are concerned about how the introduction of a stochastic short rate, *ceteris paribus*, changes the forward price volatility; and whether the exercise probability $\mathbb{Q}^S[S[T] > K]$ moves in the same direction as the forward price volatility changes.

Our conclusions, summarised in Table 3.2, are remarkably similar to those for the short sales of the discount bond. Indeed, all that changes is our definition of 'sufficiently out-of-the-money'. The cutoff 'moneyness' value for the stock hedge is

$$S_1^*[t,T,B[t,T]] = K \cdot B[t,T] \exp\left[\delta(T-t) + \tfrac{1}{2}\sigma_S\sqrt{(T-t)\Gamma[t,T]}\right] \tag{3.31d}$$

and the change from (3.31d) to (3.31c) is a direct consequence of moving from the measure $\mathbb{Q}_B^T$ to the measure $\mathbb{Q}^S$.

[1] This explains the difference between (3.31b), which concerns marginal increases in σ_r, and (3.31c), concerning the total change in σ_r.

Table 3.2: Comparison of hedge portfolio stock purchases for European equity call options.

	$\chi < \chi_c$ (i.e. stochastic interest rate decreases S/B volatility)	$\chi > \chi_c$ (i.e. stochastic interest rate increases S/B volatility)
$S[t] < S_1^*[t,T,B[t,T]]$ (i.e positive sensitivity to S/B vol changes)	$a_1 > b_1$ (OBS hedge purchases exceed VBS hedge purchases)	$a_1 < b_1$ (VBS hedge purchases exceed OBS hedge purchases)
$S[t] > S_1^*[t,T,B[t,T]]$ (i.e. negative sensitivity to S/B vol changes)	$a_1 < b_1$ (VBS hedge purchases exceed OBS hedge purchases)	$a_1 > b_1$ (OBS hedge purchases exceed VBS hedge purchases)

See (3.31d) for a definition of S_1^*.

Hedge parameter comparisons for European equity put options depend likewise on whether interest rate stochasticity increases forward price volatility, and how forward price volatility increases affect exercise probabilities. Again, the second effect is positive only when the option is sufficiently out-of-the-money. As put options confer the right to sell, not buy, the definition of 'out-of-the-moneyness' inverts, referring to stock prices exceeding a critical value.

Comparison of the OBS and VBS hedge portfolio holdings (both holdings in the discount bond and short sales of the underlying asset) are presented in Tables 3.3 and 3.4.

Table 3.3: Comparison of hedge portfolio bond purchases for European equity put options.

	$\chi < \chi_c$ (i.e. stochastic interest rate decreases S/B volatility)	$\chi > \chi_c$ (i.e. stochastic interest rate increases S/B volatility)
$S[t] < S_2^*[t,T,B[t,T]]$ (i.e negative sensitivity to S/B vol changes)	$a_2 > b_2$ (VBS hedge purchases exceed OBS hedge purchases)	$a_2 < b_2$ (OBS hedge purchases exceed VBS hedge purchases)
$S[t] > S_2^*[t,T,B[t,T]]$ (i.e. positive sensitivity to S/B vol changes)	$a_2 < b_2$ (OBS hedge purchases exceed VBS hedge purchases)	$a_2 > b_2$ (VBS hedge purchases exceed OBS hedge purchases)

See (3.31c) for a definition of S_2^*.

We conclude this section by addressing an apparent contradiction surrounding the sensi-

tivity of option prices to forward price volatility.

In comparing option prices, we noted that increasing forward price volatility (in this model) always increases European equity option prices. But when comparing hedge portfolios we noted that an increase in forward price volatility has an indeterminate effect on the portfolio constituents.

Hedge parameters are determined by some probability of exercise. Option prices, meanwhile, are an expected discounted payoff. While forward price volatility increases indeed have an indeterminate effect on exercise probabilities, they always increase the expected payoff conditional on exercise. The latter effect dominates, resolving the paradox.

Table 3.4: Comparison of hedge portfolio stock short sales for European equity put options.

	$\chi < \chi_c$ (i.e. stochastic interest rate decreases S/B volatility)	$\chi > \chi_c$ (i.e. stochastic interest rate increases S/B volatility)
$S[t] < S_1^*[t,T,B[t,T]]$ (i.e negative sensitivity to S/B vol changes)	$a_1 > b_1$ (VBS hedge short sales exceed OBS hedge short sales)	$a_1 < b_1$ (OBS hedge short sales exceed VBS hedge short sales)
$S[t] > S_1^*[t,T,B[t,T]]$ (i.e. positive sensitivity to S/B vol changes)	$a_1 > b_1$ (OBS hedge short sales exceed VBS hedge short sales)	$a_1 < b_1$ (VBS hedge short sales exceed OBS hedge short sales)

See (3.31d) for a definition of S_1^*.

Chapter 4

American Options

American contingent claims prove substantially more difficult to price than their European counterparts. This chapter addresses the pricing of American equity options in three stages. First we present some theory regarding optimal stopping. Next we price general American contingent claims, and finally we apply this to the claims of interest to us: equity options.

Remember we have a real world measure $\mathbb{P}$, and an economy with a bank account β and stock S (and, in the VBS model, a primary contingent claim X_0) all of which trade continuously and infinitesimally. From these we create a pricing measure $\mathbb{Q}$ (see (3.2a) and (3.5)) under which $S[t]$ (and $X_0[t]$) have instantaneous drift (before cash distributions) of $r[t]$.

4.1 Some Optimal Stopping Theory

Here we present those results from optimal stopping theory which we will need later in this chapter. Proofs of the statements in this section can be found in appendix D of Karatzas and Shreve (1998).

Let τ be any stopping time, and set $\mathcal{T}_{t,T}$ as the set of all stopping times τ with $\tau[\omega] \in [t,T]$ $\mathbb{P}$ – $a.s.$

For any interval $[0,T] \subset [0,\mathcal{H}]$ and any progressively measurable process $j[t,\omega]$ let $J[t,\omega]$ be the smallest $(\mathbb{Q},\mathcal{F}_t)$-supermartingale which dominates j over $[0,T]$. J is called the Snell Envelope of j, and $J[t,\omega]$ can be expressed as the random variable

$$J[t,\omega] = \operatorname*{ess\,sup}_{\tau \in \mathcal{T}_{t,T}} \mathbb{E}^{\mathbb{Q}}\left[j[\tau,\omega]\middle|\mathcal{F}_t\right] \tag{4.1a}$$

The stopping time $\eta[t,\omega] = \inf\left\{s \in [t,T] : J[s,\omega] = j[s,\omega]\right\}$ is known to be optimal for J in that no other stopping time $\tau \in \mathcal{T}_{t,T}$ will result in a larger value for $J[t,\omega]$. Subject to technical regularity conditions, we can invoke a Doob-Meyer decomposition on J such that

$$J[t,\omega] = J[0,\omega] + M[t,\omega] - N[t,\omega] \tag{4.1b}$$

where N is a continuous, non-decreasing, progressively measurable process with $N[0] = 0$, and M is a square-integrable $(\mathbb{Q},\mathcal{F}_t)$-martingale also starting at 0. By the Martingale Representation Theorem 3.1.2, there are predictable processes ϕ_M^V and ϕ_M^W such that

$$M[t,\omega] = \int_0^t \phi_M^V[s,\omega]dV_s^{\mathbb{Q}} + \int_0^t \phi_M^W[s,\omega]dW_s^{\mathbb{Q}} \tag{4.1c}$$

For $s \geq t$ the stopped process $J\left[(s \wedge \eta[t]),\omega\right]$ is a $(\mathbb{Q},\mathcal{F}_s)$-martingale, i.e. $N\left[\eta[t],\omega\right] = N[t,\omega]$.

4.2 American Contingent Claim Pricing

In this section we take some time pricing general American contingent claims. In the next section we will apply these results to American equity options.

Definition 4.2.1 *An* **American Contingent Claim** *(ACC) X_A with expiry T is the contingent claim created by the payoff set*

$$\boldsymbol{x}_A = \left\{ x[t,\omega] = A[\tau[\omega],\omega] \cdot \mathbb{I}_{\{t \geq \tau[\omega]\}} \right\}_{\tau \in \mathcal{T}_{0,T}} \tag{4.2}$$

where $A : [0,T] \times \Omega \mapsto \mathbb{R}$ is any function progressively measurable w.r.t. $\mathbb{F}$.

Notice that, whereas the European Contingent Claim has only one possible payoff stream (see definition 3.0.1), the payoff set supporting an ACC may contain uncountably many payoff streams.

Remark 4.2.2 *The seminal texts of Bensoussan (1984), Karatzas (1988) and Myneni (1992) define ACCs to include cashflows to the holder prior to exercise at τ. This extension can easily be incorporated into the format here. These cashflows have not been included here as they are not needed to address the aims of this dissertation.*

Theorem 4.2.3 *For all $t \in [0,\mathcal{H}]$ the OBS price of an (as yet unexercised) American Contingent Claim is $\mathbb{P}$ almost surely*

$$X_A[t,\omega] = \operatorname*{ess\,sup}_{\tau \in \mathcal{T}_{t,T}} \mathbb{E}^{\mathbb{Q}} \left[e^{-R(\tau - t)} A[\tau,\omega] \middle| \mathcal{F}_t \right] \cdot \mathbb{I}_{\{t<T\}} \tag{4.3}$$

Proof. Proof of Theorem 4.2.3 is simpler than, but otherwise identical to, the VBS price proof which follows next.

Theorem 4.2.4 *For all $t \in [0,\mathcal{H}]$ the VBS price of an unexercised American Contingent Claim is $\mathbb{P}$ almost surely*

$$X_A[t,\omega] = \operatorname*{ess\,sup}_{\tau \in \mathcal{T}_{t,T}} \mathbb{E}^{\mathbb{Q}} \left[\frac{\beta[t,\omega]}{\beta[\tau,\omega]} A[\tau,\omega] \middle| \mathcal{F}_t \right] \cdot \mathbb{I}_{\{t<T\}} \tag{4.4}$$

Proof. Set $\tilde{X}_A[t,\omega]$ to be our proposed price, i.e.

$$\begin{aligned} \tilde{X}_A[t,\omega] =& \operatorname*{ess\,sup}_{\tau \in \mathcal{T}_{t,T}} \mathbb{E}^{\mathbb{Q}} \left[\frac{\beta[t,\omega]}{\beta[\tau,\omega]} A[\tau,\omega] \middle| \mathcal{F}_t \right] \cdot \mathbb{I}_{\{t<T\}} \\ =& \beta[t,\omega] \operatorname*{ess\,sup}_{\tau \in \mathcal{T}_{t,T}} \mathbb{E}^{\mathbb{Q}} \left[\frac{A[\tau,\omega]}{\beta[t,\omega]} \middle| \mathcal{F}_t \right] \cdot \mathbb{I}_{\{t<T\}} \end{aligned} \tag{4.5}$$

Let $\eta_t^A = \eta_A[t] = \inf\{s \in [t,T] : \tilde{X}_A[t,\omega] = A[t,\omega]\}$ be the optimal stopping time for $\tilde{X}_A$, and define $\phi_A^W[t,\omega]$, $\phi_A^V[t,\omega]$ and $N_A[t,\omega]$ by the decomposition of $\tilde{X}_A/\beta$ over $[0,T)$ by 4.1b, i.e.

$$\begin{aligned} \frac{\tilde{X}_A[t,\omega]}{\beta[t,\omega]} =& \operatorname*{ess\,sup}_{\tau \in \mathcal{T}_{t,T}} \mathbb{E}^{\mathbb{Q}} \left[\frac{A[\tau,\omega]}{\beta[\tau,\omega]} \middle| \mathcal{F}_t \right] \\ =& \tilde{X}_A[0,\omega] + \int_0^t \phi_A^W[s,\omega] dW_s^{\mathbb{Q}} + \int_0^t \phi_A^V[s,\omega] dV_s^{\mathbb{Q}} - N_A[t,\omega] \end{aligned} \tag{4.6a}$$

so that

$$d\tilde{X}_A[t,\omega] = r[t]\tilde{X}_A[t,\omega]dt + \beta[t]\phi_A^W[t,\omega]dW_t^{\mathbb{Q}} + \beta[t]\phi_A^V[t,\omega]dV_t^{\mathbb{Q}} - \beta[t]dN_A[t,\omega] \tag{4.6b}$$

Now suppose that there is a $t < T$ for which $X_A[t,\omega] < \tilde{X}_A[t,\omega]$. Consider the portfolio which purchases X_A at such a t, exercises at η_t^A (i.e. which chooses the payoff stream $A[\eta_t^A,\omega]\cdot\mathbb{I}_{\{t\geq\eta_t^A\}}$ from the payoff set $\boldsymbol{x}_A$) and which hedges $\tilde{X}_A$ in the interim using the securities β, S and X_0. This portfolio is

$$\begin{aligned}
\Pi_A[s,\omega] =& \mathbb{I}_{\{t\leq s\leq\eta_t^A\}} \\
\Pi_0[s,\omega] =& \frac{-\beta[s]\phi_A^V[s,\omega]}{\sigma_0^V[s,\omega]X_0[s,\omega]}\mathbb{I}_{\{t\leq s\leq\eta_t^A\}} \\
\Pi_S[s,\omega] =& \left(\frac{\beta[s]\phi_A^V[s,\omega]\sigma_0^W[s,\omega]}{\sigma_0^V[s,\omega]\sigma_S\cdot S[s,\omega]} - \frac{\beta[s]\phi_A^W[s,\omega]}{\sigma_S\cdot S[s,\omega]}\right)\cdot\mathbb{I}_{\{t\leq s\leq\eta_t^A\}} \\
\Pi_\beta[s,\omega] =& \left(-\tilde{X}_A[0,\omega] - \int_0^s \phi_A^W[u,\omega]dW_u^{\mathbb{Q}} - \int_0^s \phi_A^V[u,\omega]dV_u^{\mathbb{Q}} + N_A[s,\omega]\right. \\
&\left. + \frac{\phi_A^V[s,\omega]}{\sigma_0^V[s,\omega]} - \frac{\phi_A^V[s,\omega]\sigma_0^W[s,\omega]}{\sigma_0^V[s,\omega]\sigma_S} + \frac{\phi_A^W[s,\omega]}{\sigma_S}\right)\mathbb{I}_{\{t\leq s\leq\eta_t^A\}} \\
&+ (\tilde{X}_A[t,\omega] - X[t,\omega])\tfrac{1}{\beta[t]}\mathbb{I}_{\{s\geq t\}}
\end{aligned}$$

and has the total value at time s of

$$\big(X_A[s,\omega] - \tilde{X}_A[s,\omega]\big)\mathbb{I}_{\{t\leq s\leq\eta_t^A\}} + \big(\tilde{X}_A[t,\omega] - X_A[t,\omega]\big)\frac{\beta[s]}{\beta[t]}\mathbb{I}_{\{t\leq s\}}$$

This portfolio is trivially self-financing at t. For the portfolio to be self-financing over (t,η_t^A) we need

$$\begin{aligned}
dX_A[s,\omega] - d\tilde{X}_A[s,\omega] + \big(\tilde{X}_A[t,\omega] - X_A[t,\omega]\big)\frac{\beta[s]}{\beta[t]}r[s]ds& \\
= \Pi_A[s,\omega]dX_A[s,\omega] + \Pi_0[s,\omega]\big(dX_0[s,\omega] + dx_0[s,\omega]\big)& \\
+ \Pi_S[s,\omega]\big(dS[s,\omega] + \delta S[s,\omega]ds\big) + \Pi_\beta[s,\omega]d\beta[s]&
\end{aligned}$$

which follows because Π_0 exactly hedges the V risk in $\tilde{X}_A$, Π_S hedges the W risk in $\tilde{X}_A$ (and the residual W risk from holding Π_0 units of X_0) and the drift (before cash distributions) of X_0, S, β and $\tilde{X}_A$ over (t,η_t^A) under $\mathbb{Q}$ is all $r[s]$. Finally, self-financing at exercise time η_t^A follows because

$$\begin{aligned}
\frac{A[\eta_t^A,\omega]}{\beta[\eta_t^A]} =& \frac{\tilde{X}_A[\eta_t^A,\omega]}{\beta[\eta_t^A]} \\
=& \tilde{X}_A[0,\omega] + \int_0^{\eta_t^A}\phi_A^W[u,\omega]dW_u^{\mathbb{Q}} + \int_0^{\eta_t^A}\phi_A^V[t,\omega]dV_u^{\mathbb{Q}} - N_A[\eta_t^A,\omega] \\
=& \tilde{X}_A[0,\omega] + \int_0^{\eta_t^A}\phi_A^W[u,\omega]dW_u^{\mathbb{Q}} + \int_0^{\eta_t^A}\phi_A^V[u,\omega]dV_u^{\mathbb{Q}} - N_A[t,\omega]
\end{aligned}$$

as N is level on $[t,\eta_t^A]$.

This portfolio buys the ACC X_A when it is undervalued and then sells a portfolio valued at $\tilde{X}_A$ to cover the purchase cost. The short portfolio can be rebalanced to self-finance the value $\tilde{X}_A$ up to time η_t^A. At η_t^A, exercising X_A yields the payoff $A[\eta_t^A]$ - just sufficient to cover the costs of settling the short holdings totalling $\tilde{X}_A$. The excess $\tilde{X}_A[t] - X_A[t]$ is invested in the bank account and represents the arbitrage profit, in contradiction of Assumption 2.2.A6, unless $\mathbb{P}\left[\exists t \in [0,T] : X_A[t,\omega] < \tilde{X}_A[t,\omega]\right] = 0$.

Showing that $X_A \leq \tilde{X}_A$ is more intricate. It requires taking a short position in X_A, and hence not knowing which exercise strategy the ACC holder will use (i.e. which payoff stream the buyer will choose from the payoff set). Any arbitrage strategy must hold for all possible exercise strategies.

Suppose that there is a (t,ω) for which $X_A[t,\omega] > \tilde{X}_A[t,\omega]$ at which we sell the ACC and whereupon the buyer exercises according to some stopping time $\tau' \in \mathcal{T}_{t,T}$. As the option seller, we are not aware of which stopping strategy τ' (and hence which payoff stream) the holder chooses. At any time $s > t$ this certainty is only resolved if $\tau'[\omega] \leq s$.

Suppose that for some ω that there is a $t \in [0,T]$ for which $X_A(t,\omega) > \tilde{X}_A(t,\omega)$. At this t we sell X_A, and at some random stopping time $\tau' \in \mathcal{T}_{t,T}$ the holder of X_A exercises the claim. As the option seller, we are not aware of which stopping strategy τ' (and hence which payoff stream from x_A) the holder chooses.

Invest the proceeds from the sale of X_A in securities which replicate the value of $\tilde{X}_A$ (not X_A). This requires constructing the self-financing portfolio

$$
\begin{aligned}
\Pi_A[s,\omega] &= -\mathbb{I}_{\{t\leq s\leq \mathcal{H}\}} \\
\Pi_0[s,\omega] &= \frac{\beta[s]\phi_A^V[s,\omega]}{\sigma_0^V[s,\omega]X_0[s,\omega]}\mathbb{I}_{\{t\leq s<\tau'\}} \\
\Pi_S[s,\omega] &= \left(\frac{\beta[s]\phi_A^W[s,\omega]}{\sigma_S S[s,\omega]} - \frac{\beta[s]\phi_A^V[s,\omega]\sigma_0^W[s,\omega]}{\sigma_0^V[s,\omega]\sigma_S S[s,\omega]}\right)\cdot\mathbb{I}_{\{t\leq s<\tau'\}} \\
\Pi_\beta[s,\omega] &= \left(\tilde{X}_A[0,\omega] + \int_0^s \phi_A^W[u,\omega]dW_u^{\mathbb{Q}} + \int_0^s \phi_A^V[u,\omega]dV_u^{\mathbb{Q}} - N_A[s,\omega]\right. \\
&\quad \left. - \frac{\phi_A^V[s,\omega]}{\sigma_0^V[s,\omega]} + \frac{\phi_A^V[s,\omega]\sigma_0^W[s,\omega]}{\sigma_0^V[s,\omega]\sigma_s} - \frac{\phi_A^W[s,\omega]}{\sigma_s}\right)\mathbb{I}_{\{t\leq s<\tau'\}} \\
&\quad + \left(N_A[\tau'\wedge s] - N_A[t]\right)\cdot\mathbb{I}_{\{s\geq t\}} + \left(X_A[t] - \tilde{X}_A[t]\right)\frac{1}{\beta[t]}\cdot\mathbb{I}_{\{s\geq t\}} \\
&\quad + \left(\tilde{X}_A[\tau'] - A[\tau']\right)\frac{1}{\beta[\tau']}\cdot\mathbb{I}_{\{s\geq\tau'\}}
\end{aligned}
$$

Now as N_A is a non-decreasing process, and as

$$
\tilde{X}_A[\tau',\omega] = \beta[\tau']\operatorname*{ess\,sup}_{\tau\in\mathcal{T}_{\tau',T}}\mathbb{E}^{\mathbb{Q}}\left[\frac{A[\tau',\omega]}{\beta[\tau',\omega]}\middle|\mathcal{F}_t\right] \geq A[\tau',\omega]
$$

the hedging of $\tilde{X}_A$ always produces sufficient self-financed funds to make the payoff on the ACC, no matter which exercise strategy τ' is elected. This portfolio realises arbitrage in a similar manner to that on the previous page. Selling X_A yields funds which purchase a portfolio valued at $\tilde{X}_A$ and which, through rebalancing, maintains a value of *at least* $\tilde{X}_A$. When the holder of X_A exercises, selling this portfolio *at least* covers the payoff $A[\tau']$. Excess profits at the model horizon $\mathcal{H}$ may accrue to the seller of X_A through three mechanisms:

- Sub-optimally late exercise of X_A, valued at $(N_A[\tau'] - N_A[t])\beta[\mathcal{H}]$
- Sub-optimally early exercise of X_A, valued at $(\tilde{X}_A[\tau'] - A[\tau'])\frac{\beta[\mathcal{H}]}{\beta[\tau']}$, and
- Initial overpricing of X_A, valued at $(X_A[t] - \tilde{X}_A[t])\frac{\beta[\mathcal{H}]}{\beta[t]}$.

One or both of the first two profits may accrue unless $\tau' = \eta_t^A$ (remember $\tau' \in \mathcal{T}_{t,T}$). Only the last item is independent of exercise strategy, thus representing an arbitrage opportunity - again contradicting Assumption 2.2.A6. To ensure the absence of arbitrage opportunities we require $\mathbb{P}\big[\exists t \in [0,T] : X_A[t,\omega] > \tilde{X}_A[t,\omega]\big] = 0$.

□

Remark 4.2.5 *Strictly speaking our portfolio definition (Definition 2.2.6) requires knowledge of the relevant payoff stream. As the ACC seller does not know* a priori *which exercise strategy (and hence payoff stream) is selected. the 'portfolio' process used in the second half of the proof above does not strictly meet the requirements of Definition 2.2.6.*

In essence, this portfolio assumes the payoff stream created by the exercise strategy $\tau' = \eta_t^A$. If the buyer deviates from this strategy then the seller can respond timeously to this deviation, and realises further excess profits.

Correcting this error is not straightforward. In an alternative approach, Karatzas and Shreve (1998) and Amin and Jarrow (1992) merely show that the essential supremum can be replicated, from which arbitrage opportunities are intuitive. Karatzas's (1988) seminal paper prices ACCs in a investment-consumption framework: again the link to formal arbitrage (in the probabilistic spirit of Definition 2.2.7) is intuitive, but difficult to formalise.

Alternatively, an adaption of Myneni's (1992) definition of arbitrage would permit pricing of ACCs, but would require different arbitrage definitions for European and American contingent claims.

Analogous to ECCs, ACCs have zero value after exercise, so we omit $\mathbb{I}_{\{t<T\}}$ from the pricing equation (4.4), implicitly pricing before expiry claims which have not yet been exercised.

We return our focus to equity option contracts:

4.3 American Equity Option Pricing

4.3.1 American Equity Call Option Pricing

Definition 4.3.1 *An American equity call option $X_C[t,\omega]$ with strike price K and expiry T is an American Contingent Claim with the payoff set*

$$x_C = \Big\{x[t,\omega] = \big[S[\tau] - K\big]^+ \mathbb{I}_{\{t \geq \tau\}}\Big\}_{\tau \in \mathcal{T}_{0,T}}$$

An American equity call option represents the right, but not the the obligation, to purchase the asset S for the price K at any time before expiry T. Straightforward application of Theorem 4.2.3 yields the OBS price of X_C as

$$X_C[t,\omega] = \operatorname*{ess\,sup}_{\tau \in \mathcal{T}_{t,T}} \mathbb{E}^{\mathbb{Q}}\Big[e^{-R(\tau - t)}\big[S[\tau] - K\big]^+ \Big| \mathcal{F}_t\Big]$$

Theorem 4.3.2 *The OBS price X_C is a function of only $S[t]$ and t, i.e. there exists a function $C^{\mathcal{O}}[t,S] : [0,T] \times (0,\infty) \mapsto [0,\infty)$ such that*

$$X_C[t,\omega] = C^{\mathcal{O}}\big[t, S[t,\omega]\big] \tag{4.7}$$

Proof. Theorem 1 of Fakeev (1971) proves the existence of a function $f[Y]$ such that, for any Markovian process $\{Y_t\}_{t\in[0,\infty]}$, constant $R \geq 0$ and continuous function $h[Y]$,

$$\operatorname*{ess\,sup}_{\tau\in\mathcal{T}_{t,\infty}} \mathbb{E}^{\mathbb{Q}}\Big[e^{-R\tau}h\big[Y_\tau\big]\Big|\mathcal{F}_t\Big] = f\big[Y_t\big]$$

We are interested in the American call option price

$$X_C[t,\omega] = \operatorname*{ess\,sup}_{\tau\in\mathcal{T}_{t,T}} \mathbb{E}^{\mathbb{Q}}\left[e^{-R(\tau-t)}\big[S[\tau]-K\big]^+\Big|\mathcal{F}_t\right]$$

Define $Y_t = \big[S[t,\omega],t\big]$ as vector of interest. Under the measure $\mathbb{Q}$ the process S is an Itô diffusion - see the OBS solution for S in (2.2). Ito diffusions are strongly Markovian, as shown in Øksendal (1998) Chapter 7. The vector Y is thus Markovian under the measure $\mathbb{Q}$. Define the reward function

$$h\big[Y_t\big] = \big[S[t,\omega]-K\big]^+ \cdot \mathbb{I}_{\{t\leq T\}}$$

Clearly $h\big[Y_t\big]$ is discontinuous at $t=T$. Define the sequence of functions $\{h_n\big[Y_t\big]\}_{n\in\mathbb{N}}$ by

$$h_n\big[Y_t\big] = \begin{cases} \big[S[t,\omega]-K\big]^+ & t \leq T-\frac{1}{n} \\ \big[S[t,\omega]-K\big]^+ n(t-T) & T-\frac{1}{n} < t < 1 \\ 1 & t = T \\ 0 & t \geq 1+\frac{1}{n} \end{cases}$$

which converges point-wise to $h[Y]$ from below.

By Theorem D.12 of Karatzas and Shreve (1998) there exists a stopping time $\tau^* \in \mathcal{T}_{t,\infty}$ s.t.

$$\operatorname*{ess\,sup}_{\tau\in\mathcal{T}_{t,\infty}} \mathbb{E}^{\mathbb{Q}}\left[e^{-R\tau}h[Y_\tau]\Big|\mathcal{F}_t\right] = \mathbb{E}^{\mathbb{Q}}\left[e^{-R\tau^*}h\big[Y_{\tau^*}\big]\Big|\mathcal{F}_t\right]$$

and a stopping time $\tau^n \in \mathcal{T}_{t,\infty}$ for each function h_n s.t.

$$\operatorname*{ess\,sup}_{\tau\in\mathcal{T}_{t,\infty}} \mathbb{E}^{\mathbb{Q}}\left[e^{-R\tau}h_n[Y_\tau]\Big|\mathcal{F}_t\right] = \mathbb{E}^{\mathbb{Q}}\left[e^{-R\tau^n}h_n\big[Y_{\tau^n}\big]\Big|\mathcal{F}_t\right]$$

By the definition of the essential supremum (Karatzas and Shreve (1998) Appendix A), for all $\tau \in \mathcal{T}_{t,\infty}$

$$\begin{aligned} \mathbb{E}^{\mathbb{Q}}\Big[e^{-R\tau}h\big[Y_\tau\big]\Big|\mathcal{F}_t\Big] &\leq \mathbb{E}^{\mathbb{Q}}\left[e^{-R\tau^*}h\big[Y_{\tau^*}\big]\Big|\mathcal{F}_t\right] && \mathbb{Q}\text{-a.s.} \\ \mathbb{E}^{\mathbb{Q}}\Big[e^{-R\tau}h_n\big[Y_\tau\big]\Big|\mathcal{F}_t\Big] &\leq \mathbb{E}^{\mathbb{Q}}\left[e^{-R\tau^n}h_n\big[Y_{\tau^n}\big]\Big|\mathcal{F}_t\right] && \mathbb{Q}\text{-a.s.} \end{aligned}$$

Using all this, together with application of the Dominated Convergence Theorem,

$$\begin{aligned} &\lim_{n\to\infty}\left(\operatorname*{ess\,sup}_{\tau\in\mathcal{T}_{t,\infty}} \mathbb{E}^{\mathbb{Q}}\Big[e^{-R\tau}h\big[Y_\tau\big]\Big|\mathcal{F}_t\Big] - \operatorname*{ess\,sup}_{\tau\in\mathcal{T}_{t,\infty}} \mathbb{E}^{\mathbb{Q}}\Big[e^{-R\tau}h_n\big[Y_\tau\big]\Big|\mathcal{F}_t\Big]\right) \\ &\leq \lim_{n\to\infty}\left(\mathbb{E}^{\mathbb{Q}}\Big[e^{-R\tau^*}h\big[Y_{\tau^*}\big]\Big|\mathcal{F}_t\Big] - \mathbb{E}^{\mathbb{Q}}\Big[e^{-R\tau^*}h_n\big[Y_{\tau^*}\big]\Big|\mathcal{F}_t\Big]\right) \\ &= 0 \end{aligned}$$

also

$$\begin{aligned}
&\operatorname*{ess\,sup}_{\tau\in\mathcal{T}_{t,\infty}} \mathbb{E}^{\mathbb{Q}}\Big[e^{-R\tau}h\big[Y_\tau\big]\Big|\mathcal{F}_t\Big] - \operatorname*{ess\,sup}_{\tau\in\mathcal{T}_{t,\infty}} \mathbb{E}^{\mathbb{Q}}\Big[e^{-R\tau}h_n\big[Y_\tau\big]\Big|\mathcal{F}_t\Big] \\
&\geq \mathbb{E}^{\mathbb{Q}}\Big[e^{-R\tau^n}h\big[Y_{\tau^n}\big]\Big|\mathcal{F}_t\Big] - \mathbb{E}^{\mathbb{Q}}\Big[e^{-R\tau^n}h_n\big[Y_{\tau^n}\big]\Big|\mathcal{F}_t\Big] \qquad \forall\tau^n \\
&\geq \mathbb{E}^{\mathbb{Q}}\Big[e^{-R\tau^n}h\big[Y_{\tau^n}\big]\Big|\mathcal{F}_t\Big] - \mathbb{E}^{\mathbb{Q}}\Big[e^{-R\tau^n}h\big[Y_{\tau^n}\big]\Big|\mathcal{F}_t\Big] \qquad \forall h_n \\
&= 0
\end{aligned}$$

so that

$$\lim_{n\to\infty}\left(\operatorname*{ess\,sup}_{\tau\in\mathcal{T}_{t,\infty}} \mathbb{E}^{\mathbb{Q}}\Big[e^{-R\tau}h\big[Y_\tau\big]\Big|\mathcal{F}_t\Big] - \operatorname*{ess\,sup}_{\tau\in\mathcal{T}_{t,\infty}} \mathbb{E}^{\mathbb{Q}}\Big[e^{-R\tau}h_n\big[Y_\tau\big]\Big|\mathcal{F}_t\Big]\right) \geq 0$$

and thus

$$\lim_{n\to\infty}\left(\operatorname*{ess\,sup}_{\tau\in\mathcal{T}_{t,\infty}} \mathbb{E}^{\mathbb{Q}}\Big[e^{-R\tau}h_n\big[Y_\tau\big]\Big|\mathcal{F}_t\Big]\right) = \operatorname*{ess\,sup}_{\tau\in\mathcal{T}_{t,\infty}} \mathbb{E}^{\mathbb{Q}}\Big[e^{-R\tau}h\big[Y_\tau\big]\Big|\mathcal{F}_t\Big] \qquad \mathbb{Q}\text{-a.s.} \qquad (4.8)$$

This is the first result we need.

Now define the stopping time $\tilde{\tau} \in \mathcal{T}_{t,T}$ by

$$\tilde{\tau} = \begin{cases} \tau^* & \tau^* \leq T \\ T & \tau^* > T \end{cases}$$

Clearly

$$\operatorname*{ess\,sup}_{\tau\in\mathcal{T}_{t,T}} \mathbb{E}^{\mathbb{Q}}\Big[e^{-R\tau}h\big[Y_\tau\big]\Big|\mathcal{F}_t\Big] \geq \mathbb{E}^{\mathbb{Q}}\Big[e^{-R\tilde{\tau}}h\big[Y_{\tilde{\tau}}\big]\Big|\mathcal{F}_t\Big]$$

But because $h[Y_T] \geq 0$, and $h[Y_t] = 0$ for $t \geq T$ we also have

$$\begin{aligned}
&\mathbb{E}^{\mathbb{Q}}\Big[e^{-R\tilde{\tau}}h\big[Y_{\tilde{\tau}}\big]\Big|\mathcal{F}_t\Big] \\
=&\mathbb{E}^{\mathbb{Q}}\Big[e^{-R\tilde{\tau}}h\big[Y_{\tilde{\tau}}\big]\mathbb{I}_{\{\tau^*\leq T\}}\Big|\mathcal{F}_t\Big] + \mathbb{E}^{\mathbb{Q}}\Big[e^{-rT}h\big[Y_T\big]\mathbb{I}_{\{\tau^*>T\}}\Big|\mathcal{F}_t\Big] \\
\geq&\mathbb{E}^{\mathbb{Q}}\Big[e^{-R\tau^*}h\big[Y_{\tau^*}\big]\mathbb{I}_{\{\tau^*\leq T\}}\Big|\mathcal{F}_t\Big] + \mathbb{E}^{\mathbb{Q}}\Big[e^{-R\tau^*}h\big[Y_{\tau^*}\big]\mathbb{I}_{\{\tau^*>T\}}\Big|\mathcal{F}_t\Big] \\
=&\operatorname*{ess\,sup}_{\tau\in\mathcal{T}_{t,\infty}} \mathbb{E}^{\mathbb{Q}}\Big[e^{-R\tau}h\big[Y_\tau\big]\Big|\mathcal{F}_t\Big] \\
\geq&\operatorname*{ess\,sup}_{\tau\in\mathcal{T}_{t,T}} \mathbb{E}^{\mathbb{Q}}\Big[e^{-R\tau}h\big[Y_\tau\big]\Big|\mathcal{F}_t\Big]
\end{aligned}$$

So

$$\begin{aligned}
\mathbb{E}^{\mathbb{Q}}\Big[e^{-R\tilde{\tau}}h\big[Y_{\tilde{\tau}}\big]\Big|\mathcal{F}_t\Big] =&\operatorname*{ess\,sup}_{\tau\in\mathcal{T}_{t,T}} \mathbb{E}^{\mathbb{Q}}\Big[e^{-R\tau}h\big[Y_\tau\big]\Big|\mathcal{F}_t\Big] \\
=&\operatorname*{ess\,sup}_{\tau\in\mathcal{T}_{t,\infty}} \mathbb{E}^{\mathbb{Q}}\Big[e^{-R\tau}h\big[Y_\tau\big]\Big|\mathcal{F}_t\Big] \\
=&\lim_{n\to\infty}\left(\operatorname*{ess\,sup}_{\tau\in\mathcal{T}_{t,\infty}} \mathbb{E}^{\mathbb{Q}}\Big[e^{-R\tau}h_n\big[Y_\tau\big]\Big|\mathcal{F}_t\Big]\right)
\end{aligned}$$

Now from Fakeev (1971) we know that for all $h_n[Y]$ there exists a function $f_n[Y]$ s.t.

$$\operatorname*{ess\,sup}_{\tau\in\mathcal{T}_{t,\infty}} \mathbb{E}^{\mathbb{Q}}\left[e^{-R\tau}h_n[Y_\tau]\middle|\mathcal{F}_t\right] = e^{-Rt}f_n[Y_t]$$

Set $C^{\mathcal{O}}[t,S] = \lim_{n\to\infty} f_n[Y]$ which, by (4.8) must exist. Then

$$\begin{aligned}
X_C[t,\omega] =& \operatorname*{ess\,sup}_{\tau\in\mathcal{T}_{t,T}} \mathbb{E}^{\mathbb{Q}}\left[e^{-R(\tau-t)}\left[S[\tau]-K\right]^+\middle|\mathcal{F}_t\right] \\
=& e^{Rt}\operatorname*{ess\,sup}_{\tau\in\mathcal{T}_{t,\infty}} \mathbb{E}^{\mathbb{Q}}\left[e^{-R\tau}h\left[Y_\tau\right]\middle|\mathcal{F}_t\right] \\
=& e^{Rt}\lim_{n\to\infty}\left(\operatorname*{ess\,sup}_{\tau\in\mathcal{T}_{t,\infty}} \mathbb{E}^{\mathbb{Q}}\left[e^{-R\tau}h_n\left[Y_\tau\right]\middle|\mathcal{F}_t\right]\right) \\
=& e^{Rt}\lim_{n\to\infty}\left(e^{-Rt}f_n\left[Y_t\right]\right) \\
=& C^{\mathcal{O}}\left[t,S[t,\omega]\right]
\end{aligned}$$

□

Remark 4.3.3 *From both mathematical and financial perspectives, this result is remarkable. Mathematically, we have moved from pricing over a family of random variables contingent on the whole market history $\mathcal{F}_t$ to a family contingent only on the variable $S[t]$. Financially, we are pricing a claim whose drift (in the real world) is stochastic, and possibly path-dependent. However, because the drift is linked (through the market price of equity risk λ_W) to the drift of the stock price S, all path dependency collapses to dependence only on the current price of the underlying asset.*

Theorem 4.2.3 proves the existence of a unique price for American contingent claims. However, the form

$$C^{\mathcal{O}}\left[t,S[t]\right] = \operatorname*{ess\,sup}_{\tau\in\mathcal{T}_{t,T}} \mathbb{E}^{\mathbb{Q}}\left[e^{-R(\tau-t)}\left[S[\tau]-K\right]^+|\mathcal{F}_t\right]$$

given for $C^{\mathcal{O}}$ is not particularly tractable, and hence not particularly useful for determining option prices. We derive a more tractable formulation by examining the domain of the Markovian function $C^{\mathcal{O}}$.

Set $\mathcal{D}_C^{\mathcal{O}} = [0,T]\times(0,\infty)$, the domain of $C^{\mathcal{O}}$ (which is also the domain of $c^{\mathcal{O}}[t,S]$). Divide $\mathcal{D}_C^{\mathcal{O}}$ into a stopping region $\mathcal{S}_C^{\mathcal{O}} = \left\{(t,S) : C^{\mathcal{O}}[t,S] = [S-K]^+\right\}$ where immediate exercise of the call is optimal, and a continuation region $\mathcal{C}_C^{\mathcal{O}} = \mathcal{D}_C^{\mathcal{O}}\backslash\mathcal{S}_C^{\mathcal{O}} = \left\{(t,S) : C[t,S] > [S-K]^+\right\}$ where the derivative security is better sold than exercised.

As a result of this division, the stopping time $\eta_t^C = \inf\left\{t : C^{\mathcal{O}}[t,S] = [S(t)-K]^+\right\}$ becomes a hitting time $\eta_t^C = \inf\left\{t : (t,S[t]) \in \mathcal{S}_C^{\mathcal{O}}\right\}$. Expressing $C^{\mathcal{O}}$ in terms of this hitting time and using the generalised Itô rule

$$\begin{aligned}
C^{\mathcal{O}}[t,S] =& \mathbb{E}^{\mathbb{Q}}\left[e^{-R(\eta_t^C-t)}\left[S[\eta_t^C]-K\right]^+\middle|\mathcal{F}_t\right] \\
=& \mathbb{E}^{\mathbb{Q}}\left[e^{-R(T-t)}\left[S[T]-K\right]^+\middle|\mathcal{F}_t\right] \\
& - \mathbb{E}^{\mathbb{Q}}\left[\int_{s=\eta_t^C}^{T} d\left(e^{-R(s-t)}\left[S[s]-K\right]^+\right)\middle|\mathcal{F}_t\right] \\
=& c^{\mathcal{O}}[t,S] + \mathcal{P}_C^{\mathcal{O}}[t,S]
\end{aligned} \tag{4.9}$$

where

$$\mathcal{P}_C^{\mathcal{O}}[t,S] = \mathbb{E}^{\mathbb{Q}}\left[-\int_{s=\eta_t^C}^{T} d\left(e^{-R(s-t)}\left[S[s]-K\right]^+\right)\middle|\mathcal{F}_t\right] \tag{4.10}$$

represents the excess of the price of the ACC $C^{\mathcal{O}}$ over the ECC $c^{\mathcal{O}}$, i.e. the value of the right to exercise early - known as the early exercise premium (EEP).

To better characterise $\mathcal{S}_C^{\mathcal{O}}$, and hence $\mathcal{P}_C^{\mathcal{O}}$, and also to enhance our understanding of the behaviour of the security $C^{\mathcal{O}}$, we consider bounds on the values of $C^{\mathcal{O}}$ and its derivatives.

From the optimality of η_t^C,

$$\begin{aligned} C^{\mathcal{O}}[t,S[t]] =& \mathbb{E}^{\mathbb{Q}}\left[e^{-R(\eta_t^C-t)}\left[S[\eta_t^C]-K\right]^+\middle|\mathcal{F}_t\right] \\ =& \mathbb{E}^{\mathbb{Q}}\left[\left[S[t]\cdot\exp\left[\sigma_S(W^{\mathbb{Q}}_{\eta_t^C}-W_t^{\mathbb{Q}})-\left(\delta+\tfrac{1}{2}\sigma_S^2\right)(\eta_t^C-t)\right]-Ke^{-R(\eta_t^C-t)}\right]^+\middle|\mathcal{F}_t\right] \end{aligned}$$

By the validity of differentiation under the integral,

$$\begin{aligned} \frac{\partial C[t,S]}{\partial S} &= \mathbb{E}^{\mathbb{Q}}\left[\exp\left[\sigma_S(W^{\mathbb{Q}}_{\eta_t^C}-W_t^{\mathbb{Q}})-\left(\delta+\tfrac{1}{2}\sigma_S^2\right)(\eta_t^C-t)\right]\mathbb{I}_{\{S[\eta_t^C]>K\}}\middle|\mathcal{F}_t\right] \\ &\le \mathbb{E}^{\mathbb{Q}}\left[\exp\left[\sigma_S(W^{\mathbb{Q}}_{\eta_t^C}-W_t^{\mathbb{Q}})-\tfrac{1}{2}\sigma_S^2(\eta_t^C-t)\right]\middle|\mathcal{F}_t\right] \\ &= 1 \end{aligned}$$

Now,

$$\begin{aligned} C[t,S[t]] &= \operatorname*{ess\,sup}_{\tau\in\mathcal{T}_{t,T}} \mathbb{E}^{\mathbb{Q}}\left[e^{-R(\tau-t)}\left[S[\tau]-K\right]^+\middle|\mathcal{F}_t\right] \\ &\ge \left[S[t]-K\right]^+ \end{aligned}$$

And

$$\begin{aligned} C[t,S[t]] &\ge \operatorname*{ess\,sup}_{\tau=T} \mathbb{E}^{\mathbb{Q}}\left[e^{-R(\tau-t)}\left[S[\tau]-K\right]^+\middle|\mathcal{F}_t\right] \\ &= c[t,S[t]] \\ &> 0 \text{ while } t<T \end{aligned}$$

Let $\tilde{S}_C^{\mathcal{O}}[t] = \inf\left\{S : (t,S)\in\mathcal{S}_C^{\mathcal{O}}\right\}$. As $C\ge 0$ we have $\tilde{S}_C^{\mathcal{O}}[t]\ge K$, with equality only possible at $t=T$. Using this with $\frac{\partial C}{\partial S}\le 1$ then for $S>\tilde{S}_C^{\mathcal{O}}[t]$ we have $C[t,S]\le S-K$. To satisfy $C[t,S]\ge S-K$ it must be that for all $S\ge\tilde{S}_C^{\mathcal{O}}[t]$ immediate exercise is optimal, i.e. $C[t,S]=S-K$ and $(t,S)\in\mathcal{S}_C^{\mathcal{O}}$.

The curve created by the collection of values $\left\{\tilde{S}_C^{\mathcal{O}}[t] : t\in[0,T]\right\}$ is continuous (see Peskir(2002)) and divides the continuation region $\mathcal{C}_C^{\mathcal{O}}$ from the stopping region $\mathcal{S}_C^{\mathcal{O}}$. For any option purchased in the continuation region, the optimal exercise strategy η_t^C is to exercise the first time the stock price $S[t]$ hits the curve of $\tilde{S}_C^{\mathcal{O}}[t]$. Thus this curve is known as the Optimal Exercise Boundary (OEB).

Given that $\mathcal{S}_C^{\mathcal{O}}$ can be characterised as $\mathcal{S}_C^{\mathcal{O}}=\left\{(t,S) : S\ge\tilde{S}_C^{\mathcal{O}}[t]\right\}$, some manipulation of (4.10) - expounded in Appendix B.1 - simplifies $\mathcal{P}_C^{\mathcal{O}}$ to

$$\begin{aligned} \mathcal{P}_C^{\mathcal{O}}[t,S] &= \int_t^T e^{-R(u-t)}\mathbb{E}^{\mathbb{Q}}\left[(\delta S[u]-RK)\cdot\mathbb{I}_{\{(t,S[u])\in\mathcal{S}_C^{\mathcal{O}}\}}\middle|\mathcal{F}_t\right]du \\ &= \int_t^T \delta S[t]e^{-\delta(u-t)}\Phi\left[g_1^C[t,S,u]\right] - RKe^{-R(u-t)}\Phi\left[g_2^C[t,S,u]\right]du \end{aligned} \tag{4.11}$$

$$\text{where } g_1^C[t,S,u] = \frac{\ln S[t] - \ln \tilde{S}_C^{\mathcal{O}}[u] + (R - \delta + \frac{1}{2}\sigma_S^2)(u-t)}{\sigma_S \cdot \sqrt{u-t}}$$
$$\text{and } g_2^C[t,S,u] = g_1^C[t,S,u] - \sigma_S \cdot \sqrt{u-t}$$

This provides a closed-form solution for the American call option, conditional on knowing the location of the curve critical stock prices $\{\tilde{S}_C^{\mathcal{O}}[s]\}_{s\in(t,T)}$. In all but the simplest cases locating the curve of $\tilde{S}_C^{\mathcal{O}}[t]$ proves to be an intractable problem. In chapter 6 we discuss the numerical technique used in this dissertation to locate $\tilde{S}_C^{\mathcal{O}}[t]$. However, it is worth noting here that the location of $\tilde{S}_C^{\mathcal{O}}[t]$ is dependent on the assumptions 2.1.A1-2.1.A6, in particular the values of δ, R and σ_S.

The early exercise premium $\mathcal{P}_C^{\mathcal{O}}$ carries an intuitive explaination. Within the stopping region $\mathcal{S}_C^{\mathcal{O}}$, the seller of the option may hedge his position with a long position in the intrinsic value of the option. While the option holder chooses not to exercise within the stopping area, the seller's short position of K units of cash requires funding at rate RK. This is funded from dividend payouts at rate δS. Any surplus dividends provide a windfall profit to the seller.

The corresponding losses to the option holder are not as obvious. There is an apparent gain to delayed option exercise, as more information regarding the evolution of the stock price S enters the economy. Countering this gain is the opportunity cost of dividends foregone. The exercise region $\mathcal{S}_C^{\mathcal{O}}$ constructs itself so that early exercise is only optimal where the net opportunity cost of dividends foregone (i.e. less the financing costs of the strike price paid) exceed the expected informational gains. Thus the costs to the option holder for holding the option an instant longer are $(\delta S[t] - RK) \cdot \mathbb{I}_{\{(t,S[t])\in\mathcal{S}_C^{\mathcal{O}}\}} dt$.

In comparison with an European call option, the benefits for an American option to exercise an instant earlier are $(\delta S[t] - RK) \cdot \mathbb{I}_{\{(t,S[t])\in\mathcal{S}_C^{\mathcal{O}}\}} dt$. The American call option $C^{\mathcal{O}}$ has been decomposed into its equivalent European call option $c^{\mathcal{O}}$ plus the total value $\mathcal{P}_C^{\mathcal{O}}$ of the ability to exercise before expiry.

In the special case where $\delta = 0$, it follows that $\mathcal{P}_C^{\mathcal{O}} \leq 0$. From the dominance of $c^{\mathcal{O}}$ by $C^{\mathcal{O}}$, we must have $\mathcal{P}_C^{\mathcal{O}} = 0$. This only happens if the option is optimally exercised before expiry with probability zero, i.e. if $\tilde{S}_C^{\mathcal{O}}[t] = \infty$ for all $t \in [0,T)$.

This is consistent with Merton's (1973) observation that American call options are never optimally exercised before expiry when the underlying asset makes no interim payments before option expiry. (This argument is sometimes extrapolated to all American call options; our analysis for the cases where $\delta > 0$ shows that such extrapolations are erroneous).

As with the European call option, the American call option may be hedged with holdings in the stock and the bank account. The hedge portfolio holdings $H_{C;S}^{\mathcal{O}}$ and $H_{C;\mathcal{B}}^{OBS}$ in the stock and bank account respectively are

$$H_{C;S}^{\mathcal{O}}[t,S] = e^{-\delta(T-t)}\Phi[a_1] + \delta \int_t^T e^{-\delta(u-t)}\Phi\left[g_1^C[t,S,u]\right] du + \int_t^T e^{-R(u-t)}\left(\delta\tilde{S}_C^{\mathcal{O}}[u] - RK\right)\Phi'\left[g_2^C[t,S,u]\right]\frac{1}{S\cdot\sigma_S\cdot\sqrt{u-t}}\,du \quad (4.12a)$$

$$H_{C;\mathcal{B}}^{\mathcal{O}}[t,S] = \frac{1}{\beta[t]}\left(-Ke^{-R(T-t)}\Phi[a_2] - RK\int_t^T e^{-R(u-t)}\Phi\left[g_2^C[t,S,u]\right]du - \int_t^T e^{-R(u-t)}\left(\delta\tilde{S}_C^{\mathcal{O}}[u] - RK\right)\Phi'\left[g_2^C[t,S,u]\right]\frac{1}{\sigma_S\cdot\sqrt{(u-t)}}du\right) \quad (4.12b)$$

Alternatively, note that the discount bond maturing at expiry is a constant multiple of the bank account. The bank hedge may be replaced with a hedge in the discount bond maturing at expiry, with $H^{\mathcal{O}}_{C;B(T)}[t,S] = \beta[0]e^{RT}H^{\mathcal{O}}_{C;\beta}[t,S]$.

The hedging portfolio (4.12) is super self-financing in the sense that any initial investment almost surely provides sufficient funds for future portfolios. In many cases, this investment provides an excess of funds. Such cases occur when the option has been held through the stopping region. By definition any such exercise strategy is sub-optimal; the excess funds contribute to the seller's profits.

VBS pricing of American equity call options is complicated by the additional source of noise, and not widely studied. Indeed the author has not encountered any theoretical analysis thereof, so the remainder of this subsection is an original, albeit minor, contribution to the field.

In parallel with OBS pricing, we can use our pricing theorem 4.2.4 to arrive at the VBS price for X_C:

$$X_C[t,\omega] = \operatorname*{ess\,sup}_{\tau\in\mathcal{T}_{t,T}} \mathbb{E}^{\mathbb{Q}}\left[\exp\left[-\int_t^\tau r[s]ds\right]\left[S[\tau]-K\right]^+\middle|\mathcal{F}_t\right]$$

which is useful in establishing the existence of a unique price, but not in determining the value of this price. A Markovian form of the price function is easier to manipulate.

Theorem 4.3.4 *The VBS price for X_C is jointly Markovian in the variables t, $S[t]$ and $r[t]$, i.e. there exists a function $C^{\mathcal{V}} : [0,T]\times(0,\infty)\times(-\infty,\infty)\mapsto[0,\infty)$ such that*

$$X_C[t,\omega] = C^{\mathcal{V}}\left[t,S[t,\omega],r[t,\omega]\right] \tag{4.13}$$

Proof. This proof is similar Theorem 4.3.2, but uses some subtle techniques. Set

$$Y^t_u = \left(t, S[t,\omega], r[t,\omega], \int_t^{u\vee t} r[s,\omega]ds\right)$$

which is jointly Markovian under the measure $\mathbb{Q}$. Note that $Y^t_t = (t,S,r,0)$ $\mathbb{Q}$-a.s. Consider the reward function

$$h\left[Y^t_u\right] = \exp\left[-\int_t^{u\vee t} r[s,\omega]ds\right]\left[S[t,\omega]-K\right]^+\mathbb{I}_{\{t\le T\}}$$

Again use a series of continuous functions $\left\{h_n[Y]\right\}_{n\in\mathbb{N}}$ which converge to $h[Y]$, define the functions f_n by

$$\operatorname*{ess\,sup}_{\tau\in\mathcal{T}_{u,\infty}} \mathbb{E}^{\mathbb{Q}}\left[h_n\left[Y^t_\tau\right]\middle|\mathcal{F}_u\right] = f_n\left[Y^t_u\right]$$

and set $C^{\mathcal{V}}[t,S,r] = \lim_{n\to\infty} f_n\left[Y^t_t\right]$. Then using the techniques of theorem 4.3.2,

$$\begin{aligned}
X_C[t,\omega] &= \operatorname*{ess\,sup}_{\tau\in\mathcal{T}_{t,T}} \mathbb{E}^{\mathbb{Q}}\left[\exp\left[-\int_t^\tau r[s,\omega]ds\right]\left[S[\tau]-K\right]^+\middle|\mathcal{F}_t\right]\\
&= \lim_{n\to\infty} \operatorname*{ess\,sup}_{\tau\in\mathcal{T}_{t,\infty}} \mathbb{E}^{\mathbb{Q}}\left[h_n\left[Y^t_\tau\right]\middle|\mathcal{F}_t\right]\\
&= \lim_{n\to\infty} f_n\left[Y^t_t\right]\\
&= C^{\mathcal{V}}\left[t,S[t,\omega],r[t,\omega]\right]
\end{aligned}$$

□

All state dependency in the price X_C is represented in the current values of the stock price S and the short rate r. The mathematical and financial implications discussed in remark 4.3.3 are also applicable here.

Again consideration of the domain of the Markovian function shows the optimal stopping time to be a hitting time: Divide the domain $\mathcal{D}_C^{\mathcal{V}} = \{(t,S,r) \in [0,T] \times (0.\infty) \times (-\infty,\infty)\}$ of $C^{\mathcal{V}}$ into a stopping region $\mathcal{S}_C^{\mathcal{V}}$ and a continuation region $\mathcal{C}_C^{\mathcal{V}}$. As before the stopping region $\mathcal{S}_C^{\mathcal{V}}$ is $\mathcal{S}_C^{\mathcal{V}} = \{(t,S,r) : C^{\mathcal{V}}[t,S,r] = [S-K]^+\}$ and the continuation region $\mathcal{C}_C^{\mathcal{V}} = \mathcal{D}_C^{\mathcal{V}} \backslash \mathcal{S}_C^{\mathcal{V}} = \{(t,S,r) : C^{\mathcal{V}}[t,S,r] > [S-K]^+\}$. As a result of the Markovian form for X_C, the stopping time $\eta_t^C = \inf\{s \in [t,T] : X_C[s,\omega] = [S-K]^+\}$ is the first hitting time of (t,S,r) in the stopping region $\mathcal{S}_C^{\mathcal{V}}$, i.e. $\eta_t^C = \inf\{s \in [t,T] : (s,S[s],r[s]) \in \mathcal{S}_C^{\mathcal{V}}\}$.

For further characterisation of $\mathcal{S}_C^{\mathcal{V}}$, note from the optimality of η_t^C that

$$\begin{aligned}
C^{\mathcal{V}}[t,S,r] =& \mathbb{E}^{\mathbb{Q}}\left[\frac{\mathcal{B}[t]}{\mathcal{B}[\eta_t^C]}\left[S[\eta_t^C]-K\right]^+\middle|\mathcal{F}_t\right] \\
=& \mathbb{E}^{\mathbb{Q}}\Bigg[\Bigg[S[t]\exp\left[\sigma_S(W_{\eta_t^C}^{\mathbb{Q}} - W_t^{\mathbb{Q}}) - (\delta+\tfrac{1}{2}\sigma_S^2)(\eta_t^C - t)\right] \\
& - K\exp\left[(\theta-r)D[\eta_t^C - t] - \theta(\eta_t^C - t) + \int_t^{\eta_t^C} D[\eta_t^C - u]dW_u^{\mathbb{Q}}\right]\Bigg]^+\middle|\mathcal{F}_t\Bigg]
\end{aligned}$$

By the validity of differentiation under the integral,

$$\begin{aligned}
\frac{\partial C^{\mathcal{V}}}{\partial S} &= \mathbb{E}^{\mathbb{Q}}\left[\exp\left[\sigma_S(W_{\eta_t^C}^{\mathbb{Q}} - W_t^{\mathbb{Q}}) - (\delta+\tfrac{1}{2}\sigma_s^2)(\eta_t^C - t)\right]\cdot \mathbb{I}_{\{S[\eta_t^C]>K\}}\middle|\mathcal{F}_t\right] \\
&\leq \mathbb{E}^{\mathbb{Q}}\left[\exp\left[\sigma_S(W_{\eta_t^C}^{\mathbb{Q}} - W_t^{\mathbb{Q}}) - \tfrac{1}{2}\sigma_S^2(\eta_t^C - t)\right]\middle|\mathcal{F}_t\right] \\
&= 1 \\
\frac{\partial C^{\mathcal{V}}}{\partial r} &= \mathbb{E}^{\mathbb{Q}}\Bigg[D[\eta_t^C - t]\cdot K\cdot \mathbb{I}_{\{S[\eta_t^C]>K\}} \\
&\qquad \times \exp\left[(\theta-r)D[\eta_t^C - t] - \theta(\eta_t^C - t) + \int_t^{\eta_t^C} D[\eta_t^C - u]dW_u^{\mathbb{Q}}\right]\middle|\mathcal{F}_t\Bigg] \\
&> 0
\end{aligned}$$

Also

$$\begin{aligned}
C^{\mathcal{V}}[t,S,r] &= \operatorname*{ess\,sup}_{\tau\in\mathcal{T}_{t,T}} \mathbb{E}^{\mathbb{Q}}\left[\frac{\mathcal{B}[t]}{\mathcal{B}[\tau]}\left[S[\tau]-K\right]^+\middle|\mathcal{F}_t\right] \\
&\geq \left[S[t]-K\right]^+
\end{aligned}$$

and

$$\begin{aligned}
C^{\mathcal{V}}[t,S,r] &= \operatorname*{ess\,sup}_{\tau\in\mathcal{T}_{t,T}} \mathbb{E}^{\mathbb{Q}}\left[\frac{\mathcal{B}[t]}{\mathcal{B}[\tau]}\left[S[\tau]-K\right]^+\middle|\mathcal{F}_t\right] \\
&\geq c^{\mathcal{V}}[t,S,r] \\
&> 0 \text{ while } t < T
\end{aligned}$$

We are now in a position to show that there is a single curve dividing the continuation and stopping regions, and by corollary that the continuation and stopping regions are continuous.

Let $\tilde{S}_C^{\mathcal{V}}[t,r] = \inf\{S : [t,S,r] \in \mathcal{S}_C^{\mathcal{V}}\}$. As $C^{\mathcal{V}} \geq 0$, $\tilde{S}_C^{\mathcal{V}}[t,r] \geq K$, with equality only possible at $t = T$. For all $S > \tilde{S}_C^{\mathcal{V}}[t,r]$ we have that $\frac{\partial(S-K)}{\partial S} = 1$ and $C^{\mathcal{V}} \geq S - K$ but also that $\frac{\partial C^{\mathcal{V}}}{\partial S} \leq 1$; so for all $S \geq \tilde{S}_C^{\mathcal{V}}[t,r]$ we have $\frac{\partial C^{\mathcal{V}}}{\partial S} = 1$ and hence $C^{\mathcal{V}}[S,t,r] = S - K$. So if $S \geq \tilde{S}_C^{\mathcal{V}}[t,r]$ then $(t,S,r) \in \mathcal{S}_C^{\mathcal{V}}$, and $\mathcal{S}_C^{\mathcal{V}}$ can be characterised as $\mathcal{S}_C^{\mathcal{V}} = \{(t,S,r) : S \geq \tilde{S}_C^{\mathcal{V}}[t,r]\}$.

Analagously, set $\tilde{r}_C^{\mathcal{V}}[t,S] = \sup\{r : (t,S,r) \in \mathcal{S}_C^{\mathcal{V}}\}$. Similar logic leads to $C^{\mathcal{V}}[t,S,r] = S - K \quad \forall r < \tilde{r}_C^{\mathcal{V}}[t,S]$: thus $\mathcal{S}_C^{\mathcal{V}}$ can also be characterised as $\{(t,S,r) : r \leq \tilde{r}_C^{\mathcal{V}}[t,S]\}$.

Lemma 4.3.5 *For every $t \in [0,T]$ the map $\tilde{S}_C^{\mathcal{V}}[t,r] : [0,T] \times (-\infty,\infty) \mapsto (0,\infty)$ is non-decreasing in its second parameter (i.e. in r).*

Proof. Set $r_2 > r_1$. As $(t, \tilde{S}_C^{\mathcal{V}}[t,r_2], r_2) \in \mathcal{S}_C^{\mathcal{V}}$, $C^{\mathcal{V}}[t, \tilde{S}_C^{\mathcal{V}}[t,r_2], r_2] = \tilde{S}_C^{\mathcal{V}}[t,r_2] - K$. So $\tilde{r}_C^{\mathcal{V}}[t, \tilde{S}_C^{\mathcal{V}}[t,r_2]] \geq r_2$. Thus for all $r < r_2$ we have $(t, \tilde{S}_C^{\mathcal{V}}[t,r_2], r) \in \mathcal{S}_C^{\mathcal{V}}$, including for $r = r_1$. But as $(t, \tilde{S}_C^{\mathcal{V}}[t,r_2], r_1) \in \mathcal{S}_C^{\mathcal{V}}$ we know $C^{\mathcal{V}}[t, \tilde{S}_C^{\mathcal{V}}[t,r_2], r_1] = \tilde{S}_C^{\mathcal{V}}[t,r_2] - K$. Now $\tilde{S}_C^{\mathcal{V}}[t,r_1] = \inf\{S : (t,S,r_1) \in \mathcal{S}_C^{\mathcal{V}}\}$, so we must have $\tilde{S}_C^{\mathcal{V}}[t,r_1] \leq \tilde{S}_C^{\mathcal{V}}[t,r_2]$.

□

Corollary 4.3.6 *By the same logic, $\tilde{r}_C^{\mathcal{V}}[t,S]$ is non-increasing in its second parameter.*

Conjecture 4.3.7 *The functions $\tilde{S}_C^{\mathcal{V}}[t,r]$ and $\tilde{r}_C^{\mathcal{V}}[t,S]$ are both continuous in both arguments.*

This conjecture should be provable by adapting the methodology in Peskir (2002), but the author has as yet been unable to complete this.

The hypercurve $\{(t,S,r) : S = \tilde{S}_C^{\mathcal{V}}[t,r]\}$ forms the boundary between the $\mathcal{S}_C^{\mathcal{V}}$ (in which it is included) and $\mathcal{C}_C^{\mathcal{V}}$. The optimal exercise strategy (for an option currently in $\mathcal{C}_C^{\mathcal{V}}$) is to exercise as soon as (t,S,r) hits this hypercurve. Like the OBS counterpart, this boundary is known a the Optimal Exercise Boundary.

Now as $C^{\mathcal{V}}$ and $c^{\mathcal{V}}$ are both Markovian in the triple (t,S,r) we define $\mathcal{P}_C^{\mathcal{V}}$ by

$$\mathcal{P}_C^{\mathcal{V}}[t,S,r] = C^{\mathcal{V}}[t,S,r] - c^{\mathcal{V}}[t,S,r]$$

which clearly represents the premium paid for the right to exercise before option expiry and is unsurprisingly called the early exercise premium. Again relying on the optimality of η_t^C and the Fundamental Theorem of Calculus, and invoking the generalised Itô rule for convex functions,

$$\mathcal{P}_C^{\mathcal{V}}[t,S,r] = \mathbb{E}^{\mathbb{Q}}\left[\int_{\eta_t^C}^{T} d\left(\frac{\beta[t]}{\beta[u]}\left[S[u] - K\right]^+\right) du \middle| \mathcal{F}_t\right] \tag{4.14a}$$

$$= \int_t^T \mathbb{E}^{\mathbb{Q}}\left[\frac{\beta[t]}{\beta[u]}\left(\delta \cdot S[u] - K \cdot r[u]\right)\mathbb{I}_{\{(u,S[u]),r[u]) \in \mathcal{S}_C^{\mathcal{V}}\}} \middle| \mathcal{F}_t\right] du \tag{4.14b}$$

Details are provided in Appendix B.2.

As with the OBS American equity call option, the EEP represents the excess yield to the option seller on holding an intrinsic hedge through the stopping region. The borrowing of the strike price K incurs costs at a rate $r[u] \cdot K$, which are funded from dividend payments at a rate $\delta \cdot S[u]$, with the residual yield representing excess profits to the option seller. Equations (4.14b) and (4.11) differ only in short rate stochasticity, which in turn influences the construction of the stopping region.

Remark 4.3.8 *On page 43 we showed that Merton's observation on early exercise of American equtiy options in the OBS model with $\delta = 0$ follows from the non-positivity of the early exercise premium for such options. As the VBS model allows for arbitrarily negative short rates (see remark 2.2.1), $\mathcal{P}_C^{\mathcal{V}}$ is not confined to being non-positive, even when $\delta = 0$. While probabilities under the VBS model of optimal early exercise of American equity call options on assets not paying dividends are low, they are not zero. Early exercise will be optimal for deeply in-the-money options when short rates are strongly negative.*

Unlike the OBS model, the VBS model does not permit a simple closed-form solution for $\mathcal{P}_C^{\mathcal{V}}$. This is largely due to the relationship between the stochastic variables S and r. Early exercise is dependent on both variables S and r. However, the stock price S drifts at a rate proportional to the short rate, r. Conditional on any future value of r, the distribution of the corresponding value of S depends on the path taken by r to arrive at this future value. This produces a complex conditional distribution for S involving Ornstein-Uhlenbeck bridges on r and which is not particularly tractable.

Using the Markovian formulation $X_C[t,\omega] = C^{\mathcal{V}}[t, S[t], r[t]]$ and its partial derivatives (implicitly assumed to exist on page 42), we can invoke Itô's Lemma to obtain

$$\begin{aligned} dC =& \frac{\partial C^{\mathcal{V}}}{\partial t}dt + \frac{\partial C^{\mathcal{V}}}{\partial S}dS + \frac{\partial C^{\mathcal{V}}}{\partial r}dr + \frac{1}{2}\left(\frac{\partial^2 C^{\mathcal{V}}}{\partial S^2}d\langle S\rangle + 2\frac{\partial^2 C^{\mathcal{V}}}{\partial S \partial r}d\langle S, r\rangle + \frac{\partial^2 C^{\mathcal{V}}}{\partial r^2}d\langle r\rangle\right) \\ =& \left(\frac{\partial C^{\mathcal{V}}}{\partial t} + \frac{\partial C^{\mathcal{V}}}{\partial S}rS + \frac{\partial C^{\mathcal{V}}}{\partial r}\alpha(\theta - r) + \frac{1}{2}\frac{\partial^2}{\partial S^2}\sigma_S^2 S^2 + \frac{\partial^2 C^{\mathcal{V}}}{\partial S \partial r}\sigma_r \sigma_S \chi S + \frac{1}{2}\frac{\partial^2 C^{\mathcal{V}}}{\partial r^2}\sigma_r^2\right)dt \\ &+ \frac{\partial C^{\mathcal{V}}}{\partial S}\sigma_S S d\mathbb{W}_t^{\mathbb{Q}} + \frac{\partial C^{\mathcal{V}}}{\partial r}\sigma_r D[T-t]d\mathbb{W}_t^{\mathbb{Q}} \end{aligned}$$

These dynamics are consistent with the general dynamics for American Contingent Claims which follow from the decomposition (4.6a). In particular, C is (super-)hedged by the portfolio

$$\begin{aligned} \Pi_0[s,\omega] =& H_{C;0}^{\mathcal{V}}[s,\omega] = \frac{\partial C^{\mathcal{V}}}{\partial r} \cdot \frac{\sigma_r}{\sigma_0^W[s] \cdot X_0[s]} \\ \Pi_S[s,\omega] =& H_{C;S}^{\mathcal{V}}[s,\omega] = \frac{\partial C^{\mathcal{V}}}{\partial S} - \frac{\partial C^{\mathcal{V}}}{\partial r} \cdot \frac{\sigma_0^W[s] \cdot \sigma_r}{\sigma_0^V[s] \cdot \sigma_S \cdot S[s]} \\ \Pi_{\mathcal{B}}[s,\omega] =& H_{C;\mathcal{B}}^{\mathcal{V}}[s,\omega] = C - H_{C;0}^{\mathcal{V}}[s,\omega] \cdot X_0[s] - H_{C;S}^{\mathcal{V}}[s,\omega] \cdot S[s] \end{aligned}$$

Lacking a closed-form solution for $\mathcal{P}_C^{\mathcal{V}}$ (and hence for $C^{\mathcal{V}}$), we cannot undertake the kind of analytic comparison of C^O and C^V which was possible for c^O and c^V. Comparison of C^O and C^V will have to be made numerically. In the chapter 6 we develop numerical schemes whose solutions approximate C^O and C^V, while chapter 9 presents the results from such schemes under a limited set of calibrations.

4.3.2 American Equity Put Option Pricing

Definition 4.3.9 *An American equity put option $X_P[t,\omega]$ with strike price K and expiry T is an American Contingent Claim with the payoff set*

$$\boldsymbol{x}_P = \left\{x[t,\omega] = \left[K - S[\tau]\right]^+ \mathbb{I}_{\{t \geq \tau\}}\right\}_{\tau \in \mathcal{T}_{0,T}}$$

An American equity put option represents the right, but not the the obligation, to sell the asset S for the price K at any time before expiry T. Pricing of American equity put options

is remarkably similar to that of call options: we present only the main results here, leaving the workings for the reader.

Theorem 4.2.3 immediately gives the OBS price of X_P as

$$X_P[t,\omega] = \operatorname*{ess\,sup}_{\tau \subset \mathcal{T}_{t,T}} \mathbb{E}^{\mathbb{Q}} \left[e^{-R(\tau - t)} \left[K - S[\tau] \right]^+ | \mathcal{F}_t \right]$$

and analysis along the lines of theorem 4.3.2 proves the existence of a Markovian form

$$X_P[t,\omega] = P^{\mathcal{O}}\left[t, S[t]\right]$$

exists, sharing the domain $\mathcal{D}^{\mathcal{O}}$ with $C^{\mathcal{O}}[t,S]$. $\mathcal{D}^{\mathcal{O}}$ divides into $\mathcal{S}_P^{\mathcal{O}} = \left\{(t,S) : P[t,S] = K - S\right\}$ and $\mathcal{C}_P^{\mathcal{O}} = \mathcal{D}^{\mathcal{O}} \backslash \mathcal{S}_P^{\mathcal{O}}$. This division has a single boundary $\tilde{S}_P^{\mathcal{O}}[t]$ which is continuous in t, and we can characterise $\mathcal{S}_P^{\mathcal{O}}$ as $\mathcal{S}_P^{\mathcal{O}} = \{(t,S) : S \leq \tilde{S}_P^{\mathcal{O}}[t]\}$. the curve $\tilde{S}_P^{\mathcal{O}} : [0,T) \mapsto (0,\infty)$ is known as the Optimal Exercise Boundary of P.

Analysis of the Doob-Meyer decomposition of $e^{Rt} P^{\mathcal{O}}[t,\cdot]$ leads to the early exercise premium

$$\begin{aligned}
\mathcal{P}_P^{\mathcal{O}}[t,S] =& P^{\mathcal{O}}[t,S] - p^{\mathcal{O}}[t,S] \\
\mathcal{P}_P^{\mathcal{O}}[t,S] =& \int_t^T RK e^{-R(u-t)} \Phi\left[-g_2^P[t,S,u]\right] - \delta S[t] e^{-\delta(u-t)} \Phi\left[-g_2^P[t,S,u]\right] du \\
\text{where } g_1^P[t,S,u] =& \frac{\ln S[t] - \ln \tilde{S}_P^{\mathcal{O}}[u] + \left(R - \delta + \frac{1}{2}\sigma_S^2\right)(u-t)}{\sigma_S \cdot \sqrt{u-t}} \\
\text{and} \quad g_2^P[t,S,u] =& g_1^P[t,S,u] - \sigma_S \cdot \sqrt{u-t}
\end{aligned}$$

The claim $P^{\mathcal{O}}$ can be super-replicated by a portfolio holding $H_{P,S}^{\mathcal{O}}$ and $H_{P,\beta}^{\mathcal{O}}$ of stock $S[t]$ and bank account $\beta[t]$ respectively, where

$$\begin{aligned}
H_{P,S}^{\mathcal{O}}[t,S] =& -e^{-\delta(T-t)} \Phi[-a_1] \quad \delta \int_t^T e^{-\delta(u-t)} \Phi\left[-g_1^P[t,S,u]\right] du \\
& - \int_t^T \left(RK - \delta \tilde{S}_P^{\mathcal{O}}[t]\right) e^{-R(u-t)} \Phi'\left[-g_2^P[t,S,u]\right] \frac{1}{S \cdot \sigma_S \cdot \sqrt{u-t}} du
\end{aligned}$$

$$\begin{aligned}
H_{P,\beta}^{\mathcal{O}}[t,S] =& \frac{1}{\beta[t]} \left(K e^{-R(T-t)} \Phi[-a_2] + RK \int_t^T e^{-R(u-t)} \Phi\left[-g_2^P[t,S,u]\right] du \right. \\
& \left. + \int_t^T \left(RK - \delta \tilde{S}_P^{\mathcal{O}}[t]\right) e^{-R(u-t)} \Phi'\left[-g_2^P[t,S,u]\right] \frac{1}{\sigma_S \cdot \sqrt{u-t}} du \right)
\end{aligned}$$

Applying Theorem 4.2.4 to get the VBS price of X_P,

$$X_P[t,\omega] = \operatorname*{ess\,sup}_{\tau \in \mathcal{T}_{t,T}} \mathbb{E}^{\mathbb{Q}} \left[\frac{\beta[t]}{\beta[\tau]} \left[K - S[\tau]\right]^+ \middle| \mathcal{F}_t \right]$$

and setting $\eta^P[t,\omega] = \eta_t^P = \inf\left\{ s \in [t,T] : X_P[t,\omega] = \left[K - S[t]\right]^+ \right\}$,

$$X_P[t,\omega] = \mathbb{E}^{\mathbb{Q}} \left[\frac{\beta[t]}{\beta[\eta_t^P]} \left[K - S[\eta_t^P]\right]^+ \middle| \mathcal{F}_t \right]$$

The techniques of Theorem 4.3.4 lead to the function $P^{\mathcal{V}}$ satisfying

$$X_P[t.\omega] = P^{\mathcal{V}}[r.S[t.\omega].r[t.\omega]] \tag{4.15}$$

We divide the domain $\mathcal{D}_P^{\mathcal{V}}$ of $P^{\mathcal{V}}$ (which is identical to $\mathcal{D}_C^{\mathcal{V}}$) into a stopping region $\mathcal{S}_P^{\mathcal{V}}$ where $P^{\mathcal{V}}[t,S,r] = K - S$ and a continuation region $\mathcal{C}_P^{\mathcal{V}} = \mathcal{D}_P^{\mathcal{V}} \backslash \mathcal{S}_P^{\mathcal{V}}$; the stopping time η_t^P is the first hitting time of the triple $\big(t, S[t], r[t]\big)$ in the stopping region $\mathcal{S}_P^{\mathcal{V}}$.

By the logic used for the American equity call option,

$$\begin{aligned} \frac{\partial P^{\mathcal{V}}}{\partial S} &\geq -1 \\ \frac{\partial P^{\mathcal{V}}}{\partial r} &\leq 0 \end{aligned}$$

So, setting $\tilde{S}_P^{\mathcal{V}}[t,r] = \sup\big\{S : P^{\mathcal{V}}[t,S,r] = K - S\big\}$, then for $S < \tilde{S}_P^{\mathcal{V}}[t.r]$ we have $P^{\mathcal{V}}[t,S,r] = K - S$. Similarly setting $\tilde{r}_P^{\mathcal{V}}[t.S] = \inf\big\{r : P^{\mathcal{V}}[t.S.r] = K - S\big\}$ then for $r > \tilde{r}_P^{\mathcal{V}}[t.S]$ we have $P[t,S,r] = K - S$. So $\mathcal{S}_P^{\mathcal{V}} = \big\{(t,S,r) : S \leq \tilde{S}_P^{\mathcal{V}}[t.r]\big\} = \big\{(t,S,r) : r \geq \tilde{r}_P^{\mathcal{V}}[t.S]\big\}$. Again the map $\tilde{S}_P^{\mathcal{V}}[t,r] : [0,T] \times (-\infty,\infty) \mapsto (0.\infty)$ is increasing in its second parameter.

The American equity put option price always dominates the corresponding European price. Indeed, the American equity put option decomposed into a European equity put option and an early exercise premium $\mathcal{P}_P^{\mathcal{V}}$:

$$\begin{aligned} \mathcal{P}_P^{\mathcal{V}}[t,S,r] =& P^{\mathcal{V}}[t.S,r] - p^{\mathcal{V}}[t,S.r] \\ =& \mathbb{E}^{\mathbb{Q}}\left[\int_{\eta_t^P}^{T} \frac{\beta[t]}{\beta[u]}\big(r[u]\cdot K - S[u]\cdot\delta\big)\mathbb{I}_{\{S[u]<K\}}du \,\middle|\, \mathcal{F}_t\right] \end{aligned}$$

As with $C^{\mathcal{V}}$, the complications of bridging, conditioning and correlation leave the early exercise premium representation of $P^{\mathcal{V}}$ analytically intractable. Comparisons of $P^{\mathcal{O}}$ and $P^{\mathcal{V}}$ cannot be made analytically, and must be done numerically. This is done in Chapter 10.

Chapter 5

Critique of ρ-hedging

Real world interest rates are trivially observable as stochastic, in direct contradiction of Assumptions 2.1.A3 and 2.1.A7. This stochasticity typically causes yields-to-maturity of discount bonds (i.e. spot rates) to vary with term to maturity. While acknowledging such stochasticity, many practitioners nevertheless choose to price options using the OBS model. This choice stems from the ease of use and also the widespread comprehension of this model.

Use of the OBS model requires the selection of a calibration value of R. Consistency with market values is desirable, but practitioners are faced with a choice between infinitely many different forward and spot rates. The short rate, which in one-factor models ultimately drives yield curve development in all continuous interest rate models, is an obvious candidate.

However, most (in the American case) or all (in the European case) of an option's value is determined at expiry. The spot rate maturing at option expiry, which is the natural discount rate to option expiry, is ubiquitously popular. This choice inspires our use of the symbol R to represent the instantaneous cost of money in the OBS model, in place of the more common r.

The analysis in the preceeding chapters, and also the numerical results in part III address the accuracy (or lack thereof) of such an approach, in comparison to a Vasicek-style rate. Any and all errors in OBS pricing (relative to their VBS equivalents) stem from not recognising the stochastic nature of interest rates.

Some practitioners (partially) recognise such stochasticity by measuring the sensitivity of OBS prices to a stochastic value of R. They hedge this risk through assets which also exhibit sensitivity to R, investing (borrowing) any surplus (deficit) value in (from) the riskless bank account. Because the partial derivative $\frac{\partial X^{\mathcal{O}}}{\partial R}$ which measures this sensitivity is frequently called ρ, the hedging technique described is called ρ-hedging.

Both ρ-hedging as well as the less common vega-hedging (hedging against a stochastic value of σ_S, the stock price volatility) hedge parameters which the OBS model assumes as constant. If contingent claims are priced by the OBS model, such stochasticity is external to the model, and the hedges are known as 'out-of-model' hedges. This contrasts 'in-model' hedges where the model explicitly considers and prices the relevant uncertainty.

This chapter will consider the many theoretical disadvantages, as well as possible practical advantages, of ρ-hedging.

Of course, ρ remains an important tool in sensitivity analysis. In particular, when contingent claim prices of hedges have a high absolute rate sensitivity, accurate selection of R is important and a model which includes interest rate stochasticity may be advisable.

5.1 Theoretical Disadvantages

5.1.1 Stochastic Calibration Switching

The first, obvious criticism of ρ-hedging is philosophical. The function from which the ρ-hedge is derived itself assumes constant (or at least deterministic) interest rates. Yet it is also used to gauge sensitivity to an implicitly stochastic interest rate, which cannot be consistent with the deterministic assumption.

More subtly, the OBS hedges (and therefore prices) are constructed for a single calibration value of R. Stochasticity of R implies stochastic switching between different calibrations of the model, and there is no guarantee that the 'hedge' portfolios will provide the intended hedge for the relevant claim.

The effects of calibration switching are well exhibited by the American equity call option $C^{\mathcal{O}}$. Recalling that $C^{\mathcal{O}}$ can be decomposed into the European equity call option $c^{\mathcal{O}}$ and an early exercise premium $\mathcal{P}_C^{\mathcal{O}}$ (representing payments at rate $\delta S - rK$ throughout the stopping region $\mathcal{S}_C^{\mathcal{O}}$, and using the early exercise representation of $\mathcal{P}_C^{\mathcal{O}}$ in (4.11), we get

$$\begin{aligned}
\rho_C^{\mathcal{O}}[t,S,R] =& \frac{\partial C^{\mathcal{O}}[t,S]}{\partial R} \\
=& (T-t)Ke^{-r(T-t)}\Phi[a_2] \\
&+ R\cdot K\int_t^T (u-t)e^{-R(u-t)}\Phi\left[g_2^C[t,S,u]\right]\,du \\
&+ \int_t^T e^{-R(u-t)}\left(\delta\tilde{S}_C^{\mathcal{O}}[u]-RK\right)\Phi'\left[g_2^C[t,S,u]\right]\frac{\sqrt{u-t}}{\sigma_S}\,du \\
&- K\int_t^T e^{-R(u-t)}\Phi\left[g_2^C[t,S,u]\right]\,du \\
&- \int_t^T e^{-R(u-t)}\left(\delta\tilde{S}_C^{\mathcal{O}}[u]-RK\right)\cdot\frac{\Phi'\left[g_2^C[t,S,u]\right]}{\tilde{S}_C^{\mathcal{O}}[u]\sigma_S\sqrt{u-t}}\cdot\frac{\partial\tilde{S}_C^{\mathcal{O}}[u]}{\partial R}\,du
\end{aligned}$$

The first three lines of our expansion for $\rho_C^{\mathcal{O}}[t,S,R]$ are unsurprising. They reflect the changes in value from a fixed income portfolio hedging the level (i.e. stock price independent) cashflows from $C^{\mathcal{O}}$ with the corresponding discount bonds. The total value of such a portfolio is the value of non-stock in-model hedges for $C^{\mathcal{O}}$ $\left(=\beta[t]\cdot H_{C;\beta}^{\mathcal{O}}[t,S]\Big|_R\right)$.

It is the final two lines of the expansion which yield insight into stochastic calibration switching. Firstly, calibration switches directly change the level of the early exercise payments $(\delta S - RK)$, as reflected in the penultimate line of our expansion. Secondly, following our discussion on page 43, any change in the current option value (be this from changes in $\mathcal{P}_C^{\mathcal{O}}$ or $c^{\mathcal{O}}$) will alter the tradeoffs influencing the exercise decision. As the exercise decision changes, so too will the location of the stopping area $\mathcal{S}_C^{\mathcal{O}}$, and hence the boundary $\left\{\tilde{S}_C^{\mathcal{O}}[u]\right\}_{u\in[0,T]}$ of $\mathcal{S}_C^{\mathcal{O}}$. The last line of our expansion for $\rho_C^{\mathcal{O}}$ reflects the change in the location of the OEB of $C^{\mathcal{O}}$.

The European equity call option $c^{\mathcal{O}}$ stands in contrast to the American equity call option $C^{\mathcal{O}}$. The rate sensitivity of $c^{\mathcal{O}}$ takes the form

$$\rho_c^{\mathcal{O}}[t,S,r] = \frac{\partial c^{\mathcal{O}}[t,S]\Big|_R}{\partial R} = (T-t)\,e^{-R(T-t)}\,K\,\Phi[a_2]$$

implying a sale of $K\ \Phi[a_2]$ units of the discount bond maturing at option expiry - no different to the in-model hedge $H^{\mathcal{O}}_{c;B[t]}[t,S]$.

Comparison of $c^{\mathcal{O}}$ and $C^{\mathcal{O}}$ leads to the observation that, where claim cashflows (contingent on the realisation $\{S[t]\}_{t\in[0,T]}$ are independent of the value of R, the ρ-hedged portfolio will be identical to the in-model OBS hedge portfolio invested in discount bonds corresponding to claim payment times.

While appealing, correspondence of ρ-hedges and in-model hedges is not sufficient to preclude arbitrage.

5.1.2 Flat Yield Curve Arbitrage

The OBS model prices discount bonds at a flat yield-to-maturity R, which ρ-hedges imply is stochastic. Suppose that there are two frictionlessly-traded discount bonds with maturities at $T_1 < T_2 < \mathcal{H}$ and that the bank account also trades without any friction. Consider the trading strategy for $t < T_1$ in the spirit of definition 2.2.6, holding $\Pi_1[t] = -(T_2 - t)$ of $B[t,T_1]$, also $\Pi_2[t] = (T_1 - t)e^{R(T_2-T_1)}$ of $B[t,T_2]$ and $\Pi_\beta[t] = (\Pi_1 \cdot B[t,T_1] + \Pi_2 \cdot B[t,T_2]) \div \beta[t]$ of the bank account. The dynamics of the portfolio are then

$$
\begin{aligned}
d\Pi[t] =& \Pi_\beta[t]\left(\frac{\partial \beta}{\partial t}dt\right) \\
&+ \Pi_1[t]\left(\frac{\partial B[t,T_1]}{\partial t}dt + \frac{\partial B[t,T_1]}{\partial R}dR + \frac{\partial^2 B[t,T_1]}{\partial R^2}d\langle R\rangle_t\right) \\
&+ \Pi_2[t]\left(\frac{\partial B[t,T_2]}{\partial t}dt + \frac{\partial B[t,T_2]}{\partial R}dR + \frac{\partial^2 B[t,T_2]}{\partial R^2}d\langle R\rangle_t\right) \\
=& \left(\Pi_\beta[t]\, R\, \beta[t] + \Pi_1[t] R\, B[t,T_1] + \Pi_2[t] R\, B[t,T_2]\right)dt \\
&- \left(\Pi_1[t](T_1 - t)B[t,T_1] + \Pi_2[t](T_2 - t)B[t,T_2]\right)dR \\
&+ \tfrac{1}{2}\left(\Pi_1[t](T_1 - t)^2 B[t,T_1] + \Pi_2[t](T_2 - t)^2 B[t,T_2]\right)d\langle R\rangle \\
=& 0dt \\
&- \left((T_2 - t)(T_1 - t)e^{-R(T_1 - t)} + (T_1 - t)e^{R(T_2 - T_1)}(T_2 - t)e^{-R(T_2 - t)}\right)dR \\
&+ \tfrac{1}{2}\left((T_1 - t)e^{R(T_2 - T_1)}(T_2 - t)^2 e^{R(T_1 - t)} - (T_2 - t)(T_1 - t)^2 e^{-R(T_1 - t)}\right)d\langle R\rangle \\
=& \tfrac{1}{2}(T_2 - T_1)(T_2 - t)(T_1 - t)e^{-R(T_1 - t)}d\langle R\rangle \quad > 0
\end{aligned}
$$

In particular, as R is assumed stochastic, for $s > t$ we have $\mathbb{P}\left[\langle R\rangle_s > \langle R\rangle_t \middle| \mathcal{F}_t\right] > 0$, and our portfolio represents an arbitrage opportunity in the spirit of definition 2.2.7. Indeed similar arguments imply that any (not necessarily flat) yield curve whose spot rates move in parallel permits arbitrage opportunities. The actions of arbitrageurs buying long-dated bonds and the bank account, and selling short- and medium-dated bonds, create the empirical 'hump' in yields-to-maturity. One of the many practical criticisms of the Vasicek model is that only a very limited number of calibrations permit humped yield curves.

One response to this arbitrage may be to regard R as merely the given yield on a given bond, and to price other bonds by other means. This approach leads to obvious pricing contradictions between fixed income securities and contingent claims, and to internal contradictions when pricing a portfolio of contingent claims with differing expiry times. It is also insufficient to avoid the hedging complications to be described next.

5.1.3 Intermediate Portfolio Cashflows

Remember from Chapters 3 and 4 that both American equity options (while in their continuation region) and European equity options can be expressed as expected discounted payoffs. As they satisfy the necessary technical regularity conditions (see Duffie (1996)Appendix E), we can invoke the Feynman-Kač theorem to conclude that they satisfy the PDE

$$\frac{\partial X^{\mathcal{O}}}{\partial t} + (R-\delta)\,S[t]\cdot\frac{\partial X^{\mathcal{O}}}{\partial S} + \tfrac{1}{2}\sigma_S^2\cdot S^2[t]\cdot\frac{\partial^2 X^{\mathcal{O}}}{\partial S^2} - R\cdot X^{\mathcal{O}} = 0 \tag{5.1}$$

where $X^{\mathcal{O}}$ is the OBS price of such a contingent claim.

Also, from the definition of the spot rate $R[t]$ in (3.12),

$$\begin{aligned} dR &= \frac{\partial R}{\partial t}dt + \frac{D[T-t]}{(T-t)}dr[t] \\ &= \frac{\partial R}{\partial t}dt + \frac{D[T-t]}{(T-t)}\alpha\big(\theta - r[t]\big)dt + \frac{D[T-t]}{(T-t)}\cdot\sigma_r dV_t^{\mathbb{Q}} \end{aligned} \tag{5.2}$$

From the Fundamental Theorem of Asset Pricing (see e.g. Delbaen & Schachermayer (1994A), (1994B)), any model is arbitrage-free if there exists an equivalent measure under which security prices discounted by a chosen numeraire are martingales. From here on we restrict our attention to the VBS measure $\mathbb{Q}$ defined by (3.5), where the said numeraire is the bank account, although the core arguments and conclusions are not specific to the VBS model.

Now suppose that we choose to use an OBS price $X^{\mathcal{O}}[t,S]$ within a VBS environment. As both the spot rate R and the stock price S are stochastic, by Itô's lemma it follows that

$$\begin{aligned} dX^{\mathcal{O}}[t,S]\big|_R = \frac{\partial X^{\mathcal{O}}}{\partial t}dt + \frac{\partial X^{\mathcal{O}}}{\partial S}dS[t] + \frac{\partial X^{\mathcal{O}}}{\partial R}dR \\ + \tfrac{1}{2}\left(\frac{\partial^2 X^{\mathcal{O}}}{\partial S^2}d\langle S\rangle + \frac{\partial^2 X^{\mathcal{O}}}{\partial R\partial S}d\langle S,R\rangle + \frac{\partial^2 X^{\mathcal{O}}}{\partial R^2}d\langle R\rangle\right) \end{aligned}$$

Substituting from (5.1), (5.2) and (3.7c),

$$\begin{aligned} dX^{\mathcal{O}}[t,S]\big|_R =& R\,X^{\mathcal{O}}\,dt + \frac{\partial X^{\mathcal{O}}}{\partial S}\sigma_S\,S\,dW_t^{\mathbb{Q}} + \frac{\partial X^{\mathcal{O}}}{\partial R}\frac{D[T-t]}{(T-t)}\cdot\sigma_r\,dV_t^{\mathbb{Q}} \\ &+ \left(\frac{\partial X^{\mathcal{O}}}{\partial R}\cdot\frac{D[T-t]}{(T-t)}\cdot\theta(\alpha - r[t]) + \tfrac{1}{2}\frac{\partial^2 X^{\mathcal{O}}}{\partial R^2}\frac{D^2[T-t]}{(T-t)^2}\cdot\sigma_r^2\right. \\ &\left. + \frac{\partial^2 X^{\mathcal{O}}}{\partial R\partial S}\cdot\frac{D[T-t]}{(T-t)}\cdot\sigma_s\cdot S\cdot\sigma_r\cdot\chi\right)dt \end{aligned}$$

There is no inherent reason for the drift term

$$\begin{aligned} \Bigg(R\,X^{\mathcal{O}} + \frac{\partial X^{\mathcal{O}}}{\partial R}\cdot\frac{D[T-t]}{(T-t)}\alpha\big(\theta - r[t]\big) \\ + \frac{\partial^2 X^{\mathcal{O}}}{\partial R\partial S}\frac{D[T-t]}{(T-t)}\cdot\sigma_S\cdot S\cdot\sigma_r\cdot\chi + \frac{\partial^2 X^{\mathcal{O}}}{\partial R^2}\frac{D^2[T-t]}{(T-t)^2}\sigma_r^2\Bigg) \end{aligned}$$

to equal $r[t]\cdot X^{\mathcal{O}}$. But if the drift term differs from $r[t]\cdot X^{\mathcal{O}}$, the quotient $\frac{X^{\mathcal{O}}}{\beta}$ will not be a $\mathbb{Q}$-martingale, and by the Fundamental Theorem of Asset Pricing arbitrage is possible.

Looking somewhat more closely, the three securities with which we hedge VBS claims, β, S and X_0, all drift at rate $r[t]$ proportional to their value under $\mathbb{Q}$ (by design of $\mathbb{Q}$).

As long as $X^{\mathcal{O}}$ drifts at a rate different to $r[t] \cdot X^{\mathcal{O}}$, no possible admissable self-financing trading strategy will replicate the values of $X^{\mathcal{O}}$. While $X^{\mathcal{O}}$ drifts above (below) $r[t] \cdot X^{\mathcal{O}}$, cash flows into (from) the self-financing portfolio are required to keep replicating the value of $X^{\mathcal{O}}$. Arbitrage-free contingent claim pricing will drive the price of any claim X above (below) its OBS price $X^{\mathcal{O}}$ when there is a (suitably adjusted) expectation of cash flows into (from) the replicating portfolio.

For claims with a positive cross-partial derivative $\frac{\partial^2 X^{\mathcal{O}}}{\partial S \partial R}$, including European option prices $c^{\mathcal{O}}$ and $p^{\mathcal{O}}$, the drift (and hence the price) must be an increasing function of the correlation constant χ. This is consistent with the analytic observation of the sensitivity of $c^{\mathcal{V}}$ and $p^{\mathcal{V}}$ to χ.

5.2 Practical Advantages

Having raised a number of theoretical concerns regarding ρ-hedging, we note one significant practical benefit: computational ease. As will be illustrated in the next chapter, the computational burden arising from calculating prices in the two factor VBS model may far exceed those arising in the one factor OBS model. If the OBS prices and hedges are sufficiently close to their VBS counterparts, the practical trading savings from rapid calculation may exceed any losses from a theoretically imperfect model.

We have shown that, because the value of R does not influence the level or location of the European equity option payoff function conditional the stock price path, in-model and out-of-model hedges coincide when investing only in the stock and the expiry-dated discount bond. This does not hold for American equity options.

For the sake of consistency we will consider only out-of-model hedges which achieve interest rate exposure solely through the expiry-dated discount bond. Representing the out-of-model ρ-hedge by $\tilde{H}$ it follows that the holdings of stock, bond and bank account for the ρ-hedge portfolio for $C^{\mathcal{O}}$ are

$$\begin{aligned}
\tilde{H}^{\mathcal{O}}_{C;S}[t,\omega] &= \frac{\partial C^{\mathcal{O}}}{\partial S} \\
\tilde{H}^{\mathcal{O}}_{C;B[T]}[t,\omega] &= \frac{\partial C^{\mathcal{O}}}{\partial R} \Big/ \frac{\partial B[t,T]}{\partial R} = \frac{\partial C^{\mathcal{O}}}{\partial R} \cdot \frac{e^{R(T-t)}}{(T-t)} \\
\tilde{H}^{\mathcal{O}}_{C;\beta}[t,\omega] &= C^{\mathcal{O}} - \tilde{H}^{\mathcal{O}}_{C;S}[t,\omega] \cdot S[t] - \tilde{H}^{\mathcal{O}}_{C;B[T]}[t,\omega] \cdot B[t,T]
\end{aligned}$$

Similarly, those for the ρ-hedging portfolio for $P^{\mathcal{O}}$ are

$$\begin{aligned}
\tilde{H}^{\mathcal{O}}_{P;S}[t,\omega] &= \frac{\partial P^{\mathcal{O}}}{\partial S} \\
\tilde{H}^{\mathcal{O}}_{P;B[T]}[t,\omega] &= \frac{\partial P^{\mathcal{O}}}{\partial R} \cdot \frac{e^{R(T-t)}}{(T-t)} \\
\tilde{H}^{\mathcal{O}}_{P;\beta}[t,\omega] &= P^{\mathcal{O}} - \tilde{H}^{\mathcal{O}}_{P;S}[t,\omega] \cdot S[t] - \tilde{H}^{\mathcal{O}}_{P;B[T]}[t,\omega] \cdot B[t,T]
\end{aligned}$$

Lacking any analytic hold on either the derivatives $\frac{\partial \tilde{S}^{\mathcal{O}}_C[t]}{\partial R}$ or $\frac{\partial \tilde{S}^{\mathcal{O}}_P[t]}{\partial R}$ or the VBS hedge portfolios $\left(H^{\mathcal{V}}_{C;S}, H^{\mathcal{V}}_{C;B[T]}, H^{\mathcal{V}}_{C;\beta}\right)$ and $\left(H^{\mathcal{V}}_{P;S}, H^{\mathcal{V}}_{P;B[T]}, H^{\mathcal{V}}_{P;\beta}\right)$, we have no direct means of

comparison of the OBS ρ-hedge portfolio and the corresponding VBS in-model hedge portfolios. Rather, we will rely on numerical comparison to assess any practical benefits from ρ-hedging. To achieve this, we now turn our attention to the implementation of the models discussed in this part, which will be used to generate the numerical results in part III

Part II

Implementation

In Part I we developed prices and hedges for European and American equity options. Part III will use numerical values of these prices and hedges to compare the OBS and VBS models. This part shows how the preceeding theory and succeeding practice are linked.

The first chapter of this part outlines the numerical techniques used to approximate prices and hedges. Implementation of these techniques requires values for the model parameters. Calibration of such parameter values to the South African market is discussed in the second chapter of this part.

Chapter 6

Approximation Schemes

Knowing the cumulative Gaussian density $\Phi[\cdot]$, our prices for European equity option prices are simple to calculate. The function $\Phi[\cdot]$ is known to be intractable, but highly accurate approximations of its value are widely available. We use the **EXCEL** function **NORMSDIST**$(\cdot)$ to approximate $\Phi[\cdot]$.

When evaluation of $\Phi[\cdot]$ is in its tails, the option concerned is deep in- (or out-of-) the-money, and will require very significant movements of the stock price S to move out of (or respectively into) the money. The geometric Brownian motions 2.1a and 2.5a used to model S in the respective models are known to underestimate the chances of such extreme movements relative to empirical observation - particularly for large drops in S. In statistical parlance, real world stock prices (or, more accurately, their log-returns) are leptokurtotic.

When $\Phi[\cdot]$ is in its tails we are somewhat less concerned with relatively minor errors in evaluation of the option pricing formula than we are concerned with deep flaws in the formula itself. Hence our focus away from the tails.

This brief discussion concludes our examination of European option pricing and hedging. Unfortunately, the American equivalents are not nearly as tractable.

The rest of this section discusses our approximation of American option prices and hedges. We start by giving a justification and overview of partial differential equation approximations

6.1 Overview of Approximation Schemes

American equity option prices are presented in chapter 4 as optimal stopping problems. Even in their Markovian form, such problems are be difficult to approximate numerically. Most approaches use dynamic programming to implement Bellman's backward induction. However, proving the convergence of programming results to the true American option price requires some complex topology - see du Toit (2003) for an introduction. Furthermore, accuracy of any approximation will be specific to the approximation scheme chosen.

We choose instead to reformulate these prices as a free boundary partial differential equation. Proof of the duality of optimal stopping problems and free boundary problems is beyond the scope of this dissertation. However, such duality is well established - see van Moerbeke (1976) for an introduction, or Myneni (1992) for a listing of seminal papers.

The free boundary problem is so named as a Dirichlet condition is imposed along some unspecified boundary, whose location is determined by a Neumann condition operating concurrently at this boundary. The boundary location is determined as part of the solution.

For American option prices the Neumann condition at the free boundary ensures that the solution is maximal across all possible boundary locations. As our solution is optimal, it can be restated as a variational inequality. It is this variational inequality which leads to our numerical approximation scheme.

We truncate the domain, and divide this truncated domain into a regular mesh. At each point in the mesh we apply the variational inequality. Value constraints are easy to apply, but constraints on the partial derivatives require finite difference techniques.

Finite difference techniques are a tool for numerical solution of partial differential equations. At each point in the mesh they replace partial derivatives with partial difference approximations thereof. If, as the mesh becomes infinitely fine, the partial differences converge to the partial derivatives they are approximating, then the finite difference scheme is said to be consistent with the partial differential equation it is approximating.

In keeping with most financial literature, we use central differences to approximate the spatial partial derivatives. The choice of difference approximation temporal derivatives is more important, as it affects the properties of the finite difference scheme.

Backward[1] temporal differences allow for explicit calculation of the function value at each grid point, given values at the previous time step. Consequently such schemes are known as explicit finite differences. They may be interpreted as trinomial trees, permitting three branches in each spatial dimension one time step hence.

Explicit finite difference schemes possess unfortunate complications regarding stability. Stability refers to a diminishing effect of approximation errors. In unstable schemes these approximation errors are magnified through successive iterations. Explicit finite difference schemes are only stable for a limited set of parameter values. For parameter values outside this stable set the solution may oscillate wildly (and unreasonably) in the spatial dimension.

The use of forward temporal differences leads to implicit finite difference schemes. At each time step the function value at all corresponding nodes are interdependent, and need to be calculated simultaneously. This interdependence prevents the oscillations possible in explicit schemes, and ensures that the scheme is unconditionally stable. Stability comes at the price of increased computational burden.

The Crank-Nicolson scheme uses central temporal differences across each time step to approximate the temporal partial derivative. Like the implicit scheme it requires simultaneous co-determination of function values at each temporal iteration, and is unconditionally stable. This scheme can be expressed as an average of the explicit and implicit methods, but offers increased accuracy over both. While the explicit and implicit schemes are both accurate to $O(\delta S^2, \delta t)$, the Crank-Nicolson scheme is accurate to $O(\delta S^2, \delta t^2)$.

Stability is not merely a desirable characteristic. By the Lax Equivalence Theorem (see Habermann (1998)) a stable and consistent finite difference scheme will converge to the solution of the PDE it approximates. Such convergence is necessary for our finite difference results to bear relevance to the optimal stopping problems of interest.

Returning to our variational inequality, our solution must simultaneously satisfy constraints on its value and its partial derivatives. Discretisation imposes these constraints only at grid nodes, resulting in a linear complementarity problem.

When the finite differences are explicit, function values at each node may be altered

[1]Some texts may invert terminology, calling forward what we call backward, and vice-versa. This stems from analysis of the corresponding heat equation, transformation to which requires reversing the direction of time.

individually to ensure that both constraints are satisfied. Typically the finite difference approximation to the PDE is applied first. This results in new node values, which may be adjusted to meet the value constraint. As the scheme is explicit, implementation of the value inequality and of the finite difference scheme may be done separately.

This algorithm may be interpreted as a value correction to a discrete trinomial expectation. Algebraically it is equivalent to Bellman's backwards induction in a recombining trinomial tree.

Implicit finite difference schemes are unconditionally stable because they apply spatial derivatives at the nodes to be solved, thus preventing unstable oscillations. However, this means that subsequent adjustment of individual node values alters the spatial difference approximations at neighbouring nodes, thus invalidating the finite difference scheme. The solution to this linear complementarity problem requires approximation via an convergent iterative scheme. Though Jacobi and Gauss-Seidel schemes will work, Cryer's (1971) Projected Successive Over-Relaxation (PSOR) is far more efficient, and thus the method of choice.

6.2 Approximating American Options with Constant Rates

In Chapter 4 we established that, in the OBS model, an American equity call option $C^{\mathcal{O}}[t,S]$ has a Markovian representation, and is the solution to the optimal stopping problem

$$C^{\mathcal{O}}[t,S] = \mathbb{E}^{\mathbb{Q}}\left[e^{-R(\eta_t^C - t)}\left[S[\eta_t^C] - K\right]^+ \middle| \mathcal{F}_t\right] \tag{6.1a}$$

where η_t^C is the optimal stopping time, being the first time that the call option prices at intrinsic value, i.e.

$$\eta_t^C = \inf\left\{s \in [t,T] : C^{\mathcal{O}}\left[s, S[s]\right] = \left[S[s] - K\right]^+\right\} \tag{6.1b}$$

The corresponding free boundary PDE solves

$$\frac{\partial C^{\mathcal{O}}}{\partial t} + (R - \delta)S\frac{\partial C^{\mathcal{O}}}{\partial S} + \tfrac{1}{2}\sigma_S^2 S^2 \frac{\partial^2 C^{\mathcal{O}}}{\partial S^2} - RC^{\mathcal{O}} = 0 \tag{6.2a}$$

over the continuation area $\mathcal{C}_C^{\mathcal{O}}$, subject to the terminal condition

$$C^{\mathcal{O}}[T,S] = [S-K]^+ \tag{6.2b}$$

as well as the Dirichlet boundary condition

$$\lim_{S \downarrow 0} C^{\mathcal{O}}[t,S] = 0 \tag{6.2c}$$

and the additional Dirichlet condition

$$\lim_{S \uparrow \tilde{S}_C^{\mathcal{O}}[t]} C^{\mathcal{O}}[t,S] = [S-K]^+ \tag{6.2d}$$

On their own, the conditions (6.2a) -(6.2d) are insufficient to uniquely solve for $C^{\mathcal{O}}$, as the location of optimal stopping boundary $\tilde{S}_C^{\mathcal{O}}$ is not specified exogenously. Rather, the location of $\tilde{S}_C^{\mathcal{O}}$ maximises the value of $C^{\mathcal{O}}$. As the OEB $\tilde{S}_C^{\mathcal{O}}$ determines the exercise decision, any

curve of $\tilde{S}_C^{\mathcal{O}}$ not maximising the value of $C^{\mathcal{O}}$ would imply a sub-optimal exercise strategy. It transpires that, for this problem, the additional Neumann condition at the boundary $\tilde{S}_C^{\mathcal{O}}$,

$$\lim_{S \uparrow \tilde{S}_C^{\mathcal{O}}[t]} \frac{\partial C^{\mathcal{O}}[t,S]}{\partial S} = 1 \tag{6.2c}$$

(also called the smooth fit condition) is sufficient for the maximum to be achieved. Equation (6.2e) determines the location of $\tilde{S}_C^{\mathcal{O}}$ and thereby the values of the claim $C^{\mathcal{O}}$ throughout $\mathcal{C}_C^{\mathcal{O}}$. The smooth fit condition (6.2e) also fits neatly with our financial intuition, requiring the unit holdings of the hedge portfolio to be continuous across the OEB.

The notion of American equity options being free boundary problems is introduced by McKean (1965) and van Moerbeke (1976), and adapted to the arbitrage-free framework of Black and Scholes (1973) by Merton (1973).

This free boundary problem also solves the variational inequality

$$RC^{\mathcal{O}} - \frac{\partial C^{\mathcal{O}}}{\partial t} - (R-\delta)S\frac{\partial C^{\mathcal{O}}}{\partial S} - \tfrac{1}{2}\sigma_S^2 S^2 \frac{\partial^2 C^{\mathcal{O}}}{\partial S^2} \geq 0 \tag{6.3a}$$

$$C^{\mathcal{O}}[T,S] = \left[S-K\right]^+ \tag{6.3b}$$

$$C^{\mathcal{O}}[t,y] - \left[S-K\right]^+ \geq 0 \tag{6.3c}$$

$$\left(RC^{\mathcal{O}} - \frac{\partial C^{\mathcal{O}}}{\partial t} - (R-\delta)S\frac{\partial C^{\mathcal{O}}}{\partial S} - \tfrac{1}{2}\sigma_S^2 S^2 \frac{\partial^2 C^{\mathcal{O}}}{\partial S^2}\right)\left(C^{\mathcal{O}} - \left[S-K\right]^+\right) = 0 \tag{6.3d}$$

The variable $y = \ln S$ has constant instantaneous variance. Transforming our function to $\tilde{C}^{\mathcal{O}}[t,y] = C^{\mathcal{O}}[t,e^y]$ simplifies the necessary finite difference approximations. To satisfy the variational inequality (6.3a)-(6.3d), $\tilde{C}^{\mathcal{O}}$ must solve

$$R\tilde{C}^{\mathcal{O}} - \frac{\partial \tilde{C}^{\mathcal{O}}}{\partial t} - (R-\delta-\tfrac{1}{2}\sigma_S^2)\frac{\partial \tilde{C}^{\mathcal{O}}}{\partial y} - \tfrac{1}{2}\sigma_S^2 \frac{\partial^2 \tilde{C}^{\mathcal{O}}}{\partial y^2} > 0 \tag{6.4a}$$

$$\tilde{C}^{\mathcal{O}} = \left[e^y - K\right]^+ \tag{6.4b}$$

$$\tilde{C}^{\mathcal{O}}[t,y] - \left[S-K\right]^+ \geq 0 \tag{6.4c}$$

$$\left(R\tilde{C}^{\mathcal{O}} - \frac{\partial \tilde{C}^{\mathcal{O}}}{\partial t} - (R-\delta-\tfrac{1}{2}\sigma_S^2)\frac{\partial \tilde{C}^{\mathcal{O}}}{\partial S} - \tfrac{1}{2}\sigma_S^2 \frac{\partial^2 \tilde{C}^{\mathcal{O}}}{\partial y^2}\right)\left(\tilde{C}^{\mathcal{O}} - \left[e^y - K\right]^+\right) = 0 \tag{6.4d}$$

We limit our consideration of the domain $\tilde{\mathcal{D}}_C^{\mathcal{O}} = [0,T] \times (-\infty, \infty)$ of $\tilde{C}^{\mathcal{O}}$ to the finite rectangle $[0,T] \times [y_{\min}, y_{\max}]$. We impose a uniform grid over this limited domain with n_t evenly distributed temporal steps (i.e (n_t+1) evenly distributed temporal nodes) and n_y evenly distributed spatial steps.

Approximating the PDE in (6.4a) and (6.4d) by Crank-Nicolson finite differences leads to the constrained matrix problem

$$\mathbf{A}^C \times \hat{\mathbf{C}}_i^{\mathcal{O}} - \vec{\mathbf{D}}_i^C \geq 0 \tag{6.5a}$$

$$\hat{\mathbf{C}}_i^{\mathcal{O}} - \left[e^y - K\right]^+ \geq 0 \tag{6.5b}$$

$$\left(\mathbf{A}^C \times \hat{\mathbf{C}}_i^{\mathcal{O}} - \vec{\mathbf{D}}_i^C\right)\left(\hat{\mathbf{C}}_i^{\mathcal{O}} - \left[e^y - K\right]\right) = 0 \tag{6.5c}$$

for each $i \in (0, n_t - 1)$, where each constraint is applied element-wise, the vector

$$\hat{\mathbf{C}}_i^{\mathcal{O}} = \left(\hat{C}_{i,0}^{\mathcal{O}}, \hat{C}_{i,1}^{\mathcal{O}}, \cdots, \hat{C}_{i,n_y}^{\mathcal{O}}\right)'$$

approximates the vector of American equity call option values

$$\left(\widetilde{C}^{\mathcal{O}}[t_i, y_{\min}]\,,\, \widetilde{C}^{\mathcal{O}}[t_i, y_1]\,.\,\cdots\,,\, \widetilde{C}^{\mathcal{O}}[t_i, y_{\max}]\right)'$$

and the matrix $\mathbf{A}^C$ and vector $\vec{\mathbf{D}}_i^C$ are as defined in appendix C. This collection of constrained matrix problems is initiated by the terminal constraint $\hat{C}^{\mathcal{O}}_{n_t,j} = \left[e^{y_j} - K\right]^+$. Derivation of the approximation 6.5 of the variational inequality 6.4 is provided in appendix C.1.

Each constrained matrix problem (6.5a)-(6.5c) is solved using Projected Successive Over-Relaxation (PSOR). We begin with vector $\check{\mathbf{C}}_i^{\mathcal{O}(0)}$ populated by

$$\check{C}_{i,j}^{\mathcal{O}(0)} = \text{MAX}\left[\left[e^{y_j} - K\right]^+, \left(\left(\mathbf{A}^C\right)^{-1}\vec{\mathbf{D}}_i^C\right)_j\right]$$

which is our initial estimate of $\hat{\mathbf{C}}_i^{\mathcal{O}}$. We then iteratively modify this vector to get a better estimate of $\hat{\mathbf{C}}_i^{\mathcal{O}}$.

In each iteration we solve successively for each element of the vector $\check{C}_{i,j}^{\mathcal{O}(l)}$, starting at $j = 0$. Each solution involves establishing the intermediate value ς from the equation

$$A_{j,0}^C\,\check{C}_{i,0}^{\mathcal{O}(l)} + A_{j,1}^C\,\check{C}_{i,1}^{\mathcal{O}(l)} + \cdots + A_{j,j-1}^C\,\check{C}_{i,j-1}^{\mathcal{O}(l)} + A_{j,j}^C\,\varsigma + A_{j,j+1}^C\,\check{C}_{i,j+1}^{\mathcal{O}(l-1)} + \cdots + A_{j,n_y}^C\,\check{C}_{i,n_y}^{\mathcal{O}(l-1)} = \vec{D}_{i,j}^C \quad (6.6a)$$

and then setting

$$\check{C}_{i,j}^{\mathcal{O}(l+1)} = \text{MAX}\left[\check{C}_{i,j}^{\mathcal{O}(l)} + \pi\left(\varsigma - \check{C}_{i,j}^{\mathcal{O}(l)}\right),\, \left[e^{y_j} - K\right]^+\right] \quad (6.6b)$$

Equation (6.6b) simultaneously accelerates convergence of these iterations while ensuring the solution satisfies the constrained matrix problem. The PSOR system successively 'over-relaxes' each updated value ς by the factor π (not to be confused with the portfolio variable Π), and projects onto this over-relaxed value the constraint $\hat{C}_{i,j}^{\mathcal{O}(l+1)} \geq \left[e^{y_i} - K\right]^+$.

PSOR schemes converge for values of π between 0 and 2. For values of π greater than 1 any convergence for parabolic PDE's is faster than either Jacobi or Gauss-Seidel schemes. Burden and Faires (1997) show that one can calculate a value of π which maximises the convergence rate. Clewlow and Strickland (1997) counter that, because a new value is required at each time step i, such optimisation may take longer than adopting a fixed value of π.

These PSOR iterations continue until the process converges sufficiently. The approximation $\hat{\mathbf{C}}_i^{\mathcal{O}}$ of the price vector $\widetilde{\mathbf{C}}_i^{\mathcal{O}}$ is then set to the convergent vector $\check{\mathbf{C}}_i^{\mathcal{O}(l+1)}$, and iteration begins for the next time step backwards (i.e. approximating $\widetilde{\mathbf{C}}_{i-1}^{\mathcal{O}}$).

In subsequent chapters we graph the output from this approximation scheme. Where graphing requires function values not corresponding to any of the calculated node values we interpolate using quadratic functions in the original variables t and S.

The partial derivative of the call price with respect to the stock price plays an important role in determining the constituents of the hedging portfolio. Estimates of this derivative are taken from the gradient of the interpolating quadratic.

The location of the optimal exercise boundary $\tilde{S}_C^{\mathcal{O}}[t]$ cannot be determined exactly. It is, however, trivial to find the grid interval within which $\tilde{S}_C^{\mathcal{O}}[t_i]$ lies for any $i \in \mathbb{Z} : 0 \leq i \leq n_t$. We approximate the critical stock price $\tilde{S}_C^{\mathcal{O}}[t_i]$ where the quadratic in S passing through the three spatial nodes immediately below this interval intersects the intrinsic value curve $\left[S - K\right]^+$.

Finally the partial derivative with respect to the instantaneous price of money R needs to be determined across different calibrations of the OBS model. This requires separate runs of the PSOR scheme for different values of R. We divide the range of R into uniform intervals of size ΔR, and approximate the derivative $\frac{\partial C^{\mathcal{O}}}{\partial R}$ by central differences.

American equity put options are approximated similarly. A more detailed derivation of the algorithms used to approximated both calls and puts is presented in appendix C.

6.3 Approximating American Options with Vasicek Rates

Unlike the pricing of American equity options under the OBS assumptions, the problem of pricing American equity options with stochastic interest rates is not widely studied. In particular, there are no well-developed approximation techniques which we can take 'off-the-shelf' and apply. Consequently it is necessary to develop our own scheme particular to the problem at hand.

The two-dimensional trinomial tree suggested by Hull and White (1994B) could be applied to our problem. Indeed Menkveld and Vorst (2000) apply it to a slightly more general case. However, we have concerns regarding the consistency (and hence convergence) of this scheme, discussed later in this section, and so choose to develop our own scheme.

As in the previous section, we take the optimal stopping problem of interest, viz.

$$C^{\mathcal{V}}[t,S,r] = \mathbb{E}^{\mathbb{Q}}\left[\frac{\beta[t]}{\beta[\eta_t^C]}\left[S[\eta_t^C]-K\right]^+\middle|\,\mathcal{F}_t\right] \tag{6.7a}$$

where

$$\eta_t^C = \inf\left\{s\in[t,T] : C^{\mathcal{V}}[t,S,r] = \left[S[s]-K\right]^+\right\} \tag{6.7b}$$

and transform it into the free boundary PDE satisfying

$$\frac{\partial C^{\mathcal{V}}}{\partial t} + (r-\delta)S\frac{\partial C^{\mathcal{V}}}{\partial S} + \alpha(\theta-r)\frac{\partial C^{\mathcal{V}}}{\partial r} + \tfrac{1}{2}\sigma_S^2 S^2\frac{\partial^2 C^{\mathcal{V}}}{\partial S^2} + \sigma_S\sigma_r\chi S\frac{\partial^2 C^{\mathcal{V}}}{\partial S\partial r} + \tfrac{1}{2}\sigma_r^2\frac{\partial^2 C^{\mathcal{V}}}{\partial r^2} - rC^{\mathcal{V}} = 0 \tag{6.8a}$$

over the continuation region $\mathcal{C}_C^{\mathcal{V}}$, with the terminal condition

$$C^{\mathcal{V}}[T,S,r] = \left[S-K\right]^+ \tag{6.8b}$$

subject to the Dirichlet conditions

$$\lim_{S\downarrow 0} C^{\mathcal{V}}[t,S,r] = 0 \tag{6.8c}$$

$$\lim_{r\uparrow\infty} C^{\mathcal{V}}[t,S,r] = Se^{-\delta(T-t)} \tag{6.8d}$$

with the additional Dirichlet conditions

$$\lim_{S\downarrow\hat{S}_C^{\mathcal{V}}[t,r]} C^{\mathcal{V}}[t,S,r] = \left[S-K\right]^+ \tag{6.8e}$$

$$\lim_{r\downarrow\hat{r}_C^{\mathcal{V}}[t,S]} C^{\mathcal{V}}[t,S,r] = \left[S-K\right]^+ \tag{6.8f}$$

at the optimal exercise boundary, whose location is determined by the Neumann conditions

$$\lim_{S \uparrow \tilde{S}_C^{\mathcal{V}}[t,r]} \frac{\partial C^{\mathcal{V}}[t.S,r]}{\partial S} = 1 \tag{6.8g}$$

$$\lim_{r \downarrow \tilde{r}_C^{\mathcal{V}}[t,S]} \frac{\partial C^{\mathcal{V}}[t.S,r]}{\partial r} = 0 \tag{6.8h}$$

The conditions (6.8g) and (6.8h) ensure both that the price $C^{\mathcal{V}}$ is always maximised over all possible locations of the OEB, and also that the hedge portfolio holdings are continuous over the OEB. While these conditions carry a financial intuition, they are neither mathematically obvious nor easy to prove.

However our stopping time is optimal, and the price $C^{\mathcal{V}}$ is maximal over all locations of the free boundary. Consequently, we can omit proofs of the Neumann conditions at the free boundary, restating the free boundary problem (6.8a) - (6.8h) as the variational inequality

$$\frac{\partial C^{\mathcal{V}}}{\partial t} + (r-\delta)S\frac{\partial C^{\mathcal{V}}}{\partial S} + \alpha(\theta - r)\frac{\partial C^{\mathcal{V}}}{\partial r} + \tfrac{1}{2}\sigma_S^2 S^2 \frac{\partial^2 C^{\mathcal{V}}}{\partial S^2} + \sigma_S \sigma_r \chi S \frac{\partial^2 C^{\mathcal{V}}}{\partial S \partial r} + \tfrac{1}{2}\sigma_r^2 \frac{\partial^2 C^{\mathcal{V}}}{\partial r^2} - rC^{\mathcal{V}} \geq 0 \tag{6.9a}$$

$$C^{\mathcal{V}}[T,S,r] = [S-K]^+ \tag{6.9b}$$

$$C^{\mathcal{V}}[t.S,r] \geq [S-K]^+ \tag{6.9c}$$

$$\left(\frac{\partial C^{\mathcal{V}}}{\partial t} + (r-\delta)S\frac{\partial C^{\mathcal{V}}}{\partial S} + \alpha(\theta - r)\frac{\partial C^{\mathcal{V}}}{\partial r} + \tfrac{1}{2}\sigma_S^2 S^2 \frac{\partial^2 C^{\mathcal{V}}}{\partial S^2} + \tfrac{1}{2}\sigma_r^2 \frac{\partial^2 C^{\mathcal{V}}}{\partial r^2} + \sigma_S \sigma_r S \chi \frac{\partial^2 C^{\mathcal{V}}}{\partial S \partial r} - rC^{\mathcal{V}}\right) \times \left(C^{\mathcal{V}} - [S-K]^+\right) = 0 \tag{6.9d}$$

Now define the orthogonal variables

$$z_1[S,r] = \sigma_r \cdot \ln[S] + \sigma_S \cdot r \tag{6.10a}$$

$$z_2[S,r] = \sigma_r \cdot \ln[S] - \sigma_S \cdot r \tag{6.10b}$$

both of which have constant instantaneous variance. Approximating the new function

$$\widetilde{C}^{\mathcal{V}}[t.z_1,z_2] : [0,T] \times (-\infty,\infty) \times (-\infty,\infty) \mapsto \mathbb{R}$$

defined by

$$\widetilde{C}^{\mathcal{V}}[t,z_1,z_2] = C^{\mathcal{V}}\left[t.\exp\left[\tfrac{z_1+z_2}{2\sigma_S}\right], \tfrac{z_1-z_2}{2\sigma_r}\right] \tag{6.11}$$

proves to be simpler than approximating $C^{\mathcal{V}}$ directly. In particular, the orthogonality of z_1 and z_2 assist the stability analysis later in this section.

Applied to $\widetilde{C}^{\mathcal{V}}$ the variational inequality (6.9a)-(6.9d) becomes

$$\frac{\partial \widetilde{C}^{\mathcal{V}}}{\partial t} + \mu_1 \frac{\partial \widetilde{C}^{\mathcal{V}}}{\partial z_1} + \mu_2 \frac{\partial \widetilde{C}^{\mathcal{V}}}{\partial z_2} + \tfrac{1}{2}\sigma_1^2 \frac{\partial^2 \widetilde{C}^{\mathcal{V}}}{\partial z_1^2} + \tfrac{1}{2}\sigma_2^2 \frac{\partial^2 \widetilde{C}^{\mathcal{V}}}{\partial z_2^2} - \tfrac{z_1 - z_2}{2\sigma_S} \cdot \widetilde{C}^{\mathcal{V}} \geq 0 \tag{6.12a}$$

$$\widetilde{C}^{\mathcal{V}}[T, z_1, z_2] = \left[\tfrac{z_1 + z_2}{2\sigma_r} - K\right]^+ \tag{6.12b}$$

$$\widetilde{C}^{\mathcal{V}}[t, z_1, z_2] \geq \left[\tfrac{z_1 + z_2}{2\sigma_r} - K\right]^+ \tag{6.12c}$$

$$\left(\frac{\partial \widetilde{C}^{\mathcal{V}}}{\partial t} + \mu_1 \frac{\partial \widetilde{C}^{\mathcal{V}}}{\partial z_1} - \mu_2 \frac{\partial \widetilde{C}^{\mathcal{V}}}{\partial z_2} + \tfrac{1}{2}\sigma_1^2 \frac{\partial^2 \widetilde{C}^{\mathcal{V}}}{\partial z_1^2} + \tfrac{1}{2}\sigma_2^2 \frac{\partial^2 \widetilde{C}^{\mathcal{V}}}{\partial z_2^2} - \tfrac{z_1 - z_2}{2\sigma_S} \cdot \widetilde{C}^{\mathcal{V}}\right) \times \left(\widetilde{C}^{\mathcal{V}} - \left[\tfrac{z_1 + z_2}{2\sigma_r} - K\right]^+\right) = 0 \tag{6.12d}$$

In choosing temporal differences, we reject forward (i.e. implicit) schemes in favour (simpler) explicit schemes.

With more than one spatial dimension, implicit approximation of parabolic partial differential equations becomes increasingly complex - relying on repetitive schemes such as alternating difference implied (ADI) methods. Any approximation of the solution to a variational inequality which uses implicit finite differences needs to simultaneously solve a complex finite difference scheme as well all the other constraints. The PSOR scheme in section 6.2 achieved this in one dimension. The author has seen no corresponding algorithm for more dimensions, and fears that any such algorithm may be excessively computationally burdensome.

Explicit finite difference schemes do not suffer from such complexities. As discussed, because each node is explicitly calculated independently, any value inequality may be applied independently at each node without affecting the PDE inequality. This simplicity motivates our choice explicit finite differences.

Across an appropriate subset (discussed in appendix C) of the domain of $\widetilde{C}^{\mathcal{V}}$ we place regularly spaced nodes at intervals of Δt, Δ_1 and Δ_2 in the variables t, z_1 and z_2 respectively. In order to minimise the approximation error of our partial difference equations it is appropriate (see Hull and White (1990A) of Habermann (1998) ex. 6.3.1) to set

$$\Delta_1 = \sqrt{3\sigma_1^2 \Delta t} \qquad \Delta_2 = \sqrt{3\sigma_2^2 \Delta t} \tag{6.13}$$

where σ_1 and σ_2 are the (constant) instantaneous volatilities of z_1 and z_2 respectively, defined fully in appendix C.

Setting i, j and k to index nodes in the dimensions t, z_1 and z_2 respecitively, let $\hat{C}^{\mathcal{V}}_{i,j,k}$ be our approximation of $\widetilde{C}^{\mathcal{V}}[t_i, z_{1,j}, z_{2,k}]$. Backwards temporal differences and central spatial differences approximate the variational inequality (6.12a)-(6.12d) by

$$\hat{C}^{\mathcal{V}}_{i,j,k} = \text{MAX}\left[\check{C}^{\mathcal{V}}_{i,j,k}, \left[\exp\left[\tfrac{z_1 + z_2}{2\sigma_S}\right] - K\right]^+\right] \tag{6.14a}$$

where

$$\begin{aligned}\check{C}^{\mathcal{V}}_{i-1,j,k}\left[1 + \tfrac{z_{1,j} - z_{2,k}}{2\sigma_r}\Delta t\right] = {} & q_1^d q_2^d \hat{C}^{\mathcal{V}}_{i,j-1,k-1} + q_1^d q_2^m \hat{C}^{\mathcal{V}}_{i,j-1,k} + q_1^d q_2^u \hat{C}^{\mathcal{V}}_{i,j-1,k+1} \\ & + q_1^m q_2^d \hat{C}^{\mathcal{V}}_{i,j,k-1} + q_1^m q_2^m \hat{C}^{\mathcal{V}}_{i,j,k} + q_1^m q_2^u \hat{C}^{\mathcal{V}}_{i,j,k+1} \\ & + q_1^u q_2^d \hat{C}^{\mathcal{V}}_{i,j+1,k-1} + q_1^u q_2^m \hat{C}^{\mathcal{V}}_{i,j+1,k} + q_1^u q_2^u \hat{C}^{\mathcal{V}}_{i,j+1,k+1}\end{aligned} \tag{6.14b}$$

with

$$q_1^d = \frac{1}{2}\left(\frac{1}{3} - \frac{\mu_1\Delta t}{\Delta_1} + \left(\frac{\mu_1\Delta t}{\Delta_1}\right)^2\right) \tag{6.15a}$$

$$q_1^m = \frac{2}{3} - \left(\frac{\mu_1\Delta t}{\Delta_1}\right)^2 \tag{6.15b}$$

$$q_1^u = \frac{1}{2}\left(\frac{1}{3} + \frac{\mu_1\Delta t}{\Delta_1} + \left(\frac{\mu_1\Delta t}{\Delta_1}\right)^2\right) \tag{6.15c}$$

and

$$q_2^d = \frac{1}{2}\left(\frac{1}{3} - \frac{\mu_2\Delta t}{\Delta_1} + \left(\frac{\mu_2\Delta t}{\Delta_1}\right)^2\right) \tag{6.16a}$$

$$q_2^m = \frac{2}{3} - \left(\frac{\mu_2\Delta t}{\Delta_1}\right)^2 \tag{6.16b}$$

$$q_2^u = \frac{1}{2}\left(\frac{1}{3} + \frac{\mu_2\Delta t}{\Delta_1} + \left(\frac{\mu_2\Delta t}{\Delta_1}\right)^2\right) \tag{6.16c}$$

where μ_1 and μ_2 are the instantaneous drifts of z_1 and z_2 respectively under the risk-neutral measure $\mathbb{Q}$.

Note that the q's can be interpreted as the probabilities of up, down and no movement in the z's. As the z's are orthogonal, the joint probabilities are the products of the marginal probabilities. In this interpretation the scheme (6.14a),(6.14b) is the dynamic programming solution to our optimal stopping problem. Under the probabilities q the first two centered moments of the z's agree with their moments under $\mathbb{Q}$.

The simplicity of the explicit finite difference method comes at the cost of instability. There is no guarantee that the scheme described above is stable. In general, stability analysis of multi-dimensional explicit finite difference schemes is difficult and intricate. However, for the scheme to be stable it is sufficient for the weights applied to each previous node to be positive[2] (i.e. for the 'probabilities' q to be positive.)

When the variables concerned are correlated, negative weightings may occur. Hull and White (1994B) suggest altering the correlation coefficient χ at any node where any of the joint probabilities become negative, so as to ensure non-negative weights. They concede that these alterations induce a bias in χ towards zero. Indeed the consistency (and hence convergence) of such a scheme is not immediately obvious.

Our solution to this problem is to orthogonalise the variables. This removes the scope for complexities arising out of correlation, leaving only the marginal probabilities to be examined.

Through their dependence on the drifts μ_1 and μ_2 the marginal probabilities q are quadratic functions of the short rate r. To properly consider the sign of the q's we need to consider the value of the short rate r at all points where this scheme is implemented.

Spatial boundary conditions cannot be used with the explicit scheme outlined above. In the univariate scheme known functions applied at the extrema of the domain. The interaction between separate independent variables prevents us from knowing which values to apply along the border of our domain. (Consider the example where the short rate r is at its maximum - suggesting the call is best exercised immediately - but the stock price S is at its minimum - implying no value to exercising immediately.)

[2]My thanks to Prof. Ken Vetzal for pointing this out to me

Furthermore, mean reversion of the variables z_1 and z_2 can never be sufficiently strong along the entire border to implement the implied boundary conditions discussed by Vetzal (1998).

As boundary conditions cannot be implemented, the entire domain considered must depend only on the terminal condition. In essence the twigs of the tree must branch out far enough to support calculations in the trunk. (A more apt comparison would invert the tree, requiring the roots to spread out sufficiently far to support the trunk.)

This requirement proves to be fairly onerous, demanding a very large number of calculations to support only a small area of interest. As the interval Δt (and hence also Δ_1 and Δ_2) becomes smaller, an increasingly high proportion of the calculation nodes become located in the far tails of the $\mathbb{Q}$ distributions of r and S. This waste of resources is an unfortunate necessity.

For the scheme to be stable, we will require the marginal probabilities q to positive at every calculation node. It transpires that there are two limits on the length of the life of the option - one each relating to z_1 and z_2 - beyond either of which the scheme may not be stable. These limits are

$$T < \frac{2\sigma_S\sqrt{\frac{2}{3}}}{\left(1+\frac{\sigma_2}{\sigma_1}\right)\left|\nu_1^1\right|} \tag{6.17a}$$

and

$$T < \frac{2\sigma_S\sqrt{\frac{2}{3}}}{\left(\frac{\sigma_1}{\sigma_2}+1\right)\left|\nu_2^1\right|} \tag{6.17b}$$

where σ_1 and σ_2 are the instantaneous volatilities of z_1 and z_2, while ν_1^1 and ν_2^1 are the linear coefficients of r in the drifts of z_1 and z_2 respectively.

For any option horizon satisfying these constraints it is possible to build a stable scheme. Such stability requires the time step Δt to itself satisfy an number of conditional constraints, all discussed in appendix C.

Thus we have a stable and consistent scheme for approximating $\widetilde{C}^{\mathcal{V}}$. To obtain approximations of $\widetilde{C}^{\mathcal{V}}$ for values of z_1 and z_2 not corresponding exactly to the calculated nodes we employ quadratic interpolation. We also use the interpolating quadratic to estimate partial derivatives in z_1 and z_2, from which the partial derivatives of $C^{\mathcal{V}}$ in S and r follow easily.

This scheme has been checked extensively in pricing contingent claims for which closed-form solutions exist, such as discount bonds and European equity options, and proved remarkably accurate in such tests.

A detailed derivation of this explicit finite difference scheme, including the derivation of the probabilities q and the stability inequalities, is provided in appendix C.

American put options prices and hedges are approximated similarly.

Chapter 7

Calibrations

Before we can implement numerical techniques to quantify the difference between two distinct models, we need to assign values to the parameters in each model. We will calibrate the VBS model to the South African market, and in later chapters compare the results from this model to those from the OBS model applied in this setting.

In our context, contingent claim prices will be uniquely determined by six parameters: σ_S, the volatility of the stock price S; δ, the dividend yield of the stock concerned; θ, α and σ_r, the mean, mean reversion rate and volatility respectively of the short rate r (all under the measure $\mathbb{Q}$); and by χ, the correlation between stock price uncertainty and interest rate uncertainty.

We deal with each parameter in turn. Our intention is to estimate parameters under which our models can plausibly be applied to the South African financial markets in at the beginning of 2005. Such application need only be plausible, not necessarily accurate.

Any further accuracy achieved through parameter fitting may be spurious. The models used are by construction simplistic, omitting many market features including (but not limited to) taxation, bid/ask spread, liquidity limitations and additional sources of noise (most notably stochastic volatility). This simplicity enhances model tractability at the cost of the flexibility required to increase the accuracy of market models and hence contingent claim prices[1].

Where possible we calibrate to current market prices and the prospective market dynamics which they imply. As validation of such calibrations, or where the desired information cannot be obtained from market data, we turn to observations of past market quotes.

Conventionally, statistics are estimated of an interval of equal or greater length to the interval over which they are applied. Calculations in the following chapters price options with maturities out to three years. We will estimate our parameters using market data from the beginning of 2001 to mid-February 2005. All data are taken from Bloomberg terminals, with the exception of the yield curves in figures 7.4 and 7.5 taken from the Bond Exchange of South Africa website (www.bondex.co.za) on 15 February 2005.

As a small and open economy South Africa is succeptible to external shocks, both through external events themselves and through exchange rate fluctuations affecting the terms of trade with other countries. As a prelude to our calibrations we present and briefly discuss observed

[1] As discussed in Chapter 1, the choice of the Vasicek (1977) model over the Hull-White (1990b) model for short rate movements reduces the number of parameters which induce differences between the two results sets (i.e. results with and without a stochastic shortrate). This simplifies the task of result comparison and cause determination.

value and volatility of the South African Rand (ZAR), as measured by the U.S. dollar cost of ZAR.

Figure 7.1: Observed value and historical volatility of ZAR, 2001-2004

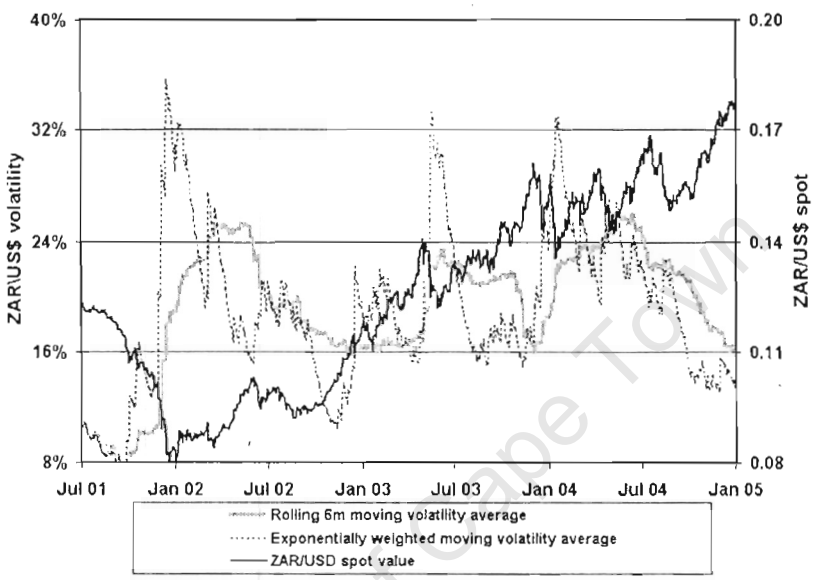

December 2001 is of particular interest. ZAR lost one fifth of its dollar value, suffering significant successive inter-day losses which drove up its observed historical volatility. As we will see, this movement impacted both South African stock and, to a lesser extent, interest rate markets.

High exchange rate volatility was also observed in both June 2003 and January 2004. These periods did not however involve material revaluation of the currency, only large but opposing daily movements. The material and unexpected currency revaluation in December 2001 appears to have impacted on domestic markets more than the increase in currency volatility.

Also, the terrorist attacks on September 11 2001 have clear effects on domestic markets, both through their interruption of global financial markets and through the uncertainty regarding their probable repercussions.

7.1 Stock Price Parameters

As a representative statistic for South African equities we select the ALSI 40 index - a weighted[2] average of the largest 40 companies traded on the JSE securities exchange[3]. The majority of equity options traded in South Africa are based on this index, giving potential practical relevance to our results. It is also frequently used as a market proxy for valuing

[2]During the estimation period such weighting changed from pure market capitalisation weighting to (more subjective) free-float weighting

[3]See www.jse.co.za, particularly the Glossary page, for details

individual equities using the Capital Asset Pricing Model - though individual shares would by-and-large exhibit larger volatility.

7.1.1 Stock Price Volatility σ_S

Since the contingent claims we price are all equity options, the most important parameter concerns the uncertainty regarding stock price movements. We desire a value of stock price volatility, σ_S, which can plausibly hold to maturities of 1 and 3 years hence (the horizons at which we price our options).

In one sense, such a value can readilly be determined from SAFEX[4] prices. Table 7.1 provides the mark-to-market implied volatilities[5] on 15 February 2005 for a selection of traded at-the-money options with differing expiries:

Table 7.1: At-the-money SAFEX ALSI volatilities, 15 February 2005

Expiry	M-T-M Implied volatility
March 2005	15%
June 2005	13%
September 2005	15%
December 2005	16%
March 2006	17%
March 2007	19%

The table exhibits increasing volatility with term to expiry, typical of most option markets. From the table also, 20% appears a reasonable flat estimate of volatility over the periods of time we will consider - slightly lower than the one-year implied volatility of around 17%, but probably slightly less than the three-year implied volatility.

In another sense such data carries little value. The volatilities listed in table 7.1 are merely that number which, when inserted into the SAFEX-Black price formula (similar to Black-Scholes), justify the current trading price. We have no knowledge of the models used by market participants, so cannot conclude that these implied volatilities are a consensus forecast of prospective volatility of the stock price volatility.

Unlike developed markets such as the U.S. or the U.K., South Africa has no openly traded measure of stock volatility. Lacking prospective estimates, our best source of information comes from observed stock movements.

We are truly interested in the volatility of S under $\mathbb{Q}$, but can only observe the dynamics of S in the real world $\mathbb{P}$. Fortunately, the Girsanov transformation (3.5) used to move from the $\mathbb{P}$-dynamics (2.5a) of S to the $\mathbb{Q}$-dynamics (3.7c) of S affect only the drift of S, not its volatility. Hence volatility is the same under the two measures, and real world estimates of volatility remain relevant to calibration.

Figure 7.2 charts two measures of observed volatility of the ALSI40: rolling six month

[4]The South African Futures Exchange, now a subsidiary of the JSE Securities Exchange

[5]See The SAFEX website www.safex.co.za for details on the pricing, marking-to-market and settlement of these traded options

historical volatility[6] and also an exponentially weighted moving average[7] with a daily residual weight of 98%[8].

Figure 7.2: Observed historical ALSI 40 volatility , 2 July 2001 to 3 January 2005

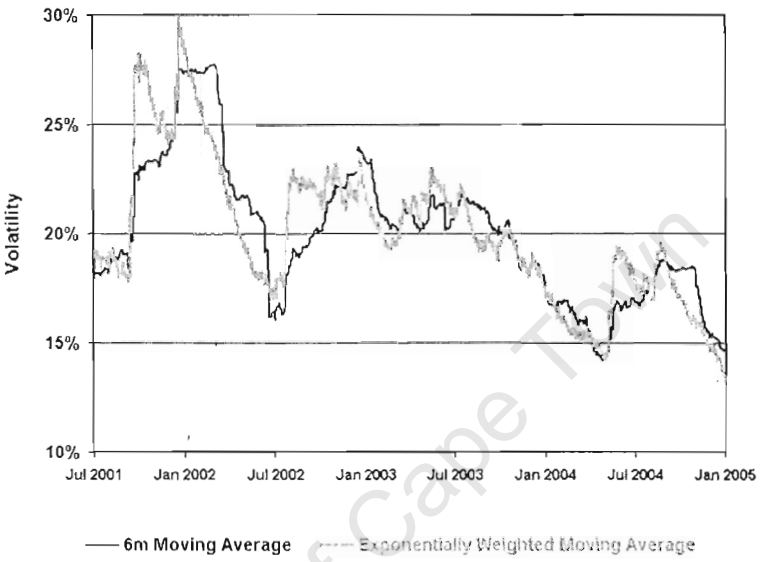

Observed ALSI volatility reached highs of over 25% after the 9/11 attacks and the December 2001 Rand crisis. For the remainder of the estimation period ALSI volatility dropped towards current lows just below 15%, with small upward shocks along the way largely associated with unexpected changes in domestic monetary policy. At the midrange of observed volatility levels over four years of estimation, our volatility estimate of 20% is within plausible bounds.

7.1.2 Stock Dividend Yields δ

The dividend yield on the ALSI, represented by δ, is a far less significant input into option pricing. Though prospective dividend yields are not directly traded, implied values can be extracted from traded futures prices[9]. Table 7.2 presents the dividend yields implied by closing quotes on 3 January 2005 for futures on the ALSI 40 with a variety of expiry dates.

[6]more precisely the standard deviation of the log-returns of the past 128 working days' log-returns, annualised at 256 working days per year

[7]Employing the methodology in Hull(2000) this is more accurately an estimate of the square root of the mean squared change. This is carried through to all other exponentially weighted moving averages. The bias between the measured value and stock volatility decreases with an increase in sampling frequency. Sampled at daily intervals, our estimates' bias is significantly less than any bounds of uncertainty or of convenient rounding.

[8]RiskMetrics use a residual weight of 94%for daily VaR calculations; we justify a larger weight due to a significantly longer horizon of consideration

[9]We extract such values by treating forward and futures prices as equivalent. It is well known (see e.g. Hull (2000) Section 3.6) that, when interest rates are stochastic and correlated with stock prices, futures and

Table 7.2: Dividend Yields implied by Closing Futures Prices, 3 January 2005

Expiry	Closing Futures Price	Spot Rate to Expiry	Implied Dividend Yield
March 2005	11633	7.7%	3.5%
June 2005	11738	7.4%	3.5%
September 2005	11816	7.4%	4.0%
December 2005	11913	7.2%	3.9%
March 2006	11988	7.3%	4.1 %
March 2007	12368	7.5%	4.3%
Spot Price :	11537	—	—

As with stock volatility levels, comparison of prospective and historic dividend yield levels is instructive. Figure 7.3 illustrates observed dividend yields[10] for the period from 1 October 2002 to 3 January 2005.[11]:

Figure 7.3: Observed dividend yields on the ALSI 40, 1 October 2002 to 3 January 2005

Both historic and implied dividend yields vary between 2% and 5%. The midpoint of this

forward prices differ. However, any peturbations in dividend yield estimates caused by stock-rate correlation will not significantly alter the numerical results in chapters 8 and 9. See section 7.3 for investigations into the level of stock-rate correlation.

[10]Measured by total dividends in the previous 12 months divided by current index level, and converted to a continuous rate for comparison to δ.

[11]Comparable dividend yields prior to October 2002 are not available due to the change of ALSI weights from market capitalisation to free-float.

range is 3.5%. but after considering the downward trend in historic yields we choose to price our options using a dividend yield of 3%. The gap between our choice of dividend yield and that implied by futures prices may be explained by an incorrect choice of yield curve or of pricing model, but shows that our choice remains plausible.

7.2 Short Rate Parameters

Consideration of prospective values for parameters of the short rate process exposes a chasm between our theory and market practice, as highlighted throught this section.

7.2.1 Yield Curve Fitting

Vasicek (1977) showed that his model for short rate movements can only produce spot rate curves which are normal (i.e. increasing with term to maturity), inverted (decreasing with term to maturity) or, under a very limited range of parameters, humped.(i.e. increase, then decrease. with term to maturity).

Throughout early 2005 the South African yield curve has exhibited a strong dip around one year to maturity, with a mild hump around nine years to maturity. Figure 7.4 illustrates this clearly:

Figure 7.4: South African Yield Curve on 15 February 2005

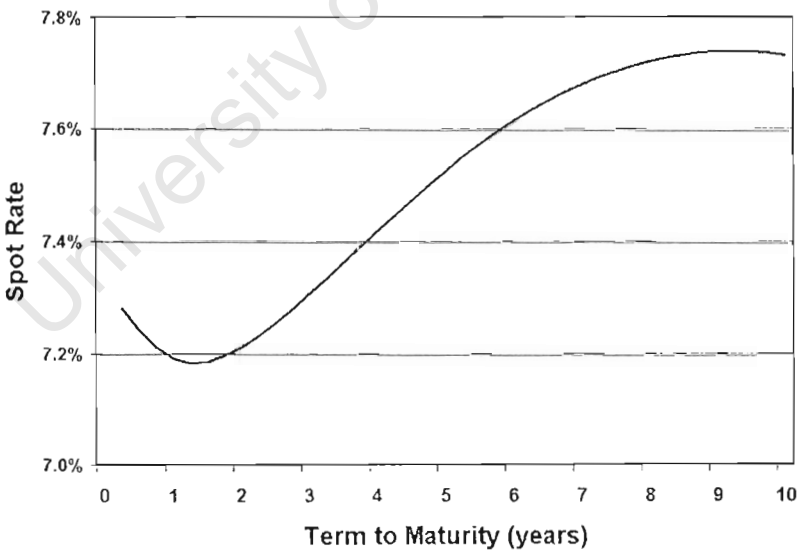

The Vasicek model cannot be calibrated to reproduce a spot rate curve with these shapes. A bit of investigation leads to at least one major discrepancy between theoretical assumptions and practical execution.

All short-term (three month and shorter) interest rates in South Africa closely follow the South African Reserve Bank (SARB) repurchase (repo) rate. Far from following a (continuous) mean-reverting Brownian motion with instantaneous trading and infinitely many

potential values, the repo rate is reset by the SARB only at its Monetary Policy Committee meetings - typically bimonthly - and only moves in units of 25 basis points[12]. While our assumptions regarding interest rate dynamics may be sufficiently accurate for long- and even perhaps medium-term views, they fail dismally in the short term.

Since March 2000 the SARB has been tasked to use its control of monetary policy solely to target inflation. The relevant inflation level at the time of calibration (early 2005) is approaching the lower end of its target band. The spot curve dip reflects market expectations of coming repo rate cuts in order to keep inflation within its targets. Thereafter rising spot rates are caused both by expectations of repo rate increases to tame rising inflationary pressures, and by a growing contribution of term premia to spot rates.

If we conveniently ignore the first two years of the spot rate curve, covering the observed dip, a satisfactory visual fit to the remainder of the curve can be achieved using the parameter values

$$\alpha = 6.666\% = \frac{1}{15} \qquad \theta = 9\%$$
$$\sigma_r = 2\% \qquad r = 6.8\%$$

Figure 7.5 compares the yield curve obtained from these parameters to the one illustrated in figure 7.4. It could be argued that the fitted curve resembles the yield curve which may arise should the SARB immediately effect a 50 b.p. cut in the repo rate - a cut which was considered a possibility for the December MPC meeting[13].

Figure 7.5: Fitted and Observed Yield Curves, 15 February 2005

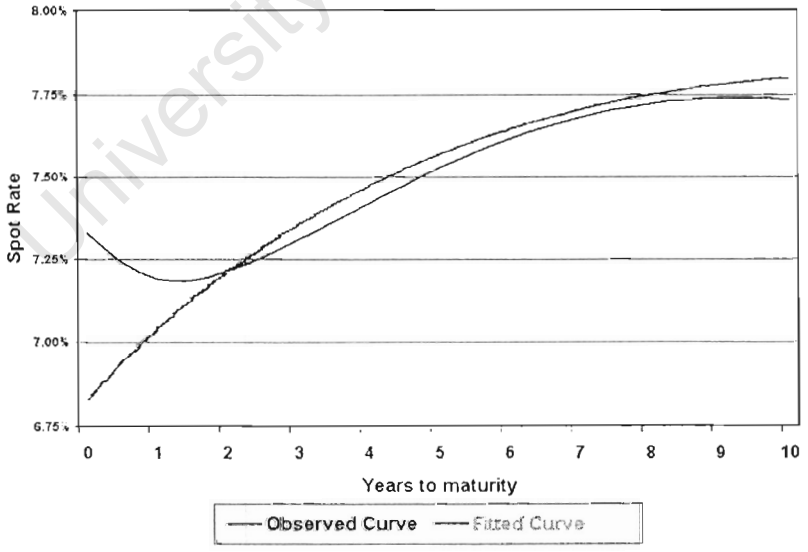

We note here that we have started to fit the market to the model, not vice-versa. This is justifiable only in light of this dissertation's stated aim of comparing two pricing models.

[12] 1 basis point (b.p.) = 0.01%

[13] Indeed a cut of 50 basis points followed this calibration at the MPC meeting on 18 April 2005

But it results in calculated option prices which may differ substantially from observed market prices.

7.2.2 Spot Rate Volatility σ_r

As with the stock price, the Girsanov kernel which transforms the dynamics of the short rate r from the real world probability measure $\mathbb{P}$ to the risk-neutral probability measure $\mathbb{Q}$ leaves the short rate volatility σ_r unaffected. Thus we can compare our fitted value of σ_r to past observations of short rate volatility. (This is not true for θ and α, both of which are drift-related, and hence affected by the transformation).

Because of the discrete movements in time and level of the repo rate, overnight borrowing rates are a poor statistic from which to estimate short rate volatility. We choose instead the volatility of the 3×6 FRA[14], which closely approximates the short rate volatility[15]. Figure 7.6 charts both a six month rolling moving average and an exponentially weighted moving average of observed 3×6 FRA rate volatility, calculated from data for the years 2001-2004. During periods of stable monetary policy, FRA volatility appears to stay between 1% and $1\frac{1}{2}$%. This observation is consistent with estimates derived in Svoboda (2001) for a related model by inverting the price of over-the-counter bond option trades, estimated over a similarly stable period of monetary policy.

Figure 7.6: Observed 3×6 FRA volatility, 2 July 2001 to 3 January 2005

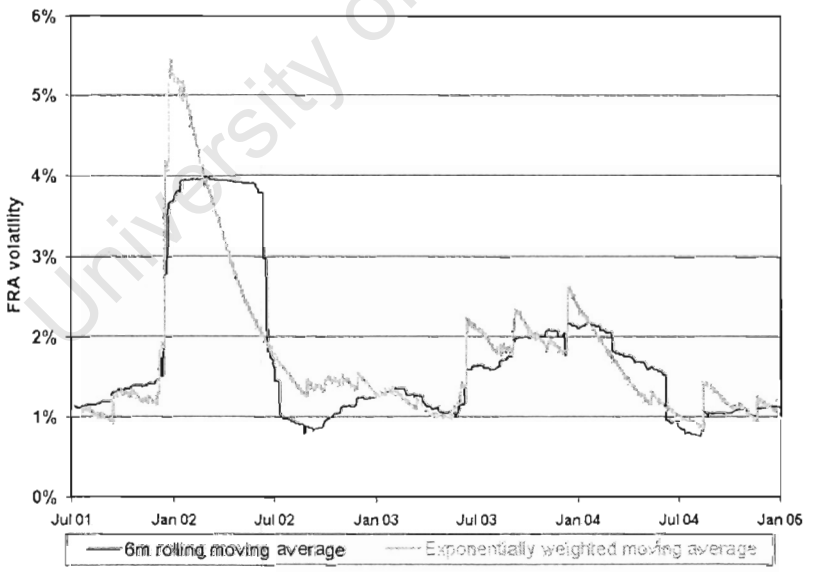

There are, however, periods where FRA volatility breaks out to values significantly above this stable interval. The largest such breaks coincide with external shocks, notably the Rand crisis of December 2001; other breaks are induced by unexpected changes in domestic monetary policy. Such breaks are much too regular to be discarded as statistical anomalies. So

[14] Forward Rate Agreement. See e.g. Jarrow and Turnbull (2000) for theoretical details.

[15] Some algebra shows that, in the Vasicek model, the volatility of the 3×6 FRA rate is equal to $4\sigma_r e^{-0.25\alpha} D[0.25]$ - which, for our purposes of estimation, is sufficiently close to equality.

our fitted value for σ_r of 2% seems a plausible tradeoff between the stable interval of 1% - $1\frac{1}{2}$% and those periods of heightened monetary instability.

7.2.3 Comparison of Spot Rates and Short Rates

By (3.12) at any fixed time to maturity spot rates are a linear function of the ruling short rate. The gradient of this line is determined solely by alpha, and decreases with increasing time to maturity in an exponential fashion. The relationship between the short rate and spot rates for maturities of interest to us under our chosen calibration and across a wide variety of short rates is given in figure 7.7.

Figure 7.7: Relationship between Short and Spot Rates

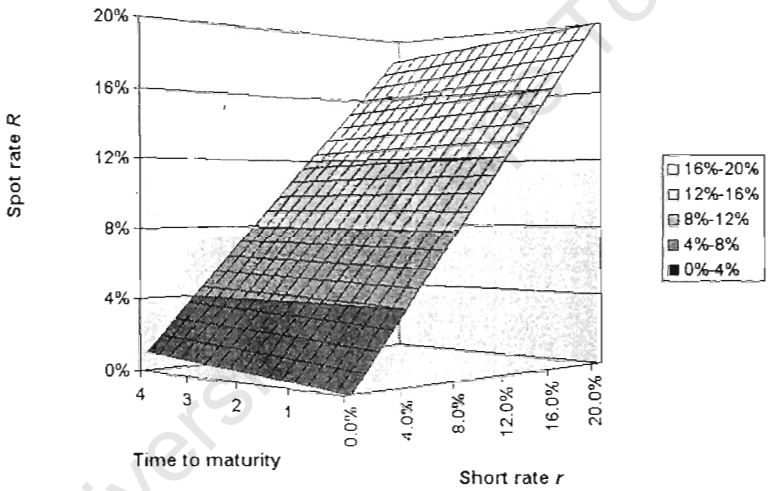

Very close to maturity short and spot rates will be indistinguishable under all calibrations. For our calibration spot rates closely resemble short rates even at three years to maturity. This is largely a result of a low value for α, necessitated to match the low curvature of the observed yield curve for maturities of two through to seven years. The inverse function from spot rates back to short rates will look remarkably similar to figure 7.7, but with gradient steepening mildly with term to maturity (as opposed to the mild flattening in figure 7.7).

7.3 Correlation

As with the dividend yield on the ALSI 40, there is no market which directly trades the correlation between short rate and stock price noise. Theoretically it could be obtained from inverting equity option prices, but in practice any such information would be strongly diluted by incorrect model selection and calibration, amongst others.

Along with the volatility structure, the Girsanov transformation from $\mathbb{P}$ to $\mathbb{Q}$ also leaves correlation structure unchanged. Observed historical correlation between the changes in 3×6

FRAs and log-returns of the ALSI 40 - both rolling 6 month moving average and exponentially weighted moving average[16] - as calculated from daily closing quotes for the years 2001-2004 is presented in figure 7.8.

Figure 7.8: Observed FRA-ALSI correlation, 2 July 2001 to 3 January 2005

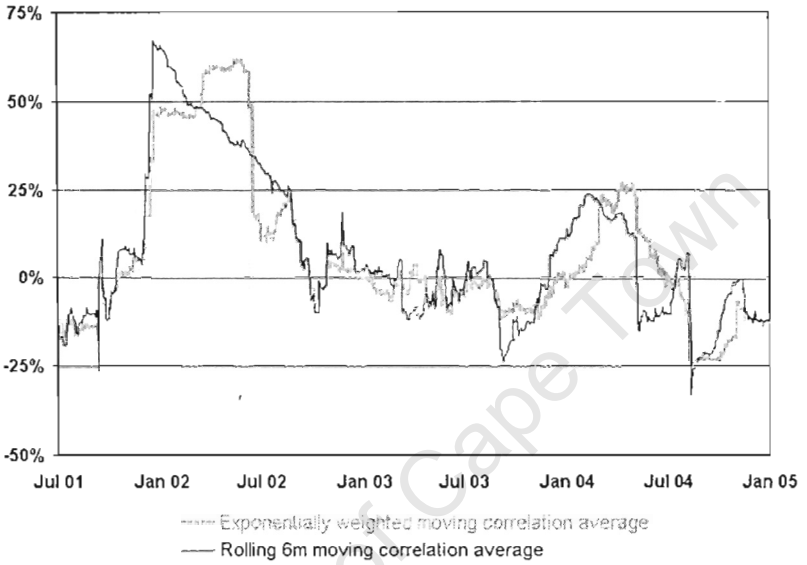

Unlike the previous parameters considered, estimates of the correlation coefficient χ show no discernible level or trend. There are some periods worth discussing.

September 2001 shows large opposing fluctuations in observed correlation. This is a function of increased market uncertainty rather than fundamental correlation changes.

However, the Rand crisis of December 2001 induced large ALSI and FRA movements in the same direction, driving observed correlation into highly positive territory - quite the opposite sign to the postulations in remark 2.2.2. An ex-post justification of this sign can be made using the dominance of resource stocks in the ALSI 40, combined with the inflation targeting of monetary policy.

With depreciating value of the Rand the local price of resource stocks climbs strongly, pulling the ALSI 40 up with them. At the same time depreciating Rand value increases the cost of imported goods, increasing anticipated inflation and hence anticipations of the repo rate rises to control such inflation. Appreciation of the Rand has the reverse effect.

Whenever ZAR moves strongly, FRA rates move in the same direction as the ALSI 40 - hence the positive correlation observation.

Finally, the last two years of observations reveal negative correlation shocks which coincide with unexpected changes in the repo rate, and are consistent with the mechanism postulated in 2.2.2.

Other than the discussed events, observed correlation cannot be said to differ significantly from zero.

[16]EWMA calculation methodology is again taken from Hull(2000)

This very brief discussion supports an argument that the ALSI and repo rates are uncorrelated during calm periods, and display negative correlation during domestic shocks but positive correlation during external shocks. This argues for inclusion of currency, as well as possibly stock price volatility, as additional explanatory variables - variables beyond the scope of this dissertation.

None of which leaves us much closer to chosing a calibration of χ. Instead of one value we chose three. A value of zero for χ approximates the calmer market periods, as well providing benchmark values with uncorrelated processes. To this we add the calibration $\chi = 25\%$ as representative of periods subject to external shocks. Finally $\chi = -25\%$ is included for times of domestic shocks, and also for indicative results which can be applied to more traditional economies which exhibit negative correlation.

We will calculate results for all three scenarios of χ. Amongst others this will indicate the sensitivity of our results to the chosen value of χ.

Part III

Numerical Results

This part completes the main body of this dissertation. It presents and comments on the results of our numerical investigations. We apply the numerical techniques described in chapter 6, together with the calibration described in chapter 7, to investigate the properties of the results derived in part I.

Consideration is given to European and American put and call options. We also investigate both in-model hedges and out-of-model ρ-hedges for all these options. together with the Optimal Exercise Boundaries for American puts and calls.

Chapter 8 covers all European options. Analysis of Americans is divided over chapters 9 (calls) and 10 (puts). Lastly chapter 11 covers the conclusions of the entire document.

Chapter 8

Numerical Results I: European Options

This chapter explores the differences between the Original Black-Scholes (OBS) and the Vasicek-augmented Black-Scholes (VBS) model results with respect to European options. In particular we examine differences in the values of option price, stock hedge and bond hedge for a variety of stock price and spot rate levels, at both one and three years to option expiry.

8.0.1 Difference Symmetry

Price Differences

Our comparisons control for stock price and for the price of the discount bond maturing at option expiry. Thus, from the put-call parities

$$\begin{aligned} c^{\mathcal{V}}[t,S,r] &= p^{\mathcal{V}}[t,S,r] + S[t]\cdot e^{-\delta(T-t)} - K\cdot B^{V}BS[t,T,r[t]] \\ c^{\mathcal{O}}[t,S] &= p^{\mathcal{V}}[t,S] + S[t]\cdot e^{-\delta(T-t)} - K\cdot B^{O}BS[t,T] \end{aligned}$$

we can conclude that

$$c^{\mathcal{O}}[t,S]\Big|_R - c^{\mathcal{V}}[t,S,R^{-1}[t,T,R]] = p^{\mathcal{O}}[t,S]\Big|_R - p^{\mathcal{V}}[t,S,R^{-1}[t,T,R]] \tag{8.1}$$

Our interest is primarily in model differences rather than absolute prices. Thus we need only examine the difference in call prices; put price differences will be identical.

Hedge Differences

Recall from chapter 3 that the OBS hedge portfolio holdings in the stock price S are

$$H^{\mathcal{O}}_{c;S}[t,S] = e^{-\delta(T-t)}\Phi[a_1] \qquad H^{\mathcal{O}}_{p;S}[t,S] = -e^{-\delta(T-t)}\Phi[-a_1]$$

for European calls and puts respectively, while the corresponding VBS portfolio holdings are

$$H^{\mathcal{V}}_{c;S}[t,S,r] = e^{-\delta(T-t)}\Phi[b_1] \qquad H^{\mathcal{V}}_{p;S}[t,S,r] = -e^{-\delta(T-t)}\Phi[-b_1]$$

Properties of the standard univariate Gaussian distribution (or alternatively differentiating (8.1)) yield

$$\Phi[b_1] - \Phi[a_1] = \Phi[-a_1] - \Phi[-b_1] \quad (8.2a)$$

$$\Phi[b_2] - \Phi[a_2] = \Phi[-a_2] - \Phi[-b_2] \quad (8.2b)$$

So when the stock purchases hedging a call option are greater (less) under the approximate OBS model than under the true VBS model. stock short sales hedging the corresponding put option will be less (greater) under the aproximate OBS model than under the true VBS model, and these differences will be of the same magnitude. The same result holds for discound bond sales (purchases) hedging call (put) options.

8.0.2 Correlation and Forward Price Variance

Critical Correlation

Comparison of the European option pricing formulae (3.14b), (3.27), (3.14b) and (3.28) shows that, after controlling for the stock and bond prices, the European option prices differ between models only through different variance of the forward price $\frac{S[t]}{B[t,T]}$.

Figure 8.1: Critical Correlation Path

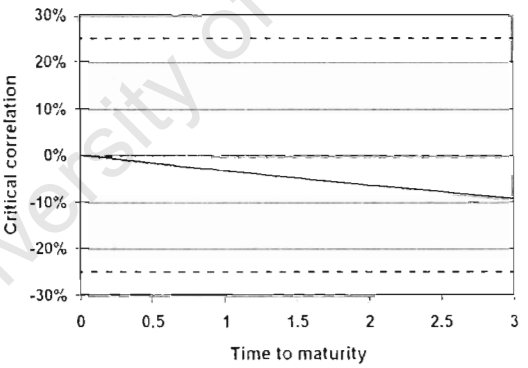

On page 29 we established a time-dependent level of correlation, $\chi_c[t,T]$, such that VBS total forward price variance exceeds OBS total forward price variance over the life of the option only when stock-rate correlation exceeds $\chi_c[t,T]$. Figure 8.1 plots the path of this critical correlation under our calibrations and for times to expiry of interest to us[1], with the three calibration correlations included for reference.

Total Forward Price Variance

The total forward price variance until option expiry is exactly $\sigma_S^2(T-t)$ and $\Gamma[t,T]$ under the OBS and VBS models respectively. Comparison of these values for the calibrations $\chi = -25\%$, $\chi = 0$ and $\chi = 25\%$ is shown in Figure 8.2.

[1]The approximate linear relationship of χ_c and time to expiry fails only very close to expiry (within 0.001 years) where other aspects - including transaction costs and discrete asset movements - create significant discrepancies between models and reality.

Figure 8.2: Total Forward Price Variance

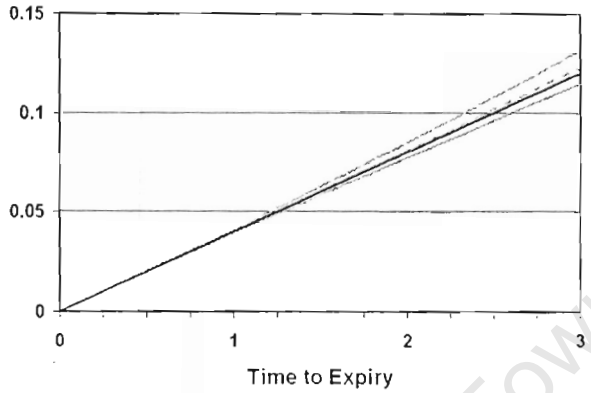

$$\text{—}\ \sigma_S^2(T-t)\quad \text{---}\ \Gamma[t,T]\big|_{\chi=25\%}\quad \cdots\ \Gamma[t,T]\big|_{\chi=0}\quad -\ \Gamma[t,T]\big|_{\chi=-25\%}$$

Within one year of option expiry the graphs of $\sigma_S^2(T-t)$ and $\Gamma[t,T]$ are practically indistinguishable. From this we anticipate that all the models and calibrations considered will deliver similar numerical results.

Three years from expiry the various graphs in figure 8.2 become distinct, though still within close range of each other. Considering results from the various models and calibrations at a three year horizon gives an indication of the importance of total forward price volatility, in addition to stock prices and spot rates, on option prices and hedges.

8.1 Option Prices

As option prices are monotonically increasing in $\Gamma[t,T]$, OBS option prices will only exceed their VBS counterparts when $\sigma_S^2(T-t) > \Gamma[t,T]$. From figure 8.1 it is apparent that at all times to expiry of interest OBS option prices will exceed VBS option prices only for $\chi = -25\%$; for $\chi = 0$ and $\chi = 25\%$ VBS prices will exceed OBS prices. To determine the magnitude of these differences we explore specific cases, starting with options with one year to expiry.

8.1.1 Shorter-term options: $T - t = 1$

Each comparison of OBS and VBS results can be considered an experiment. For every calibration the VBS price is assumed to be the true price, thus acting as the control. The OBS price is a simplification, and can be considered the hypothesis.

However, the VBS price varies across experiments. After conditioning on the spot rate, the same OBS price price is used in each experiment. Because of this consistency we choose to present this OBS price as a common baseline indication of option price levels, even though it is the hypothesis function.

Figure 8.3 shows the price of European call and put options with one year to expiry and

Figure 8.3: OBS Call and Put prices at $T - t = 1$

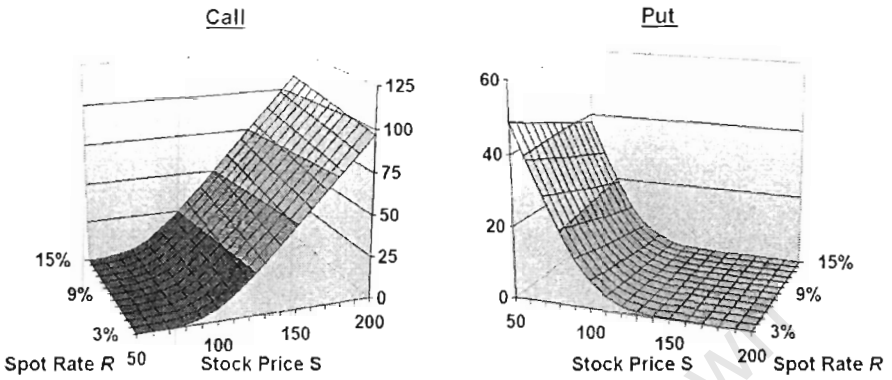

a strike price of 100, as a function of both stock price S and spot rate R. The majority of variance in OBS option prices results from changes in S. Indeed, the low sensitivity of option prices to spot rates is an early indication of model similarity at this time.

$\underline{\chi = -25\%}$

Prices resulting from the VBS model are remarkably similar. The excess of OBS prices over corresponding VBS prices for $\chi = -25\%$ is illustrated in figure 8.4 - all values are positive, as per our conclusions regarding correlation structure.

Figure 8.4: Total Pricing Error at $T - t = 1$ for $\chi = -25\%$

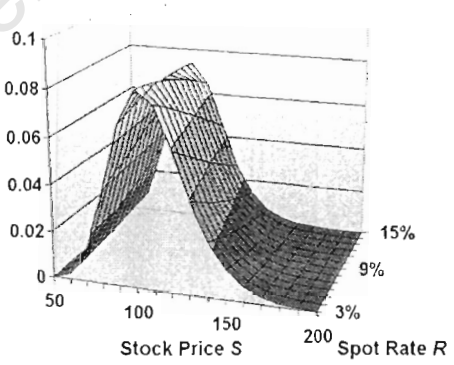

The total pricing error is greatest when the option is at-the-money. At these locations certainty about the eventual exercise decision is lowest, hence any neglect of risk sources creates the greatest price impact. Like option prices, total price differences at this time to expiry are relatively insensitive to spot rate levels.

As an alternative measure of model difference we consider the error proportional to the correct VBS price.

Unlike total error, proportional error increases steadily as the option moves out-of-the-money - driven largely by decreasing option prices. However, these relative errors are mostly

Figure 8.5: Proportional Pricing Error at $T - t = 1$ for $\chi = -25\%$

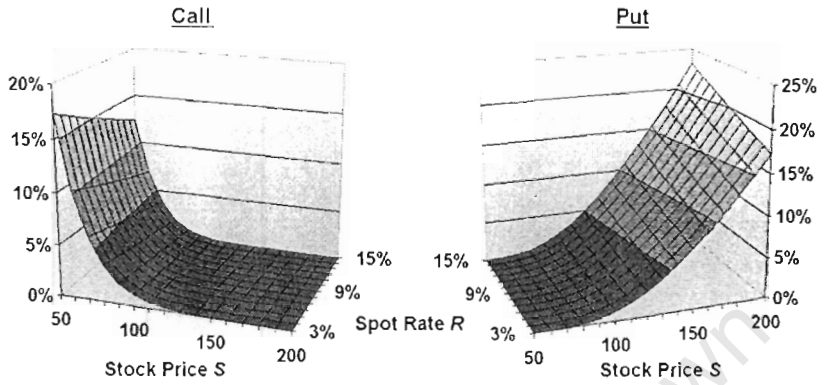

within 5%. The underlying asset needs to move at least 20% - and often more - out-of-the-money for proportional pricing errors at one year to expiry for $\chi = -25\%$ to exceed 5%.

$\underline{\chi = 0}$

At one year to option expiry the critical level of correlation is approximately -3%. The calibration value $\chi = 0$ is remarkably close to this value, so it is no surprise that option prices approximated using the OBS formulae are remarkably close the true underlying VBS price - although always marginally below them.

Figure 8.6: Total Pricing Error at $T - t = 1$ for $\chi = 0$

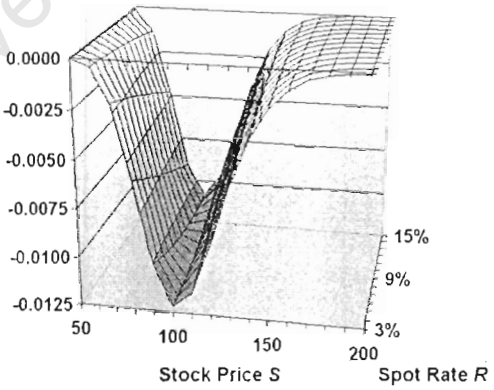

Again, total difference is largest while options are at-the-money while proportional error grows as the option moves out-of-the-money. The similarity of VBS and OBS prices with $\chi = 0$ at $T - t = 1$ is such that the relative error remains less than 3% for both puts and calls over the domain $(S, R) \in [50, 200] \times [0\%, 15\%]$.

$\chi = 25\%$

For the calibration $\chi = 25\%$, the magnitude of total price errors bears a very strong resemblance to the results with $\chi = -25\%$, though the differences are of a different sign (as follows from a correlation exceeding χ_c). Comparison of figures 8.4 and 8.7 demonstrates this well.

Figure 8.7: Total Pricing Error at $T - t = 1$ for $\chi = 25\%$

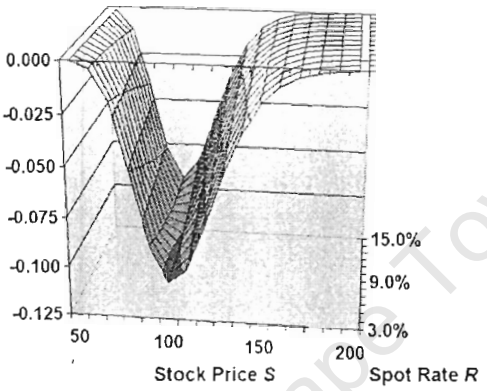

Proportional price differences for $\chi = 25\%$ and $\chi = -25\%$ exhibit similarly strong resemblance, again with inverse signs.

8.1.2 Longer-term options: $T - t = 3$

At three years to option expiry the differences between models are more varied, more significant and altogether more interesting than those at one year to expiry.

Figure 8.8: OBS Call and Put Prices at $T - t = 3$

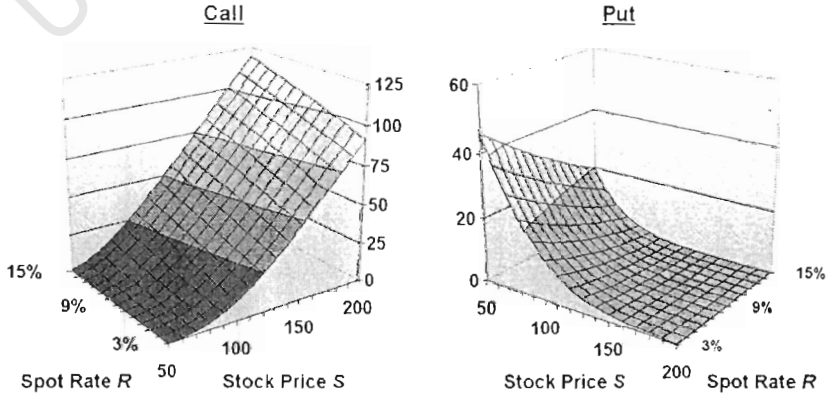

As depicted in figure 8.8, OBS option prices three years from expiry exhibit similar levels and shape to those at one year to expiry. However, they are smoother than their shorter counterparts: the expectations operator increasingly smooths the corner occuring at the strike

price around option expiry. More importantly, they are noticably more sensitive to changes in the spot rate than their shorter term counterparts.

$\underline{\chi = -25\%}$

Over a three year horizon any additional uncertainty arising from stochastic interest rates

Figure 8.9: Total Price Errors at $T - t = 3$ for $\chi = -25\%$

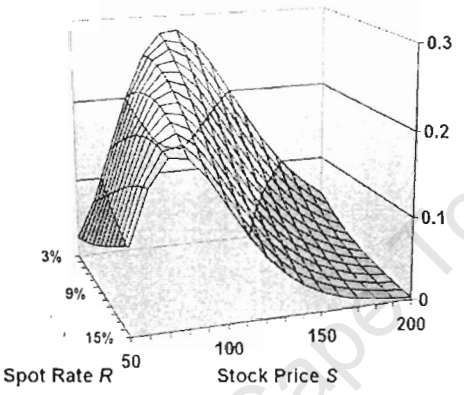

has a longer period to impact option prices than over a one year horizon. It comes as no surprise that the total option price differences at three years depicted in figures 8.9, 8.11 and 8.13 are substantially larger than their one year counterparts.

The direction of the price errors for $\chi = -25\%$ illustrated in figure 8.9 is consistent with the path of χ_C. Furthermore, as with the one year options, maximum pricing error occurs when the option is at-the-money. However, analysis of the three year errors shows that 'at-the-moniness' needs to consider the price of the underlying asset relative to the discount bond maturing at option expiry, and not relative to the (undiscounted) strike price. At high interest rates an underlying price less than the strike price may still be considered 'at-the-money'. This consideration implies a comparison of the the constituents of the hedge portfolio (i.e stock versus discount bond), which is intuitively appealing.

More intriguingly, after controlling for 'moneyness', the magnitude of the total price difference for the negative correlation calibration appears to be a decreasing function of interest rates. In other words, all else equal, price differences between two models are lowest when spot rates are high.

Proportional pricing errors, depicted in figure 8.11, remain a decreasing function of the extent to which the option is in-the-money.

For call options, despite increasing absolute error with time to expiry, the largest relative error experienced at three years to expiry over the considered domain is of the order of 15% - a similar result to that at one year to expiry.

Relative pricing errors at-the-money, although somewhat larger than those for shorter term call options, remain between 1% and 5%. However these proportional errors - like their absolute counterparts - do exhibit stronger short rate sensitivity at longer horizons.

On the other hand, put options show a marked increase in proportional error over the longer time horizon. For very deep out-of-the-money options considered, use of OBS pricing

Figure 8.10: Proportional Price Errors at $T - t = 3$ for $\chi = -25\%$

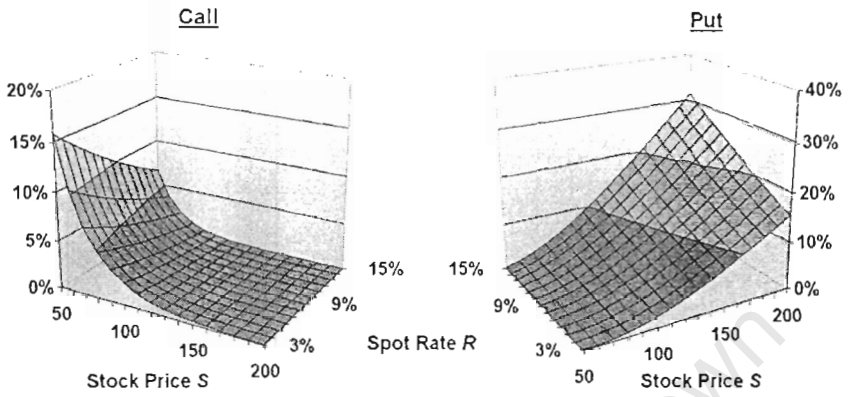

may lead to overpricing by as much as 30%. Even at-the-money options may be overpriced by between 5% and 10%.

$\underline{\chi = 0}$

Total and proportional pricing errors of options with three years to expiry for the calibration $\chi = 0$ are shown in figures 8.11 and 8.12 respectively. They are a near reflection across the (S, R) axis of the corresponding results with $\chi = -25\%$.

Figure 8.11: Total Price Errors at $T - t = 3$ for $\chi = 0$

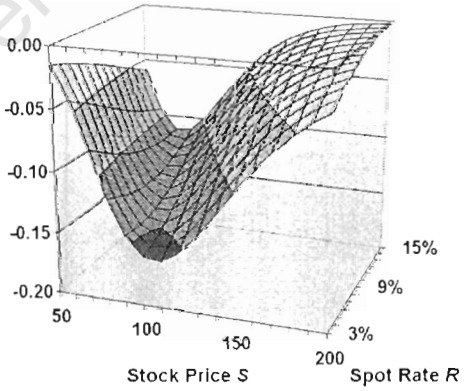

$\underline{\chi = 25\%}$

At one year from expiry the calibrations $\chi = -25\%$ and $\chi = 25\%$ were approximately equidistant from the critical correlation $\chi_c[t, T] \approx -3\%$. These calibrations produced results closely mirroring each other.

Three years from option expiry, the critical correlation value $\chi_c[t, T]$ which equates the VBS and OBS models is close to -10%. Calibrations $\chi = -25\%$ and $\chi = 0$ are nearly

Figure 8.12: Proportional Price Errors at $T - t = 3$ for $\chi = 0$

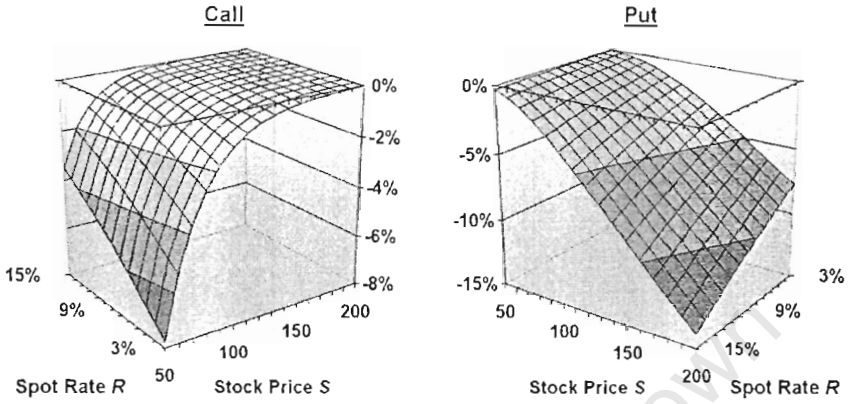

equidistant from this value of $\chi_c[t,T]$, and produce results of very similar magnitude.

Our brief numerical investigations suggest that, while the direction of approximation errors from using the OBS pricing formulae in a VBS context is determined by the relationship between the calibration value of χ to the critical correlation $\chi_c[t,T]$, the magnitude of such errors is roughly symmetrical across $\chi_c[t,T]$ in the value of χ.

Pricing errors for the calibration $\chi = 25\%$ at three years to expiry show all the characterics discussed previously, but are of a far greater magnitude than any of the other cases considered. Total pricing errors, depicted in figure 8.13, are maximal when the option is at-the-money, and decrease as the spot rate increases (again, after controlling for the moniness of the option). These values are up to six times larger than for $\chi = 25\%$ at one year to expiry.

Figure 8.13: Total Price Errors at $T - t = 3$ for $\chi = 25\%$

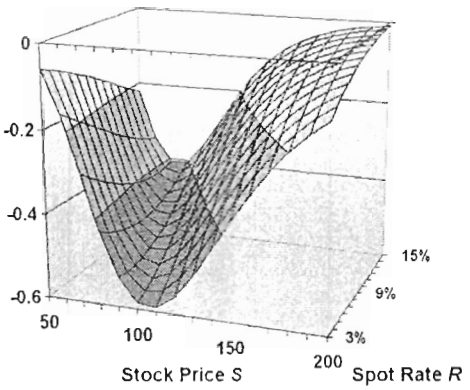

Proportional pricing errors, depicted in figure 8.14, increase as the option moves out-of-the-money. Once again the relative errors for puts appear to be more extreme than those for call options. However, in this final case the relative pricing error is substantial. For call options at-the-money, using OBS prices to approximate VBS prices leads to underpricing by

5%. The errors for put options are around 10% when the option is at-the-money, increasing to a maximum of 40% when the option is deep out-of-the-money. All the effects documented

Figure 8.14: Proportional Price Errors at $T - t = 3$ for $\chi = 25\%$

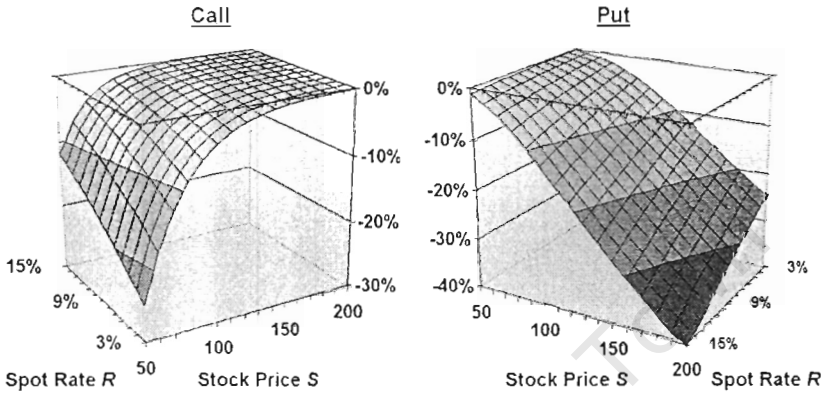

at the three year horizon were also present at the one year horizon. However, some of these only became sufficiently pronounced to be noticable at the longer horizon.

Of all these effects, the tendency for total pricing error to decrease with increasing spot rate is arguably the effect least anticipated. An attempted explanation of this effect could be made around bond durations:

Trivially, the duration of the discount bond maturing at option expiry is three years. But duration is a measure of price sensitivity relative to current price. As high spot rates imply low bond prices, they also imply a low total option price sensitivity of discount bonds to interest rates. And as we have observed, model differences appear to be larger when OBS prices are more sensitive to interest rates.

This explanation is however only an initial speculation. It requires rigorous mathematical treatment to be placed on a sound theoretical footing. We turn now to considering the numerical values of the hedge parameters between the OBS and VBS models.

8.2 Hedge Parameters

In section 3.2.2 we argued that differences between the OBS and VBS models regarding quantities of stock and discount bond purchased or sold for hedging purposes depends jointly on two factors:

- how exclusion of short rate stochasticity affects the total forward price variance, and
- whether the option is sufficiently out-of-the-money to increase in price when total forward price variance increases.

The first factor is dependent solely on the relationship between $\chi_c[t,T]$, whose path is plotted in figure 8.1, and the calibration correlation.

The second factor is determined by the location of the current stock price in relation to a level dependent both on time and the spot rate to expiry. This critical stock level is calibration specific, and different levels apply for the stock and bond hedge parameters.

Cross-correlation differences in these stock prices are largest far away from option expiry. Also, cross-correlation differences are marginally larger for stock hedge parameters than for bond hedge parameters.

Table 8.1: $S_1^*[t, t+1, B]$ for various correlations and three year spot rates

Spot rate	3%	6%	9%	12%%	15%
$\chi = -25\%$	106.04	96.91	88.57	80.95	73.98
$\chi = \chi_c[t, t+1]$	106.24	97.09	88.74	81.10	74.12
$\chi = 0$	106.27	97.12	88.76	81.12	74.14
$\chi = 25\%$	106.48	97.32	88.94	81.29	74.29

Table 8.1 shows critical stock prices for the stock hedge parameter three years from expiry, for a selection of correlations and of three-year spot rates. This critical stock price is clearly very robust to correlation changes. The critical stock price for bond hedge parameters is likewise insensitive to correlation.

8.2.1 Shorter-term options: $T - t = 1$

We begin our consideration of hedge parameters one year from expiry with plots of the critical stock levels for the stock and bond hedge parameters. Figure 8.15 depicts these for $\chi = \chi_c[t, t+1]$; from the conclusions following from table 8.1 we know that the graphs of our three calibrations of χ will be virtually indistinguishable from those plotted.

Figure 8.15: Critical stock prices one year from expiry for $\chi = \chi_c[t, t+1]$

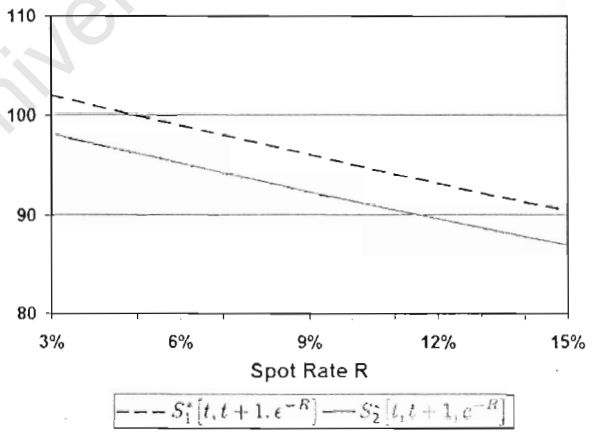

Though the graphs in figure 8.15 are exponential functions of the spot rate, the short time to option expiry induces first order terms to dominate, making the graphs approximately linear. As with the discussion regarding price comparisons, hedge comparisons need to consider stock price, spot rates and dividend yields jointly when the degree to which options are in- or out-of- the money.

Figures 8.16 and 8.17 show the quantities of stock and discount bond respectively purchased to replicate both call and put options under the common OBS approximation to our three VBS models. (Negative amounts indicate short sales). They show the familiar structure of increasing hedge position sizes as options move into-the-money. Call hedges purchase stock and short bonds, while put hedges do the reverse. At all times the put and call hedge purchases differ by a constant.

Figure 8.16: OBS hedge purchases of stock at $T - t = 1$

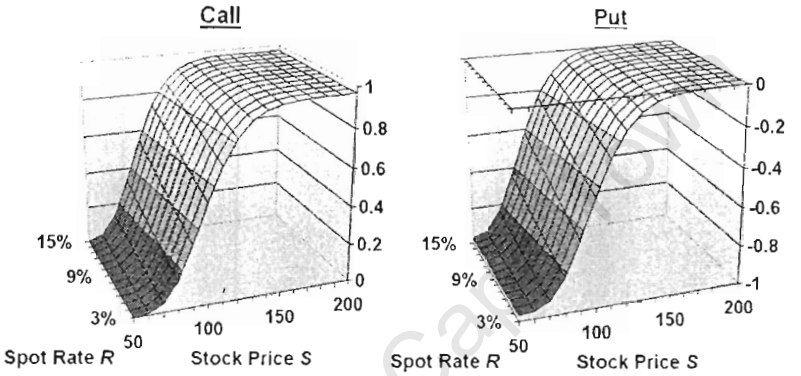

Figure 8.17: OBS hedge purchases of discount bonds at $T - t = 1$

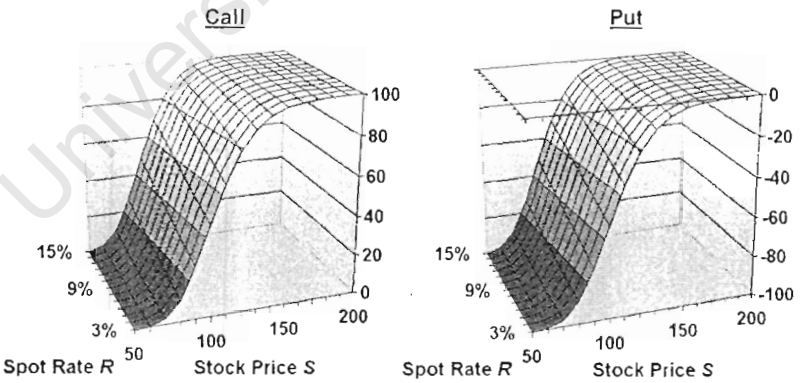

As with option prices, option hedge ratios one year from expiry are relatively insensitive to changes in the prevailing spot rate to option expiry. Again, this indicates a low sensitivity to the level of interest rate stochasticity.

$\underline{\chi = -25\%}$

The calibration value $\chi = -25\%$ lies below $\chi_c[t, t+1]$ implying in this case that the OBS model over-estimates total forward price variance. Following our conclusions regarding hedge differences, in comparison to the VBS model with $\chi = 25\%$ the OBS model will magnify

Figure 8.18: Total Hedging Error at $T - t = 1$ for $\chi = -25\%$

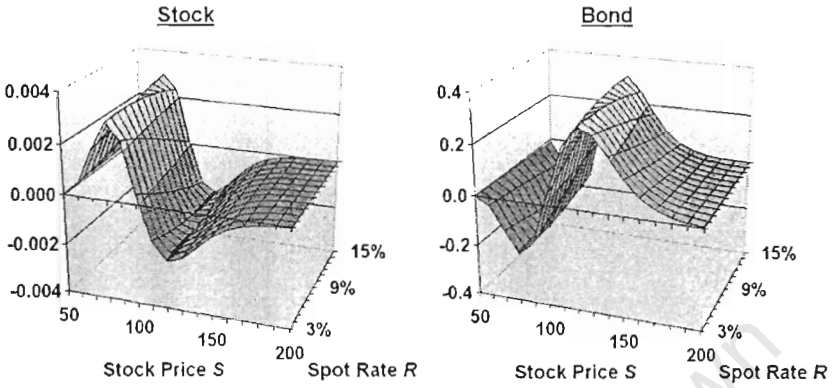

hedge positions when options are out-of-the-money and reduce positions then in-the-money. This is illustrated in figure 8.18.

The wave-like appearance of hedge differences deserves attention. All hedge parameters are determined largely by the cumulative Gaussian function $\Phi[\cdot]$. Near to critical stock prices, diverging hedge parameters are driven by diverging values of the input to $\Phi[\cdot]$. Far from the critical stock prices the model differences are dampened as the VBS and OBS returns from the common function Φ converge to a common value.

Below the appropriate critical stock prices stock puchases are over-estimated, and bond purchases under-estimated. Call hedges purchase stock and short bonds. As purchase under-estimation is just sale over-estimation, both stock purchases and bond sales are over-estimated for out-of-the-money calls. Similar intuition can be applied to in-the-money call hedges and to put hedges.

Figure 8.19: Proportional Hedging Errors at $T - t = 1$ for $\chi = -25\%$

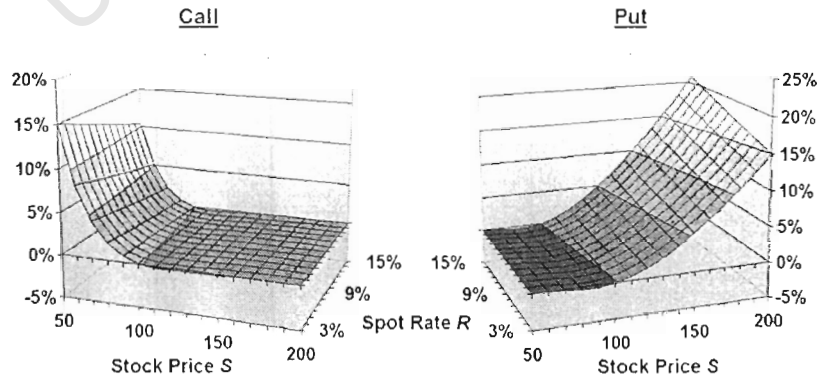

Figure 8.19 shows proportional hedging errors (defined as total hedging error divided by the correct VBS value) for puts and calls. Proportional hedging errors are for all intents and purposes indistinguishable between stocks and bonds.

Comparison with figure 8.5 shows that when options are out-of-the-money (and where proportinal errors are most concerning) hedge and price errors are almost identical. Deep out-of-the-money relative pricing errors are not driven by any systematic bias towards either of the hedging instruments, but rather by a near-uniform mis-estimation of exercise probabilities and hence of hedge parameters. This probability mis-estimation is induced by incorrect total forward price variance.

Of course, at- and in-the-money the sign of proportional price and proportional hedge errors differ, but here the errors are in any case negligible.

$\underline{\chi = 0}$

For the calibration $\chi = 0$. differences between the VBS and OBS hedges are minuscule. Proportional hedging errors remain within 3% while absolute pricing errors demonstrate the shape and sign of those for the calibration $\chi = 25\%$.

$\underline{\chi = 25\%}$

Figure 8.20 shows total hedging errors when $\chi = 25\%$. The errors are determined by the

Figure 8.20: Total Hedging Errors at $T - t = 1$ for $\chi = 25\%$

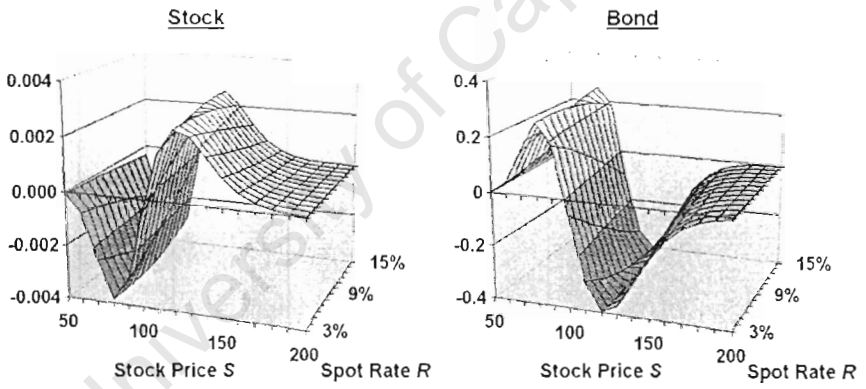

same factors as those for $\chi = -25\%$, though in this case the OBS model under-estimates total forward price variance. Replicating the characteristics of price errors. hedging errors for $\chi = 25\%$ are an approximate image of those for $\chi = -25\%$, mirrored across the (S, R)-axis.

Proportional hedging errors for $\chi = 25\%$ at one year from expiry (not shown here) also mirror those for $\chi = -25\%$. and closely follow the relative pricing errors. Once again the pricing error presents no systematic bias towards either of the hedging instruments.

8.2.2 Longer-term options: $T - t = 3$

Three years from expiry. critical stock prices still show surprisingly little curvature. as illustrated in figure 8.21. However. in comparison to their one-year counterparts they are far more sensitive to spot rate changes. and also demonstrate a larger difference between critical prices for the stock and bond hedge values.

OBS hedge parameters for options three years from expiry are smoother than their one year counterparts and converge at a slower speed towards their limiting values. More impor-

Figure 8.21: Critical stock prices three years from expiry for $\chi = \chi_c[t, t+3]$

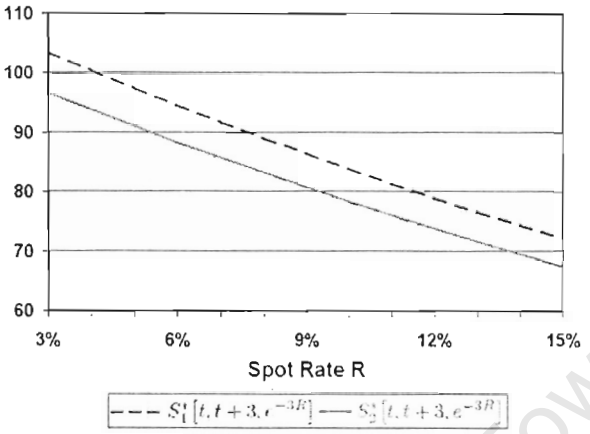

Figure 8.22: OBS Hedge Stock Purchases at $T - t = 3$

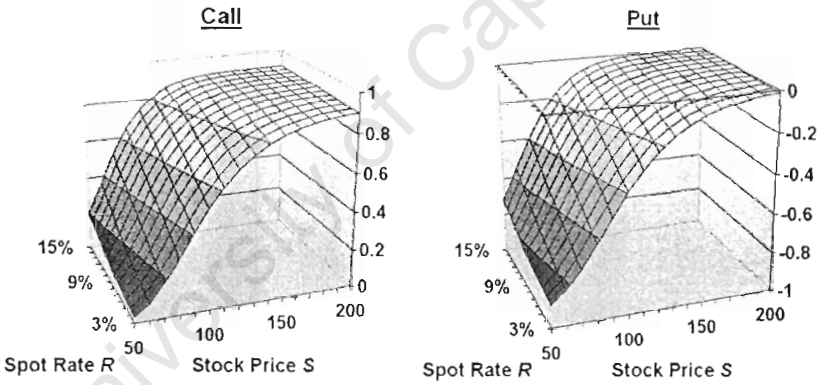

tantly, they exhibit more sensitivity to changes in spot rates than their shorter counterparts. Interestingly, they better illustrate the contour of hedge parameters along constant values of $S[t] \cdot \exp[(R-\delta)(T-t)]$.

$\chi = -25\%$

Differences in total forward price variance between the VBS model with $\chi = -25\%$ and its OBS approximation diverge as time to option expiry increases to three years. Additionally, OBS prices three years from expiry show more spot rate sensitivity than prices one year from expiry. Given both these effects, we are not surprised that the total hedge differences shown in figure 8.24 exceed the differences for $\chi = -25\%$ at one year from option expiry as plotted in figure 8.18.

$\chi = -25\%$ is below the critical correlation for options three years from expiry. Consequently, any OBS approximation to the VBS prices will over-estimate total forward price variance to option expiry - just as with one year options. Thus call hedges are magnified

Figure 8.23: OBS Hedge Discount Bond Purchases at $T - t = 3$

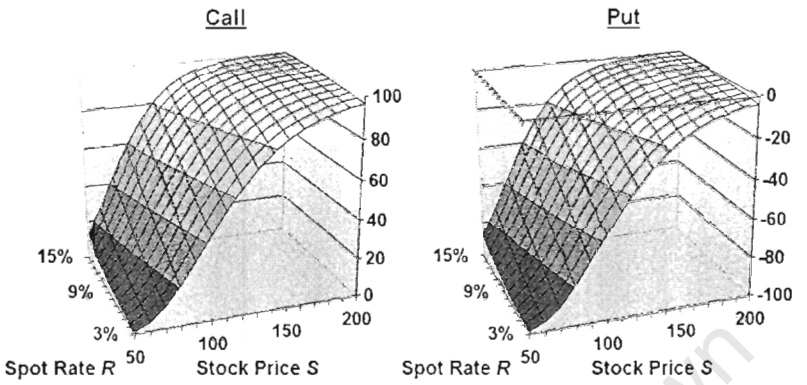

(reduced) and put hedges reduced (magnified) when the stock price lies below (above) the critical levels plotted in figure 8.21.

VBS hedge parameter contour lines, like those of their OBS approximations, trace the curves where $S[t] \cdot \exp[(R - \delta)(T - t)]$ remains constant. As a result the total hedging error is unchanging while $S[t] \cdot \exp[(R - \delta)(T - t)]$ is unchanging.

Figure 8.24: Total Hedge Errors at $T - t = 3$ for $\chi = -25\%$.

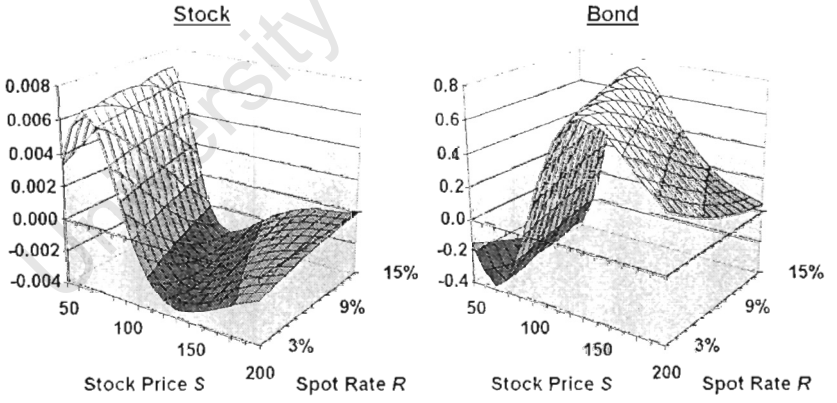

$\chi = 0$

Total hedging errors for three year options under the calibration $\chi = 0$ are a near mirror image of those for $\chi = -25\%$ across the (S, R)-axis. This is consistent with the total pricing errors at the same horizon.

$\chi = 25\%$

For the calibration $\chi = 25\%$ OBS approximations will under-estimate total forward price volatility, and so stock hedge purchases are under-estimated and bond hedge purchases over-estimated when stock prices are low. The total hedging errors for $\chi = 25\%$, shown in figure

Figure 8.25: Total Hedge Errors at $T - t = 3$ for $\chi = 25\%$.

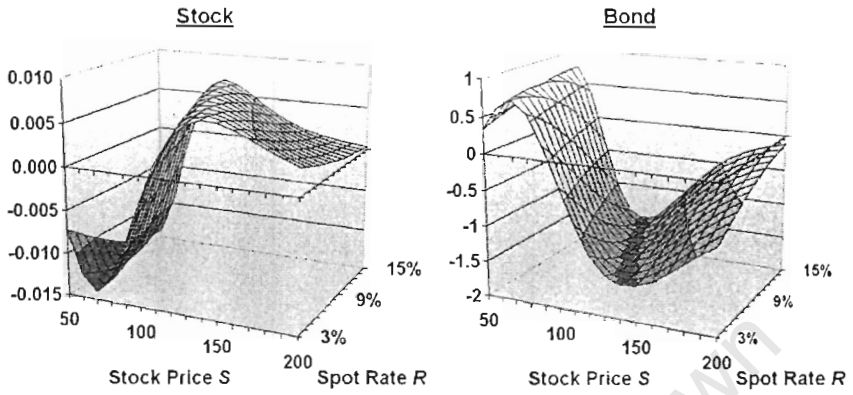

8.25, are the largest of all scenarios considered.

As with one year options, proportional hedging errors for three year horizon options are indistinguishable between stock and bond hedges, both being reflections of the relative percentage errors. Any significant pricing error remains equally spread across both hedging instruments. We do not plot the proportional hedging error for options with three year horizons, noting that for all practical purposes they are indistinguishable from figures 8.10, 8.12 and 8.14.

Chapter 9

Numerical Results II: American Call Options

Chapter 8 began by showing that put-call parity for European options resulted in OBS pricing errors in a VBS world being identical for puts and calls. Only one set of absolute errors needed to be presented.

This parity results from European puts and calls being two sides of the same coin: either the put will be exercised at expiry, or the call will be exercised at expiry. For American options, the early exercise feature destroys this parity: it is entirely possible for a put option to be exercised before expiry, but for the corresponding call option to be optimally exercised only at expiry.

As American put and call options are totally different problems, linked only vaguely through put-call symmetry[1], we present numerical results for each problem in a separate chapter. This chapter deals with American call options, analysing the accuracy of OBS approximations (both in- and out-of-model) to VBS prices and hedges. The following chapter presents a similar analysis, but with respect to American put options.

9.0.3 Approximation Scheme Details

OBS call prices are obtained using the methodology described in section 6.2. We set n_t, the number of time steps, to 12 per month (or approximately one every second working day). As elaborated in appendix C, to ensure that the OEB $\tilde{S}_C^{\mathcal{O}}$ is included in the scheme, it is necessary to vary the upper bound of spatial domain considered with the interest rate R. We divide this spatial domain into n_y=750 sub-intervals. The spacial step size Δy necessarily varies across interest rate calibration. The scheme is unconditionally stable and convergent.

VBS call prices are obtained using the methodology described in section 6.3. We set the domain of interest to $(S, r) \in [40, 330] \times [0\%, 20\%]$. For consistency with the OBS scheme we set $\Delta t = \frac{1}{144}$, or 12 steps per month. The explicit scheme used for VBS prices is stable only conditionally. The stability horizon is limited by inequalities 6.17a and 6.17b. A quick check of these inequalities shows that the scheme may be applied within the horizons 5.52, 4.90 and 4.28 years for the calibrations $\chi = -25\%$, $\chi = 0$ and $\chi = 25\%$ respectively. The longest time to option expiry we consider remains three years, and comfortably lies within limitation for each calibration.

[1] see e.g. Kwok (1998) for a discussion of put-call symmetry.

Within these horizons, stability requires satisfaction of the inequalities (C-27a)-(C-27d) discussed in Appendix C. Collectively these require a timestep Δt less than 0.262, 0.151 and 0.067 for the calibrations $\chi = -25\%$, $\chi = 0$ and $\chi = 25\%$ respectively. Our choice of $\Delta t = \frac{1}{144} \approx 0.007$ clearly satisfies all these inequalities, so the scheme is stable and convergent.

For more details of the schemes used see the discussion in chapter 6 or the derivations in appendix C. The Matlab code used to obtain the results in this chapter is provided in appendix D.

9.1 Optimal Exercise Boundaries

Following from the American contingent claim pricing theorems 4.2.3 and 4.2.4, section 4.3 showed that the American call option prices $C^{\mathcal{O}}$ and $C^{\mathcal{V}}$ are both solutions to optimal stopping problems. Analysing the optimal stopping rule, i.e. the exercise strategy which maximises each call price, adds insight into the characteristics and comparisons of $C^{\mathcal{O}}$ and $C^{\mathcal{V}}$. We examine this optimal stopping rule in this section, before moving to option prices in the next section and option hedges in the section thereafter.

The call option $C^{\mathcal{O}}$ is optimally exercised when the option price is first equal to the intrinsic value of the option - i.e. the option payoff. Starting on page 41 we showed that the optimal stopping time is equivalent to the first time that the path of the stock price $S[t]$ touches the curve $\tilde{S}^{\mathcal{O}}_C[t]$. This curve $\tilde{S}^{\mathcal{O}}_C[t]$ is known as the Optimal Exercise Boundary (OEB).

The location of the OEB is dependent on the tradeoff between exercising and holding the option, and is hence dependent on the calibration values of the model parameters - including the interest rate R. Figure 9.1 shows the hypercurve created by a collection of OEBs for the OBS model calibrated to a variety of interest rates R.

Figure 9.1: Optimal Exercise Boundary $\tilde{S}^{\mathcal{O}}_C[t]$ for $R \in [3\%, 15\%]$

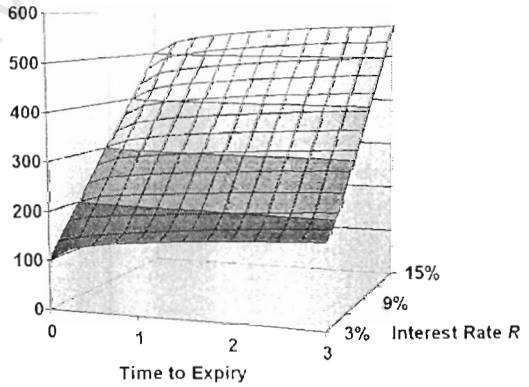

To understand the behaviour of the OEB we must recall the reasons for exercising the call option before expiry. The costs of early exercise are twofold. Firstly, the strike price must be paid early. Time value of money makes early payment dearer (while $R > 0$); the instantaneous marginal cost of this is $R \cdot K\, dt$. Secondly, by exercising the option before expiry one sacrafices the ability to wait for more information regarding the state of the world

before chosing to exercise. This optionality has a monetary value which increases with time to expiry.

The benefits of early exercise are the dividends received from the stock before the option expires - carrying an instantaneous marginal value of $\delta \cdot S[t]dt$. Only when these benefits of early exercise exceed the costs will early exercise be beneficial.

Returning to figure 9.1, three features are noteworthy. Firstly, for fixed R (i.e. for any given calibration of the OBS model), the OEB is increasing with time to expiry. This reflects the increased cost of optionality foregone. As time to expiry increases, the benefits to early exercise (viz. dividends received prior to expiry, whose value is positively related to $S[t]$) need to to increase to compensate for the increased costs of exercise.

More noticeably the OEB increases almost linearly in the interest rate R. Following from the discussion in the previous paragraph, an increase in R requires the option to be deeper in-the-money before the increase in benefits to early exercise outweigh the costs, making such exercise rational.

(Increases in R also have subtle effects on $\tilde{S}_C^{\mathcal{O}}$ through the drift of the asset S under the measure $\mathbb{Q}$. Changes in $\tilde{S}_C^{\mathcal{O}}$ with changing R are however dominantly driven by changes in the time value of the strike price).

However, most striking is the level of the OEB in comparison to the strike price K. For an interest rate of 3% the OEB ranges between 100% and 170% of the strike price, but for an interest rate of 15% the OEB ranges between 500% and 575% of the strike price. Indeed, for the majority of cases exhibited in figure 9.1 the stock price needs to exceed 300% of the strike price before early exercise becomes optimal.

At levels this deep in-the-money, errors regarding assumed volatility levels and/or assumed asset price dynamics may well dominate any pricing and hedging errors stemming from an incorrect interest rate assumption.

Moreover, for the most range of stock prices we consider - $S[t] \in [50, 200]$ - the probability of the stock price reaching the OEB, and hence of the option being exercised before expiry, are minimal. Consequently we anticipate that American call options priced within the OBS framework will very closely resemble their European conterparts.

Due to our choice of numerical method for approximating VBS American prices, estimates of the location of the exercise boundary $\tilde{S}_C^{\mathcal{V}}$ are only available when such estimates lie within the domain of interest. The calculations producing the results in this chapter use the domain of interest $(S, R) \in [40, 330] \times [3\%, 15\%]$, implicitly excluding any estimates of $\tilde{S}_C^{\mathcal{V}}$ above 330.

As discussed in chapter 7, three separate calibrations of the VBS model are considered. Where estimates of $\tilde{S}_C^{\mathcal{V}}$ are possible, such estimates far more closely resemble estimates under other VBS calibrations than they resemble estimates for the corresponding location of $\tilde{S}_C^{\mathcal{O}}$. Figure 9.2 shows the error induced using an OBS model to locate the OEB for a VBS model with $\chi = 0$ (errors for $\chi = -25\%$ and $\chi = 25\%$ are remarkably similar).

At all available sample points the OBS model underestimates the location of the VBS Optimal Exercise Boundary. This occurs presumably because the VBS model contains greater uncertainty, which raises the optionality costs of early exercise - forcing the option to be deeper in-the-money before early exercise is optimal.

The extent of underestimation increases as time to expiry increases, and also as the ruling spot rate to maturity increases. (Lack of smoothness in the graph is induced by inefficient methods of interpolating $\tilde{S}_C^{\mathcal{V}}$ from a collection of point estimates for $C^{\mathcal{V}}$).

Figure 9.2: Errors in OEB estimation: $\tilde{S}_C^{\mathcal{O}}$ - $\tilde{S}_C^{\mathcal{V}}$ for $\chi = 0$

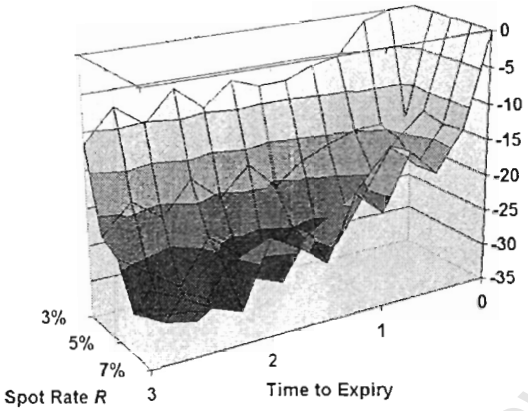

The location of $\tilde{S}_C^{\mathcal{O}}$ suggested a low probability of early exercise under OBS dynamics. Though the VBS model includes more uncertainty, critical stock prices for the calibrations considered uniformly exceed their OBS counterparts. Consequently, the probability of early exercise of an American call option is likewise low.

As American equity call options priced under both OBS and VBS models have low probabilities of early exercise, it is reasonable to postulate that both will closely resemble their European counterparts - and hence that the OBS pricing errors will closely resemble those errors presented in the previous chapter. The following sections show this to be largely true, though slight anomalies occur around the early exercise boundary.

9.2 Premia and Prices

9.2.1 Early Exercise Premia

Before considering call option pricing, and estimation error therein, we briefly examine the early exercise premia $\mathcal{P}_C^{\mathcal{O}}$ and $\mathcal{P}_C^{\mathcal{V}}$ - defined as the difference between the American and corresponding European equity call options. In section 4.3 we showed that this premium represents the value of all excess profits accruing to the option seller should the holder, before maturity, fail to exercise the option within the optimal stopping region.

Early Exercise Premium Characteristics

Figure 9.3 illustrates this premium for OBS option prices with one and three years to maturity. Resulting from the high - and relatively inaccessible - location of the boundary $\tilde{S}_C^{\mathcal{O}}$, the early exercise premium $\mathcal{P}_C^{\mathcal{O}}$ is close to zero for most of the domain $(S, R) \in [50, 200] \times [3\%, 15\%]$.

Only when the option is deeply in-the-money (i.e. both a high stock price and low spot rates), and early exercise becomes likely (or even probable), does $\mathcal{P}_C^{\mathcal{O}}$ differ significantly from zero. Low spot rates and high stock prices push the European price below intrinsic value; the early exercise premium rises to maintain the arbitrage requirement $C^{\mathcal{O}}[t, S] \geq [S - K]^+$, i.e. that American call option prices are never strictly dominated by their intrinsic value.

VBS early exercise premia dislay similar characteristics.

Figure 9.3: Early Exercise Premium $\mathcal{P}_C^{\mathcal{O}}$ for $T-t=1$ and $T-t=3$

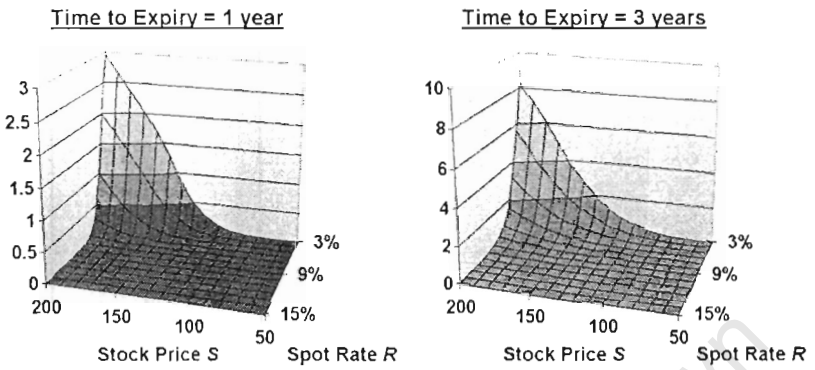

Early Exercise Premia Comparison

Previous chapters established that American call options are optimally exercised when they first reach intrinsic value: this notion was indeed used to define the stopping areas $\mathcal{S}_C^{\mathcal{O}}$ and $\mathcal{S}_C^{\mathcal{V}}$. The opening pages of this chapter established that, by under-estimating total uncertainty, the OBS model under-estimates the location of the optimal exercise boundary.

This under-estimation results in OBS decision rules exercising early (based on ruling stock prices and spot rates to expiry) whenever VBS decision rules exercise early, but also exercising early on a limited set of stock prices and spot rates where the option is optimally held (i.e. sold rather than exercised) under the corresponding VBS model.

Figure 9.4: Errors in EEP estimation: $\mathcal{P}_C^{\mathcal{O}} - \mathcal{P}_C^{\mathcal{V}}$ for $\chi = 0$

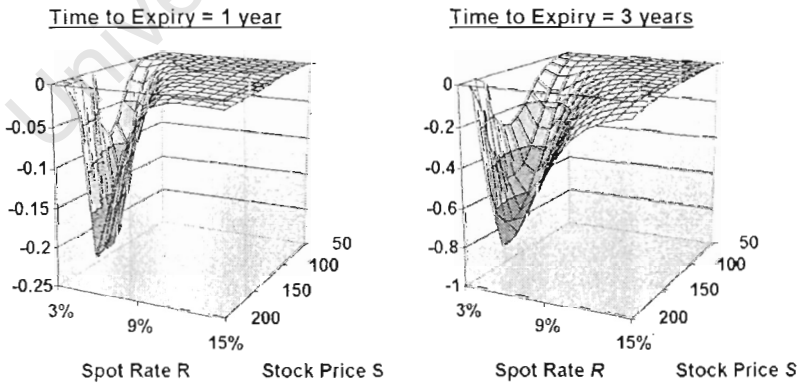

This portion of the early exercise region unique to the OBS model dominates differences in early exercise premia. Here OBS prices equal intrinsic value while VBS prices, which in this area are optimally sold rather than exercised, must exceed their intrinsic value. The discrepancy implies that, within the stopping area unique to the OBS model, VBS prices must exceed their OBS approximations, and as such that OBS approximations $\mathcal{P}_C^{\mathcal{O}}$ to the corresponding early exercise premium $\mathcal{P}_C^{\mathcal{V}}$ are under-estimates. This relationship is clearly

illustrated (for the VBS calibration $\chi = 0$) in figure 9.4.

For options one year from expiry, the calibrations $\chi = -25\%$ and $\chi = 25\%$ produce graphs almost identical to that in figure 9.4. Three years from expiry $\chi = -25\%$ and $\chi = 0$ agree, while $\chi = 25\%$ has the OBS model slightly over-estimating the $\mathcal{P}_C^{\mathcal{V}}$ within the stopping region common to both models. In the common stopping area both options carry intrinsic value, and the mis-estimation of $\mathcal{P}_C^{\mathcal{V}}$ stems from a slight under-estimation of the European option (See figure 8.13 on page 89).

9.2.2 Call Option Prices

Prices of American equity call options are implicitly the sum of their European counterparts and their early exercise premium. Given the predominantly low level of the early exercise premium (shown in figure 9.3). American equity call options differ perceptibly from European equity call options only when deep in-the-money. Even so, the broad shape and level of American equity call option prices is not significantly different from the European prices shown in figures 8.3 and 8.8.

Figure 9.5: Total pricing errors at $T - t = 1$ for $\chi = -25\%$ and $\chi = 25\%$

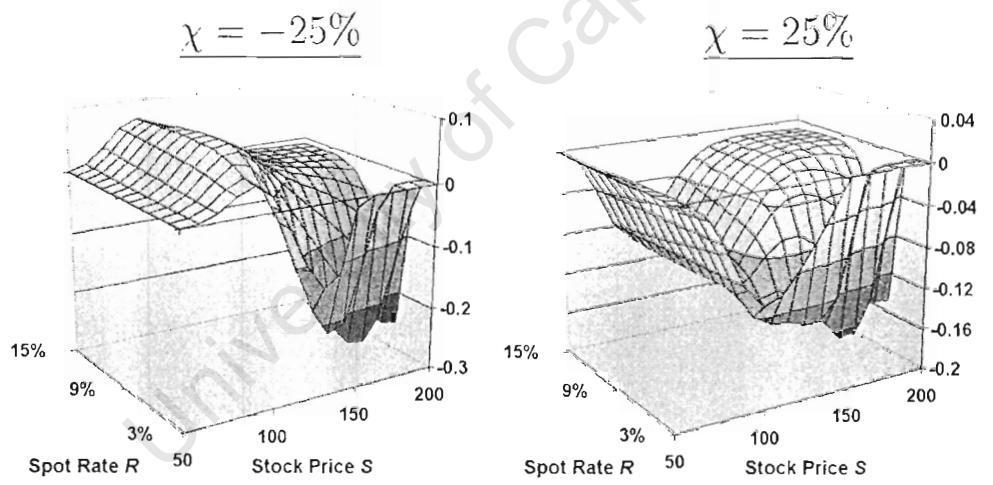

Of more immediate concern to us than price levels is the difference between OBS and VBS prices for these options. This is just the sum of European pricing errors and errors pricing the early exercise premium. These distinct effects are clearly visible both at one and three years to maturity, as shown in figures 9.5 and 9.6.

The hill (valley) for $\chi = -25\%$ ($\chi = 25\%$) occurring while the option is at-the-money reflects mispricing of the underlying European claim, discussed in detail in the previous chapter. The steep valley occurring for deep in-the-money options reflects mispricing of $\mathcal{P}_C^{\mathcal{V}}$: for $\chi = 25\%$ this is of equal magnitude to mispricing of the European component, while for $\chi = -25\%$ underestimation of $\mathcal{P}_C^{\mathcal{V}}$ is two to three times the magnitude of $c^{\mathcal{V}}$ mispricing errors.

However, mispricing attributed to the early exercise premium is minimal as a proportion of the total option price. This is largely because such mispricing occurs when the option is close to being exercised, and carries a high price.

Figure 9.6: Total pricing errors at $T - t = 3$ for $\chi = -25\%$ and $\chi = 25\%$

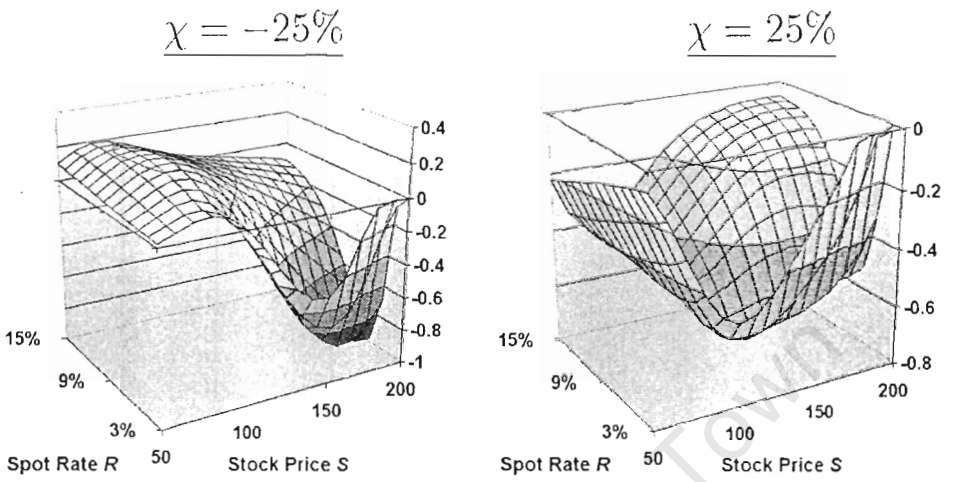

Figure 9.7[2] shows how, despite $\mathcal{P}_C^{\mathcal{V}}$ errors being visible as a slight twist in the foreground, pricing errors as a proportion of option price remain dominated by the corresponding European effects, which are largest when the option is deep out-of-the-money. (Refer also to figures 8.5 and 8.10).

Figure 9.7: Relative pricing errors for $\chi = 25\%$

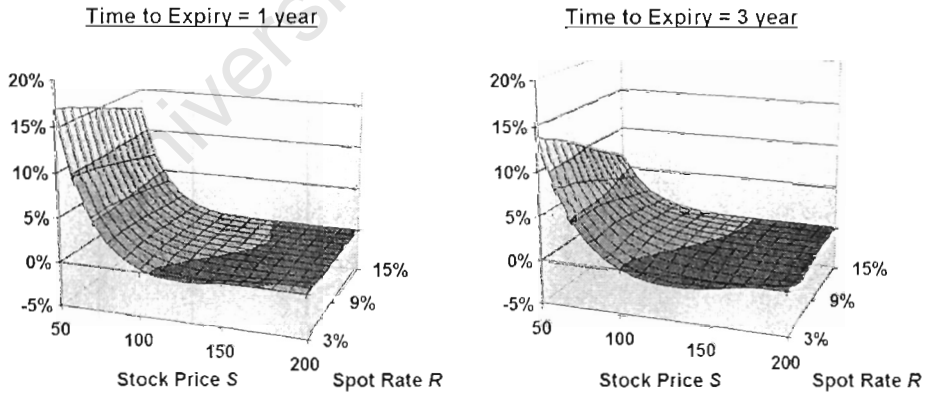

[2]This figure paradoxically exhibits decreasing proportional pricing error with increasing time to expiry. This is explained by 1) the denominator (option price) increasing with time to expiry, and 2) critical correlation χ_c decreasing towards -25% as time to expiry increases, thereby minimising increases in the numerator (total pricing error).

9.3 Call Hedge Parameters

Our techniques for option pricing rely on the ability to hedge all market risk. Accurate and appropriate pricing requires accurate hedging. We will examine both the in-model hedges used to arrive at option prices, as well out-of-model ρ-hedges discussed in chapter 5.

9.3.1 In-Model Hedges

Stock Transactions

We consider first the units of stock used to hedge American call options. Figure 9.8 shows the OBS American call option stock purchases to be (unsurirpsingly) very similar in shape to the European counterparts illustrated in figures 8.16 and 8.22, displaying increasing sensitivity to spot rates with increasing time to expiry. However, the early exercise possibility drives the American hedge up to a value of one within the stopping region.

Figure 9.8: OBS Stock Hedges for $T-t=1$ and $T-t=3$

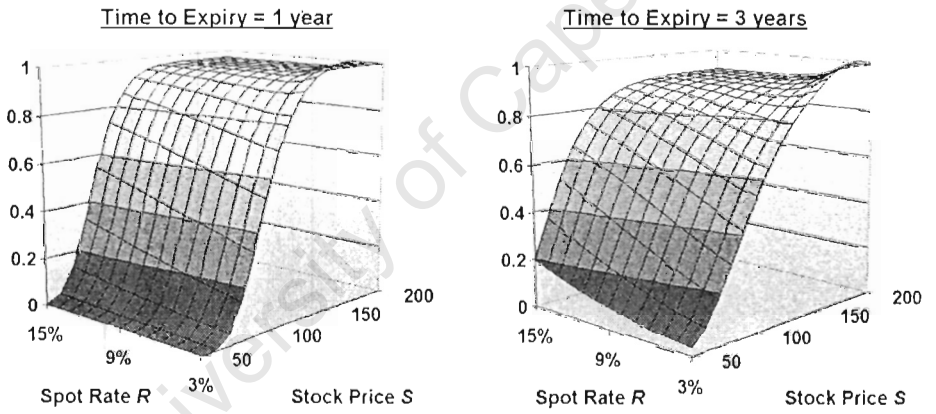

This plateau at unity induces an interesting effect. While European stock hedges uniformly increase with increasing spot rates, for high stock prices American stock hedges may be either increasing or decreasing in the spot rate. We merely note this property here, and leave its investigation to other studies.

Stock hedges in a VBS model are accurately approximated in level and shape by the simpler to obtain OBS value. VBS stock hedges exhibit all the characteristics of their OBS approximations, including indeterminate sensitivity to spot rates at high stock prices.

Figure 9.9 shows errors from approximating VBS American call stock hedges by simpler (and quicker) OBS hedges for call options one year from expiry. As with price errors, the distinct effects stemming from European mis-estimation and from early exercise premium mis-estimation are clearly visible. While the European portion of the error is sensitive in direction and magnitude to the chosen correlation calibration, the early exercise premium portion is relatively insensitive in both aspects.

As with price approximation errors, hedge approximation errors arising from differences in the early exercise premium occur near the zenith of the hedge value. As such they have little effect on the proportional error in approximating the units of stock held to hedge the

Figure 9.9: Total Stock Hedge Errors at $T - t = 1$

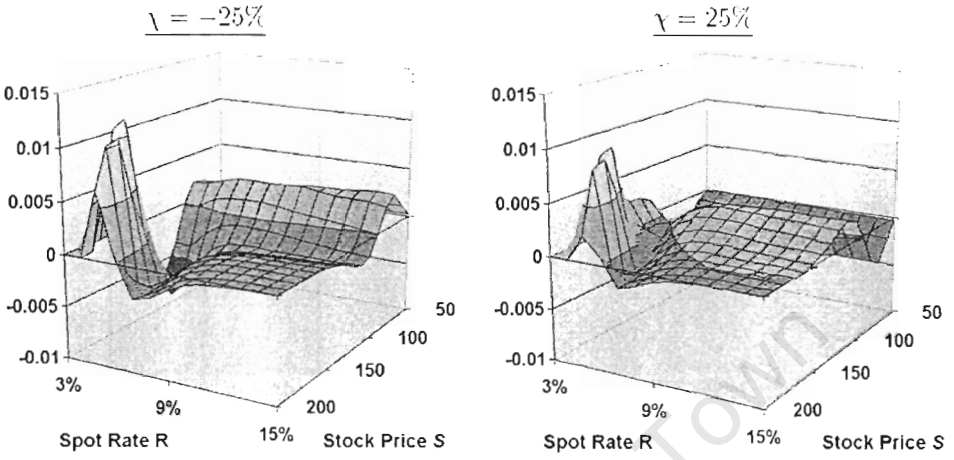

American call option. The proportional error is dominated by European errors when the option moves out-of-the-money, as illustrated in figure 9.10.

Figure 9.10: Proportional Stock Hedge Errors at $T - t = 1$

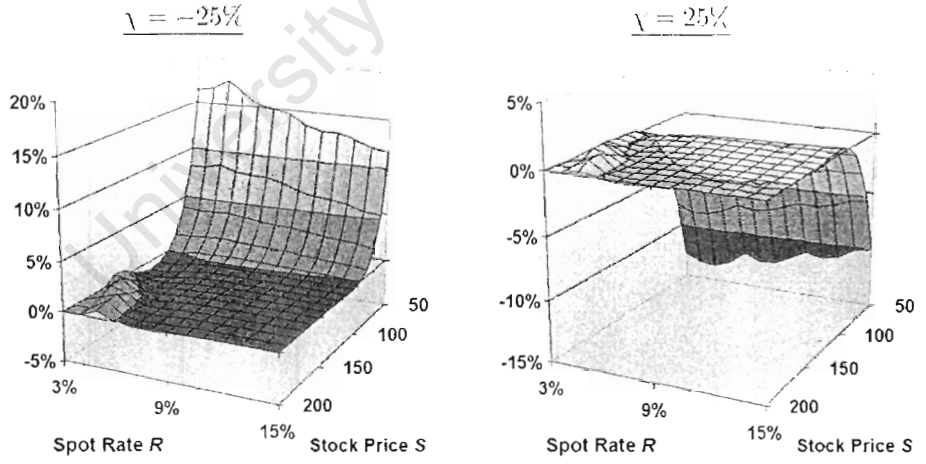

This analysis for stock hedge errors remains true even at three years from option expiry. Figure 9.11 depicts stock hedge errors three years from option expiry for $\lambda = 0$. European errors dominate the proportional error, while EEP errors remain quite insensitive to correlation. Indeed, the value of the stock hedge error resulting from differences in the EEP changes little between one and three years to expiry. Total stock hedge errors for $\chi = -25\%$ and $\chi = 25\%$ likewise exhibit distinct European and EEP effects, while proportional errors are still dominated by European effects.

Figure 9.11: Total Stock Hedge Errors at $T - t = 3$ for $\chi = 0$

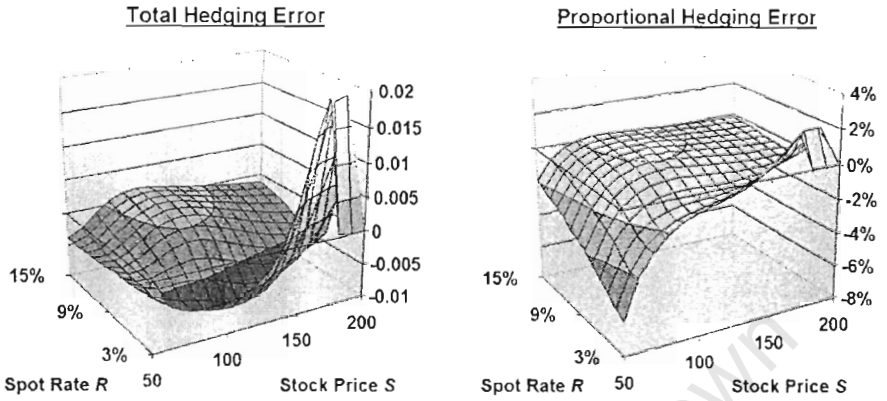

Fixed Income Transactions

Having invested part of the replicating portfolio in the underlying equity security, both OBS and VBS models invest the residual amount in either cash or bonds. In the case of call options the stock investment exceeds the option premium, so this 'residual' is negative, implying either borrowing cash or shorting bonds.

The OBS assumptions imply that cash and bonds are indistinguishable (see section 3.1.2), and so that the hedge may be arbitrarily split between these assets. Due to this indistinction, to make a valid comparison between VBS values and their OBS estimates we compare the total *value* of investment in cash and bonds within each model (i.e. compare $\beta[t] \cdot H^{\mathcal{O}}_{C;\beta}[t,\omega]$ to $\beta[t] \cdot H^{\mathcal{V}}_{C;\beta}[t,\omega] + B^{\mathcal{V}}[t,T.R] \cdot H^{\mathcal{V}}_{C;B[T]}[t,\omega]$).

Knowing that both price and stock hedge approximations by OBS values are reasonably accurate, we have *a priori* evidence suggesting that the total value of the hedge portfolio invested in what we shall call fixed income assets[3] will not differ between models.

As a baseline for comparison, figure 9.12 shows the total value of hedge purchases in fixed income assets under OBS pricing; negative values indicate short sales, as ever. As with stock hedges, fixed income hedges approximately equal those of their European counterparts, but for deviations at and near to the stopping region. (Note that figures 9.12 shows a measurement of cash value, whereas figures 8.17 and 8.23 show unit purchases. While comparable, the two measures are not equal.).

Like stock hedge values, the cash value of fixed income hedges exhibit changing direction of sensitivity to spot rates for high stock prices.

Model differences still exhibit distinct European and early exercise premium effects: figure 9.13 shows a sample of this at $T - t = 1$. The European effects were discussed in detail in the previous chapter. Early exercise premium effects remain relatively insensitive to changes in correlation or in time to maturity; they consistently reach a maximum magnitude of under-buying (i.e. over-shorting) by 2% of the strike price.

Fixed income hedge errors three years from option expiry are a composite of the European effects (discussed in the previous chapter) and early exercise effects (which closely resemble the early exercise effects one year from option expiry).

[3]Traditional definitions of fixed income assets do not include cash. Ours does.

Figure 9.12: OBS Fixed Income Hedge Values at $T-t=1$ and $T-t=3$

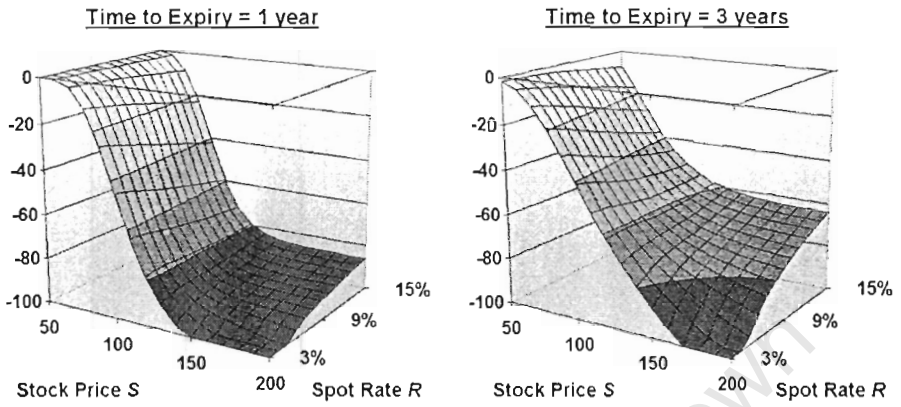

Figure 9.13: Fixed Income Hedge errors at $T-t=1$

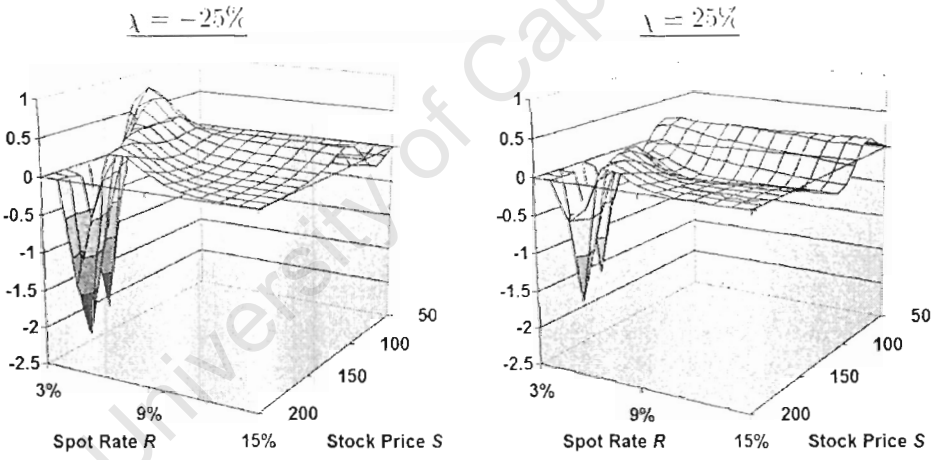

As in other analyses, proportional errors are dominated by European effects out-of-the-money; effects associated with the early exercise premium are negligible in proportion to the total fixed income holdings.

9.3.2 Out-of-Model ρ-hedges

ρ-hedging involves hedging the sensitivity of the OBS price to the (assumed-constant) interest rate R. Chapter 5 discussed this technique in detail. The discussion described theoretical inconsistencies in the notion of ρ-hedging, but concluded that the technique may have practical computational benefits.

Computational benefits involve a tradeoff between speed and accuracy. We know that OBS prices are far less intricate, hence faster to calculate. Our numerical results permit us

to examine the accuracy of so-called ρ-hedging in removing interest rate risk from portfolios holding American equity options here.

ρ-Hedge Characteristics

ρ-hedging techniques leave hedge portfolio purchases of the underlying stock unchanged. Hence we only consider fixed income security transactions.

First we consider the broad level and shape of the functions to be compared. Figure 9.14 shows the ρ-hedge purchases under OBS pricing of the discount bond maturing at option expiry. (Once more negative purchases indicate short sales). Two features stand out.

Figure 9.14: OBS ρ-hedge bond purchases for $T - t = 1$ and $T - t = 3$

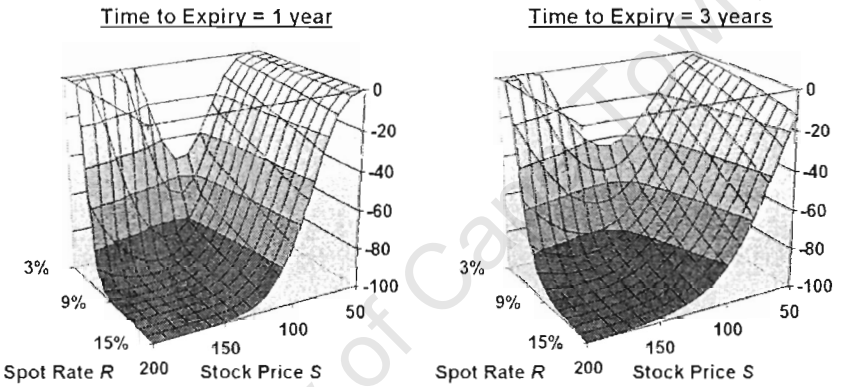

Firstly, from a floor of short sales with face value almost equivalent to the strike price, ρ-hedge purchases rise (short sales decrease) with decreasing stock price. For the majority of the domain $(S, R) \in [50, 200] \times [3\%, 15\%]$ the American call option is either not nearly sufficiently in-the-money, or spot rates are simply too high, for early exercise to be likely - and hence to have a meaningful impact on the option's characteristics.

So, in this majority of the domain, the American call option behaves much like a European option. In this case ρ-hedges correspond closely to the European hedges, where all fixed-income short sales are transacted in the T-discount bond. Decreasing short sales with decreasing stock price indicates decreasing probability of option exercise at maturity under the measure $\mathbb{Q}_B^T$.

The second feature occurs at high stock prices and low spot rates, where the number of ρ-hedge short sales decreases dramatically with decreasing spot rate. It is only here, with low and decreasing opportunity costs of early exercise, that such exercise becomes beneficial.

With the option this deep in-the-money, it is almost certain to be exercised. The European hedge short-sells nearly the full strike price in face value of the discount bond, to hedge the anticipated cash inflow of the strike price at option expiry.

The decreasing spot rate, as said, decreases the opportunity costs of early exercise and, when low enough, makes such exercise optimal. As we approach this early exercise, the the anticipated receipt of the strike price migrates forward in time from maturity to the present. The fixed income position hedging the call adjusts correspondingly from a short position in discount bonds only to a short position in cash only. This adjustment creates the second

Figure 9.15: Comparison of bond purchases for OBS ρ-hedge and VBS hedge at $T-t=3$ for $S[t]=200$

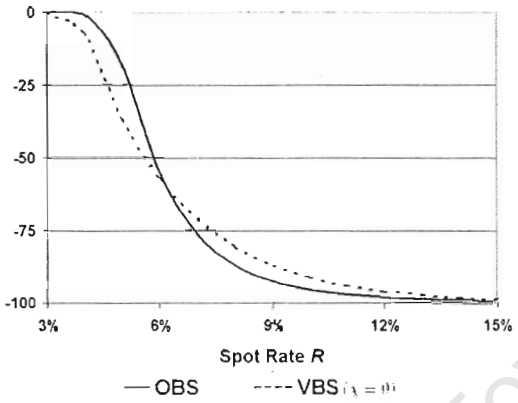

feature.

Though both effects are steeper at one year from expiry than three, the steepening over time is less pronounced for the early exercise effect, which retains a very steep gradient at both horizons. As with standard Black-Scholes delta-hedging, the steep gradient of a hedge parameter creates potential substantial hedging losses in actual markets (which in practice trade discretely) should the underlying stochastic parameter fluctuate within the area of steep gradient.

In the Black-Scholes case this is sometimes referred to as the Gamma trap. In our case the partial derivative of concern is the second derivative with respect to the spot rate, and the stochastic variable of concern is again the spot rate (or equivalently, through the inverse of (3.12), the short rate).

ρ-Hedge Accuracy

Now let us compare our two models. Examination of effectiveness of ρ-hedging in eliminating interest-rate risk of the American equity call option requires comparing the VBS in-model discount bond purchases $H^{\mathcal{V}}_{C;B[T]}[t,S,r]$ to the OBS out-of-model approximation $\tilde{H}^{\mathcal{O}}_{C;B[T]}[t,S]\Big|_{R[t,T,r]}$.

Figure 9.15 depicts the number of discount bonds purchased for the portfolio replicating an American equity call option three years from expiry for $S[t]=200$, under both the OBS (ρ-hedge) and VBS ($\chi=0$) models. The switch from bonds to cash as the spot rate decreases is evidently far more sudden for the OBS model than the VBS model. Smoothness in the VBS model results from explicitly modelling interest rate stochasticity. Other values of S and χ produce similar conclusions.

It is this discrepancy regarding the speed of switching from bonds to cash which dominates differences in bond holdings, illustrated in figure 9.16 at three years to expiry. As spot rates decline, VBS models start switching to cash earlier, initially leading to OBS under-estimation of bond purchases (i.e. over-estimation of bond short sales). Thereafter OBS models react strongly to decreasing spot rates, exercising too early and holding too few bonds. The models

naturally agree within the common stopping region.

Figure 9.16: Total errors in ρ-hedge bond purchases for $\chi = 25\%$ and $\chi = -25\%$

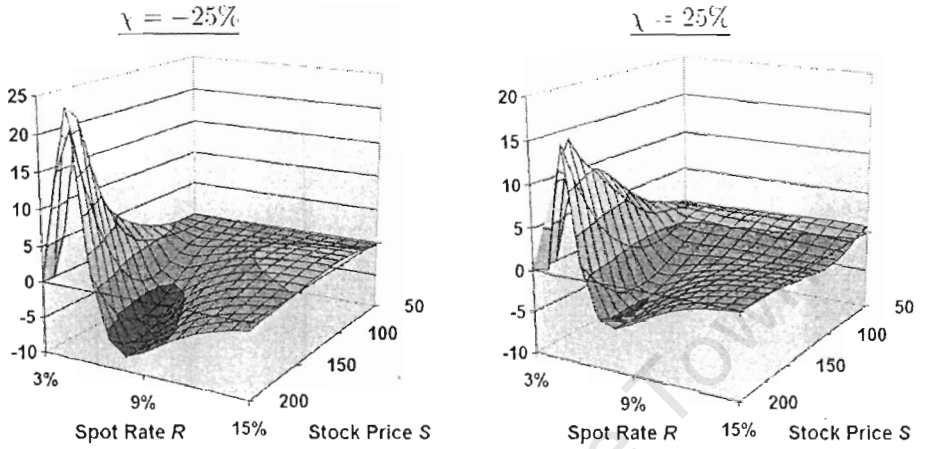

In the stopping region unique to OBS models, by holding all non-equity assets in cash only any OBS approximation must under-estimate bond short sales by 100%. Relative ρ-hedging errors are dominated by this spike to -100% throughout the unique stopping region.

Sources of ρ-hedge error may be viewed another way. Within the common exercise area the two models agree on option price and option hedges. And suitably far away from this area both models price (and hedge) the American call option indistinguishably from the European. Chapter 5 showed the European ρ-hedge to be the discount bond hedge, while chapter 8 showed that numerical differences in discount bond hedges to be insubstantial.

ρ-hedge differences are then driven by the transition of the two models from one area of ρ-hedge agreement to another area of agreement. As exhibited in figure 9.15, the OBS model makes this transition far faster than the VBS model, creating the errors in figure 9.16.

Comparisons one year from expiry of OBS ρ-hedge results to VBS results reveal similar patterns. Total differences are lower in magnitude, but ρ-hedge (and also in-model VBS) short sales of discount bonds display, near to early exercise, a steeper gradient in the spot rate than displayed three years from expiry.

Chapter 10

Numerical Results III: American Put Options

In this final results chapter we present numerical comparisons of VBS and OBS model outputs regarding American equity put options. This process mirrors the analysis in chapter 9, which considered American equity call options. We investigate Optimal Exercise Boundaries (OEBs), option prices, and in the last section hedge parameters regarding stock purchases, in-model fixed income purchases as well as out-of-model bond purchases.

10.0.3 Approximation Scheme Details

Consistent with the preceeding chapter, OBS numerics use 12 time steps per month, with 750 spatial steps spanning the price interval concerned. The lower bound of this interval must be lowered to $\tilde{S}_P^{\mathcal{O}}[\infty]$, while an upper bound of 250 is imposed. In general this leads to a smaller interval than that used for pricing calls, providing marginally better precision.

VBS estimates use the explicit scheme, again with $\Delta t = \frac{1}{144}$. As with OBS calculations, the stock prices interval considered is lower than for calls, catering for the characteristics of put options. The domain of interest for the calculations used in this chapter is set to (S, r) in $[25, 250] \times [0\%, 20\%]$.

The stability horizons are calibration-specific, and remain unchanged from those presented for American call options. However, the changed domain of interest leads to the new upper bounds on Δt of 0.241, 0.140 and 0.062 for the calibrations $\chi = -25\%$, $\chi = 0\%$ and $\chi = 25$ respectively. Our choice of $\Delta t \approx 0.007$ clearly satisfies these limits.

Again, discussion and derivation of the schemes used here are presented in chapter 6 and appendix C, while the Matlab code used to obtain out results is provided in appendix D.

10.1 Optimal Exercise Boundaries

We start our analysis in the same way as in the previous chapter, examining the optimal exercise rules which characterise the solution to our exercise problem. Figure 10.1 illustrates a collection of OBS optimal stopping boundaries $\tilde{S}_P^{\mathcal{O}}[t]$ for calibration spot rates ranging from 3% to 15%.

Representing the right to sell equities, the American equity put option exhibits very different features to the call option. The option moves in-the-money as stock prices decrease,

Figure 10.1: Optimal Exercise Boundary $\tilde{S}_P^{\mathcal{O}}[t]$ for $R \in [3\%, 15\%]$

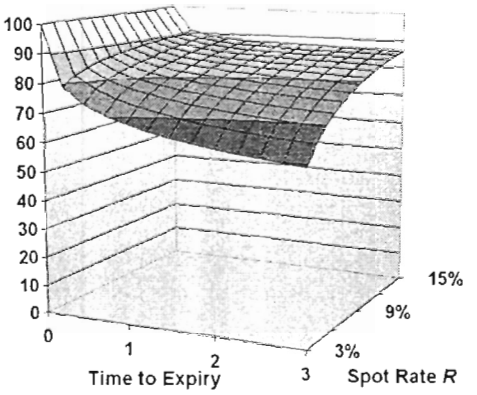

More importantly, the roles of dividends and interest rates are reversed: following early exercise, interest is received on the strike price while dividends on the stock are foregone. As the spot rates considered are large relative to the calibration $\delta = 3\%$ for the dividend yield, early exercise becomes more lucrative and hence more likely.

Returning to figure 10.1, we identify three features, as with figure 9.1. Firstly, the optimal exercise curves are decreasing with increasing time to expiry - reflecting greater optionality foregone, hence a need to be deeper in-the-money before exercise is optimal.

Secondly, the curves increase for increasing spot rate. Naturally the larger the rewards for early exercise, the less in-the-money the option needs be before early exercise is optimal.

But in strong contrast to figure 9.1, the optimal exercise boundary $\tilde{S}_P^{\mathcal{O}}[t]$ remains within the range considered ($S \in [50, 200]$) for all spot rates and times to maturity considered. The relative accessibility of this OEB results from the relatively high value of benefit rate (R) in comparison to the cost rate (δ).

Whereas the OEB limit at expiry for call options was linear in the spot rate, this same limit for put options is perfectly horizontal at $S = K$. In fact, graphs of both call and put OEB limits at expiry exhibit a constant section and a section linear in R, separated across the value $R = \delta$. By calibrating $R = \delta$ as the lower bound of spot rates for consideration, we have inadvertently hidden this characteristic.

The relative accessibility of $\tilde{S}_P^{\mathcal{O}}[t]$ suggests that early exercise premia may have a larger influence on the accuracy of OBS approximations for put options than they did for call options. Interpretation of any such differences is aided by a comparison of optimal exercise boundaries across different models.

Figure 10.2 shows the OEB $\tilde{S}_P^{\mathcal{V}}[t, R^{-1}[R]]$ for the calibration $\chi = 0$; the locations of $\tilde{S}_P^{\mathcal{V}}$ for $\chi = -25\%$ and $\chi = 25\%$ are remarkably similar. (For $(R, T - t) \in [3\%, 15\%] \times [0, 3]$, $\tilde{S}_P^{\mathcal{V}}$ - unlike $\tilde{S}_C^{\mathcal{V}}$ - remains within the bounds of S used in our numerical approximation. Thus we can present estimates of $\tilde{S}_P^{\mathcal{V}}$ throughout the domain of figure 10.2.)

It is immediately apparent that, for low spot rates and large times to expiry, OBS estimates of the stock price below which exercise is optimal are far larger than the true VBS values.

However, as shown in figure 10.3, large magnitude errors are localised to low spot rates.

Figure 10.2: Optimal Exercise Boundary $\tilde{S}_P^{\mathcal{V}}[t, R^{-1}[R]]$ for $\chi = 0$

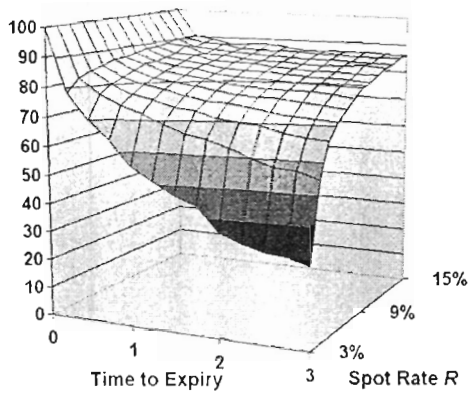

Figure 10.3: Errors in OEB estimation: $\tilde{S}_P^{\mathcal{O}}$ - $\tilde{S}_P^{\mathcal{V}}$ for $\chi = 0$

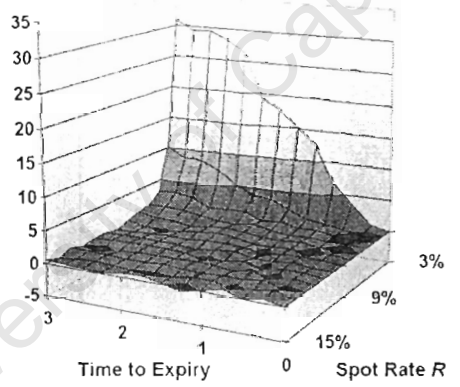

For most of the domain of $\tilde{S}_P^{\mathcal{V}}$ considered, the difference between $\tilde{S}_P^{\mathcal{V}}$ and $\tilde{S}_P^{\mathcal{O}}$ is negligible. In some areas the price process $P^{\mathcal{O}}$ even under-estimates the optimal stock price, though this minority is probably due to inaccurate numerical estimation of $\tilde{S}_P^{\mathcal{V}}$ rather than to differences in the true processes.

Indeed, supposing the under-estimates are numerical irregularities rather than actual phenomena, then - as with American equity call options - the VBS stopping region for American put options is a proper sub-set of the corresponding OBS stopping region. In addition to this common exercise area, there is also a set of points (S, R, t) where only $P^{\mathcal{O}}$ is exercised - a stopping region unique to $P^{\mathcal{O}}$. Other than at very low spot rates, this unique stopping region is minimal.

The accessibility of the boundaries $\tilde{S}_P^{\mathcal{O}}$ and $\tilde{S}_P^{\mathcal{V}}$ suggests that the early exercise premia $\mathcal{P}_P^{\mathcal{O}}$ and $\mathcal{P}_P^{\mathcal{V}}$ will contribute a more significant portion to American put option prices $P^{\mathcal{O}}$ and $P^{\mathcal{V}}$ than $\mathcal{P}_C^{\mathcal{O}}$ and $\mathcal{P}_C^{\mathcal{V}}$ did to $C^{\mathcal{O}}$ and $C^{\mathcal{V}}$. However, this dissertation is primarily concerned with price differences. The broad agreement of boundaries $\tilde{S}_P^{\mathcal{O}}$ and $\tilde{S}_P^{\mathcal{V}}$ indicates that, despite greater price contribution, the put early exercise premia will not contribute significantly to

differences in option prices and hedges between OBS and VBS price models. We investigate this more fully in the following sections.

10.2 Premia and Prices

10.2.1 Early Exercise Premia

As with American call options, American put options can be split into their corresponding European claim plus an early exercise premium. This early exercise premium represents the arbitrage profits accruing to the option seller should the holder not exercise optimally prior to expiry.

For the put option, such arbitrage profits are the interest received on the strike price held, less any dividends paid on the short position in stock. The stopping region constructs itself so that such profits are necessarily positive.

Before comparing early exercise premia across different models, we first consider the characteristics of the early exercise premium.

Early Exercise Premium Characteristics

Figure 10.4 depicts the early exercise premium for OBS put prices one and three years from expiry.

Figure 10.4: OBS Early Exercise Premium $\mathcal{P}_P^{\mathcal{O}}$ at $T-t=1$ and $T-t=3$

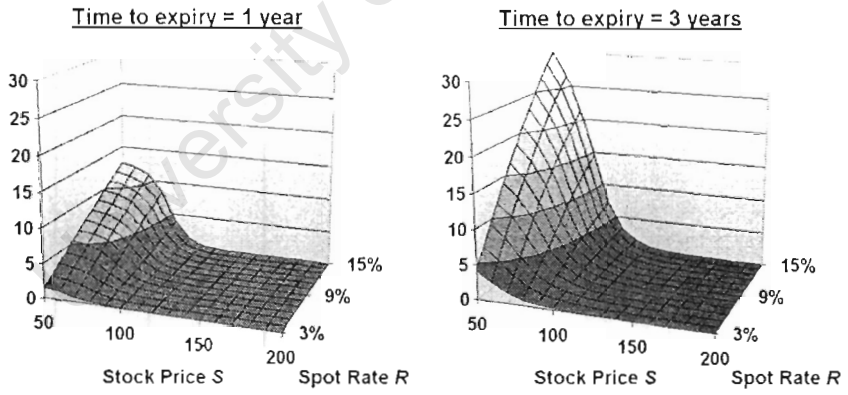

Several features deserve comment. Firstly, while the stock price lies above the strike price the early exercise premium is, for all intents and purposes, indistinguishable from zero. Then, as the option moves into-the-money, exercise before expiry becomes increasingly likely as the net benefits of such exercise increase. The early exercise premium rises steeply, reflecting this increase.

$\mathcal{P}_P^{\mathcal{O}}$ is also strongly increasing with increasing spot rates. European put option prices are decreasing functions of the spot rate (see section 8.1), but increasing interest rates make early exercise more attractive, inducing exercise at higher stock prices - exhibited in figure 10.1. Indeed, throughout the stopping region $\mathcal{S}_P^{\mathcal{O}}$ American put option prices must be insensitive to spot rates - so $\mathcal{P}_P^{\mathcal{O}}$ must increase with spot rates to offset the European sensitivity.

Finally, particularly at 1 year to expiry, the early exercise premium appears to reach a plateau with decreasing stock price. The second graph for $\mathcal{P}_P^{\mathcal{O}}$ suggests that this effect may also present three years from expiry, but is not visible within the domain considered.

Over the domain considered, the early exercise premium constitutes up to 42% of the American equity put option price at one year from expiry, and up to 74% three years from expiry. This contrasts strongly with the American equity call option, for which the early exercise premium never exceeded 8% of the option price throughout the domain considered.

Early Exercise Premia Comparisons

In chapter 9 the differences in American equity call option prices and hedges between the true VBS and approximate OBS models decomposed neatly into two apparently independent effects - a European effect, and the residual effect attributed to the early exercise premium. While this decomposition remains valid for American equity put options, interaction between the two effects reduces the explanatory power of the decomposition.

To better understand this interaction, consider figure 10.5:

Figure 10.5: OEBs $\tilde{S}_P^{\mathcal{O}}$ and $\tilde{S}_P^{\mathcal{V}}$ at $T-t=3$ against contours of $p^{\mathcal{O}}-p^{\mathcal{V}}$, all for $\chi=0$

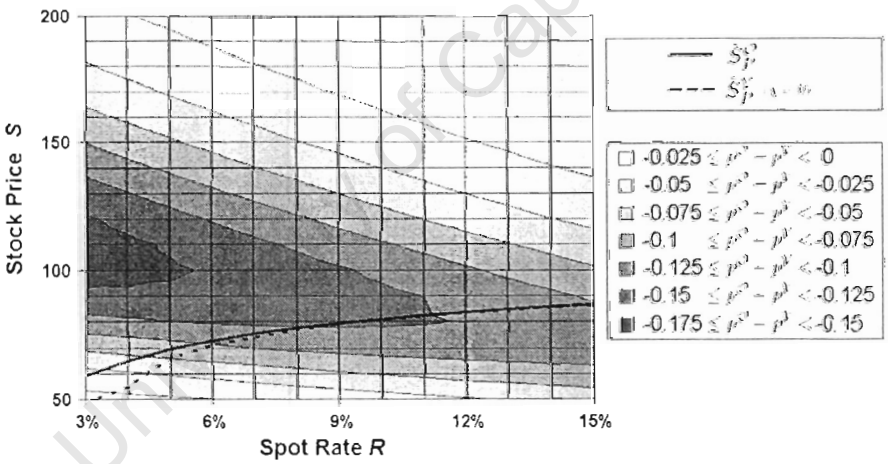

The background of figure 10.5 shows contours of the difference between the OBS and VBS models in the price of a European equity put option (viz. $p^{\mathcal{O}}-p^{\mathcal{V}}$). The foreground graphs the optimal exercise boundaries $\tilde{S}_P^{\mathcal{O}}$ and $\tilde{S}_P^{\mathcal{V}}$ for an American equity put option under the OBS and VBS models respectively, for $T-t=3$. Both foreground and background use the calibration correlation $\chi=0$.

In the common exercise area - below the lowest exercise boundary - both models value the option at intrinsic value, and hence the model pricing difference is zero. However, within this region the European prices may differ by as much as 0.15 currency units per contract. Consequently, within this common exercise area the early exercise premia $\mathcal{P}_P^{\mathcal{O}}$ and $\mathcal{P}_P^{\mathcal{V}}$ must differ by the reverse of the European difference, so that the net American option price difference remains zero.

This necessary counter-acting effect distorts interpretation of the early exercise premium. Figure 10.6 illustrates the differences in the early exercise premia $\mathcal{P}_P^{\mathcal{O}}$ and $\mathcal{P}_P^{\mathcal{V}}$ at three years

from expiry for the VBS calibration $\chi = 0$.

Figure 10.6: Total EEP error $\mathcal{P}_P^{\mathcal{O}} - \mathcal{P}_P^{\mathcal{V}}$ at $T - t = 3$ for $\chi = 0$

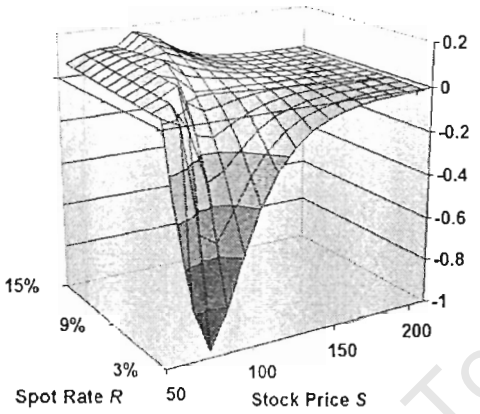

The valley occurring at low spot rates reflects the consistent over-estimation of the OEB, and corresponding under-estimation of the optimal stopping time, by the OBS model. The mechanisms inducing the valley are the same as those operating for the American equity call options (see section 9.2).

However, the slight ridge occurring for high spot rates merely reflects the need for the early exercise premium to remove differences in European option prices throughout the common stopping area (compare to figure 8.11). Differences between OBS and VBS models regarding the early exercise premium at different times, and/or for different correlation calibrations, reflect similar interactions with differences in the European prices.

As a result of this interaction, analysis in isolation of the differences in early exercise premia provides limited insight into the differences in American equity put option pricing between the models considered. Consequently, we bypass further analysis of early exercise premia and move directly to differences in option pricing.

10.2.2 Put Option Prices

The crucial differences between American and European equity put options have already been alluded to. Figure 10.7 presents the prices of American put options under the OBS model for comparison to figures 8.3 and 8.8, as well as for completeness.

American put option prices differ most notably from European put options at low stock prices. Here the American strongly exceeds the European, and displays little or no sensitivity to changes in interest rates - in contrast to the European. In addition, the early exercise feature makes the American put option far less sensitive to changes in time to option expiry.

While VBS prices for the American equity put option do differ from the OBS prices in figure 10.7, their broad price level and shape is not visibly substantially different from the OBS graphs.

Errors in OBS approximations to the true VBS prices behave differently for American and European equity put options. At both one and three years to expiry, total pricing errors are dominated by the price under-estimate at low spot rates and low stock prices generated

Figure 10.7: OBS Prices at $T-t=1$ and $T-t=3$

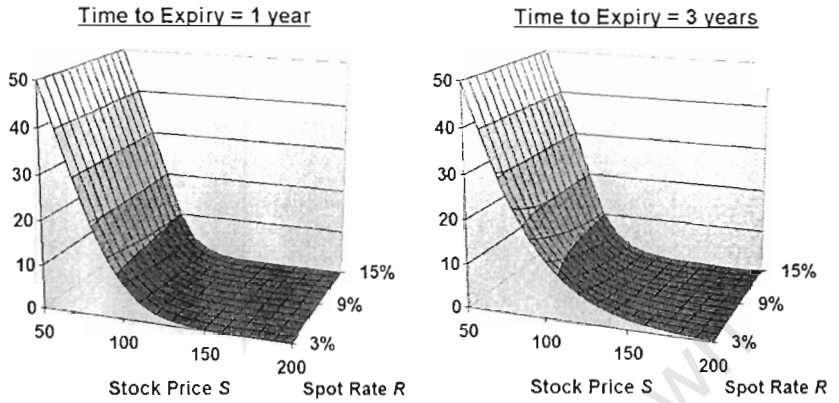

Figure 10.8: Total pricing error at $T-t=1$

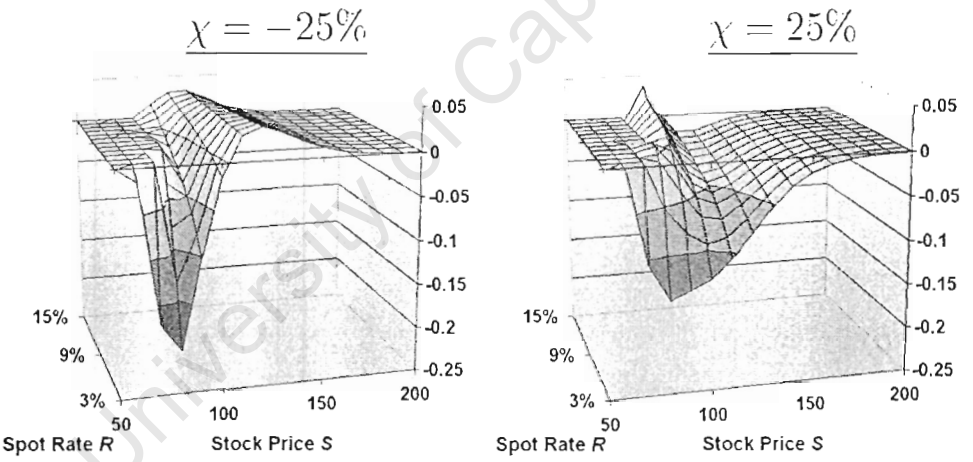

by mis-specification of the OEB. This error is relatively stable across different correlation calibrations.

Effects stemming from the European component are still visible, with the OBS model over-estimating at-the-money option prices for $\chi=-25\%$ and under-estimating for $\chi=25\%$. However, in comparison to the full European error analysed in Chapter 8, the errors here are dampened in amplitude by approximately half (compare to figures 8.4, 8.7, 8.9 and 8.13). This dampening is induced by the levelling effects of common early exercise through areas of large European differences, as illustrated through figure 10.5, as well as the continuity of the price function carrying such levelling effects into the continuation regions.

Finally, a peculiar effect presents itself within the common continuation region. Here, for all times to expiry considered, and at high spot rates and very near to the OEB, there exists a small area where OBS approximations paradoxically exceed the true VBS price, even for $\chi=25\%$. This effect also occurs for $\chi=0$ (not graphed), as well as for $\chi=-25\%$, for which

Figure 10.9: Total pricing error at $T - t = 3$

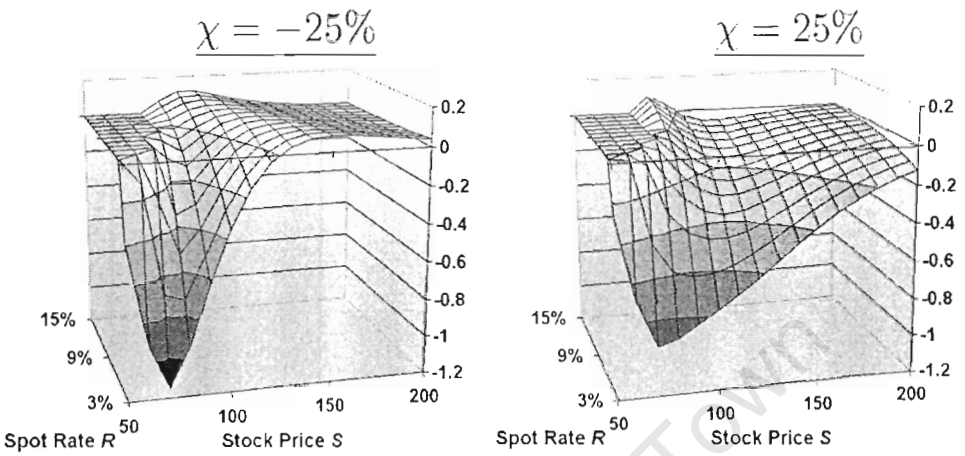

it is most visible through the changing inflection at high rates in figure 10.6.

This peculiarity reflects differing second derivatives of the OBS and VBS put option prices with respect to the underlying stock price - as illustrated (rather exaggeratedly) in figure 10.10. As the causes of such differences are as yet unexplained - and appear counter to initial intuition - we term this price over-estimate the 'convexity paradox'.

Figure 10.10: Exaggerated illustration of the 'convexity paradox'

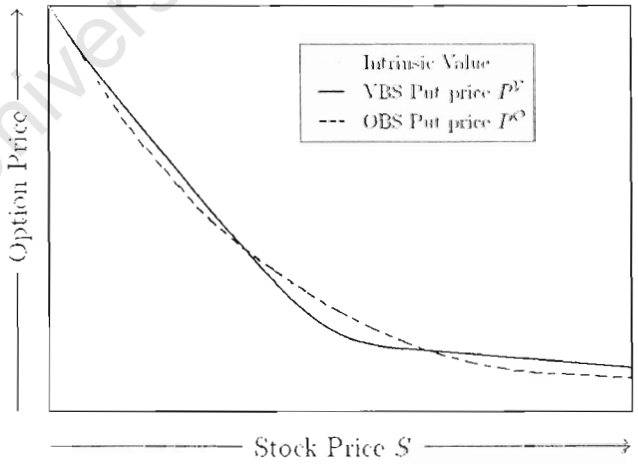

Price differences between OBS and VBS models showed interesting characteristics for American equity put options not present for European equity put options. However, such new differences are negligible when compared to the option price. Figure 10.11 shows (for $\chi = -25\%$) that, proportional the VBS option price, pricing errors remain dominated by the European effects deep out-of-the-money, induced the option price converging to zero faster

than the pricing error.

For a very substantial proportion of the domain of parameters considered, the OBS approximation to a VBS price with $\chi = -25\%$ remains accurate to within 5%. This is also true for the two other correlation calibrations.

Figure 10.11: Proportional pricing error for $\chi = -25\%$ for $T - t = 1$ and $T - t = 3$

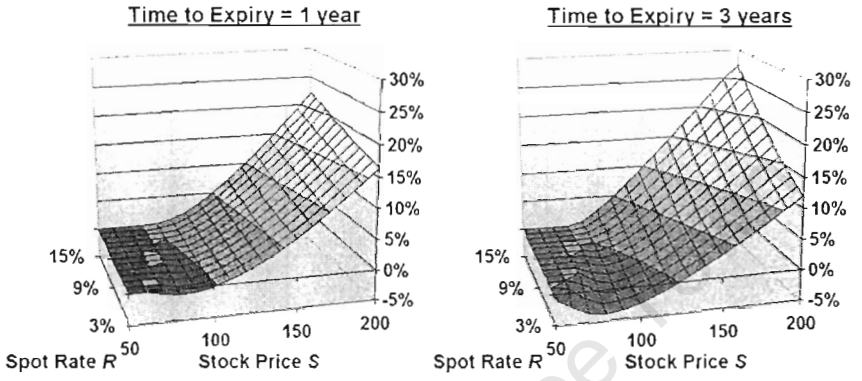

10.3 Put Hedge Parameters

Accuracy of hedge parameters remains necessary for the implementation of our arbitrage-free option prices. We will consider both the in-model hedges which create the replicating portfolio from which option prices are derived, as well as the ρ-hedging technique which attempts to hedge interest rate risk using the sensitivity of the OBS price to the fixed input R.

10.3.1 In-Model Hedges

Stock Transactions

Figure 10.12 shows the number of units of the underlying stock purchased in order to hedge an OBS American put option. (As ever, negative purchases indicate short sales).

In comparison to the stock hedges for the European put option (presented in chapter 8) two features deserve comment. Firstly, while the European option hedge increases uniformly with increasing spot rates, the early exercise feature causes American option hedges near to early exercise to be decreasing with increasing spot rates.

Secondly, the strong possibility of early exercise, particularly for high spot rates, limits the extent to which American option prices become smoother and more uniform over time. As a result of this the American stock hedge retains a steep gradient near the exercise boundary, even three years from option expiry. This gradient may give rise to 'Gamma risk' of trading losses, which for European options is limited to at-the-money options close to expiry.

VBS prices also exhibit both these effects.

Total errors when using the OBS model to estimate a VBS stock hedge are displayed in figure 10.13 at $T - t = 3$ for $\chi = -25\%$, where they are largest. (Over-estimation of stock

Figure 10.12: OBS Stock Hedges for $T - t = 1$ and $T - t = 3$

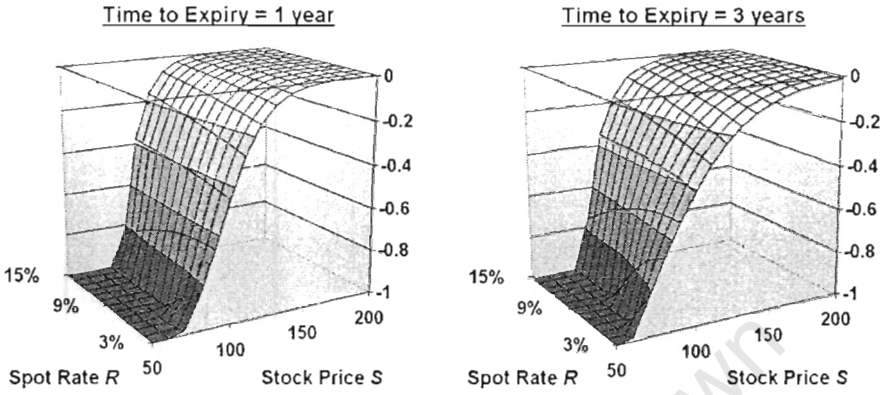

Figure 10.13: Total stock hedge error at $T - t = 3$ for $\chi = 25\%$

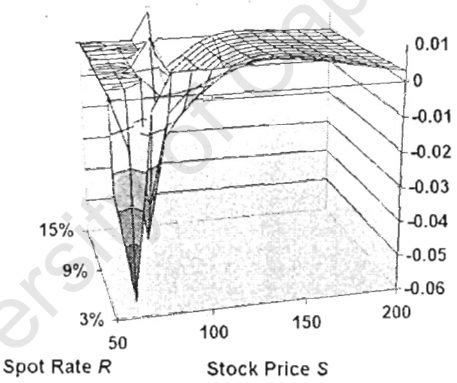

hedge purchases reflects under-estimation of short sales). The shape of this error curve is driven by factors discussed in the previous section on option pricing.

The wave-like form of the corresponding European estimate remains present, though muted through the possibility of mutually optimal early exercise. The direction and magnitude of this error remain dependent jointly on the correlation calibration and on the extent to which the option is in-the-money. However, this effect is dominated by others created by the early exercise feature.

At low spot rates the OBS model significantly over-estimates the stock price at which the option is first exercised. While in between the OBS and VBS OEBs the OBS model hedge shorts fully one unit of stock, while the VBS model shorts less than this. This creates under-purchases of as much as 0.05 units per contract for $\chi = 25\%$.

Finally, at high spot rates and close to the OEB, the OBS model exhibits mild over-purchases of stock associated with the convexity paradox. This error, like the under-purchases occurring in between OEBs, is relatively stable across the three correlation calibrations considered.

Figure 10.14: Proportional stock hedge error at $T - t = 3$ for $\lambda = 25\%$

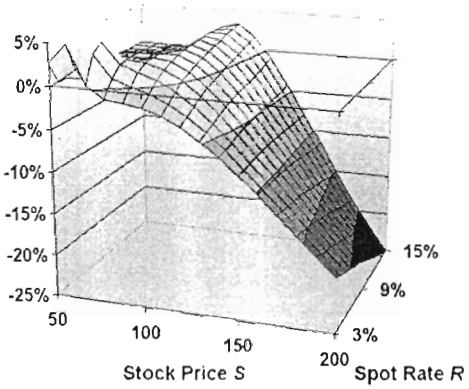

Again, despite the interesting nature of such differences, they remain largely insignificant as a proportion of total stock hedge purchases. Figure 10.14 exhibits such proportional error for $\chi = 25\%$, illustrating that the early exercise hedge errors never exceed 5% of total hedge, and that proportional errors are largest for deep out-of-the-money options. Proportional errors for the other two calibrations, as well as for one year options, display similar characteristics but are of lower magnitude.

Fixed Income Transactions

After stock purchases to hedge the option, the residual receipts from the option price are invested in fixed income instruments - cash and bonds. For put options this residual equals the option premium plus the proceeds from the short sales of stock. Substantial concurrence of the OBS and VBS models regarding option price and also stock hedge suggest that differences in fixed income hedges across the two models will not be large.

Figure 10.15: OBS Fixed Income Hedge Purchases at $T - t = 1$ and $T - t = 3$.

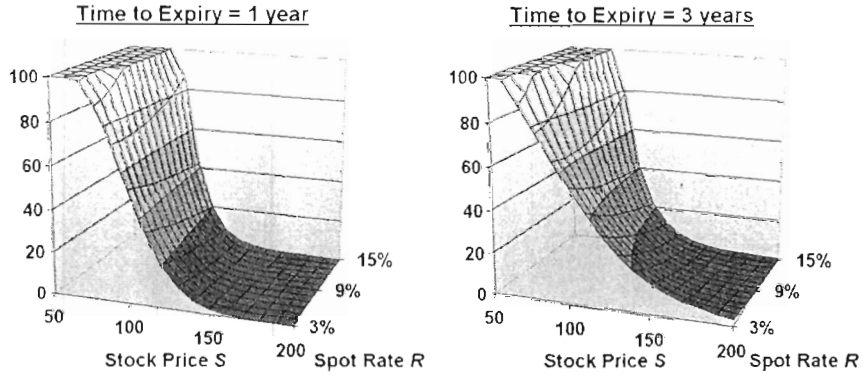

Fixed income purchases hedging an American equity put option under the OBS model are depicted in figure 10.15. As with the graph presented in chapter 9 this represents a cash

value, not a unit number of any security. They exhibit the anticipated shift from zero (when the option is very deep out-of-the-money) to the full strike price (within the optimal exercise area $\mathcal{S}_P^{\mathcal{O}}$).

Consistent with observations for stock short sales - and in contrast to the European put option - the early exercise feature induces the sensitiviy of fixed income purchases to spot rates to change sign with changing stock prices. and - when at-the-money - also with changing spot rates.

Figure 10.16: Total Error in Fixed Income Hedge Purchases at $T - t = 3$.

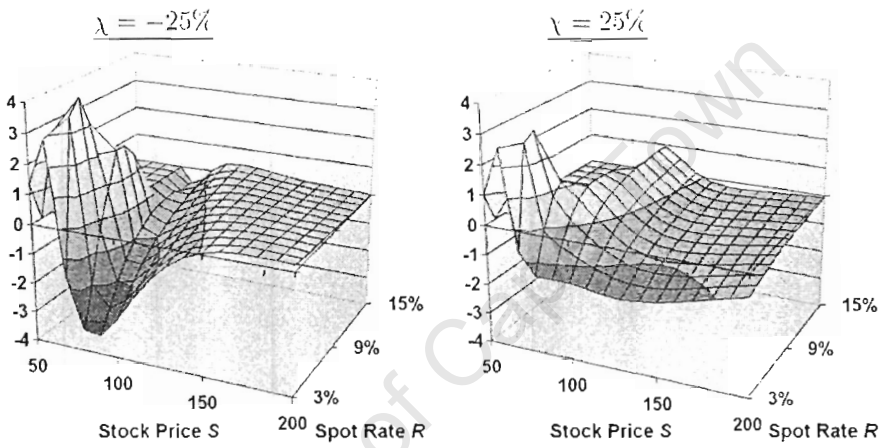

Figure 10.16 illustrates the difference between the OBS and VBS models regarding fixed income hedge purchases at $T - t = 3$. Similarly to the rest of this chapter, three effects are visible.

For large values of the stock price S, the hedge error is dominated by the corresponding European error - somewhat muted in magnitude by the effects of mutually optimal early exercise discussed on page 118.

For low spot rates and low stock price, as the stock price approaches $\tilde{S}_P^{\mathcal{V}}$ the OBS model over-estimates VBS fixed income hedge purchases. Here earlier exercise of the option under the OBS model requires the whole of the strike price held in fixed income assets, whereas the VBS models - still pricing the possibility that the option will never be optimally exercised - hold slightly less than this. This early exercise error is not particularly sensitive to the choice of correlation calibration.

Finally, for high spot rates and low stock price, the convexity paradox induces an over-estimation of the fixed income purchases for the hedging portfolio. This effect is strongest for $\chi = 25\%$, and remains unexplained.

Following the trend exhibited throughout this dissertation, proportional errors - shown in figure 10.17 - are immaterial for the majority of the domain of concern. Three years from option expiry, proportional errors only broach 5% when the option is deep out-of-the-money. The same patterns are visible for proportional fixed income hedge errors for $\chi = -25\%$ and $\chi = 0\%$.

Fixed income errors one year from option expiry exhibit the the same patterns as those three years from expiry, only over a more compressed area of the domain and with diminished

Figure 10.17: Proportional Error in Fixed Income Hedge Purchases at $T - t = 3$.

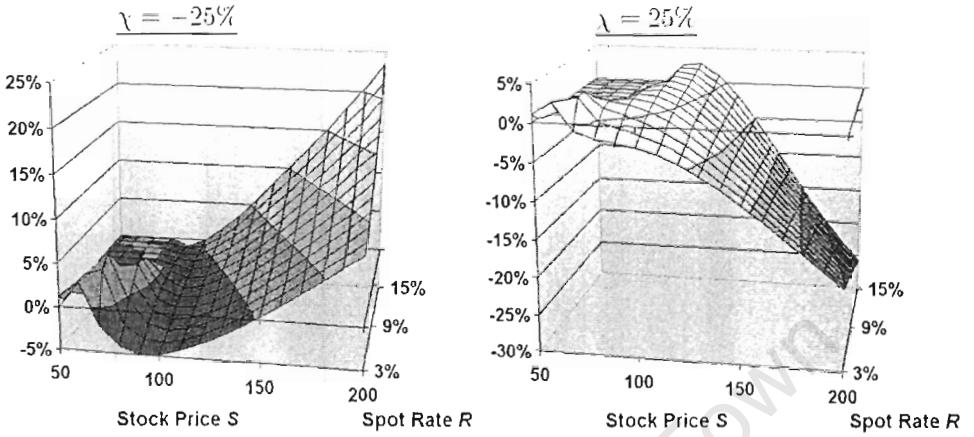

magnitude.

10.3.2 Out-of-Model ρ-hedges

The fixed income hedges above merely represent the use of residual funds. Such investments do not guarantee that the interest rate risk inherent in the American equity put option will be hedged. For interest rate risk to be hedged, the fixed income hedge must be divided appropriately amongst securities exhibiting interest rate risk. We assume that such a split is between the money market account and the discount bond maturing at option expiry.

OBS results may also be used to attempt hedging interest rate risk by using out-of-model hedging statistics, as discussed in chapter 5. We are interested in the accuracy of the ρ-hedge $\tilde{H}^{\mathcal{O}}_{P;B[T]}[t,S]$ as an estimator of the in-model VBS hedge statistic $H^{\mathcal{V}}_{P;B[T]}[t,S,r]$.

ρ-Hedge Characteristics

Figure 10.18 illustrates the number of discount bonds (maturing at option expiry) purchased to ρ-hedge an American equity put option, for both one and three years to option expiry.

For out-of-the-money options, ρ-hedge bond purchases increase as the stock price decreases. Such increases reflect an increase in the probability of exercise, with the discount bond purchases hedging an anticipated future cash outflow. However, for in-the-money options such purchases increase with decreasing stock price. Here the option is highly likely to be exercised within its lifespan; with the stock price approaching the optimal exercise boundary $\tilde{S}^{\mathcal{O}}_P$ from above, the expected time of exercise migrates from option expiry towards the present. Decreases in ρ-hedge purchases reflect a shift of total fixed income hedge from discount bonds (which hedge exercise at expiry) to cash (which hedges immediate exercise).

Throughout the domains presented in figure 10.18, discount bond purchases ρ-hedging the American equity put option are decreasing in the spot rate. This effect has two primary causes. In the OBS model, the stock price S drifts under the risk-neutral pricing measure $\mathbb{Q}$ at the interest rate R. Increasing R enhances this drift and so also all future values of the S, hence reducing the probability of exercise and consequently all fixed income hedge purchases,

Figure 10.18: OBS ρ-hedge bond purchases for $T-t=1$ and $T-t=3$

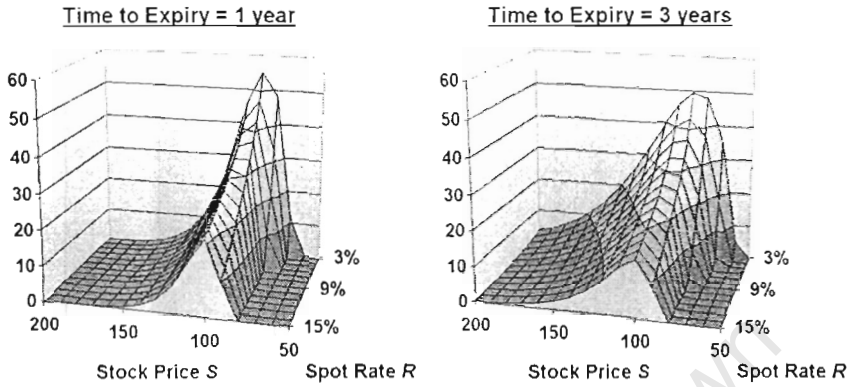

bonds included.

The second effect concerns early exercise. Larger spot rates indicate larger benefits to early exercise, and raises the OEB $\tilde{S}_P^{\mathcal{O}}[t]$. For any given path of $S[t]$ an increase in the spot rate R may bring the optimal time of exercise closer to the present, but never move it further into the future. Reacting to this, the (already reduced) fixed income hedge purchases are weighted more towards cash, further reducing bond purchases.

The hump through varying stock prices and the decrease with increasing spot rate both become steeper as the option approaches expiry. Such erratic behaviour at-the-money and near to option expiry is typical of most option contracts. However, where such behaviour merely represents switching assets between bonds and cash the economic significance is minimal - as, near to option expiry, cash becomes an increasingly close substitute for the dicsount bond maturing at option expiry.

Our final comment regarding figure 10.18 concerns its level. We are intrigued that the face value of discount bonds purchased to hedge the American put option only exceeds 50% of the strike price in a very limited number of scenarios. This characteristic reflects low probabilities of the option being exercised at maturity. In most scenarios the option is more likely to either be exercised before maturity, or not at all, than to be exercised at maturity.

ρ-Hedge Accuracy

We return to analysing the use of OBS results in a VBS economy, which is the focus of this dissertation.

Figure 10.19 shows the difference in discount bond purchases between OBS ρ-hedge portfolios and VBS hedge portfolios for $\chi=0$; coinciding graphs for other correlation calibrations exhibit similar shape, location and level. Other than the familiar mis-estimation in between $\tilde{S}_P^{\mathcal{O}}$ and $\tilde{S}_P^{\mathcal{V}}$, the inter-model difference regarding discount bond purchases is remarkably small. As established earlier, for low spot rates the OBS model exercises the American put option at materially higher stock prices than those at which the VBS model exercises. In the interregnum where the OBS model exercises and the VBS does not, OBS ρ-hedges hold no bonds and all cash, while VBS hedges hold some bonds to hedge interest rates ruling between the option valutation date and optimal exercise time. This discrepancy creates the downward spike in bond purchase differences present at low interest rates. At its maximum this difference can

Figure 10.19: Total error in ρ-hedge bond purchases at $T - t = 1$ and 3

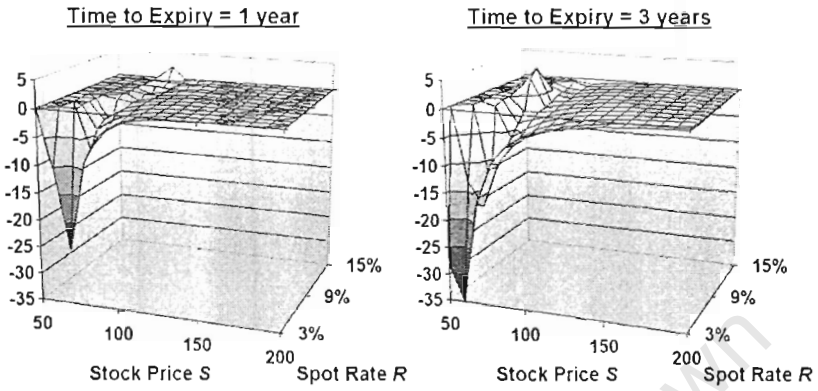

exceed (in face value of bonds) one third of the strike price.

At both one and three years to option expiry, for high spot rates and near to the OEBs there exist limited areas where the OBS model over-estimates discount bond purchases. There exist, amongst other possible explainations for this, two of which are associated with the numerical scheme.

The first considers that these over-estimates may simply be the results of inaccuracy of the schemes used to estimate hedge parameters via option prices. In this case more accurate estimates would show OBS under-estimation throughout the entire domain considered.

Secondly, the limited location may result from sparse sampling of prices. Were this over-estimation systemic but very localised - for example being a product of the convexity paradox - then finer price sampling, possibly combined with more accurate numerical schemes, would reveal such over-estimates over a larger portion of the domain.

Should VBS discount bond purchases uniformly exceed their OBS estimates, speculation regarding causation would intuitively focus on the relative location of the OEBs. Note however that the OBS model, in the calibrations considered, under-estimates the time of exercise for *both* American equity call options and American equity put options. However, while ρ-hedges for the put are consistent under-estimates, for calls the direction of mis-estimation changes over the domain considered. OEB mis-estimation may indeed not be the reason for the constant direction of bond purchase errors.

Proportional errors for concerning ρ-hedging are not presented here. Firstly, we know that in between the OEBs $\tilde{S}_p^{\mathcal{V}}$ and $\tilde{S}_p^{\mathcal{O}}$ the extent of mis-estimation will be 100% of the true VBS value. This will dominate proportional error plots. Secondly, ρ-hedges are only part of the fixed income portion of the replicating portfolio. While cash and bonds are not perfect substitutes, they far more closely resemble each other than either resembles stock. Proportional errors for fixed income hedge, presented earlier in this section, give better insight into the hedging process.

In our final piece of analysis, we consider the practical applicability of ρ-hedging.

As with the American equity call option, the ρ-hedge for American equity put options will agree with the VBS hedge within the common exercise region. Where the early exercise premium contributes little to either VBS or OBS option price, the options will be approximately

European; chapter 5 showed that the European ρ-hedge places all fixed income assets in the discount bond, and chapter 8 showed that numerical differences in European bond hedges are minimal.

Only where the early exercise premium contributes significantly to American option price, but where one or both options are still optimally held (i.e. not exercised), is there potential for ρ-hedges to be significantly erroneous. The difference in the rates at which option prices in the two models (i.e OBS and VBS) move from being indistinguishable from European to being priced at intrinsic value determines the size of such errors.

Figure 10.20: OEBs $\tilde{S}_P^{\mathcal{O}}$ and $\tilde{S}_P^{\mathcal{V}}$ against contours of $\left(\mathcal{P}_P^{\mathcal{O}}/P^{\mathcal{O}}\right)$ at $T-t=3$ for $\chi=0$.

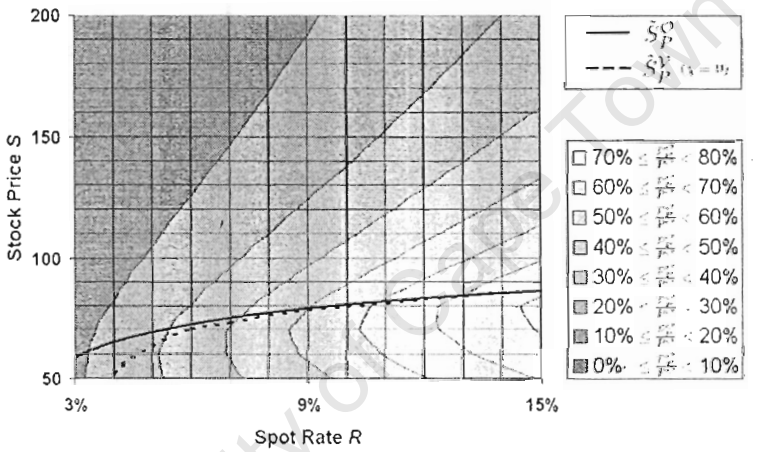

Figure 10.20 plots the OEBs $\tilde{S}_P^{\mathcal{O}}$ and $\tilde{S}_P^{\mathcal{V}}$ at $T-t=3$ for $\chi=0$; the two other values of χ produce very similar OEBs. As a background we provide contours of the proportional contribution of the early exercise premium $\mathcal{P}_P^{\mathcal{O}}$ to the American equity put option price $P^{\mathcal{O}}$. The lower this proportion the more closely the American option (and hence its hedges) resembles its European counterpart.

For American equity call options, examined in the previous chapter, the early exercise premium never contributed more than 10% of the option price. It was then unsurprising that the ρ-hedges, like their European counterparts, differed little across models.

For the put options examined here, even within the mutual continuation region the early exercise premium may contribute as much as half the option price. It is hence striking, given the size of the early exercise premium, that despite the theoretical criticisms raised in section 5.1, ρ-hedges provide such accurate estimates of VBS bond hedges.

This accuracy, combined with the substantial speed advantage offered by OBS estimate calculation over true VBS hedge calculation, justifies most practical use of ρ-hedging. Such use is subject to the caveat that, for low spot rates and with stock prices just below the OBS OEB, ρ-hedges may severely under-estimate discount bond purchases.

Chapter 11

Conclusions

This dissertation set out to examine the nature and causes of the errors induced when using standard Black-Scholes option prices to estimate true equity option prices in a world where short rates follow an Ornstein-Uhlenbeck process. In this final chapter we review the major results obtained.

Black-Scholes prices for European option prices are widely understood and are presented in most finance textbooks. American option prices, the solution to an optimal stopping problem, are slightly more complicated. They are nevertheless very well studied throughout academic literature. Subject to knowledge of the optimal exercise boundary, American option prices may be decomposed into their corresponding European option and an early exercise premium. The early exercise premium represents the arbitrage profits accruing to the option seller should the option holder never exercise the option before expiry.

11.1 Pricing and Hedging Theory

Adding a Vasicek-type short rate to the standard Black-Scholes model introduces an additional source of market risk. Arbitrage-free contingent claim pricing in such a world requires one more primary risky security (i.e. in addition to the stock price S) so that the market prices of each risk source may be determined. The two primary securities, in conjunction with a bank account, may be used to hedge contingent claims. Both market risk prices must be reflected appropriately in the Radon-Nikodym derivative $\frac{d\mathbb{Q}}{d\mathbb{P}}$ used to create the risk-neutral pricing measure.

11.1.1 European Option Prices

VBS prices for European equity options are relatively easily obtained using an appropriate change of numéraire. This technique highlights the exchange nature of European options. Because the strike price at option expiry is independent of the short rate path, European options are truly options to exchange the stock S for the discount bond maturing at option expiry. Accordingly, European options may be hedged using only stock and expiry-dated discount bonds (i.e. no bank account).

The resulting VBS European equity option prices bear a strong functional resemblance to standard Black-Scholes prices. Indeed, comparing OBS prices (calibrated at the spot rate ruling to option expiry) to VBS prices, the price difference is dependent (through total

forward price variance) on the calibration of χ. This variable χ is the correlation between unexpected stock price movements and unexpected short rate movements. Only for χ less than a time-dependent critical level $\chi_c[t,T]$ will OBS option prices exceed corresponding VBS prices.

When hedging, we make the assumption that the primary asset determining the market price of interest rate risk is the discount bond maturing at option expiry, and that this bond is used to hedge contingent claims. In both models, hedge purchases of stock and of bonds are proportional to an appropriate probability of exercise. This makes cross-model differences in hedge purchases jointly dependent on correlation calibration and on the extent to which the option is in-the-money. For $\chi < \chi_c[t,T]$, total forward price variance is larger under OBS pricing than under VBS pricing, and vice-versa. Only for options sufficiently out-of-the-money will any increase in total forward price variance increase exercise probabilities (and hence affect hedge purchases). 'Sufficiently out-of-the-money' describes the stock price level in relation to a spot rate-dependent critical price level.

11.1.2 American Option Prices

American equity option prices remain the solution to an optimal stopping problem. Within our stochastic short rate economy these prices are Markovian in one temporal and two spatial variables. This Markovian property collapses the general optimal stopping problem into a hitting time problem involving only the triple of inputs to the Markovian price formulation. The relevant optimal exercise boundary (OEB) needs to be placed in three dimensions, whereas a standard Black-Scholes OEB can be placed within two dimensions.

For all American options, the time of option exercise is not known at option expiry. Within our context, this prevents us from selecting an appropriate forward measure for option pricing, and hence from using change of numéraire techniques. The three-dimensional nature of the OEB, combined with the complex inter-relationships between future values of S and r, makes the early exercise representation of the American option price complex beyond practical use. Lacking tractable analytic prices for American options, we must turn to numerical results to compare models.

11.1.3 ρ-Hedging

The parameter ρ measures the sensitivity of OBS option prices to the assumed level of the constant interest rate input. It provides an important tool in determining a necessary order of accuracy when regarding this input. It may, however, also be used in an attempt to hedge interest rate risk present in option contracts but not modelled within the standard Black-Scholes framework. Such hedging may be referred to as ρ-hedging, or as out-of-model hedging.

Invoking ρ-hedging results in a philosophical inconsistency between a pricing model ignoring interest rate risk and practical acceptance of the existence of such risk. Out-of-model hedging (of any kind) implies stochastic switching between various model calibrations.

In our situation if, conditional upon the path of the in-model risky asset S, contingent claim cashflows are unaffected by changes in calibration of R, then the ρ-hedge portfolio is identical to an in-model hedge with all cash payments having been hedged by purchases of the corresponding discount bonds. This applies to European equity options. American equity

options are optimally exercised at the OEB, whose location is dependent on the choice of R, thus voiding the correspondence of in- and out-of-model hedges.

The inherent inconsistencies of ρ-hedging also permit arbitrage. The first arbitrage occurs within the bond market, where assumed parallel movements of the yield curve may be exploited for riskless profit.

The second results from the failure of the Fundamental Theorem of Asset Pricing. A standard Black-Scholes price, when substituted into a model with stochastic interest rates, will not necessarily drift under the risk-neutral measure at the risk-free rate. Yet all the primary assets which complete the stochastic interest rate economy must (by definition) drift under the risk-neutral measure at the risk-free rate. The divergence of drifts opens up the possibility of arbitrage.

Despite these concerns, ρ-hedging may offer tangible benefits as a fast and relatively accurate estimate of true hedge portfolios in the stochastic interest rate economy. The evaluation of this tradeoff requires a numerical investigation, whose results are discussed shortly.

11.2 Approximation

Numerical values for European option contracts require only accurate estimates of the cumulative Gaussian distribution, which are commony available. Intricate approximation schemes are required for American option values.

Such schemes are well established for standard Black-Scholes pricing. We have employed a Crank-Nicolson scheme with Dirichlet boundary conditions to obtain price estimates, a scheme which is unconditionally stable. From these prices we derived OEB estimates.

Numerical schemes approximating the heat equation in more than one dimension are less well documented. Unsatisfied with the schemes available, we developed our own scheme to suit the purposes of this dissertation. We selected an explicit finite difference scheme to reduce processing time and facilitate easier stability analysis. The scheme is rather intricate and, due to lack of obvious boundary conditions, needed to be applied over a massive domain. Analysis reveals that stability only occurs within a limited horizon, and even then for only a limited step size. Our investigation satisfies all these constraints.

11.3 Numerical Investigations

For numerical comparison we calibrated to a combination of prospective market expectations implied by ruling prices and restospective historical data as appropriate. Such data was taken for South African markets and ruling at, or covering the period to, the end of February 2005.

Of all the constants to be calibrated, χ exhibited the most volatility. Stock-rate correlation appeared positive across external shocks, negative across internal shocks and neutral in between. To accommodate this we considered three values for χ, each covering one of these scenarios. This also facilitated a partial sensitivity analysis.

11.3.1 European Options

To ensure consistency, numerical comparisons are made between VBS option prices and OBS option prices at the same stock price, with the OBS model calibrated to the spot rate to

option expiry ruling in the VBS model. Comparisons are made at one and three years to option expiry, for all three correlation calibrations ($\chi = -25\%$, $\chi = 0$ and $\chi = 25\%$).

Put-call parity shows that, for both option price and hedge portfolios, differences between OBS and VBS values are identical for European puts and calls. The critical correlation level $\chi_c[t,T]$ which determines the relative size of OBS and VBS total forward price variance appears approximately linear in time. While differences in total forward price variance exist between the three VBS calibrations and the comparable OBS model, such differences are relatively small even three years from option expiry.

Total price differences for European equity options are largest when the option is at-the-money. Here the exercise decision is least certain, and uncertainty mis-estimation has the largest price impact. Analysis three years from option expiry shows the at-the-money level to be sensitive to the spot rate R, again highlighting the exchange nature of European options. Total price difference magnitudes appear to be symmetric in χ across χ_c.

The differences between OBS and VBS European equity option prices, as a proportion of the correct VBS price, are largest when the option is deep out-of-the-money. For the majority of cases and domains considered such proportional errors are within $\pm 5\%$ of the true price, though for deep out-of-the money puts three years from option expiry this may rise to 40% of the true price.

European hedge errors are largest near (but not at) the critical stock price S^*. These hedge errors contour along constant values of $S \cdot e^{-R(T-t)}$. As a proportion of true VBS purchases, errors are indistinguishable between stock and bond, or even between hedge and price. European equity option price errors are not created by a systematic bias to one or other of the hedging instruments. Rather, these errors stem from a near-uniform mis-estimation of forward price variance and hence exercise probabilities.

11.3.2 American Call Options

Unlike European options, American puts and calls are distinctly different problems, and need to be considered separately. We begin with American equity call options.

The calibration dividend yield δ is relatively low in relation to the spot rates R considered. Because of this, American equity call options - under both OBS and VBS models - are only optimally exercised before expiry at very high stock price levels. Interestingly, OBS approximations consistently and for all calibrations under-estimate the location of the OEB $\tilde{S}_C^{\mathcal{V}}$, so OBS exercise strategies never exercise no later than VBS exercise strategies.

Whilst exercise strategies are based jointly upon stock price and spot rate to expiry, the VBS stopping domain is a proper subset of the OBS stopping domain, and here OBS and VBS prices must agree. However, in the exercise area unique to OBS strategies, OBS prices must be less than the VBS prices they approximate.

Total price estimate errors display two distinct and independent effects. A European effect as described above is present when the option is at-the-money. There is a larger error deep in-the-money within the unique stopping region where the OBS price under-estimates option prices. This early exercise under-estimate appears relatively insensitive to correlation χ.

Proportional price estimates remain dominated by the European effects out-of-the-money. Early exercise effects occur when the option carries a large value, and do not contribute a significant portion of option price where they occur.

Stock hedge puchases are over-estimated in the unique exercise area, in addition to the European effects displayed around stock prices S^*. Proportional errors concerning stock hedge

purchases are also dominated by European effects. Similar conclusions apply to short sales of fixed income instruments (i.e. cash and bonds).

Discount bond sales indicated by ρ-hedges appear largely accurate. However, with decreasing spot rates they converge to early exercise at an excessive rate - indicating possible Gamma-type trading losses in a hedge portfolio. The American equity call option price is very strongly dominated over the domains considered by its European component. This domination, and the theoretical applicability of ρ-hedges for European options discussed earlier, make this ρ-hedge accuracy unsurprising.

11.3.3 American Put Options

Conditional upon any path of the stock price S, OBS pricing may under-estimate but never over-estimates the exercise time of American equity put options. For put options, time under-estimation is associated with an over-estimation of the OEB location. This OEB over-estimation is negligible for most of the domains considered, though may be considerable at low spot rates. This OEB mis-estimation is remarkably consistent across correlation calibrations.

As with American equity call options, this OEB mis-estimation results in a stopping area common to the two models and a stopping area unique to OBS exercise strategies, with the remainder of the domain being a mutual continuation region.

The spot rates considered, reflecting a benefit to early put exercise, are large in relation to stock dividend yield (which relates to early exercise costs). Consequently, optimal exercise stock prices for the put option do not differ substantially from the strike price. The area of mutual exercise, where both model prices equal intrinsic value, overlaps partially with areas of large European put price difference. This overlap dampens the magnitude of European put errors carried into American put errors. Within the unique exercise region, and particularly for low spot rates (where this region is wide) OBS prices noticeably under-estimate true VBS prices. In addition, at-the-money the European option price differences remain present, though reduced in amplitude by price convergence in the mutually optimal exercise region. Lastly, a strange - albeit minor - OBS price over-estimate appears to occur at high spot rates just before optimal exercise. We term this counter-intuitive effect the 'convexity paradox'.

Total American equity put price under-estimates within the unique exercise region, and over-estimates associated with the convexity paradox, contribute little to proportional price errors. OBS prices remain within 5% of the true VBS price for most of the domains considered, moving beyond 10% of the true price only when options move deep out-of-the-money.

Stock and fixed income purchases hedging the American put option exhibit corresponding properties. OBS hedges under-estimatine the magnitude of VBS hedges within the unique stopping area while the corresponding European errors carry through, still somewhat dampened by mutual exercise. Proportional hedge errors remain substantially similar to the European counterparts.

Unlike the American equity call option, American equity put option price may be up to three times the corresponding European price. Given this significant early exercise contribution, ρ-hedges perform surprising well. Indeed, ρ-hedging provides very accurate estimates for purchases of expiry-dated discount bonds for most of the domains considered. The only exceptions to this accuracy occur within the unique exercise region.

11.4 Further Research

This dissertation has analysed the difference between equity options priced in an economy subject to a Vasicek-style short rate, and their approximations using the standard Black-Scholes model. Where possible we have examined these estimation errors analytically. We have also considered numerical values of the errors occurring in a model plausibly calibrated to the South African market.

For the most part the errors induced in option prices by ignoring short rate stochasticity are not material. In certain cases, notably deep out-of-the-money, proportional pricing errors may become material. Furthermore, we have highlighted the significant factors causing these errors, which may aid consideration of errors in alternative parametrisations or in alternate functional model forms. However, despite the detailed calculus and algebra presented, this is only an initial investigation of this problem. Numerous areas of further research present themselves.

Alternative models for the interest rate process may be considered. These may include different forms of short rate diffusion (e.g. Black, Derman & Toy (1990)), multi-factor models (e.g. Schaefer & Schwartz (1979), Duffie & Kan (1996)), no-arbitrage models which fit the entire yield curve (as pioneered by Hull & White (1990)) and market models (e.g. Brace, Gatarek & Musiela (1997)). Note again that our analysis of European option price errors remains valid within the Hull and White (1990) no-arbitrage extension of the Vasicek model, due to the exchange option characteristics of European options.

An explicit finite difference scheme was chosen for obtaining equity option prices where interest rates are stochastic. The explicit choice was intended to speed calculations, but stability considerations imposed substantial additional computational burdens. Our scheme appears relatively inefficient, but estimation time was not a significant constraint. Other approximation schemes may be far more efficient and faster. In particular, implicit finite difference schemes provide guaranteed stability and would also, through implicit boundary conditions, limit the domain over which calculations need be conducted. Any numerical technique incorporating stochastic interest rates which can provide real-time prices for equity options will make it unnecessary to use standard Black-Scholes price estimates.

American options have always proved more mathematically difficult than European options, and our considerations are no exception. The apparently consistent under-estimation of the optimal exercise time by the standard Black-Scholes model is an unexpected result. Theoretical comparisons of stopping times between the models presented in this dissertation, as well as other models, may yield insight into the role of interest rates in the early exercise decision. In addition, the convexity paradox is a numerical result not anticipated, and can be subjected to analytic scrutiny.

Finally, we may concern ourselves over the sensitivity of price and hedge estimation errors to the calibrated model parameters, and the conditions under which such errors become material. Two parameters appear to keep our price estimates low. Short rate volatility is very low in comparison to stock price volatility, though this is repeatedly justified by prospective and retrospective data. The rate α of short rate mean reversion is relatively slow, though higher rates would imply larger yield curve convexity. This begs inquiry into the parameter levels at which option valuation estimation errors become material, and whether such levels are plausible.

Part IV

Appendices

Appendix A

Girsanov's Theorem for Correlated Brownian Motions

Given the $\mathbb{P}$-Brownian motions $W_t^{\mathbb{P}}$ and $V_t^{\mathbb{P}}$ with correlation χ and the Radon-Nikodym derivative

$$\frac{d\mathbb{Q}}{d\mathbb{P}} = \exp\left[-\int_0^{\mathcal{H}} \frac{\lambda_W[t] - \chi \cdot \lambda_V}{1-\chi^2} dW_t^{\mathbb{P}} - \int_0^{\mathcal{H}} \frac{\lambda_V - \chi \cdot \lambda_W[t]}{1-\chi^2} dV_t^{\mathbb{P}} - \tfrac{1}{2}\int_0^{\mathcal{H}} \lambda_W^2[t] - 2\chi \cdot \lambda_W[t] \cdot \lambda_V + \lambda_V^2 dt\right] \quad \text{(A-1)}$$

we wish to show that the processes $W_t^{\mathbb{Q}}$ and $V_t^{\mathbb{Q}}$ defined by

$$W_t^{\mathbb{Q}} = W_t^{\mathbb{P}} + \int_0^t \lambda_W[s] ds$$
$$V_t^{\mathbb{Q}} = V_t^{\mathbb{P}} + \lambda_V \cdot t$$

are $\mathbb{Q}$-Brownian motions with correlation χ.

Note that

$$W_0^{\mathbb{Q}} = W_0^{\mathbb{P}} = 0 \qquad \text{and} \qquad V_0^{\mathbb{Q}} = V_0^{\mathbb{P}} = 0$$

and also

$$d\langle W^{\mathbb{Q}}\rangle_t = d\langle W^{\mathbb{P}}\rangle_t = dt \qquad d\langle W^{\mathbb{Q}} V^{\mathbb{Q}}\rangle_t = d\langle W^{\mathbb{P}} V^{\mathbb{P}}\rangle_t = \chi dt$$
$$d\langle V^{\mathbb{Q}}\rangle_t = d\langle V^{\mathbb{P}}\rangle_t = dt$$

All that remains is to show that $W^{\mathbb{Q}}$ and $V^{\mathbb{Q}}$ are $\mathbb{Q}$-martingales.

It suffices to show that $\xi_t W_t^{\mathbb{Q}}$ and $\xi_t W_t^{\mathbb{Q}}$ are $\mathbb{P}$-martingales, where

$$\xi_t = \mathbb{E}^{\mathbb{P}}\left[\frac{d\mathbb{Q}}{d\mathbb{P}}\middle| \mathcal{F}_t\right]$$

is already a $\mathbb{P}$-martingale.

Now $\xi_t = \mathcal{E}\left[\frac{\chi\lambda_V - \lambda_W}{1-\chi^2}W_t^{\mathbb{P}} + \frac{\chi\lambda_W - \lambda_V}{1-\chi^2}V_t^{\mathbb{P}}\right]$

So that $d\xi_t = \xi_t\left(\frac{\chi\lambda_V - \lambda_W}{1-\chi^2}dW_t^{\mathbb{P}} + \frac{\chi\lambda_W - \lambda_V}{1-\chi^2}dV_t^{\mathbb{P}}\right)$

Therefore

$$\begin{aligned}
d\left(\xi_t W_t^{\mathbb{Q}}\right) =& W_t^{\mathbb{Q}}d\xi_t + \xi_t dW_t^{\mathbb{Q}} + d\xi_t dW_t^{\mathbb{Q}} \\
=& W_t^{\mathbb{Q}}d\xi_t + \xi_t\left(dW_t^{\mathbb{P}} + \lambda_W dt\right) \\
&+ \xi_t\left(dW_t^{\mathbb{P}} + \lambda_W dt\right)\left(\frac{\chi\lambda_V - \lambda_W}{1-\chi^2}dW_t^{\mathbb{P}} + \frac{\chi\lambda_W - \lambda_V}{1-\chi^2}dV_t^{\mathbb{P}}\right) \\
=& W_t^{\mathbb{Q}}d\xi_t + \xi_t dW_t^{\mathbb{P}} + \xi_t\left(\lambda_W + \frac{\chi\lambda_V - \lambda_W}{1-\chi^2} + \chi\frac{\chi\lambda_W - \lambda_V}{1-\chi^2}\right)dt \\
=& W_t^{\mathbb{Q}}d\xi_t + \xi_t dW_t^{\mathbb{P}}
\end{aligned}$$

so $\xi_t W_t^{\mathbb{Q}}$ is a $\mathbb{P}$-martingale. Similarly, $\xi_t V_t^{\widehat{\chi}}$ is a $\mathbb{P}$-martingale.

Thus, by Lévy's characterisation of Brownian motion, $W_t^{\mathbb{Q}}$ and $V_t^{\mathbb{Q}}$ are $\mathbb{Q}$-Brownian motions with constant correlation χ.

Application of the same methodology shows that $W^{\mathbb{Q}^S}$, $V^{\mathbb{Q}^S}$, $W_t^{\mathbb{Q}_B^T}$ and $V_t^{\mathbb{Q}_B^T}$ are Brownian motions under the relevant measure, with the correlation between W and V still χ.

Appendix B

Early Exercise Premia

B.1 OBS Early Exercise Premia

From (4.10) we know that

$$\mathcal{P}_C^{\mathcal{O}}[t,S] = \mathbb{E}^{\mathbb{Q}}\left[-\int_{s=\eta_t^C}^{T} d\left(e^{-R(s-t)}[S[s]-K]^+\right)\middle|\mathcal{F}_t\right] \tag{B-1}$$

Now using the generalised Itô rule for convex functions,

$$\begin{aligned}\mathcal{P}_C^{\mathcal{O}}[t,S] =& \mathbb{E}^{\mathbb{Q}}\left[\int_{\eta_t^C}^{T} e^{-R(u-t)}\left(\delta S[u]-RK\right)\cdot \mathbb{I}_{\{S[u]>K\}}du\middle|\mathcal{F}_t^W\right] \\ &- \mathbb{E}^{\mathbb{Q}}\left[\int_{\eta_t^C}^{T} e^{-R(u-t)}dL_u[S[u]-K]\middle|\mathcal{F}_t^W\right]\end{aligned} \tag{B-2}$$

where $L_t[X]$ is the local time of the process X spent at zero, i.e.

$$L_t[X] = \lim_{\epsilon\downarrow 0}\frac{1}{2\epsilon}\Lambda\left[\{u\in[0,t] : X[u]\in(-\epsilon,\epsilon)\}\right]$$

Now define $\mathcal{M}_C^{\mathcal{O}}$ and $\mathcal{N}_C^{\mathcal{O}}$ by

$$\begin{aligned}\mathcal{M}_C^{\mathcal{O}}[t,\omega] &= \int_0^t e^{-Ru}\left(\delta S[u]-RK\right)\cdot \mathbb{I}_{\{(u,S[u])\in\mathcal{C}_C^{\mathcal{O}}\}}\cdot \mathbb{I}_{\{S[u]>K\}}du \\ &\quad - \int_0^t e^{-Ru}\mathbb{I}_{\{(u,S[u])\subset\mathcal{C}_C^{\mathcal{O}}\}}dL_u[S[u]-K] \\ \mathcal{N}_C^{\mathcal{O}}[t,\omega] &= \int_0^t e^{-Ru}\left(\delta S[u]-RK\right)\cdot \mathbb{I}_{\{(u,S[u])\in\mathcal{S}_C^{\mathcal{O}}\}}\cdot \mathbb{I}_{\{S[u]>K\}}du \\ &\quad - \int_0^t e^{-Ru}\cdot \mathbb{I}_{\{(u,S[u])\in\mathcal{S}_C^{\mathcal{O}}\}}dL_u[S[u]-K]\end{aligned}$$

$\mathcal{M}_C^{\mathcal{O}}$ and $\mathcal{N}_C^{\mathcal{O}}$ are constant on the stopping region $\mathcal{S}_C^{\mathcal{O}}$ and continuation region $\mathcal{C}_C^{\mathcal{O}}$ respectively, and $\mathcal{P}_C^{\mathcal{O}}$ can be expressed as

$$\mathcal{P}_C^{\mathcal{O}}[t,S] = e^{Rt}\mathbb{E}^{\mathbb{Q}}\left[\left(\mathcal{N}_C^{\mathcal{O}}[T]-\mathcal{N}_C^{\mathcal{O}}[\eta_t^C]\right)+\left(\mathcal{M}_C^{\mathcal{O}}[T]-\mathcal{M}_C^{\mathcal{O}}[\eta_t^C]\right)\middle|\mathcal{F}_t^W\right] \tag{B-3}$$

$\mathcal{N}_C^{\mathcal{O}}$ will turn out to be the finite variation portion of the Doob-Meyer decomposition of the $\mathbb{Q}$-supermartingale $C^{\mathcal{O}}$. $(\mathcal{M}_C^{\mathcal{O}} + c^{\mathcal{O}})$ will be the corresponding martingale portion. Though we still need to prove this fact, it motivates our choice of symbol.

On page 42 we showed that $\mathcal{S}_C^{\mathcal{O}} = \{(t,S) : S \geq \tilde{S}_C^{\mathcal{O}}[t]\}$ and also $\Lambda[\tilde{S}_C^{\mathcal{O}}[t] \leq K] = 0$, which together imply that

$$\int_0^T \mathbb{I}_{\{(u,S[u])\in\mathcal{S}_C^{\mathcal{O}}\}} dL_u[S[u] - K] = 0 \tag{B-4a}$$

From the property $\eta_t^C = \inf\{t : (t, S[t]) \in \mathcal{S}_C^{\mathcal{O}}\}$ presented on page 41,

$$\int_{\eta_t^C}^T \mathbb{I}_{\{(u,S[u])\in\mathcal{S}_C^{\mathcal{O}}\}} du = \int_t^T \mathbb{I}_{\{(u,S[u])\in\mathcal{S}_C^{\mathcal{O}}\}} du \tag{B-4b}$$

Together (B-4a) and (B-4b) permit the simplification

$$e^{Rt}\mathbb{E}^{\mathbb{Q}}\left[\mathcal{N}_C^{\mathcal{O}}[T] - \mathcal{M}_C^{\mathcal{O}}[\eta_t^C]\middle|\mathcal{F}_t^W\right] = \int_t^T e^{-R(u-t)}\mathbb{E}^{\mathbb{Q}}\left[\left(\delta S[u] - RK\right)\cdot \mathbb{I}_{\{(u,S[u])\in\mathcal{S}_C^{\mathcal{O}}\}}\middle|\mathcal{F}_t^W\right] du \tag{B-5a}$$

Simplifying $\mathcal{M}_C^{\mathcal{O}}$ requires considerbly more work. We avoid this, presenting instead a heuristic argument. We know that in the continuation region $\mathcal{C}_C^{\mathcal{O}}$, $C^{\mathcal{O}}$ is a $(\mathbb{Q},\mathbb{F})$-local martingale. As $c^{\mathcal{O}}$ is a $(\mathbb{Q},\mathbb{F})$-local martingale throughout the domain $\mathcal{D}_C^{\mathcal{O}}$, $\mathcal{P}_C^{\mathcal{O}}$ must also be a $(\mathbb{Q},\mathbb{F})$-local martingale throughout $\mathcal{C}_C^{\mathcal{O}}$. Then applying tower property of conditional expectation yields

$$\mathbb{E}^{\mathbb{Q}}\left[\mathcal{M}_C^{\mathcal{O}}[T] - \mathcal{M}_C^{\mathcal{O}}[\eta_t^C]\middle|\mathcal{F}_t^W\right] = 0. \tag{B-5b}$$

For formalisation see the proof in Myneni(1992) and the references therein; also Karatzas and Shreve (1998).

Putting (B-5a) and (B-5b) into (B-3) we get

$$\begin{aligned}\mathcal{P}_C^{\mathcal{O}}[t,S] &= \int_t^T e^{-R(u-t)}\mathbb{E}^{\mathbb{Q}}\left[\left(\delta S[u] - RK\right)\cdot \mathbb{I}_{\{(t,S[u]\in\mathcal{S}_C^{\mathcal{O}}\}}\middle|\mathcal{F}_t^W\right] du \\ &= \int_t^T e^{-R(u-t)}\mathbb{E}^{\mathbb{Q}}\left[\left(\delta S[u] - RK\right)\cdot \mathbb{I}_{\{S[u]\geq\tilde{S}_C^{\mathcal{O}}[u]\}}\middle|\mathcal{F}_t^W\right] du\end{aligned}$$

and applying similar calculus to that needed for $c^{\mathcal{O}}$ in (3.14b) yields

$$\mathcal{P}_C^{\mathcal{O}}[t,S] = \int_t^T \delta S[t]e^{-\delta(u-t)}\Phi\left[g_1^C[t,S,u]\right] - RKe^{-R(u-t)}\Phi\left[g_2^C[t,S,u]\right]du$$

$$\text{where } g_1^C[t,S,u] = \frac{\ln S[t] - \ln\tilde{S}_C^{\mathcal{O}}[u] + (R - \delta + \frac{1}{2}\sigma_S^2)(u-t)}{\sigma_S\cdot\sqrt{u-t}}$$
$$\text{and } g_2^C[t,S,u] = g_1^C[t,S,u] - \sigma_S\cdot\sqrt{u-t}$$

as required.

□

B.2 VBS Early Exercise Premia

The first stage in simplifying VBS early exercise premia follows many of the techniques used above. From (4.14a)

$$\mathcal{P}_C^{\mathcal{V}}[t,S,r] = \mathbb{E}^{\mathbb{Q}}\left[\int_{\eta_t^C}^{T} d\left(\frac{\beta[t]}{\beta[u]}\left[S[u]-K\right]^+\right)du\middle|\mathcal{F}_t\right]$$

Using a the generalised Itô rule for convex functions we get

$$\begin{aligned}\mathcal{P}_C^{\mathcal{V}}[t,S,r] = \mathbb{E}^{\mathbb{Q}}\left[\int_{\eta_t^C}^{T}\frac{\beta[t]}{\beta[u]}\left(\delta\cdot S[u]-K\cdot r[u]\right)\mathbb{I}_{\{S[u]>K\}}du\middle|\mathcal{F}_t\right]\\ -\mathbb{E}^{\mathbb{Q}}\left[\int_{\eta_t^C}^{T}\frac{\beta[t]}{\beta[u]}dL_u\left[S[u]-K\right]\middle|\mathcal{F}_t\right]\end{aligned}\tag{B-6}$$

Which simplifies to

$$\mathcal{P}_C^{\mathcal{V}}[t,S,r] = \beta[t]\mathbb{E}^{\mathbb{Q}}\left[\left(\mathcal{N}_C^{\mathcal{V}}[T]-\mathcal{N}_C^{\mathcal{V}}[\eta_t^C]\right)+\left(\mathcal{M}_C^{\mathcal{V}}[T]-\mathcal{M}_C^{\mathcal{V}}[\eta_t^C]\right)\middle|\mathcal{F}_t\right]$$

where

$$\begin{aligned}\mathcal{N}_C^{\mathcal{V}}[t,\omega] &= \int_0^t \frac{\delta\cdot S[u]-K\cdot r[u]}{\beta[u]}\cdot\mathbb{I}_{\{S[u]>K\}}\cdot\mathbb{I}_{\{(u,S[u],r[u])\in\mathcal{S}_C^{\mathcal{V}}\}}du\\ &\quad-\int_0^t\frac{1}{\beta[u]}\cdot\mathbb{I}_{\{(u,S[u],r[u])\in\mathcal{S}_C^{\mathcal{V}}\}}dL_u\left[S[u]-K\right]\\ \mathcal{N}_C^{\mathcal{V}}[t,\omega] &= \int_0^t \frac{\delta\cdot S[u]-K\cdot r[u]}{\beta[u]}\cdot\mathbb{I}_{\{S[u]>K\}}\cdot\mathbb{I}_{\{(u,S[u],r[u])\in\mathcal{C}_C^{\mathcal{V}}\}}du\\ &\quad-\int_0^t\frac{1}{\beta[u]}\cdot\mathbb{I}_{\{(u,S[u],r[u])\in\mathcal{C}_C^{\mathcal{V}}\}}dL_u\left[S[u]-K\right]\end{aligned}$$

As $\tilde{S}_C^{\mathcal{V}}[t,r] > K$ for all $(t,r)\in[0,T)\times(-\infty,\infty)$ (see page 46) we have that $L_u\left[S[u]-K\right]$ must be level while $(u,S[u],r[u])\in\mathcal{S}_C^{\mathcal{V}}$ and so

$$\mathbb{E}^{\mathbb{Q}}\left[\mathcal{N}_C^{\mathcal{V}}[T]-\mathcal{N}_C^{\mathcal{V}}[\eta_t^C]\middle|\mathcal{F}_t\right] = \int_t^T\mathbb{E}^{\mathbb{Q}}\left[\frac{\delta\cdot S[u]-K\cdot r[u]}{\beta[u]}\cdot\mathbb{I}_{\{(u,S[u],r[u])\in\mathcal{S}_C^{\mathcal{V}}\}}\middle|\mathcal{F}_t\right]du$$

As in the previous section we argue heurisitically that $\mathcal{N}_C^{\mathcal{C}}$ must be a martingale in $\mathcal{C}_C^{\mathcal{V}}$ for $\frac{C^{\mathcal{V}}}{\beta}$ to be a martingale within $\mathcal{C}_C^{\mathcal{V}}$. Trivially $\mathcal{N}_C^{\mathcal{C}}$ is a martingale through $\mathcal{S}_C^{\mathcal{V}}$, and so

$$\begin{aligned}\mathcal{P}_C^{\mathcal{V}}[t,S,r] &= \beta[t]\mathbb{E}^{\mathbb{Q}}\left[\mathcal{N}_C^{\mathcal{V}}[T]-\mathcal{N}_C^{\mathcal{V}}[\eta_t^C]\middle|\mathcal{F}_t\right]\\ &= \beta[t]\int_t^T\mathbb{E}^{\mathbb{Q}}\left[\frac{\delta\cdot S[u]-K\cdot r[u]}{\beta[u]}\cdot\mathbb{I}_{\{(u,S[u],r[u])\in\mathcal{S}_C^{\mathcal{V}}\}}|\mathcal{F}_t\right]du\end{aligned}\tag{B-7}$$

□

As discussed in section 4.3.1, simplification of B-7 is intricate, and does not yield a particularly tractable closed-form solution. These complications are created by the complex interactions between the stochastic variables S and r.

Appendix C

Approximation Schemes: Derivations

C.1 American Options with Constant Short Rate

We are interested in solving (more appropriately, approximating the solution to) the variational inequality (6.5a), viz.

$$R\widetilde{C}^{\mathcal{O}} - \frac{\partial \widetilde{C}^{\mathcal{O}}}{\partial t} - (R - \delta - \tfrac{1}{2}\sigma_S^2)\frac{\partial \widetilde{C}^{\mathcal{O}}}{\partial y} - \tfrac{1}{2}\sigma_S^2 \frac{\partial^2 \widetilde{C}^{\mathcal{O}}}{\partial y^2} \geq 0 \qquad \text{(C-1a)}$$

$$\widetilde{C}^{\mathcal{O}} = \left[e^y - K\right]^+ \qquad \text{(C-1b)}$$

$$\widetilde{C}^{\mathcal{O}}[t, y] - \left[S - K\right]^+ \geq 0 \qquad \text{(C-1c)}$$

$$\left(R\widetilde{C}^{\mathcal{O}} - \frac{\partial \widetilde{C}^{\mathcal{O}}}{\partial t} - (R - \delta - \tfrac{1}{2}\sigma_S^2)\frac{\partial \widetilde{C}^{\mathcal{O}}}{\partial S} - \tfrac{1}{2}\sigma_S^2 \frac{\partial^2 \widetilde{C}^{\mathcal{O}}}{\partial y^2}\right)\left(\widetilde{C}^{\mathcal{O}} - \left[e^y - K\right]^+\right) = 0 \qquad \text{(C-1d)}$$

We limit our consideration of $\widetilde{C}^{\mathcal{O}}$ to the subset $[0, T] \times [y_{\min}, y_{\max}]$ of the domain $\widetilde{\mathcal{D}}_C^{\mathcal{O}} = [0, T] \times (-\infty, \infty)$ of $\widetilde{C}^{\mathcal{O}}$. Divide the rectangle $[0, T] \times [y_{\min}, y_{\max}]$ into a uniform grid with $(n_t + 1)$ temporal points and $(n_y + 1)$ spatial points, setting

$$\Delta t = \frac{T - 0}{n_t} \qquad \Delta y = \frac{y_{\max} - y_{\min}}{n_y}$$

$$t_i = 0 + i \times \Delta t \qquad y_j = y_{\min} + j \times \Delta y$$

$$i \in \mathbb{Z}\,;\, 0 \leq i \leq n_t \qquad j \in \mathbb{Z}\,;\, 0 \leq j \leq n_y$$

Using this grid we develop a finite difference scheme to approximate the PDE (C-1). Setting $\widetilde{C}_{i,j}^{\mathcal{O}} = \widetilde{C}^{\mathcal{O}}[t_i, y_i]$ and using central differences to approximate the spatial derivatives,

$$\frac{\partial \widetilde{C}_{i,j}^{\mathcal{O}}}{\partial y} \approx \frac{\widetilde{C}^{\mathcal{O}}[t_i, y_{j+1}] - \widetilde{C}^{\mathcal{O}}[t_i, y_{j-1}]}{2\Delta y} \qquad \text{(C-2a)}$$

$$\frac{\partial^2 \widetilde{C}_{i,j}^{\mathcal{O}}}{\partial y^2} \approx \frac{\widetilde{C}^{\mathcal{O}}[t_i, y_{j+1}] + \widetilde{C}^{\mathcal{O}}[t_i, y_{j-1}] - 2\widetilde{C}^{\mathcal{O}}[t_i, y_j]}{(\Delta y)^2} \qquad \text{(C-2b)}$$

Then using central temporal differences at the artificial grid point $(i+\frac{1}{2}, j) = \left((i+\frac{1}{2})\Delta t, y_{\min} + j\Delta y\right)$, for $0 \leq i \leq n_t - 1$ and $1 \leq n_j \leq n_y - 1$:

$$\widetilde{C}^{\mathcal{O}}_{i+\frac{1}{2},j} \approx \tfrac{1}{2}\left(\widetilde{C}^{\mathcal{O}}_{i,j} + \widetilde{C}^{\mathcal{O}}_{i+1,j}\right) \tag{C-3a}$$

$$\frac{\partial \widetilde{C}^{\mathcal{O}}_{i+\frac{1}{2},j}}{\partial t} \approx \frac{\widetilde{C}^{\mathcal{O}}_{i+1,j} - \widetilde{C}^{\mathcal{O}}_{i,j}}{\Delta t} \tag{C-3b}$$

$$\frac{\partial \widetilde{C}^{\mathcal{O}}_{i+\frac{1}{2},j}}{\partial y} \approx \tfrac{1}{2}\left(\frac{\partial \widetilde{C}^{\mathcal{O}}_{i+1,j}}{\partial y} + \frac{\partial \widetilde{C}^{\mathcal{O}}_{i,j}}{\partial y}\right) \tag{C-3c}$$

$$\frac{\partial^2 \widetilde{C}^{\mathcal{O}}_{i+\frac{1}{2},j}}{\partial y^2} \approx \tfrac{1}{2}\left(\frac{\partial^2 \widetilde{C}^{\mathcal{O}}_{i+1,j}}{\partial y^2} + \frac{\partial^2 \widetilde{C}^{\mathcal{O}}_{i,j}}{\partial y^2}\right) \tag{C-3d}$$

and substituting the approximations in (C-2) and (C-3) into the Partial Differential Inequality (C-1a) gives the matrix inequality

$$\mathbf{A}^{-} \times \hat{\mathbf{C}}^{\mathcal{O}}_{i} \geq \mathbf{B} \times \hat{\mathbf{C}}^{\mathcal{O}}_{i+1} \tag{C-4}$$

where $\mathbf{A}^{-}$ is the tri-diagonal $(n_y - 1) \times (n_y + 1)$ matrix

$$\mathbf{A}^{-} = \begin{pmatrix} A_{1,0} & A_{1,1} & A_{1,2} & 0 & 0 & \cdots & 0 \\ 0 & A_{1,0} & A_{1,1} & A_{1,2} & 0 & \cdots & 0 \\ 0 & 0 & A_{1,0} & A_{1,1} & A_{1,2} & \cdots & 0 \\ \vdots & \vdots & \ddots & \ddots & \ddots & \ddots & \vdots \\ 0 & 0 & \cdots & 0 & A_{1,0} & A_{1,1} & A_{1,2} \end{pmatrix}$$

with

$$\begin{aligned} A_{1,0} &= \tfrac{1}{2}\left(R - \delta - \tfrac{1}{2}\sigma_S^2\right)\frac{\Delta t}{\Delta y} - \tfrac{1}{2}\sigma_S^2\frac{\Delta t}{(\Delta y)^2} \\ A_{1,1} &= 2 + \sigma_S^2\frac{\Delta t}{(\Delta y)^2} + R\,\Delta t \\ A_{1,2} &= -\tfrac{1}{2}\left(R - \delta - \tfrac{1}{2}\sigma_S^2\right)\frac{\Delta t}{\Delta y} - \tfrac{1}{2}\sigma_S^2\frac{\Delta t}{(\Delta y)^2} \end{aligned}$$

$\mathbf{B}$ is the tri-diagonal $(n_y - 1) \times (n_y + 1)$ matrix

$$\mathbf{B} = \begin{pmatrix} B_{0,0} & B_{0,1} & B_{0,2} & 0 & 0 & \cdots & 0 \\ 0 & B_{0,0} & B_{0,1} & B_{0,2} & 0 & \cdots & 0 \\ 0 & 0 & B_{0,0} & B_{0,1} & B_{0,2} & \cdots & 0 \\ \vdots & \vdots & \ddots & \ddots & \ddots & \ddots & \vdots \\ 0 & 0 & \cdots & 0 & B_{0,0} & B_{0,1} & B_{0,2} \end{pmatrix}$$

with

$$\begin{aligned} B_{0,0} &= \tfrac{1}{2}\sigma_S^2\frac{\Delta t}{(\Delta y)^2} - \tfrac{1}{2}\left(R - \delta - \tfrac{1}{2}\sigma_S^2\right)\frac{\Delta t}{\Delta y} \\ B_{0,1} &= 2 - \sigma_S^2\frac{\Delta t}{(\Delta y)^2} - R\,\Delta t \\ B_{0,2} &= \tfrac{1}{2}\left(R - \delta - \tfrac{1}{2}\sigma_S^2\right)\frac{\Delta t}{\Delta y} + \tfrac{1}{2}\sigma_S^2\frac{\Delta t}{(\Delta y)^2} \end{aligned}$$

and finally $\hat{\mathbf{C}}_i^{\mathcal{O}}$ is the (n_y+1) vector

$$\hat{\mathbf{C}}_i^{\mathcal{O}} = \left(\hat{C}_{i,0}^{\mathcal{O}}, \hat{C}_{i,1}^{\mathcal{O}}, \cdots, \hat{C}_{i,n_y}^{\mathcal{O}}\right)'$$

which approximates the vector of American equity call option values

$$\left(\widetilde{C}^{\mathcal{O}}[t_i, y_{\min}], \widetilde{C}^{\mathcal{O}}[t_i, y_1], \cdots, \widetilde{C}^{\mathcal{O}}[t_i, y_{\max}]\right)'$$

The Crank-Nicolson finite difference scheme is known to be stable for all parabolic PDEs. From the consistency and stability of our PdE we can conclude that the PdE solution converges to the PDE solution.

Now, the constraint (C-1b) gives us the terminal values of $\widetilde{C}^{\mathcal{O}}$. and hence lets us populate the vector $\hat{\mathbf{C}}_{n_t}^{\mathcal{O}}$. The update equation (C-4) is an under-determined system, giving $(n_y - 1)$ simultaneous inequalities for the $(n_y + 1)$ unknowns in $\hat{\mathbf{C}}_{n_t-1}^{\mathcal{O}}$.

The variational inequality C-1 applies over the entire domain of $\widetilde{C}^{\mathcal{O}}$; as we have truncated the spatial dimension of this domain we need to augment (C-4) with spatial boundary conditions.

The first obvious additional equation $\hat{C}_{(n_t-1),0}^{\mathcal{O}} = 0$ follows from the Dirichlet boundary condition (6.2b): $\lim_{S \downarrow 0} C^{\mathcal{O}}[t, S] = 0$ implies $\widetilde{C}^{\mathcal{O}}[t, y] \approx 0$ for small y, so set $\hat{C}^{\mathcal{O}}[t_i, y_{\min}] = 0$ for all $i < n_t$.

Secondly, it follows from the definition

$$\tilde{S}_C^{\mathcal{O}}[t_i] = \inf\left\{S : C^{\mathcal{O}}[t_i, S] = \left[S - K\right]^+\right\}$$

that if $e^{y_{\max}} \geq \tilde{S}_C^{\mathcal{O}}[t_i]$ then $\hat{C}_{i,n_y}^{\mathcal{O}} = \left[e^{y_{\max}} - K\right]^+$.

We have previously noted that the map $\tilde{S}_C^{\mathcal{O}}[t] : [0, T) \mapsto (0, \infty)$ is monotonically decreasing in t. For $t = 0$ and T very large, the value of $\tilde{S}_C^{\mathcal{O}}[t]$ approaches the limiting upper bound $\frac{\kappa_1}{\kappa_1 - 1} \cdot K$, with κ_1 the positive root of the quadratic in S

$$\tfrac{1}{2}\sigma_S^2 S^2 + \left(R - \delta - \tfrac{1}{2}\sigma_S^2\right) S - R = 0 \tag{C-5}$$

(For proofs and further details of this upper bound for $\tilde{S}_C^{\mathcal{O}}[t]$ see Kwok (1998) or Wilmott (1999).)

So long as $y_{\max} \geq \ln\left[\frac{\kappa_1}{\kappa_1 - 1} \cdot K\right]$ we are guaranteed at this upper limit $y_{\max}$ that $\widetilde{C}^{\mathcal{O}}[t_i, y_{\max}] = \left[e^{y_{\max}} - K\right]^+$ for all i.

Using these exact solutions for $\hat{C}_{i,0}^{\mathcal{O}}$ and $\hat{C}_{i,n_y}^{\mathcal{O}}$ gives the complete system of inequalities

$$\mathbf{A}^C \times \hat{\mathbf{C}}_i^{\mathcal{O}} \geq \vec{\mathbf{D}}_i^C$$

where $\mathbf{A}^C$ is the square matrix

$$\mathbf{A}^C = \begin{pmatrix} 0 & 0 & \cdots & 0 & 0 \\ & & \mathbf{A}^- & & \\ 0 & 0 & \cdots & 0 & 1 \end{pmatrix}$$

$\vec{\mathbf{D}}_i^C$ is the vector

$$\vec{\mathbf{D}}_i^C = \left(0, \left(\mathbf{B} \times \hat{\mathbf{C}}_{i+1}^{\mathcal{O}}\right)', \left[e^{y_{\max}} - K\right]^+\right)'$$

and $\hat{\mathbf{C}}_i^{\mathcal{O}}$ is as previously defined.

Thus (C-1a), (C-1c) and (C-1d) lead to the family of constrained matrix problems

$$\begin{aligned} \mathbf{A}^C \times \hat{\mathbf{C}}_i^{\mathcal{O}} - \vec{\mathbf{D}}_i^C &\geq 0 && \text{(C-6a)} \\ \hat{\mathbf{C}}_i^{\mathcal{O}} - \left[e^{\mathbf{y}} - K\right]^+ &\geq 0 && \text{(C-6b)} \\ \left(\mathbf{A} \times \hat{\mathbf{C}}_i^{\mathcal{O}} - \vec{\mathbf{D}}_i^C\right)\left(\hat{\mathbf{C}}_i^{\mathcal{O}} - \left[e^{\mathbf{y}} - K\right]\right) &= 0 && \text{(C-6c)} \end{aligned}$$

while (C-1b) lets us initialise this family with $\hat{C}^{\mathcal{O}}_{n_t,j} = \left[e^{y_j} - K\right]^+$.

The American equity put option price $P^{\mathcal{O}}[t, S]$ is approximated similarly. The only difference of consequence regards the boundary problems: we set $\hat{P}^{\mathcal{O}}_{i,n_y} = 0$, while $\hat{P}^{\mathcal{O}}_{i,0} = [K - S_{\min}]^+$ so long as $S_{\min} \leq \frac{\kappa_2}{\kappa_2 - 1} \cdot K$, where κ_2 is the negative root of (C-5). This results in the family of constrained matrix problems

$$\begin{aligned} \mathbf{A}^P \times \hat{\mathbf{C}}_i^{\mathcal{O}} - \vec{\mathbf{D}}_i^C &\geq 0 && \text{(C-7a)} \\ \hat{\mathbf{C}}_i^{\mathcal{O}} - \left[e^{\mathbf{y}} - K\right]^+ &\geq 0 && \text{(C-7b)} \\ \left(\mathbf{A} \times \hat{\mathbf{C}}_i^{\mathcal{O}} - \vec{\mathbf{D}}_i^C\right)\left(\hat{\mathbf{C}}_i^{\mathcal{O}} - \left[e^{\mathbf{y}} - K\right]\right) &= 0 && \text{(C-7c)} \end{aligned}$$

where $\mathbf{A}^P$ is the square matrix

$$\mathbf{A}^C = \begin{pmatrix} 1 & 0 & \cdots & 0 & 0 \\ & & \mathbf{A}^- & & \\ 0 & 0 & \cdots & 0 & 0 \end{pmatrix}$$

$\vec{\mathbf{D}}_i^P$ is the vector

$$\vec{\mathbf{D}}_i^P = \left(\left[K - e^{y_{\max}}\right]^+ \cdot \left(\mathbf{B} \times \hat{\mathbf{P}}_{i+1}^{\mathcal{O}}\right)', 0\right)'$$

$\mathbf{A}^-$ and $\mathbf{B}$ are the matrices defined for (C-4) and $\hat{\mathbf{P}}_i^{\mathcal{O}}$ is the $(n_y + 1)$ vector

$$\hat{\mathbf{P}}_i^{\mathcal{O}} = \left(\hat{P}^{\mathcal{O}}_{i,0}, \hat{P}^{\mathcal{O}}_{i,1}, \cdots, \hat{P}^{\mathcal{O}}_{i,n_y}\right)'$$

which approximates the vector of American equity put option values

$$\left(\widetilde{P}^{\mathcal{O}}[t_i, y_{\min}], \widetilde{P}^{\mathcal{O}}[t_i, y_1], \cdots, \widetilde{P}^{\mathcal{O}}[t_i, y_{\max}]\right)'$$

Again a PSOR scheme is used to solve this constrained matrix problem.

C.2 American Options with Vasicek Short Rate

We are interested in approximating the variational inequality

$$\frac{\partial \widetilde{C}^{\mathcal{V}}}{\partial t} + \mu_1 \frac{\partial \widetilde{C}^{\mathcal{V}}}{\partial z_1} + \mu_2 \frac{\partial \widetilde{C}^{\mathcal{V}}}{\partial z_2} + \tfrac{1}{2}\sigma_1^2 \frac{\partial^2 \widetilde{C}^{\mathcal{V}}}{\partial z_1^2} + \tfrac{1}{2}\sigma_2^2 \frac{\partial^2 \widetilde{C}^{\mathcal{V}}}{\partial z_2^2} - \tfrac{z_1 - z_2}{2\sigma_S} \cdot \widetilde{C}^{\mathcal{V}} \geq 0 \tag{C-8a}$$

$$\widetilde{C}^{\mathcal{V}}[T, z_1, z_2] = \left[\tfrac{z_1+z_2}{2\sigma_r} - K\right]^+ \tag{C-8b}$$

$$\widetilde{C}^{\mathcal{V}}[t, z_1, z_2] \geq \left[\tfrac{z_1+z_2}{2\sigma_r} - K\right]^+ \tag{C-8c}$$

$$\left(\frac{\partial \widetilde{C}^{\mathcal{V}}}{\partial t} + \mu_1 \frac{\partial \widetilde{C}^{\mathcal{V}}}{\partial z_1} + \mu_2 \frac{\partial \widetilde{C}^{\mathcal{V}}}{\partial z_2} + \tfrac{1}{2}\sigma_1^2 \frac{\partial^2 \widetilde{C}^{\mathcal{V}}}{\partial z_1^2} + \tfrac{1}{2}\sigma_2^2 \frac{\partial^2 \widetilde{C}^{\mathcal{V}}}{\partial z_2^2} - \tfrac{z_1 - z_2}{2\sigma_S} \cdot \widetilde{C}^{\mathcal{V}}\right) \times \left(\widetilde{C}^{\mathcal{V}} - \left[\tfrac{z_1+z_2}{2\sigma_r} - K\right]^+\right) = 0 \tag{C-8d}$$

Where the variables z_1 and z_2 are defined by

$$z_1[S, r] = \sigma_r \cdot \ln[S] + \sigma_S \cdot r \qquad z_2[S, r] = \sigma_r \cdot \ln[S] - \sigma_S \cdot r \tag{C-9a}$$

having the respective drifts

$$\mu_1 = \nu_1^0 + \nu_1^1 \cdot r \qquad \mu_2 = \nu_2^0 + \nu_2^1 \cdot r \tag{C-9b}$$

where

$$\nu_1^0 = \alpha\theta\sigma_S - \sigma_r\delta - \tfrac{1}{2}\sigma_r\sigma_S^2 \qquad \nu_1^1 = \tfrac{\sigma_r}{\sigma_s} - \alpha$$
$$\nu_2^0 = -\alpha\theta\sigma_S - \sigma_r\delta - \tfrac{1}{2}\sigma_r\sigma_S^2 \qquad \nu_2^1 = \tfrac{\sigma_r}{\sigma_s} + \alpha$$

and the respective instantaneous volatilities

$$\sigma_1 = \sigma_S \cdot \sigma_r \cdot \sqrt{2(1+\chi)} \qquad \sigma_2 = \sigma_S \cdot \sigma_r \cdot \sqrt{2(1-\chi)} \tag{C-9c}$$

and are orthogonal. The reverse transforms are

$$S = \exp\left[\tfrac{z_1+z_2}{2\sigma_r}\right] \qquad r = \tfrac{z_1-z_2}{2\sigma_S} \tag{C-9d}$$

The function $\widetilde{C}^{\mathcal{V}}$ is defined by

$$\widetilde{C}^{\mathcal{V}}[t, z_1, z_2] = C^{\mathcal{V}}\left[t, \exp\left[\tfrac{z_1+z_2}{2\sigma_S}\right], \tfrac{z_1-z_2}{2\sigma_r}\right]$$

so that approximation of $\widetilde{C}^{\mathcal{V}}$ is sufficient to obtain an approximation of $C^{\mathcal{V}}$ via the reverse transform

$$C^{\mathcal{V}}[t, S, r] = \widetilde{C}^{\mathcal{V}}\left[t, (\sigma_r \cdot \ln[s] + \sigma_S \cdot r), (\sigma_r \cdot \ln[s] - \sigma_S \cdot r)\right]$$

In section C.1 the correspondence between the area of interest in the transformed domain $\widetilde{\mathcal{D}}_C^{\mathcal{O}}$ and the area if interest in the original domain $\mathcal{D}_C^{\mathcal{O}}$ was trivial. However, the transformations leading to $\widetilde{C}^{\mathcal{V}}$ are more extensive than those for $\widetilde{C}^{\mathcal{O}}$. Consequently the correspondnce

between the area of calculation in the transformed domain $\widetilde{\mathcal{D}}_C^{\mathcal{V}} = [0,T] \times (-\infty,\infty) \times (\infty,\infty)$ and the original domain $\mathcal{D}_C^{\mathcal{V}}$ is not at all obvious.

For the moment we will state an interest in the behaviour of $C^{\mathcal{V}}$ limited to the hyper-rectangle $[0.T] \times (S_{\min}, S_{\max}) \times (r_{\min}, r_{\max}) \in \mathcal{D}_C^{\mathcal{V}}$, and will follow the implications for the sub-space of $\widetilde{\mathcal{D}}_C^{\mathcal{V}}$ we need to study.

We divide the temporal domain $[0,T]$ into (n_t+1) separate time points, setting

$$t_i = 0 + i \times \Delta t$$

where

$$\Delta t = \frac{T-0}{n_t}$$

and

$$i \in [0, n_t] \cap \mathbb{Z}$$

Rather than exogenously specifying the numbers of spatial points as in section C.1, we choose to impose fixed spatial step sizes Δ_1 and Δ_2, and to determine the numbers of spatial points accordingly.

Assuming that we are concerned with z_1 over the interval $[z_1^{\text{MIN}}, z_1^{\text{MAX}}]$ and z_2 over $[z_2^{\text{MIN}}, z_2^{\text{MAX}}]$, set

$$\begin{aligned} n_1 &= \inf\{j \in \mathbb{Z} : z_1^{\text{MAX}} \leq z_1^{\text{MIN}} + j \times \Delta_1\} \\ n_2 &= \inf\{k \in \mathbb{Z} : z_2^{\text{MAX}} \leq z_2^{\text{MIN}} + k \times \Delta_2\} \end{aligned}$$

then let

$$\begin{aligned} z_{1,j} &= z_1^{\text{MIN}} + j \cdot \Delta_1 \qquad & j \in [0, n_1] \cap \mathbb{Z} \\ z_{2,k} &= z_2^{\text{MIN}} + k \cdot \Delta_2 \qquad & k \in [0, n_2] \cap \mathbb{Z} \end{aligned} \tag{C-10}$$

Setting $\widetilde{C}_{i,j,k}^{\mathcal{V}} = \widetilde{C}^{\mathcal{V}}[t_i, z_{1,j}, z_{2,k}]$ and using central differences to approximate spatial differences,

$$\frac{\partial \widetilde{C}_{i,j,k}^{\mathcal{V}}}{\partial z_1} \approx \frac{\widetilde{C}_{i,j+1,k}^{\mathcal{V}} - \widetilde{C}_{i,j-1,k}^{\mathcal{V}}}{2\Delta_1} \tag{C-11a}$$

$$\frac{\partial^2 \widetilde{C}_{i,j,k}^{\mathcal{V}}}{\partial z_1^2} \approx \frac{\widetilde{C}_{i,j+1,k}^{\mathcal{V}} + \widetilde{C}_{i,j-1,k}^{\mathcal{V}} - 2\widetilde{C}_{i,j,k}^{\mathcal{V}}}{(\Delta_1)^2} \tag{C-11b}$$

$$\frac{\partial \widetilde{C}_{i,j,k}^{\mathcal{V}}}{\partial z_2} \approx \frac{\widetilde{C}_{i,j,k+1}^{\mathcal{V}} - \widetilde{C}_{i,j,k-1}^{\mathcal{V}}}{2\Delta_2} \tag{C-11c}$$

$$\frac{\partial^2 \widetilde{C}_{i,j,k}^{\mathcal{V}}}{\partial z_2^2} \approx \frac{\widetilde{C}_{i,j,k+1}^{\mathcal{V}} + \widetilde{C}_{i,j,k-1}^{\mathcal{V}} + 2\widetilde{C}_{i,j,k}^{\mathcal{V}}}{(\Delta_2)^2} \tag{C-11d}$$

while a forward difference approximation for the temporal derivative yields

$$\frac{\partial \widetilde{C}_{i,j,k}^{\mathcal{V}}}{\partial t} \approx \frac{\widetilde{C}_{i,j,k}^{\mathcal{V}} - \widetilde{C}_{i-1,j,k}^{\mathcal{V}}}{\Delta t} \tag{C-11e}$$

The spatial approximations (C-11a),(C-11b) and (C-11c),(C-11d) are accurate to $O\big((\Delta_1)^2\big)$ and $\big((\Delta_2)^2\big)$ respectively, while the temporal approximation (C-11e) is accurate to $O(\Delta t)$. Substituting (C-11a)-(C-11e) into (C-8a) yields[1]

$$\begin{aligned}\left[1+\tfrac{z_{1,j}-z_{2,k}}{2\sigma_S}\right]\widetilde{C}^{\mathcal{V}}_{i-1,j,k} \approx{}& \tfrac{1}{2}\left(\tfrac{\sigma_1^2\Delta t}{(\Delta_1)^2}+\tfrac{\mu_1\Delta t}{\Delta_1}\right)\widetilde{C}^{\mathcal{V}}_{i,j+1,k}\\ &+\tfrac{1}{2}\left(\tfrac{\sigma_1^2\Delta t}{(\Delta_1)^2}-\tfrac{\mu_1\Delta t}{\Delta_1}\right)\widetilde{C}^{\mathcal{V}}_{i,j-1,k}+\left(1-\tfrac{\sigma_1^2\Delta t}{(\Delta_1)^2}-\tfrac{\sigma_2^2\Delta t}{(\Delta_2)^2}\right)\widetilde{C}^{\mathcal{V}}_{i,j,k}\\ &+\tfrac{1}{2}\left(\tfrac{\sigma_2^2\Delta t}{(\Delta_2)^2}+\tfrac{\mu_2\Delta t}{\Delta_2}\right)\widetilde{C}^{\mathcal{V}}_{i,j,k+1}+\tfrac{1}{2}\left(\tfrac{\sigma_2^2\Delta t}{(\Delta_2)^2}-\tfrac{\mu_2\Delta t}{\Delta_2}\right)\widetilde{C}^{\mathcal{V}}_{i,j,k-1}\end{aligned}\tag{C-12}$$

which is accurate to $O\big(\Delta t,(\Delta_1)^2,(\Delta_2)^2\big)$. In order to minimise the approximation error in (C-12) it is appropriate (see Hull and White (1990A) or Habermann (1998) ex. 6.3.1) to set

$$\Delta_1=\sqrt{3\sigma_1^2\Delta t}\qquad\qquad \Delta_2=\sqrt{3\sigma_2^2\Delta t}\tag{C-13}$$

in which case $O(\Delta t)=O\big((\Delta_1)^2\big)=O\big((\Delta_2)^2\big)$.

We note that

$$\begin{aligned}\widetilde{C}^{\mathcal{V}}_{i,j,k-1} &= \tfrac{1}{2}\left(\widetilde{C}^{\mathcal{V}}_{i,j-1,k-1}+\widetilde{C}^{\mathcal{V}}_{i,j+1,k-1}\right)+\frac{\partial^2\widetilde{C}^{\mathcal{V}}_{i,j,k-1}}{\partial z_1^2}(\Delta_1^2)+O\big((\Delta_1)^2\big)\\ &= \tfrac{1}{2}\left(\widetilde{C}^{\mathcal{V}}_{i,j-1,k-1}+\widetilde{C}^{\mathcal{V}}_{i,j+1,k-1}\right)\\ &\quad+\left(\frac{\partial^2\widetilde{C}^{\mathcal{V}}_{i,j,k}}{\partial z_1^2}-\frac{\partial^3\widetilde{C}^{\mathcal{V}}_{i,j,k}}{\partial z_1^2 z_2}\Delta_2+O\big((\Delta_2)^2\big)\right)(\Delta_1)^2+O\big((\Delta_1)^2\big)\\ &= \tfrac{1}{2}\left(\widetilde{C}^{\mathcal{V}}_{i,j-1,k-1}+\widetilde{C}^{\mathcal{V}}_{i,j+1,k-1}\right)+\frac{\partial^2\widetilde{C}^{\mathcal{V}}_{i,j,k}}{\partial z_1^2}(\Delta_1)^2+O(\Delta t)\end{aligned}\tag{C-14a}$$

and similarly that

$$\widetilde{C}^{\mathcal{V}}_{i,j,k}=\tfrac{1}{2}\left(\widetilde{C}^{\mathcal{V}}_{i,j-1,k}+\widetilde{C}^{\mathcal{V}}_{i,j+1,k}\right)+\frac{\partial^2\widetilde{C}^{\mathcal{V}}_{i,j,k}}{\partial z_1^2}(\Delta_1)^2+O(\Delta t)\tag{C-14b}$$

$$\widetilde{C}^{\mathcal{V}}_{i,j,k+1}=\tfrac{1}{2}\left(\widetilde{C}^{\mathcal{V}}_{i,j-1,k+1}+\widetilde{C}^{\mathcal{V}}_{i,j+1,k-1}\right)+\frac{\partial^2\widetilde{C}^{\mathcal{V}}_{i,j,k}}{\partial z_1^2}(\Delta_1)^2+O(\Delta t)\tag{C-14c}$$

Now $\frac{4}{36}\times$ (C-14b) $-\frac{2}{36}\times\big($(C-14a) + (C-14c)$\big)$ gives

$$\begin{aligned}&\tfrac{1}{36}\widetilde{C}^{\mathcal{V}}_{i,j-1,k-1}-\tfrac{2}{36}\widetilde{C}^{\mathcal{V}}_{i,j-1,k}+\tfrac{1}{36}\widetilde{C}^{\mathcal{V}}_{i,j-1,k+1}\\ &\quad-\tfrac{2}{36}\widetilde{C}^{\mathcal{V}}_{i,j,k-1}+\tfrac{4}{36}\widetilde{C}^{\mathcal{V}}_{i,j,k}-\tfrac{2}{36}\widetilde{C}^{\mathcal{V}}_{i,j,k+1}\\ &\quad+\tfrac{1}{36}\widetilde{C}^{\mathcal{V}}_{i,j+1,k-1}-\tfrac{2}{36}\widetilde{C}^{\mathcal{V}}_{i,j+1,k}+\tfrac{1}{36}\widetilde{C}^{\mathcal{V}}_{i,j+1,k+1}=O(\Delta t)\end{aligned}\tag{C-15a}$$

[1] As we are approximating (C-8a) at $\widetilde{C}^{\mathcal{V}}_{i,j,k}$, the value of $r\cdot\widetilde{C}^{\mathcal{V}}$ should be approximated at $\widetilde{C}^{\mathcal{V}}_{i,j,k}$. We rather adopt the convention, popular in financial applications of explicit finite difference techniques, of approximating $r\cdot\widetilde{C}^{\mathcal{V}}$ at $\widetilde{C}^{\mathcal{V}}_{i-1,j,k}$. This permits our scheme to be interpreted in some sense as an expected discounted payoff. As $\widetilde{C}^{\mathcal{V}}_{i-1,j,k}=\widetilde{C}^{\mathcal{V}}_{i,j,k}+O(\Delta t)$, the accuracy of (C-12) remains unchanged.

while $\frac{1}{6}\frac{\mu_1\Delta t}{\Delta_1}$((C-14a)-(C-14c)) gives

$$\frac{\mu_1\Delta t}{\Delta_1}\left(\frac{3}{36}\widetilde{C}^{\mathcal{V}}_{i,j+1,k+1} - \frac{6}{36}\widetilde{C}^{\mathcal{V}}_{i,j+1,k} + \frac{3}{36}\widetilde{C}^{\mathcal{V}}_{i,j+1,k-1} + - \frac{3}{36}\widetilde{C}^{\mathcal{V}}_{i,j-1,k+1} + \frac{6}{36}\widetilde{C}^{\mathcal{V}}_{i,j-1,k} - \frac{3}{36}\widetilde{C}^{\mathcal{V}}_{i,j-1,k-1}\right) = O(\Delta t) \quad \text{(C-15b)}$$

and similarly

$$\frac{\mu_2\Delta t}{\Delta_2}\left(\frac{3}{36}\widetilde{C}^{\mathcal{V}}_{i,j+1,k+1} - \frac{6}{36}\widetilde{C}^{\mathcal{V}}_{i,j,k+1} + \frac{3}{36}\widetilde{C}^{\mathcal{V}}_{i,j-1,k+1} - \frac{3}{36}\widetilde{C}^{\mathcal{V}}_{i,j+1,k-1} + \frac{6}{36}\widetilde{C}^{\mathcal{V}}_{i,j,k-1} - \frac{3}{36}\widetilde{C}^{\mathcal{V}}_{i,j-1,k-1}\right) = O(\Delta t) \quad \text{(C-15c)}$$

Finally, the step sizes (C-13) imply

$$\left(\frac{\mu_1\Delta t}{\Delta_1}\right)\left(\frac{\mu_2\Delta t}{\Delta_2}\right) = \frac{\mu_1\mu_2}{\sigma_1\sigma_2}\Delta t$$

so that

$$\frac{1}{4}\left(\frac{\mu_1\Delta t}{\Delta_1}\right)\left(\frac{\mu_2\Delta t}{\Delta_2}\right)\left(\widetilde{C}^{\mathcal{V}}_{i,j-1,k-1} - \widetilde{C}^{\mathcal{V}}_{i,j-1,k+1} - \widetilde{C}^{\mathcal{V}}_{i,j+1,k-1} + \widetilde{C}^{\mathcal{V}}_{i,j+1,k+1}\right) = O(\Delta t) \quad \text{(C-15d)}$$

Adding all of (C-15a) -(C-15d) to (C-12) and using (C-13),

$$\begin{aligned}
&\left[1 + \tfrac{z_{1,j}-z_{2,k}}{2\sigma_S}\right]\widetilde{C}^{\mathcal{V}}_{i-1,j,k} \\
&\approx \left(\tfrac{1}{6} - \tfrac{1}{2}\tfrac{\mu_1\Delta t}{\Delta_1}\right)\left(\tfrac{1}{6} - \tfrac{1}{2}\tfrac{\mu_2\Delta t}{\Delta_2}\right)\widetilde{C}^{\mathcal{V}}_{i,j-1,k-1} + \left(\tfrac{1}{6} - \tfrac{1}{2}\tfrac{\mu_1\Delta t}{\Delta_1}\right)\cdot\tfrac{2}{3}\cdot\widetilde{C}^{\mathcal{V}}_{i,j-1,k} \\
&\quad + \left(\tfrac{1}{6} - \tfrac{1}{2}\tfrac{\mu_1\Delta t}{\Delta_1}\right)\left(\tfrac{1}{6} + \tfrac{1}{2}\tfrac{\mu_2\Delta t}{\Delta_2}\right)\widetilde{C}^{\mathcal{V}}_{i,j-1,k+1} + \tfrac{2}{3}\left(\tfrac{1}{6} - \tfrac{1}{2}\tfrac{\mu_2\Delta t}{\Delta_2}\right)\widetilde{C}^{\mathcal{V}}_{i,j,k-1} \\
&\quad + \tfrac{2}{3}\cdot\tfrac{2}{3}\cdot\widetilde{C}^{\mathcal{V}}_{i,j,k} + \tfrac{2}{3}\left(\tfrac{1}{6} + \tfrac{1}{2}\tfrac{\mu_2\Delta t}{\Delta_2}\right)\widetilde{C}^{\mathcal{V}}_{i,j,k+1} \\
&\quad + \left(\tfrac{1}{6} + \tfrac{1}{2}\tfrac{\mu_1\Delta t}{\Delta_1}\right)\left(\tfrac{1}{6} - \tfrac{1}{2}\tfrac{\mu_2\Delta t}{\Delta_2}\right)\widetilde{C}^{\mathcal{V}}_{i,j+1,k-1} + \left(\tfrac{1}{6} + \tfrac{1}{2}\tfrac{\mu_1\Delta t}{\Delta_1}\right)\cdot\tfrac{2}{3}\cdot\widetilde{C}^{\mathcal{V}}_{i,j+1,k} \\
&\quad + \left(\tfrac{1}{6} + \tfrac{1}{2}\tfrac{\mu_1\Delta t}{\Delta_1}\right)\left(\tfrac{1}{6} + \tfrac{1}{2}\tfrac{\mu_2\Delta t}{\Delta_2}\right)\widetilde{C}^{\mathcal{V}}_{i,j+1,k+1}
\end{aligned} \quad \text{(C-16)}$$

which remains accurate to $O(\Delta t)$. Indeed, as both $\left(\frac{\mu_1\Delta t}{\Delta_1}\right)^2$ and $\left(\frac{\mu_2\Delta t}{\Delta_2}\right)^2$ are of $O(\Delta t)$, we can further amend (C-16), without affecting its accuracy, to

$$\begin{aligned}
&\left[1 + \tfrac{z_{1,j}-z_{2,k}}{2\sigma_S}\right]\widetilde{C}^{\mathcal{V}}_{i-1,j,k} \\
&\quad \approx q_1^d q_2^d \widetilde{C}^{\mathcal{V}}_{i,j-1,k-1} + q_1^2 q_2^m \widetilde{C}^{\mathcal{V}}_{i,j-1,k} + q_1^d q_2^u \widetilde{C}^{\mathcal{V}}_{i,j-1,k+1} \\
&\quad + q_1^m q_2^d \widetilde{C}^{\mathcal{V}}_{i,j,k-1} + q_1^m q_2^m \widetilde{C}^{\mathcal{V}}_{i,j,k} + q_1^m q_2^u \widetilde{C}^{\mathcal{V}}_{i,j,k+1} \\
&\quad + q_1^u q_2^d \widetilde{C}^{\mathcal{V}}_{i,j+1,k-1} + q_1^u q_2^m \widetilde{C}^{\mathcal{V}}_{i,j,k} + q_1^u q_2^u \widetilde{C}^{\mathcal{V}}_{i,j+1,k+1}
\end{aligned} \quad \text{(C-17)}$$

where

$$q_1^d = \tfrac{1}{2}\left(\tfrac{1}{3} - \tfrac{\mu_1\Delta t}{\Delta_1} + \left(\tfrac{\mu_1\Delta t}{\Delta_1}\right)^2\right) \quad \text{(C-18a)}$$

$$q_1^m = \tfrac{2}{3} - \left(\tfrac{\mu_1\Delta t}{\Delta_1}\right)^2 \quad \text{(C-18b)}$$

$$q_1^u = \tfrac{1}{2}\left(\tfrac{1}{3} + \tfrac{\mu_1\Delta t}{\Delta_1} + \left(\tfrac{\mu_1\Delta t}{\Delta_1}\right)^2\right) \quad \text{(C-18c)}$$

and

$$q_2^d = \frac{1}{2}\left(\frac{1}{3} - \frac{\mu_2\Delta t}{\Delta_1} + \left(\frac{\mu_2\Delta t}{\Delta_1}\right)^2\right) \tag{C-19a}$$

$$q_2^m = \frac{2}{3} - \left(\frac{\mu_2\Delta t}{\Delta_1}\right)^2 \tag{C-19b}$$

$$q_2^u = \frac{1}{2}\left(\frac{1}{3} + \frac{\mu_2\Delta t}{\Delta_1} + \left(\frac{\mu_2\Delta t}{\Delta_1}\right)^2\right) \tag{C-19c}$$

We return to the linear complimentarity problem (C-8a) - (C-8d). Following from (C-8d) the unique solution will instantaneously satisfy either

$$\frac{\partial\widetilde{C}^{\mathcal{V}}}{\partial t} + \mu_1\frac{\partial\widetilde{C}^{\mathcal{V}}}{\partial z_1} + \mu_2\frac{\partial\widetilde{C}^{\mathcal{V}}}{\partial z_2} + \frac{1}{2}\sigma_1^2\frac{\partial^2\widetilde{C}^{\mathcal{V}}}{\partial z_1^2} - \frac{1}{2}\sigma_2^2\frac{\partial^2\widetilde{C}^{\mathcal{V}}}{\partial z_2^2} - \frac{z_1-z_2}{2\sigma_S}\cdot\widetilde{C}^{\mathcal{V}} = 0 \tag{C-20a}$$

or

$$\widetilde{C}^{\mathcal{V}}[t,z_1,z_2] = \left[\exp\left[\frac{z_1+z_2}{2\sigma_r}\right] - K\right]^+ \tag{C-20b}$$

subject to

$$\widetilde{C}^{\mathcal{V}}[T,z_1,z_2] = \left[\exp\left[\frac{z_1+z_2}{2\sigma_r}\right] - K\right]^+ \tag{C-20c}$$

We introduce the iterative function $\hat{C}^{\mathcal{V}}_{i,j,k}$, defined only on $\{(i,j,k) : i \in [0,n_t]\cap\mathbb{Z},\ j \in [0,n_1]\cap\mathbb{Z}, k \in [0,n_2]\times\mathbb{Z}\}$ to approximate the values of $\widetilde{C}^{\mathcal{V}}_{i,j,k}$. Set

$$\hat{C}^{\mathcal{V}}_{n_t,j,k} = \left[\exp\left[\frac{z_{1,j}+z_{2,k}}{2\sigma_r}\right] - K\right]^+ \tag{C-21}$$

so that $\hat{C}^{\mathcal{V}}_{n_t,j,k} = \widetilde{C}^{\mathcal{V}}_{n_t,j,k}$ exactly. Using the definitions of q in (C-18) and (C-19), the intermediate variable $\check{C}^{\mathcal{V}}_{i-1,j,k}$ defined by

$$\begin{aligned}\check{C}^{\mathcal{V}}_{i-1,j,k}\left[1 + \frac{z_{1,j}-z_{2,k}}{2\sigma_r}\Delta t\right] = {} & q_1^d q_2^d \hat{C}^{\mathcal{V}}_{i,j-1,k-1} - q_1^d q_2^m \hat{C}^{\mathcal{V}}_{i,j-1,k} + q_1^d q_2^u \hat{C}^{\mathcal{V}}_{i,j-1,k+1} \\ & + q_1^m 1_2^d \hat{C}^{\mathcal{V}}_{i,j,k-1} + q_1^m q_2^m \hat{C}^{\mathcal{V}}_{i,j,k} + q_1^m q_2^u \hat{C}^{\mathcal{V}}_{i,j,k+1} \\ & + q_1^u q_2^d \hat{C}^{\mathcal{V}}_{i,j+1,k-1} + q_1^u q_2^m \hat{C}^{\mathcal{V}}_{i,j+1,k} + q_1^u q_2^u \hat{C}^{\mathcal{V}}_{i,j+1,k+1}\end{aligned} \tag{C-22a}$$

exactly solves the approximation (C-17) of the PDE in (C-8a).

The solution of a finite difference equation, $\hat{C}^{\mathcal{V}}_{i,j,k}$ can also be interpreted as the discounted expected value of the future value of $\hat{C}^{\mathcal{V}}$. Discounting is done over the time length Δt at the short rate prevailing when z_1 and z_2 take the values $z_{1,j}$ and $z_{2,k}$ respectively. Expectations are taken over a measure where z_1 can move from $z_{1,j}$ up to $z_{1,j+1}$, down to $z_{1,j-1}$ or stay constant with probabilities q_1^u, q_1^d and q_1^m respectively, and z_2 likewise moves to $z_{2,k-1}$, $z_{2,k}$ or $z_{2,k+1}$ with probabilities q_2^u, q_2^m and q_2^d independently of z_1. By (C-9b), (C-9d), (C-18) and (C-19) these probabilities are specific to the index values j and k.

This probabilistic interpretation motivates the calculations linking (C-17) to (C-12). The approximations (C-15a)-(C-15d) distribute the weights in (C-12) across the nine nodes to enable interpretation as joint probabilities of independent processes. These probabilities match the first conditional moments of z_1 and z_2, and approximate the second (uncentered) conditional moment z_1 and z_2 with their conditional variances. In most problems these distributed weights will reduce the scheme error.

The minor adjustments to arrive at (C-17) maintain the independent process interpretation, and eliminate the bias in the the second uncentered conditional moment. This further reduces scheme error. More usefully to us, the second moment matching substantially broadens the range of parameter values under which we can conclude scheme stability. (See discussion starting on page 153).

The individual values of $\check{C}^{\mathcal{V}}_{i-1,j,k}$ are explicitly determined by the future values $\hat{C}^{\mathcal{V}}_{i,j,k}$, and the finite difference scheme is hence termed explicit. The values of $\check{C}^{\mathcal{V}}_{i-1,j,k}$ are independent of each other other than through any mutual dependence on values of $\hat{C}^{\mathcal{V}}_{i,j,k}$.

Figure C-1: Explicit determination of $\check{C}^{\mathcal{V}}$ from $\hat{C}^{\mathcal{V}}$.

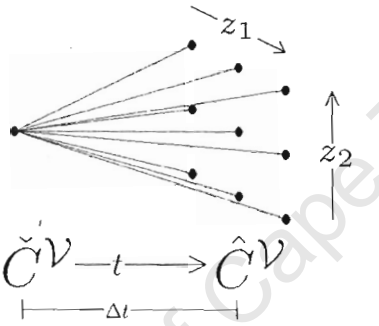

Unlike the implicit scheme in section C.1, the explicit scheme employed here permits node-by-node adjustments. This is feasible because the nodes are explicitly determined, independently of each other, not relying on each other for stability.

To complete the iterative process for $\hat{C}^{\mathcal{V}}$ at time t_i, wherever $\check{C}^{\mathcal{V}}_{i,j,k}$ is defined we set

$$\hat{C}^{\mathcal{V}}_{i,j,k} = \text{MAX}\left[\check{C}^{\mathcal{V}}_{i,j,k}, \left[\exp\left[\frac{z_1+z_2}{2\sigma_S}\right] - K\right]^+\right] \tag{C-22b}$$

so that any approximation of $\tilde{C}^{\mathcal{V}}$ solves (C-8c).

From a financial perspective, $\check{C}^{\mathcal{V}}_{i,j,k}$ represents the value at time t_i of holding $C^{\mathcal{V}}$ for a further time step Δt (i.e. until time t_{i+1}). From simple arbitrage arguments $C^{\mathcal{V}}$ must dominate the value of immediate exercise (viz. intrinsic value), leading to (C-8c). The inclusion of (C-22b) in the iterative process for $\hat{C}^{\mathcal{V}}$ enforces this inequality by allowing for early exercise of $C^{\mathcal{V}}$ at any time t_i.

The iterative scheme determined by (C-22a) and (C-22b) permits the calculation of most values of $\hat{C}^{\mathcal{V}}_{i,j,k}$ given the values of $\hat{C}^{\mathcal{V}}_{i+1,j,k}$. From the terminal values in (C-8b) we can calculate $\hat{C}^{\mathcal{V}}_{i,j,k}$ many time steps before expiry T.

The calculation permits calculation of many, but not all, of the the values of $\hat{C}^{\mathcal{V}}_{i,j,k}$ because each expectation in (C-22a) requires a spread of possible future outcomes to reflect the underlying uncertainty. This permits pricing at any time step t_i only on the interior nodes at time t_{i+1} - at every time step we lose the perimiter nodes. This creates a collapsing cone where pricing is feasible. The cone can be visualised as similar to a pyramid (see figure C-6).

In section C.1 we encountered a similar loss of perimiter values. We overcame this by introducing boundary values at every time step. (See the definitions accompanying (C.1)).

Such boundary conditions are infeasible in our current model with two stochastic variables. To see this consider a cross-section th the domain $\mathcal{D}_C^{\mathcal{V}}$ at a fixed time as illustrated in figure C-2[2].

Figure C-2: Cross-section through $\mathcal{D}_C^{\mathcal{V}}$ at fixed time

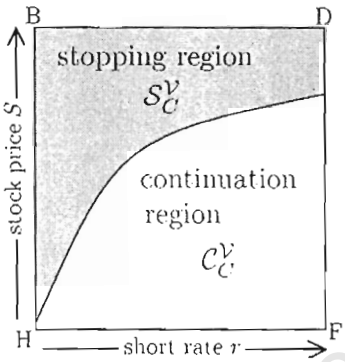

The excess of the call price $C^{\mathcal{V}}$ over intrinsic value is an increasing function of r and a decreasing function of S. Near the corner B in figure C-2 it is reasonable to assign intrinsic value to the perimiter values. Similar arguments applied to the early exercise premium may reasonaby assign the price of the corresponding European equity call option at perimiter nodes near the corner F (though the mean-reverting nature of r makes the accuracy of even this European approximation doubtful).

Approaching the corners D and H we are forced to consider the tradeoffs induced by moving the stock price and short rate in the same direction. Somewhere between B and F the perimiter of BDFH will cross the OEB. However, the OEB location needs to be determined within the calculation. There is hence no possible method to determine *a priori* which perimiter nodes lie within the stopping area $\mathcal{S}_C^{\mathcal{V}}$ and which lie in the continuation region $\mathcal{C}_C^{\mathcal{V}}$, and to impose such locations onto the perimeter values.

Some explicit finite difference schemes with mean-reverting variables permit implicit boundary conditions within certain ranges. Vetzal (1998) provides a highly accessible justificaiton of such methods. Our transformed variables z_1 and z_2 are not necessarily mean-reverting. Indeed, it can be shown that implicit boundary conditions on either z_1 or z_2 cannot be stable at both their upper and lower bounds.

We adopted a forward time difference because of the consequent ease of intrinsic update in (C-22b). We pay twice for this. Firstly, we need to calculate results in a sufficiently large 'pyramid' to cover all the prices within the subset of the domain $\mathcal{D}_C^{\mathcal{V}}$ which interest us. We discuss this calculation pyramid next.

The second cost concerns scheme stability. As mentioned earlier, explicit finite difference schemes are typically only stable conditional on the variables lying within specific ranges. These ranges depend on the domain over which the scheme is applied, so we first address the problem of domain size.

[2]The slope of the OEB was determined in Lemma 4.3.5: its curvature is at this point only speculated.

We have expressed interest in a hyper-rectangular sub-space of $\mathcal{D}_C^{\mathcal{V}}$ (a time cross-section of which is illustrated in figure C-2). The transformation of this cross-section to (z_1, z_2)-space rotates and stretches this cross section.

The finite difference scheme introduced in (C-22a)-(C-22b)operates on a rectangle in (z_1, z_2)-space whose sides are parallel with the axes of this space. This rectangle needs to include all the points of the transformation of the area of interest, as depicted in figure C-3:

Figure C-3: Domains of interest and concern in (z_1, z_2)-space

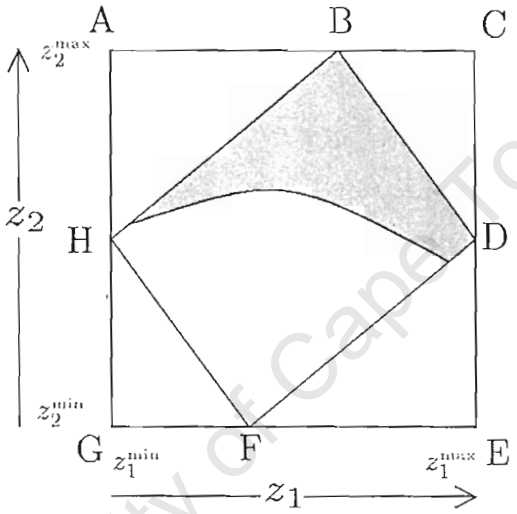

This inclusion is achieved so long as the rectangle in (z_1, z_2)-space is bounded by

$$z_1^{\min} \leq \sigma_r \cdot S_{\min} + \sigma_S \cdot r_{\min} \qquad z_2^{\min} \leq \sigma_r \cdot S_{\min} - \sigma_S \cdot r_{\max}$$
$$z_1^{\max} \geq \sigma_r \cdot S_{\max} + \sigma_S \cdot r_{\max} \qquad z_2^{\max} \geq \sigma_r \cdot S_{\max} - \sigma_S \cdot r_{\min}$$

We will call the trapezium BDFH the domain of interest, and the rectangle ACEG the domain of concern. Though we are interested only in BDFH, we need to concern ourselves at all times with ACEG in order to guarantee prices within all of BDFH.

As previously discussed, at each time step we lose the ability to calculate option prices at the perimiter spatial nodes of the previous time step. This creates a collapsing cone of prices. To ensure that we have prices within the domain of concern ACEG at all times, the hyper-rectangle $[0, T] \times$ACEG must be fully contained within this collapsing cone.

Viewed differently, because we cannot correctly apply the boundary conditions presented in (6.8c) and (6.8d) along the perimiter of the domain of concern, we increase our reliance upon the terminal condition (6.8b). The hyper-rectangle $[0, T] \times$ACEG must be part of that domain which is dependent only on the terminal condition. In effect the PDE (less the free boundary constraints) becomes only an initial value problem, omitting the boundary conditions (6.8c) and (6.8d). (The free boundary constraints (6.8e)-(6.8h) enter through the intrinsic adjustment (C-22b) and its impact on subsequent iterations).

By increasing the area of (z_1, z_2)-space over which we apply the terminal condition, we can increase the 'volume' of the cone dependent on the terminal condition only. This is done

until the cone fully contains the domain of concern for all times of interest. To discover how large a space we need apply the initial condition over, we start with the size of ACEG.

We lose one spatial step at each boundary at every time step. Clearly the strongest restriction occurs furthest from expiry, i.e. at $t = 0$. To ensure that the entire domain of concern at $t = 0$ falls within the domain dependent only on the terminal condition, it is sufficient that the terminal condition is applied over a rectangle containing

$$z_1^{\text{MIN}} = z_1^{\min} - n_t \cdot \Delta_1 \qquad z_2^{\text{MIN}} = z_2^{\min} - n_t \cdot \Delta_2 \qquad \text{(C-23)}$$
$$z_1^{\text{MAX}} = z_1^{\max} + n_t \cdot \Delta_1 \qquad z_2^{\text{MAX}} = z_2^{\max} + n_t \cdot \Delta_2$$

As the domain of concern is time-independent, this ensures that the entire domain of concern is calculable for all times of interest.

Figure C-4: Cross-sectional extension of terminal condition

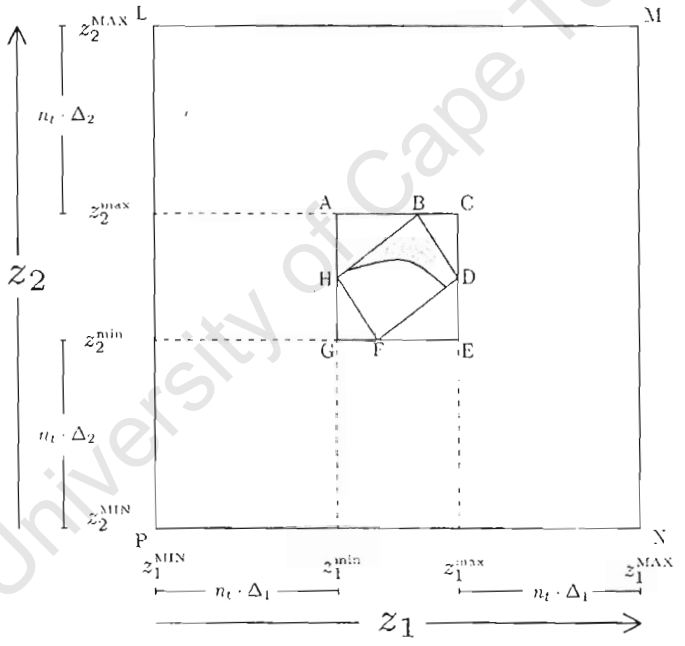

A final subtlety regards the location of nodes. The spatial step sizes Δ_1 and Δ_2 are determined in (C-13) in terms of the step size Δt. They will probably not span the domain of concern (or hence the rectangle LMNP in figure C-4) perfectly without remainder.

With the values of z_1^{MIN}, z_1^{MAX}, z_2^{MIN} and z_2^{MAX} determined in (C-23), the node positions are fixed by the equation (C-10) on page 145. They start along the lines LP and PN in figure C-4, and extend just far enough to include the lines LM and MN. Nodes will also lie exactly on AG and GE.

The terminal condition must be applied to the rectangle QRSP in figure C-5 so that prices are available at all times of interest within the rectangle IJKG, and hence the domain of concern.

Figure C-5: Location of nodes within Domain of Calculation

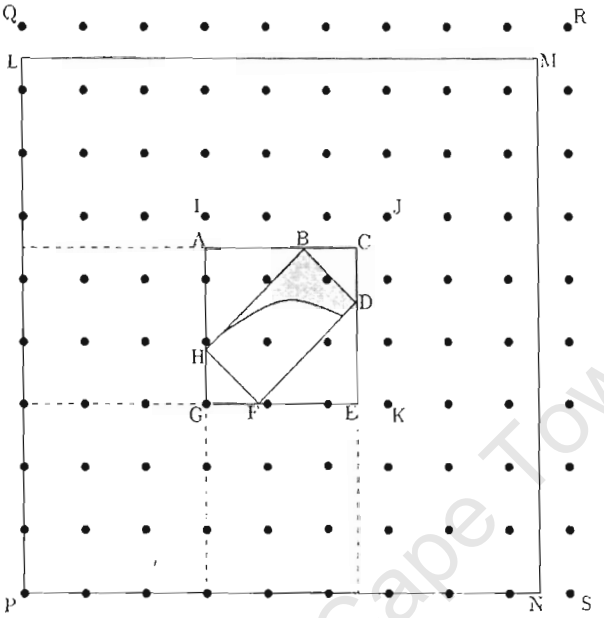

Consider the subspace of $\widetilde{\mathcal{D}}_C^{\mathcal{V}}$ created by all possible straight lines joining QRSP at time T to IJKG at time 0 (see figure C-6). With the terminal condition applied over QRSP, it is only at nodes within this space that we will be able to calculate option prices. Hence we term this subspace the domain of calculation.

Having established the domain over which we will be applying our scheme, we are in a position to consider the stability of the scheme.

Stability analysis of univariate explicit finite difference schemes is trivial: positivity of all 'probabilites' is both a necessary and a sufficient requirement for stability.

Multivariate explicit finite difference schemes are more intricate to analyse. While positivity of the 'probabilities' is no longer necessary for stability, it remains a sufficient condition[3]. In order to simplify the analysis required, we will consider only schemes with positive probabilities. These are guaranteed to be stable.

As the variables z_1 and z_2 are independent under the probabilities q, positivity of the joint probabilities requires positivity of the marginal probabilities. The 'up' and 'down' probabilities in (C-18) and C-19 are quadratics in $\left(\frac{\mu.\Delta t}{\Delta_1}\right)$ which are always positive. Only the probabilities q_1^m and q_2^m may drop below zero. This happens when the value of $\left|\mu_1 \frac{\Delta t}{\Delta_1}\right|$ or of $\left|\mu_2 \frac{\Delta t}{\Delta_2}\right|$ exceeds $\sqrt{\frac{2}{3}}$.

From their definitions in (C-9b) the drifts μ_1 and μ_2 are linear functions of the short rate r. So long as these drifts give positive probabilities at both the smallest and largest values of the short rate within the domain of calculation, they will give positive probabilities througout

[3]Personal communication with Prof. K. Vetzal

Figure C-6: Domain of Calculation

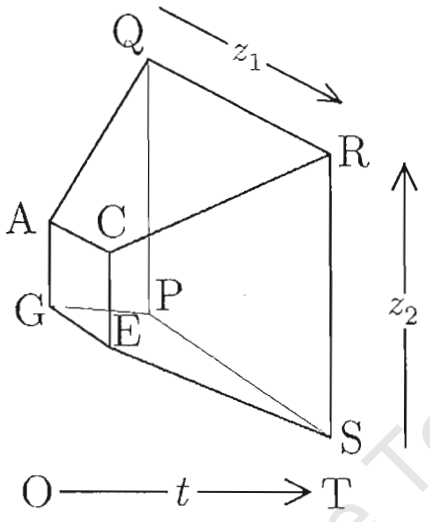

the domain of calculation.

The short rate r is the difference $\frac{z_1 - z_1}{2\sigma_S}$. Within QRSP it will reach minimum and maximum values at the corners Q and S respectively. These values can be shown to be[4]:

$$r_{\text{MIN}} = r_{\min} - \frac{\sigma_r}{2\sigma_S} \ln \frac{S_{\max}}{S_{\min}} - \frac{n_t}{2\sigma_S} (\Delta_1 + \Delta_2) \tag{C-24a}$$

$$r_{\text{MAX}} = r_{\max} + \frac{\sigma_r}{2\sigma_S} \ln \frac{S_{\max}}{S_{\min}} + \frac{n_t}{2\sigma_S} (\Delta_1 + \Delta_2) \tag{C-24b}$$

Considering the drift μ_1 at r_{MIN} and amending (C-13) to $\frac{\Delta_1}{\sigma_1} = \frac{\Delta_2}{\sigma_2}$ we get

$$\begin{aligned} \sqrt{\tfrac{2}{3}} &> \left|\mu_1 \tfrac{\Delta t}{\Delta_1}\right| \\ &= \left|\tfrac{\Delta t}{\Delta_1}\left(\nu_1^0 + \nu_1^1 r_{\min} - \nu_1^1 \tfrac{\sigma_r}{2\sigma_S} \ln \tfrac{S_{\max}}{S_{\min}}\right) - \nu_1^1 \tfrac{\Delta t}{\Delta_1} \tfrac{T/\Delta t}{2\sigma_S} \Delta_1 \left(1 + \tfrac{\sigma_2}{\sigma_1}\right)\right| \\ &= \left|\tfrac{\Delta t}{\Delta_1}\left(\nu_1^0 + \nu_1^1 r_{\min} - \nu_1^1 \tfrac{\sigma_r}{2\sigma_S} \ln \tfrac{S_{\max}}{S_{\min}}\right) - \tfrac{\nu_1^1 T}{2\sigma_S}\left(1 + \tfrac{\sigma_1}{\sigma_2}\right)\right| \end{aligned} \tag{C-25a}$$

Likewise from μ_1 at r_{MAX}, for $\left|\mu_1 \frac{\Delta t}{\Delta_1}\right| < \sqrt{\frac{2}{3}}$ we require

$$\sqrt{\tfrac{2}{3}} > \left|\tfrac{\Delta t}{\Delta_1}\left(\nu_1^0 + \nu_1^1 r_{\max} + \nu_1^1 \tfrac{\sigma_r}{2\sigma_S} \ln \tfrac{S_{\max}}{S_{\min}}\right) + \tfrac{\nu_1^1 T}{2\sigma_S}\left(1 + \tfrac{\sigma_1}{\sigma_2}\right)\right| \tag{C-25b}$$

A necessary condition for (C-25a) and (C-25b) to hold concurrently is

$$T < \frac{2\sigma_S \sqrt{\frac{2}{3}}}{\left(1 - \frac{\sigma_2}{\sigma_1}\right)\left|\nu_1^1\right|} \tag{C-26a}$$

[4]Technically r_{MIN} corresponds to the node L; evaluated at Q the short rate r lies in the interval $(r_{\text{MIN}} - \frac{\Delta_2}{2\sigma_S}, r_{\text{MIN}}]$. However, the smallest value of r for which we will need to evaluate q_1^m and q_2^m lies in $(r_{\text{MIN}}, r_{\text{MIN}} + \frac{\Delta_1}{2\sigma_S}]$. Ensuring positivity at r_{MIN} is slightly excessive. Such excess vanishes at $\Delta t \downarrow 0$. Similar arguments apply for r_{MAX} at S

Similarly, $\left|\mu_2 \frac{\Delta t}{\Delta_2}\right| < \sqrt{\frac{2}{3}}$ demands

$$T < \frac{2\sigma_S \sqrt{\frac{2}{3}}}{\left(\frac{\sigma_1}{\sigma_2} + 1\right) \left|\nu_2^1\right|} \tag{C-26b}$$

So, regardless of the size Δt of the temporal divisions, there is a fixed time to maturity beyond which we cannot guarantee positive probabilities. Because σ_r, σ_S and α are all positive by assumption, the Cauchy-Schwartz inequality gives $\left|\nu_2^1\right| \geq \left|\nu_1^1\right|$. Frin this inequality, (C-26b) is normally a stronger condition than (C-26a), unless the correlation coefficient χ is sufficiently below zero.

Assuming that our times of interest lie within this window, we still need to satisfy the drift inequalities (C-25a) and (C-25b) and the corresponding inequalities arising from $\left|\mu_2 \frac{\Delta t}{\Delta_1}\right| < \sqrt{\frac{2}{3}}$. Inequality (C-25a) can be rewritten in terms of a linear function of $\sqrt{\Delta t}$ with the intercept on the dependent variable axis located by the horizon limit (C-26a) in the interval $(-\sqrt{\frac{2}{3}}, \sqrt{\frac{2}{3}})$:

$$\left|\left(\nu_1^0 + \nu_1^1 r_{\min} - \nu_1^1 \frac{\sigma_r}{2\sigma_s} \ln \frac{S_{\max}}{S_{\min}}\right) \frac{\sqrt{\Delta t}}{\sigma_1 \sqrt{3}} - \nu_1^1 \frac{T\Delta_1}{2\sigma_S} \left(1 + \frac{\sigma_2}{\sigma_1}\right)\right| < \sqrt{\frac{2}{3}}$$

from which we can deduce that

$$\Delta t < \begin{cases} 3\sigma_1^2 \left(\frac{\sqrt{\frac{2}{3}} + \nu_1^1 \frac{T\Delta_1}{2\sigma_S}\left(1+\frac{\sigma_2}{\sigma_1}\right)}{\nu_1^0 + \nu_1^1 r_{\min} - \nu_1^1 \frac{\sigma_r}{2\sigma_S} \ln \frac{S_{\max}}{S_{\min}}} \right)^2 & \nu_1^0 + \nu_1^1 r_{\min} - \nu_1^1 \frac{\sigma_r}{2\sigma_S} \ln \frac{S_{\max}}{S_{\min}} > 0 \\ \infty & \nu_1^0 + \nu_1^1 r_{\min} - \nu_1^1 \frac{\sigma_r}{2\sigma_S} \ln \frac{S_{\max}}{S_{\min}} = 0 \\ 3\sigma_1^2 \left(\frac{\sqrt{\frac{2}{3}} - \nu_1^1 \frac{T\Delta_1}{2\sigma_S}\left(1+\frac{\sigma_2}{\sigma_1}\right)}{\nu_1^0 + \nu_1^1 r_{\min} - \nu_1^1 \frac{\sigma_r}{2\sigma_S} \ln \frac{S_{\max}}{S_{\min}}} \right)^2 & \nu_1^0 + \nu_1^1 r_{\min} - \nu_1^1 \frac{\sigma_r}{2\sigma_S} \ln \frac{S_{\max}}{S_{\min}} < 0 \end{cases} \tag{C-27a}$$

Similarly (C-25b) leads to

$$\Delta t < \begin{cases} 3\sigma_1^2 \left(\frac{\sqrt{\frac{2}{3}} - \nu_1^1 \frac{T\Delta_1}{2\sigma_S}\left(1+\frac{\sigma_2}{\sigma_1}\right)}{\nu_1^0 + \nu_1^1 r_{\max} + \nu_1^1 \frac{\sigma_r}{2\sigma_S} \ln \frac{S_{\max}}{S_{\min}}} \right)^2 & \nu_1^0 + \nu_1^1 r_{\max} + \nu_1^1 \frac{\sigma_r}{2\sigma_S} \ln \frac{S_{\max}}{S_{\min}} > 0 \\ \infty & \nu_1^0 + \nu_1^1 r_{\max} + \nu_1^1 \frac{\sigma_r}{2\sigma_S} \ln \frac{S_{\max}}{S_{\min}} = 0 \\ 3\sigma_1^2 \left(\frac{\sqrt{\frac{2}{3}} + \nu_1^1 \frac{T\Delta_1}{2\sigma_S}\left(1+\frac{\sigma_2}{\sigma_1}\right)}{\nu_1^0 + \nu_1^1 r_{\max} + \nu_1^1 \frac{\sigma_r}{2\sigma_S} \ln \frac{S_{\max}}{S_{\min}}} \right)^2 & \nu_1^0 + \nu_1^1 r_{\max} + \nu_1^1 \frac{\sigma_r}{2\sigma_S} \ln \frac{S_{\max}}{S_{\min}} < 0 \end{cases} \tag{C-27b}$$

while from the constraints on μ_2,

$$\Delta t < \begin{cases} 3\sigma_2^2 \left(\frac{\sqrt{\frac{2}{3}} + \nu_2^1 \frac{T\Delta_2}{2\sigma_S}\left(\frac{\sigma_1}{\sigma_2}+1\right)}{\nu_2^0 + \nu_2^1 r_{\min} - \nu_2^1 \frac{\sigma_r}{2\sigma_S} \ln \frac{S_{\max}}{S_{\min}}} \right)^2 & \nu_2^0 + \nu_2^1 r_{\min} - \nu_2^1 \frac{\sigma_r}{2\sigma_S} \ln \frac{S_{\max}}{S_{\min}} > 0 \\ \infty & \nu_2^0 + \nu_2^1 r_{\min} - \nu_2^1 \frac{\sigma_r}{2\sigma_S} \ln \frac{S_{\max}}{S_{\min}} = 0 \\ 3\sigma_2^2 \left(\frac{\sqrt{\frac{2}{3}} - \nu_2^1 \frac{T\Delta_2}{2\sigma_S}\left(\frac{\sigma_1}{\sigma_2}+1\right)}{\nu_2^0 + \nu_2^1 r_{\min} - \nu_2^1 \frac{\sigma_r}{2\sigma_S} \ln \frac{S_{\max}}{S_{\min}}} \right)^2 & \nu_2^0 + \nu_2^1 r_{\min} - \nu_2^1 \frac{\sigma_r}{2\sigma_S} \ln \frac{S_{\max}}{S_{\min}} < 0 \end{cases} \tag{C-27c}$$

and also

$$\Delta t < \begin{cases} 3\sigma_2^2 \left(\dfrac{\sqrt{\frac{2}{3}} - \nu_2^1 \frac{T\Delta_2}{2\sigma_S}\left(\frac{\sigma_1}{\sigma_2}+1\right)}{\nu_2^0 + \nu_2^1 r_{\max} + \nu_2^1 \frac{\sigma_r}{2\sigma_S} \ln \frac{S_{\max}}{S_{\min}}} \right)^2 & \nu_2^0 + \nu_2^1 r_{\max} + \nu_2^1 \frac{\sigma_r}{2\sigma_S} \ln \frac{S_{\max}}{S_{\min}} > 0 \\ \infty & \nu_2^0 + \nu_2^1 r_{\max} + \nu_2^1 \frac{\sigma_r}{2\sigma_S} \ln \frac{S_{\max}}{S_{\min}} = 0 \\ 3\sigma_2^2 \left(\dfrac{\sqrt{\frac{2}{3}} + \nu_2^1 \frac{T\Delta_2}{2\sigma_S}\left(\frac{\sigma_1}{\sigma_2}+1\right)}{\nu_2^0 + \nu_2^1 r_{\max} + \nu_2^1 \frac{\sigma_r}{2\sigma_S} \ln \frac{S_{\max}}{S_{\min}}} \right)^2 & \nu_2^0 + \nu_2^1 r_{\max} + \nu_2^1 \frac{\sigma_r}{2\sigma_S} \ln \frac{S_{\max}}{S_{\min}} < 0 \end{cases} \qquad \text{(C-27d)}$$

Thus while the option's time to expiry remains less than the limits set by (C-26a) and (C-26b), we can always set Δt small enough to satisfy all of (C-27a) - (C-27d). This guarantees the positive probabilities for which we are searching, and hence scheme stability.

The major drawback of our approach regards the number of nodes to be calculated. Figure C-7 illustrates how the domain of concern is dwarfed in the domain of calculation. The number of nodes in the domain of concern is of the order of (n_t^3).

Figure C-7: Spatial cross-section of the domain of calculation through QAES

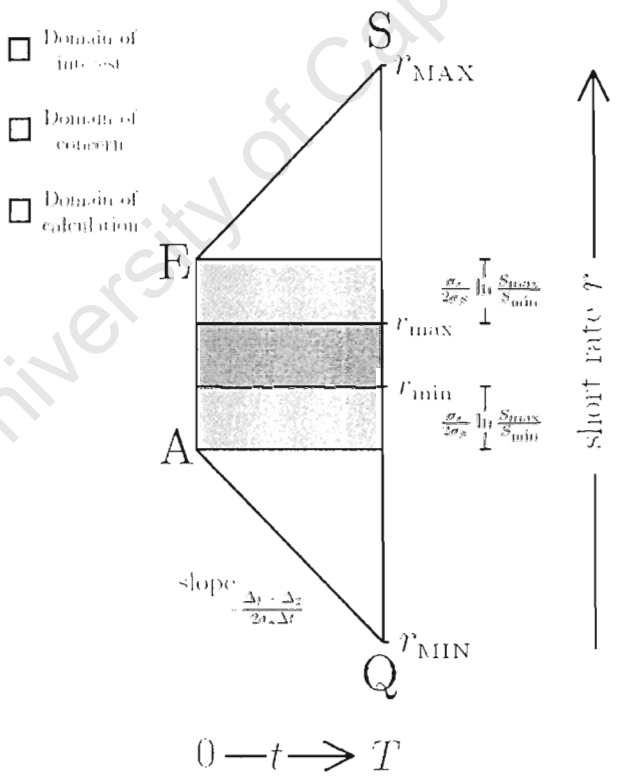

We have determined that the scheme determined by (C-21), (C-22a) and (C-22b) for $\hat{C}^{\mathcal{V}}$ is stable and also consistent with the variational inequality (C-8a)- (C-8d) for $\widetilde{C}^{\mathcal{V}}$. By the Lax Equivalency Theorem again $\hat{C}^{\mathcal{V}}$ will converge to the unique solution of (C-8a)- (C-8d). The convergence of the same order as the consistency - i.e. $O(\Delta t)$.

Appendix D

Matlab Code

D.1 Code for OBS American Call $C^{\mathcal{O}}$

D.1.1 AmCallMaster.m

```
OnePrice = zeros(17,1);
for i = 2 : 17
    OnePrice(i) = 30+10*i;
end
%
OneDelta = OnePrice;
ThreePrice = OnePrice;
ThreeDelta = ThreePrice;
%
CallBoundary = zeros(39,1);
for i = 4 : 39
    CallBoundary(i) = (i-3)/12;
end
%
%
for h = 1 : 13
    SpotRate = 0.0175+0.01*h;
        AmCall;
        OnePrice = [OnePrice,[SpotRate;OneCallVector(:,2)]];
        OneDelta = [OneDelta,[SpotRate;OneCallVector(:,3)]];
        ThreePrice = [ThreePrice,[SpotRate;ThreeCallVector(:,2)]];
        ThreeDelta = [ThreeDelta,[SpotRate;ThreeCallVector(:,3)]];
        CallBoundary = [CallBoundary,[SpotRate;RootCount;CallOEB(:,2)]];
    SpotRate = 0.02+0.01*h;
        AmCall;
        OnePrice = [OnePrice,[SpotRate;OneCallVector(:,2)]];
        OneDelta = [OneDelta,[SpotRate;OneCallVector(:,3)]];
        ThreePrice = [ThreePrice,[SpotRate;ThreeCallVector(:,2)]];
        ThreeDelta = [ThreeDelta,[SpotRate;ThreeCallVector(:,3)]];
        CallBoundary = [CallBoundary,[SpotRate;RootCount;CallOEB(:,2)]];
    SpotRate = 0.0225+0.01*h;
        AmCall;
        OnePrice = [OnePrice,[SpotRate;OneCallVector(:,2)]];
        OneDelta = [OneDelta,[SpotRate;OneCallVector(:,3)]];
        ThreePrice = [ThreePrice,[SpotRate;ThreeCallVector(:,2)]];
        ThreeDelta = [ThreeDelta,[SpotRate;ThreeCallVector(:,3)]];
        CallBoundary = [CallBoundary,[SpotRate;RootCount;CallOEB(:,2)]];
end
```

D.1.2 AmCall.m

```
%
```

```
% Take input values
%
Strike = 100;
divyield=0.03;
StockVol = 0.2;
%
Smax = max(PerpCallOEB(Strike,SpotRate,divyield,StockVol*StockVol),250);
Smin = 40;
%
StepsPerMonth = 12;
SpaceSteps = 750;
%
RootCount = 0;
%
% ----------------------------------------
% Determine intermediate variables
%
SigSq = StockVol*StockVol;
%
ymin = log(Smin);
ymax = log(Smax);
%
SpaceNodes = SpaceSteps+1;
%
Delta_y = (ymax-ymin)/(SpaceSteps);
Delta_t = 1/12/StepsPerMonth;
%
% ----------------------------------------------------
% Initialise constants and matrices used in FDE and PSOR
%
TempOne = 0.5*(SpotRate-divyield-0.5*SigSq)*(Delta_t/Delta_y);
TempTwo = (Delta_t/Delta_y)*0.5*SigSq/Delta_y;
%
Aoz=TempOne-TempTwo;
Aoo=2+2*TempTwo+SpotRate*Delta_t;
Aot=-TempTwo-TempOne;
%
Bzz=TempTwo-TempOne;
Bzo=2-2*TempTwo-SpotRate*Delta_t;
Bzt=TempOne+TempTwo;
%
MatrixA = [diag(Aoz*ones(SpaceNodes-2,1)),zeros(SpaceNodes-2,2)];
MatrixA = MatrixA + [zeros(SpaceNodes-2,1),diag(Aoo*ones(SpaceNodes- 2,1)),zeros(SpaceNodes -2,1)];
MatrixA = MatrixA + [zeros(SpaceNodes-2,2),diag(Aot*ones(SpaceNodes-2,1))];
MatrixA = [zeros(1,SpaceNodes);MatrixA;zeros(1,SpaceNodes)];
MatrixA(1,1)=1;
MatrixA(SpaceNodes,SpaceNodes)=1;
%
MatrixB = [diag(Bzz*ones(SpaceNodes-2,1)),zeros(SpaceNodes-2,2)];
MatrixB = MatrixB + [zeros(SpaceNodes-2,1),diag(Bzo*ones(SpaceNodes -2,1)),zeros(SpaceNodes- 2,1)];
MatrixB = MatrixB + [zeros(SpaceNodes-2,2),diag(Bzt*ones(SpaceNodes- 2,1))];
%
clear TempOne
clear TempTwo
%
%----------
%    Initialise stock, payoff, call and OEB vectors
%
StockVector = ones(SpaceNodes,1);
PayoffVector = ones(SpaceNodes,1);
%
StockNow = Smin;
StockVector(1) = StockNow;
PayoffVector(1) = max(StockNow- Strike,0);
%
for i = 2 : SpaceNodes
```

```
    StockNow = StockNow*exp(Delta_y);
    %
    StockVector(i) = StockNow;
    PayoffVector(i) = max(StockNow-Strike,0);
    %
end
%
OldCallVector = PayoffVector;
CallOEB = [0,max(1,SpotRate/divyield)*Strike];
%
% ------------------------------------------------------------------
%
TimeToExpiry = 0;
%
% Looping through the first twelve months, to get results at T=1
for i = 1 : 12
    %
    % Solve the constrained matrix problem at intervals of Delta_t
    for j = 1 : StepsPerMonth
        %
        TimeToExpiry = TimeToExpiry + Delta_t;
        %
        SolveCallPSOR
        %
    end
    %
    %Locate the OEB at monthly intervals
    LocateOBSCallOEB
    %%
end
%
OneCallVector = ones(16,3);
%
for i = 1 : 16
    StockPrice = 40 + 10*i;
    InterpolateCall;
    OneCallVector(i,1) = StockPrice;
    OneCallVector(i,2) = CallPrice;
    StockPrice = StockPrice+1;
    InterpolateCall;
    Delta = 0.5*CallPrice;
    StockPrice = StockPrice-2;
    InterpolateCall;
    Delta = Delta - 0.5*CallPrice;
    OneCallVector(i,3) = Delta;
end
%
%
% Looping through remaining twenty-four months, to get results at T=4
for i = 13 : 36
    %
    % Solve the constrained matrix problem at intervals of Delta_t
    for j = 1 : StepsPerMonth
        %
        TimeToExpiry = TimeToExpiry + Delta_t;
        %
        SolveCallPSOR
        %
    end
    %
    %Locate the OEB at monthly intervals
    LocateOBSCallOEB
    %%
end
%
ThreeCallVector = ones(16,3);
```

```
%
for i = 1 : 16
    StockPrice = 40 + 10*i;
    InterpolateCall;
    ThreeCallVector(i,1) = StockPrice;
    ThreeCallVector(i,2) = CallPrice;
    StockPrice = StockPrice+1;
    InterpolateCall;
    Delta = 0.5*CallPrice;
    StockPrice = StockPrice-2;
    InterpolateCall;
    Delta = Delta - 0.5*CallPrice;
    ThreeCallVector(i,3) = Delta;
end
```

D.1.3 SolveCallPSOR.m

```
VectorD = [0;MatrixB*OldCallVector;0];
LowerBound = BScall(StockVector(1),Strike,SpotRate,divyield,StockVol,TimeToExpiry);
VectorD(1) = LowerBound;
VectorD(SpaceNodes) = PayoffVector(SpaceNodes);
%
NewCallVector = MatrixA\VectorD;
for k = 2 : SpaceNodes-1
    NewCallVector(k) = max(NewCallVector(k),PayoffVector(k));
end
OldCallVector = NewCallVector;
%
Iterations = 0;
Continue = 1;
%
while Continue == 1
    %
    Continue = 0;
    %
    LoopA = MatrixA;
    LoopD = VectorD;
    %
    for k = 1 : SpaceNodes
        %
        if OldCallVector(k) == PayoffVector(k)
            %
            LoopA(k,:) = zeros(1,SpaceNodes);
            LoopA(k,k) = 1;
            LoopD(k) = PayoffVector(k);
            %
        end
    end
    %
    NewCallVector = LoopA \ LoopD;
    OldCallVector = NewCallVector;
    %
    for k = 2 : SpaceNodes-1
        %
        Intermediate = (VectorD(k)-Aoz * NewCallVector(k-1)-Aot * OldCallVector(k+1))/Aoo;
        NewCallVector(k) = max(PayoffVector(k),1.5*Intermediate-0.5*OldCallVector(k));
        %
        if NewCallVector(k) - OldCallVector(k) >= 1.0e-010
            Continue = 1;
        end
        %
    end
    %
    OldCallVector = NewCallVector;
    %
    Iterations = Iterations + 1;
```

```
    %
end
```

D.1.4 BScall.m

```
function Call=BScall(Stock,Strike,SpotRate,divyield,StockVol,Expiry)
LimitOne=(log(Stock)-log(Strike)+(SpotRate-divyield+0.5*StockVol*StockVol)*Expiry)/(StockVol*sqrt(Expiry));
LimitTwo=LimitOne-StockVol*sqrt(Expiry);
Call=Stock*exp(-divyield*Expiry)*normcdf(LimitOne)-Strike*exp(-SpotRate*Expiry)*normcdf(LimitTwo);
```

D.1.5 LocateOBSCallOEB.m

```
ExIndex = 1;
%
while abs(OldCallVector(ExIndex)-PayoffVector(ExIndex))<0.001
    ExIndex = ExIndex + 1;
end

while OldCallVector(ExIndex) > PayoffVector(ExIndex)
    ExIndex = ExIndex + 1;
end
%
QuadCoeff = [(StockVector(ExIndex-3))^2,StockVector(ExIndex-3),1];
QuadCoeff = [QuadCoeff;(StockVector(ExIndex-2))^2,StockVector(ExIndex-2),1];
QuadCoeff = [QuadCoeff;(StockVector(ExIndex-1))^2,StockVector(ExIndex-1),1];
QuadCoeff = QuadCoeff\[OldCallVector(ExIndex-3);OldCallVector(ExIndex-2);OldCallVector(ExIndex-1)];
%
Determinant = (QuadCoeff(2) -1)^2- 4*QuadCoeff(1)*(QuadCoeff(3)+Strike);
if Determinant < 0
    CallOEB = [CallOEB;TimeToExpiry,StockVector(ExIndex)];
    RootCount = RootCount + 1;
else
    CallOEB = [CallOEB;TimeToExpiry,min(StockVector(ExIndex),(1-QuadCoeff(2)-sqrt(Determinant))/(2*
        QuadCoeff(1)))];
end
```

D.1.6 InterpolateCall.m

```
yValue = log(StockPrice);
LowNode = floor((yValue-ymin)/Delta_y)+1;
HiNode = LowNode+1;
%
if StockPrice > CallOEB(length(CallOEB(:,2)),2)
    CallPrice = max(StockPrice-Strike,0);
elseif StockVector(HiNode)>CallOEB(length(CallOEB(:,2)),2)
    MatrixX = [(StockVector(LowNode-2))^2,StockVector(LowNode-2),1;(StockVector(LowNode-1))^2,StockVector
        (LowNode-1),1;(StockVector(LowNode))^2,StockVector(LowNode),1];
    VectorY = [OldCallVector(LowNode-2);OldCallVector(LowNode-1);OldCallVector(LowNode)];
    QuadCoeff = MatrixX\VectorY;
    CallPrice = QuadCoeff'*[StockPrice^2;StockPrice;1];
elseif StockVector(HiNode+1)>CallOEB(length(CallOEB(:,2)),2)
    MatrixX = [(StockVector(LowNode-1))^2,StockVector(LowNode-1),1;(StockVector(LowNode))^2,StockVector(
        LowNode),1;(StockVector(HiNode))^2,StockVector(HiNode),1];
    VectorY = [OldCallVector(LowNode-1);OldCallVector(LowNode);OldCallVector(HiNode)];
    QuadCoeff = MatrixX\VectorY;
    CallPrice = QuadCoeff'*[StockPrice^2;StockPrice;1];
else
    MatrixX = [(StockVector(LowNode-1))^2,StockVector(LowNode-1),1;(StockVector(LowNode))^2,StockVector(
        LowNode),1;(StockVector(HiNode))^2,StockVector(HiNode),1];
    VectorY = [OldCallVector(LowNode-1);OldCallVector(LowNode);OldCallVector(HiNode)];
    QuadCoeff = MatrixX\VectorY;
    CallPrice = QuadCoeff'*[StockPrice^2;StockPrice;1];
    %
    MatrixX = [(StockVector(LowNode))^2,StockVector(LowNode),1;(StockVector(HiNode))^2,StockVector(HiNode)
        ,1;(StockVector(HiNode+1))^2,StockVector(HiNode+1),1];
```

```
    VectorY = [OldCallVector(LowNode);OldCallVector(HiNode);OldCallVector(HiNode+1)];
    QuadCoeff = MatrixX\VectorY;
    CallPrice = 0.5*CallPrice+0.5*QuadCoeff'*[StockPrice^2;StockPrice;1];
end
```

D.1.7 PerpCallOEB

```
function Boundary=PerpCallOEB(Strike,SpotRate,divyield,SigSq)
% Function to calculate the critical stock price
% (i.e. Optimal Exercise Boundary)
% of a perpetual call option.

TempVarOne = SpotRate-divyield-0.5*SigSq;
TempVarTwo = sqrt(TempVarOne^2+2*SpotRate*SigSq);
Root = (-TempVarOne+TempVarTwo)/SigSq;
Boundary = Root*Strike/(Root-1);
```

D.2 Code for OBS American Put $P^{\mathcal{O}}$

D.2.1 AmPutMaster.m

```
OnePrice = zeros(17,1);
for i = 2 : 17
    OnePrice(i) = 30+10*i;
end
%
OneDelta = OnePrice;
ThreePrice = OnePrice;
ThreeDelta = ThreePrice;
%
PutBoundary = zeros(39,1);
for i = 3 : 39
    PutBoundary(i) = (i-3)/12;
end
%
%
%
for h = 1 : 13
    SpotRate = 0.0175+0.01*h;
        AmPut;
        OnePrice = [OnePrice,[SpotRate;OnePutVector(:,2)]];
        OneDelta = [OneDelta,[SpotRate;OnePutVector(:,3)]];
        ThreePrice = [ThreePrice,[SpotRate;ThreePutVector(:,2)]];
        ThreeDelta = [ThreeDelta,[SpotRate;ThreePutVector(:,3)]];
        PutBoundary = [PutBoundary,[SpotRate;RootCount;PutOEB(:,2)]];
    SpotRate = 0.02+0.01*h;
        AmPut;
        OnePrice = [OnePrice,[SpotRate;OnePutVector(:,2)]];
        OneDelta = [OneDelta,[SpotRate;OnePutVector(:,3)]];
        ThreePrice = [ThreePrice,[SpotRate;ThreePutVector(:,2)]];
        ThreeDelta = [ThreeDelta,[SpotRate;ThreePutVector(:,3)]];
        PutBoundary = [PutBoundary,[SpotRate;RootCount;PutOEB(:,2)]];
    SpotRate = 0.0225+0.01*h;
        AmPut;
        OnePrice = [OnePrice,[SpotRate;OnePutVector(:,2)]];
        OneDelta = [OneDelta,[SpotRate;OnePutVector(:,3)]];
        ThreePrice = [ThreePrice,[SpotRate;ThreePutVector(:,2)]];
        ThreeDelta = [ThreeDelta,[SpotRate;ThreePutVector(:,3)]];
        PutBoundary = [PutBoundary,[SpotRate;RootCount;PutOEB(:,2)]];
end
```

D.2.2 AmPut.m

```
% Take input values
```

```
%
Strike = 100;
divyield=0.03;
StockVol = 0.2;
%
Smax = 250;
Smin = min(PerpPutOEB(Strike,SpotRate,divyield,StockVol*StockVol),40);
%
StepsPerMonth = 12;
SpaceSteps = 750;
%
RootCount = 0;
%
% ----------------------------------------
% Determine intermediate variables
%
SigSq = StockVol*StockVol;
%
ymin = log(Smin);
ymax = log(Smax);
%
SpaceNodes = SpaceSteps+1;
%
Delta_y = (ymax-ymin)/(SpaceSteps);
Delta_t = 1/12/StepsPerMonth;
%
% ----------------------------------------------
% Initialise constants and matrices used in FDE and PSOR
%
TempOne = 0.5*(SpotRate-divyield-0.5*SigSq)*(Delta_t/Delta_y);
TempTwo = (Delta_t/Delta_y)*0.5*SigSq/Delta_y;
%
Aoz=TempOne-TempTwo;
Aoo=2+2*TempTwo+SpotRate*Delta_t;
Aot=-TempTwo-TempOne;
%
Bzz=TempTwo-TempOne;
Bzo=2-2*TempTwo-SpotRate*Delta_t;
Bzt=TempOne+TempTwo;
%
MatrixA = [diag(Aoz*ones(SpaceNodes-2,1)),zeros(SpaceNodes-2,2)];
MatrixA = MatrixA + [zeros(SpaceNodes-2,1),diag(Aoo*ones(SpaceNodes-2,1)),zeros(SpaceNodes-2,1)];
MatrixA = MatrixA + [zeros(SpaceNodes-2,2),diag(Aot*ones(SpaceNodes- 2,1))];
MatrixA = [zeros(1,SpaceNodes);MatrixA;zeros(1,SpaceNodes)];
MatrixA(1,1)=1;
MatrixA(SpaceNodes,SpaceNodes)=1;
%
MatrixB = [diag(Bzz*ones(SpaceNodes-2,1)),zeros(SpaceNodes-2,2)];
MatrixB = MatrixB + [zeros(SpaceNodes-2,1),diag(Bzo*ones(SpaceNodes-2,1)),zeros(SpaceNodes-2,1)];
MatrixB = MatrixB + [zeros(SpaceNodes -2,2),diag(Bzt*ones(SpaceNodes-2,1))];
%
clear TempOne
clear TempTwo
%
%----------
%    Initialise stock, payoff, put and OEB vectors
%
StockVector = ones(SpaceNodes,1);
PayoffVector = ones(SpaceNodes,1);
%
StockNow = Smin;
StockVector(1) = StockNow;
PayoffVector(1) = max(Strike -StockNow,0);
%
for i = 2 : SpaceNodes
    StockNow = StockNow*exp(Delta_y);
```

```
    %
    StockVector(i) = StockNow;
    PayoffVector(i) = max(Strike-StockNow,0);
    %
end
%
OldPutVector = PayoffVector;
PutOEB = [0,min(1,SpotRate/divyield)*Strike];
%
% ------------------------------------------------------------
%
TimeToExpiry = 0;
%
% Looping through the first twelve months, to get results at T=1
for i = 1 : 12
    %
    % Solve the constrained matrix problem at intervals of Delta_t
    for j = 1 : StepsPerMonth
        %
        TimeToExpiry = TimeToExpiry + Delta_t;
        %
        SolvePutPSOR
        %
    end
    %
    %Locate the OEB at monthly intervals
    LocateOBSPutOEB
    %%
end
%
OnePutVector = ones(16,3);
%
for i = 1 : 16
    StockPrice = 40 + 10*i;
    InterpolateOBSPut;
    OnePutVector(i,1) = StockPrice;
    OnePutVector(i,2) = PutPrice;
    StockPrice = StockPrice+1;
    InterpolateOBSPut;
    Delta = 0.5*PutPrice;
    StockPrice = StockPrice-2;
    InterpolateOBSPut;
    Delta = Delta - 0.5*PutPrice;
    OnePutVector(i,3) = Delta;
end
%
%
% Looping through remaining twenty-four months, to get results at T=4
for i = 13 : 36
    %
    % Solve the constrained matrix problem at intervals of Delta_t
    for j = 1 : StepsPerMonth
        %
        TimeToExpiry = TimeToExpiry + Delta_t;
        %
        SolvePutPSOR
        %
    end
    %
    %Locate the OEB at monthly intervals
    LocateOBSPutOEB
    %%
end
%
ThreePutVector = ones(16,3);
%
```

```
for i = 1 : 16
    StockPrice = 40 + 10*i;
    InterpolateOBSPut;
    ThreePutVector(i,1) = StockPrice;
    ThreePutVector(i,2) = PutPrice;
    StockPrice = StockPrice+1;
    InterpolateOBSPut;
    Delta = 0.5*PutPrice;
    StockPrice = StockPrice-2;
    InterpolateOBSPut;
    Delta = Delta - 0.5*PutPrice;
    ThreePutVector(i,3) = Delta;
end
%
% ------------------------
% Display information of interest to user(s)
%
TimeNow = clock;
disp([TimeNow(4)+0.01*TimeNow(5)+0.0001*TimeNow(6),100*SpotRate,Smin,Smax,RootCount,PutOEB(1,2),
    PutOEB(13,2),PutOEB(37,2)])
```

D.2.3 SolvePutPSOR.m

```
LowerBound = PayoffVector(SpaceNodes);
UpperBound = BSput(StockVector(SpaceNodes),Strike,SpotRate,divyield,StockVol,TimeToExpiry);
%
VectorD = [LowerBound;MatrixB*OldPutVector;UpperBound];
%
NewPutVector = MatrixA\VectorD;
for k = 2 : SpaceNodes-1
    NewPutVector(k) = max(NewPutVector(k),PayoffVector(k));
end
OldPutVector = NewPutVector;
%
Iterations = 0;
Continue = 1;
%
while Continue == 1
    %
    Continue = 0;
    %
    LoopA = MatrixA;
    LoopD = VectorD;
    %
    for k = 1 : SpaceNodes
        %
        if OldPutVector(k) == PayoffVector(k)
            %
            LoopA(k,:) = zeros(1,SpaceNodes);
            LoopA(k,k) = 1;
            LoopD(k) = PayoffVector(k);
            %
        end
    end
    %
    NewPutVector = LoopA \ LoopD;
    OldPutVector = NewPutVector;
    %
    for k = SpaceNodes-1 : -1 : 2
        %
        Intermediate = (VectorD(k)-Aoz * OldPutVector(k-1)-Aot * NewPutVector(k+1))/Aoo;
        NewPutVector(k) = max(PayoffVector(k),1.5*Intermediate-0.5*OldPutVector(k));
        %
        if NewPutVector(k) - OldPutVector(k) >= 1.0e-010
            Continue = 1;
        end
```

```
        %
    end
    %
    OldPutVector = NewPutVector;
    %
    Iterations = Iterations + 1;
    %
end
```

D.2.4 BSput.m

```
function Put=BSput(Stock,Strike,SpotRate,divyield,StockVol,Expiry)
LimitOne=(log(Stock)-log(Strike)+(SpotRate-divyield+0.5*StockVol*StockVol)*Expiry)/(StockVol*sqrt(Expiry));
LimitTwo=LimitOne-StockVol*sqrt(Expiry);
Put=Strike*exp(-SpotRate*Expiry)*normcdf(-LimitTwo)- Stock*exp(-divyield*Expiry)*normcdf(-LimitOne);
```

D.2.5 LocateOBSPutOEB.m

```
ExIndex = SpaceNodes;
%
while abs(OldPutVector(ExIndex)-PayoffVector(ExIndex))<0.001
    ExIndex = ExIndex - 1;
end

while OldPutVector(ExIndex) > PayoffVector(ExIndex)
    ExIndex = ExIndex - 1;
end
%
QuadCoeff = [(StockVector(ExIndex+1))^2,StockVector(ExIndex+1),1];
QuadCoeff = [QuadCoeff;(StockVector(ExIndex+2))^2,StockVector(ExIndex+2),1];
QuadCoeff = [QuadCoeff;(StockVector(ExIndex+3))^2,StockVector(ExIndex+3),1];
QuadCoeff = QuadCoeff\[OldPutVector(ExIndex+1);OldPutVector(ExIndex+2);OldPutVector(ExIndex+3)];
%

Determinant = (QuadCoeff(2)+1)^2-4*QuadCoeff(1)*(QuadCoeff(3)-Strike);
if Determinant < 0
    PutOEB = [PutOEB;TimeToExpiry,StockVector(ExIndex)];
    RootCount = RootCount + 1;
else
    PutOEB = [PutOEB;TimeToExpiry,max(StockVector(ExIndex),(-1-QuadCoeff(2)+sqrt(Determinant))/(2*
        QuadCoeff(1)))];
end
```

D.2.6 InterpolatePut.m

```
yValue = log(StockPrice);
LowNode = floor((yValue-ymin)/Delta_y)+1;
HiNode = LowNode+1;
%
if StockPrice <= PutOEB(length(PutOEB(:,2)),2)
    PutPrice = max(Strike-StockPrice,0);
elseif StockVector(LowNode)<=PutOEB(length(PutOEB(:,2)),2)
    MatrixX = [(StockVector(HiNode))^2,StockVector(HiNode),1;(StockVector(HiNode+1))^2,StockVector(HiNode
        +1),1;(StockVector(HiNode+2))^2,StockVector(HiNode+2),1];
    VectorY = [OldPutVector(HiNode);OldPutVector(HiNode+1);OldPutVector(HiNode+2)];
    QuadCoeff = MatrixX\VectorY;
    PutPrice = QuadCoeff'*[StockPrice^2;StockPrice;1];
elseif StockVector(LowNode-1)<=PutOEB(length(PutOEB(:,2)),2)
    MatrixX = [(StockVector(LowNode))^2,StockVector(LowNode),1;(StockVector(HiNode))^2,StockVector(HiNode)
        ,1;(StockVector(HiNode+1))^2,StockVector(HiNode+1),1];
    VectorY = [OldPutVector(LowNode);OldPutVector(HiNode);OldPutVector(HiNode+1)];
    QuadCoeff = MatrixX\VectorY;
    PutPrice = QuadCoeff'*[StockPrice^2;StockPrice;1];
else
    MatrixX = [(StockVector(LowNode-1))^2,StockVector(LowNode-1),1;(StockVector(LowNode))^2,StockVector(
        LowNode),1;(StockVector(HiNode))^2,StockVector(HiNode),1];
```

```
    VectorY = [OldPutVector(LowNode-1);OldPutVector(LowNode);OldPutVector(HiNode)];
    QuadCoeff = MatrixX\VectorY;
    PutPrice =  QuadCoeff'*[StockPrice^2;StockPrice;1];
    %
    MatrixX = [(StockVector(LowNode))^2,StockVector(LowNode),1;(StockVector(HiNode))^2,StockVector(HiNode)
        ,1;(StockVector(HiNode+1))^2,StockVector(HiNode+1),1];
    VectorY = [OldPutVector(LowNode);OldPutVector(HiNode);OldPutVector(HiNode+1)];
    QuadCoeff = MatrixX\VectorY;
    PutPrice = 0.5*PutPrice+0.5*QuadCoeff'*[StockPrice^2;StockPrice;1];
end
```

D.2.7 PerpPutOEB

```
function Boundary=PerpPutOEB(Strike,SpotRate,divyield,SigSq)
% Function to calculate the critical stock price
% (i.e. Optimal Exercise Boundary)
% of a perpetual put option.
TempVarOne = SpotRate-divyield-0.5*SigSq;
TempVarTwo = sqrt(TempVarOne^2+2*SpotRate*SigSq);
Root = (-TempVarOne-TempVarTwo)/SigSq;
Boundary = Root*Strike/(Root-1);
```

D.3 Code for VBS American Call $C^{\mathcal{V}}$

D.3.1 AmCallVBS.m

```
% Orthogonalised Explicit Finite Difference scheme
% for a correlated GBM stock / Vasicek short rate model.
%
% Aims:
% 1.  To price an American Call option
%     at various spot rates to expiry and
%     at various stock levels , at one and
%     three years to option expiry;
%
% 2.  To establish sensitivities of said prices
%     to short rate and stock price levels ;
%
% 3.  To establish the location of the OEB.
%
% ********************************************************************
%
% Clear the current workspace
%
clear
%
% Accept Model Parameters
%
Horizon = 3;
alpha = 1/15;
theta = 0.09;
VolStock = 0.2;
VolRate = 0.02;
divyield = 0.03;
chi = 0.25;
Strike = 100;
%
% Accept Domain Limits
%
Smin = 40;
Smax = 330;
rmin = 0;
rmax = 0.2;
%
% Set Grid Mesh
```

```
%
StepsPerMonth = 12;
%
% Set Estimation Intervals
%
StockBoundaryEstimationStep = 0.125;
StockBoundaryMaximumMargin = 0.05;
%
% Points at which to extract values of interest
%
SpotRatesOfInterest    = [0.03,0.04,0.05,0.06,0.07,0.08,0.09,0.10,0.11,0.12,0.13,0.14,0.15]';
StocksOfInterest  = [50,60,70,80,90,100,110,120,130,140,150,160,170,180,190,200] ';
%
SpotRates = length(SpotRatesOfInterest);
Stocks = length(StocksOfInterest);
%
%*************************************************************************
%
disp('Calculating_Working_Parameters')
% Calculate Corresponding Volatilities , Drifts and and StepSizes
%
VolOne = VolStock * VolRate * sqrt(2*(1+chi));
VolTwo = VolStock * VolRate * sqrt(2*(1-chi));
%
DriftConstOne = VolStock*alpha*theta - VolRate*divyield - VolRate*VolStock*VolStock/2;
DriftConstTwo = -VolStock*alpha*theta '- VolRate*divyield - VolRate*VolStock*VolStock/2;
%
DriftCoeffOne = VolRate - VolStock*alpha;
DriftCoeffTwo = VolRate + VolStock*alpha;
%
TimeSteps = ceil(Horizon*12)*StepsPerMonth;
Delta_t = Horizon / TimeSteps;
%
DeltaOne = VolOne*sqrt(3*Delta_t);
DeltaTwo = VolTwo*sqrt(3*Delta_t);
%
%*************************************************************************
%
% Determine Limits of Orthogonal Vectors, Number of Orthogonal Steps,
%       and initialise vectors of Orthogonal Variables
%
ymin = log(Smin);
ymax = log(Smax);
%
MinOneConcern = VolRate*ymin + VolStock*rmin;
OneConcernSteps = ceil((VolRate*ymax + VolStock*rmax - MinOneConcern)/DeltaOne);
MaxOneConcern = MinOneConcern + OneConcernSteps*DeltaOne;
%
MinTwoConcern = VolRate*ymin - VolStock*rmax;
TwoConcernSteps = ceil((VolRate*ymax - VolStock*rmin - MinTwoConcern)/DeltaTwo);
MaxTwoConcern = MinTwoConcern + TwoConcernSteps*DeltaTwo;
%
MinOneCalc = MinOneConcern - TimeSteps * DeltaOne;
MaxOneCalc = MaxOneConcern + TimeSteps * DeltaOne;
MinTwoCalc = MinTwoConcern - TimeSteps * DeltaTwo;
MaxTwoCalc = MaxTwoConcern + TimeSteps * DeltaTwo;
%
OneCalcSteps = OneConcernSteps + 2 * TimeSteps;
TwoCalcSteps = TwoConcernSteps + 2 * TimeSteps;
%
OneConcernNodes = OneConcernSteps + 1;
TwoConcernNodes = TwoConcernSteps + 1;
OneCalcNodes = OneCalcSteps + 1;
TwoCalcNodes = TwoCalcSteps + 1;
%
OneValues = zeros(OneCalcNodes,1);
```

```
TwoValues = zeros(TwoCalcNodes,1);
%
for i = 1 : OneCalcNodes
    OneValues(i) = MinOneCalc + (i-1) * DeltaOne;
end
for i = 1 : TwoCalcNodes
    TwoValues(i) = MinTwoCalc + (i-1) * DeltaTwo;
end
%
% ************************************************************
%
% Populate Matrices containing Stock, Intrinsic , Short Rate and Call Values.
%
RateMatrix = zeros(OneCalcNodes,TwoCalcNodes);
StockMatrix = zeros(OneCalcNodes,TwoCalcNodes);
IntrinsicMatrix = zeros(OneCalcNodes,TwoCalcNodes);
%
for i = 1 : OneCalcNodes
    for j = 1 : TwoCalcNodes
        StockMatrix(i,j) = exp((OneValues(i)+TwoValues(j))/2/VolRate);
        RateMatrix(i,j)  = (OneValues(i)-TwoValues(j))/2/VolStock;
        IntrinsicMatrix(i,j) = max(StockMatrix(i,j)-Strike,0);
    end
end
%
OldCallMatrix = IntrinsicMatrix;
NewCallMatrix = IntrinsicMatrix;
%
% ************************************************************
%
% Create and populate vectors and values used in OEB estimation
%
VectorNodes = ceil((Smax*(1-StockBoundaryMaximumMargin)-Strike)/StockBoundaryEstimationStep)+1;
StockVector = ones(VectorNodes,1);
IntrinsicVector = StockVector;
CallVector = StockVector;
%
for i = 1 : VectorNodes
    StockVector(i) = Strike + (i-1) * StockBoundaryEstimationStep;
end
%
BoundaryVector = zeros(1,SpotRates);
%
CallOEB = [0,SpotRatesOfInterest];
CallOEB = [CallOEB;CallOEB];
for i = 1 : SpotRates
    CallOEB(2,i+1) = max( SpotRatesOfInterest(i)/divyield , 1) * Strike;
end
%
% ************************************************************
%
disp('Calculating Probabilities')
% Populate Matrices of Conditional Movement Probabilities.
%
UpLeft = zeros(OneCalcNodes,TwoCalcNodes);
UpFlat = zeros(OneCalcNodes,TwoCalcNodes);
UpRight = zeros(OneCalcNodes,TwoCalcNodes);
FlatLeft = zeros(OneCalcNodes,TwoCalcNodes);
FlatFlat = zeros(OneCalcNodes,TwoCalcNodes);
FlatRight = zeros(OneCalcNodes,TwoCalcNodes);
DownLeft = zeros(OneCalcNodes,TwoCalcNodes);
DownFlat = zeros(OneCalcNodes,TwoCalcNodes);
DownRight = zeros(OneCalcNodes,TwoCalcNodes);
%

%
```

```
for i = 1 : OneCalcNodes
    for j = 1 : TwoCalcNodes
        %
        OneExpChange = (DriftConstOne + DriftCoeffOne * RateMatrix(i,j))*Delta_t/DeltaOne;
        TwoExpChange = (DriftConstTwo + DriftCoeffTwo * RateMatrix(i,j))*Delta_t/DeltaTwo;
        %
        OEC = OneExpChange;
        TEC = TwoExpChange;
        %
        UpProb = 0.5*(1/3 - OEC + OEC^2);
        FlatProb = 2/3 - OEC^2;
        DownProb = 0.5*(1/3 + OEC + OEC^2);
        %
        ProbLeft = 0.5*(1/3 - TEC + TEC^2);
        ProbFlat = 2/3 - TEC^2;
        ProbRight = 0.5*(1/3 + TEC + TEC^2);
        %
        UpLeft(i,j) = UpProb * ProbLeft;
        UpFlat(i,j) = UpProb * ProbFlat;
        UpRight(i,j) = UpProb * ProbRight;
        FlatLeft(i,j) = FlatProb * ProbLeft;
        FlatFlat(i,j) = FlatProb * ProbFlat;
        FlatRight(i,j) = FlatProb * ProbRight;
        DownLeft(i,j) = DownProb * ProbLeft;
        DownFlat(i,j) = DownProb * ProbFlat;
        DownRight(i,j) = DownProb * ProbRight;
        %
    end
end
%
% ********************************************************************
disp('Beginning Stepping Process...')
disp(' ')
%
StepsProcessed = 0;
for Month = 1 : 12
    for MonthlyStep = 1 : StepsPerMonth
        %
        for i = 2 + StepsProcessed : OneCalcNodes - 1 - StepsProcessed
            for j = 2 + StepsProcessed : TwoCalcNodes - 1 - StepsProcessed
                NewCallMatrix(i,j) = (UpLeft(i,j)*OldCallMatrix(i-1,j-1) + UpFlat(i,j)*OldCallMatrix(i-1,j) +
                    UpRight(i,j)*OldCallMatrix(i-1,j+1) + FlatLeft(i,j)*OldCallMatrix(i,j-1) + FlatFlat(i,j)*
                    OldCallMatrix(i,j) + FlatRight(i,j)*OldCallMatrix(i,j+1) + DownLeft(i,j)*OldCallMatrix(i+1,j
                    -1) + DownFlat(i,j)*OldCallMatrix(i+1,j) + DownRight(i,j)*OldCallMatrix(i+1,j+1))/(1+
                    RateMatrix(i,j)*Delta_t);
                NewCallMatrix(i,j) = max(NewCallMatrix(i,j),IntrinsicMatrix(i,j));
            end
        end
        %
        OldCallMatrix = NewCallMatrix;
        %
        StepsProcessed = StepsProcessed+1;
        TimeToExpiry = StepsProcessed * Delta_t;
        TimeNow = clock;
        Hours = num2str(TimeNow(4));
        if TimeNow(5) < 10
            Minutes = ['0',num2str(TimeNow(5))];
        else
            Minutes = num2str(TimeNow(5));
        end
        if TimeNow(6) < 10
            Seconds = ['0',num2str(floor(TimeNow(6)))];
        else
            Seconds = num2str(floor(TimeNow(6)));
        end
        disp(['Steps Processed: ',num2str(StepsProcessed),' of ',num2str(StepsPerMonth*Horizon*12),' (at ',
```

```
            Hours,'h',Minutes,':',Seconds,').__TimeToExpiry_=_',num2str(TimeToExpiry),'.__Horizon_=_',
            num2str(Horizon)])
    end
    %
    disp(['Locating_OEB_for_t_=_',num2str(TimeToExpiry)])
    disp('_')
    LocateVBSCallOEB
    %
end
%
%**********************************************************************
%
disp('Extracting_Values_of_Interest_at_t_=_1')
% Extract Values of Interest
%
ShortRatesOfInterest = SpotToShort(alpha,theta,VolRate,TimeToExpiry,SpotRatesOfInterest);
%
OneCallPrice = zeros(Stocks,SpotRates);
OneCallPrice = [StocksOfInterest,OneCallPrice];
OneCallPrice = [0,SpotRatesOfInterest;OneCallPrice];
%
OneCallStockDelta = OneCallPrice;
OneCallRateDelta = OneCallPrice;
%
CallNodesOfInterest = zeros(4,4);
%
for i = 1 : Stocks
    %
    for j = 1 : SpotRates
        %
        % ********** PRICE AND SENSITIVITY APPROXIMATIONS ***********
        %
        WantedOne = VolRate * log(StocksOfInterest(i)) + VolStock * ShortRatesOfInterest(j);
        WantedOnes(i+1,j+1) = WantedOne;
        WantedTwo = VolRate * log(StocksOfInterest(i)) - VolStock * ShortRatesOfInterest(j);
        WantedTwos(i+1,j+1) = WantedTwo;
        %
        LOI = floor((WantedOne-MinOneCalc)/DeltaOne)+1;
        UOI = LOI + 1;
        LTI = floor((WantedTwo - MinTwoCalc)/DeltaTwo)+1;
        UTI = LTI + 1;
        %
        OnePreMult = 0.5*([(OneValues(LOI-1))^2,OneValues(LOI -1),1;(OneValues(LOI))^2,OneValues(LOI),1;(
            OneValues(LOI+1))^2,OneValues(LOI+1),1]^-1) * [1,0,0,0;0,1,0,0;0,0,1,0];
        OnePreMult = OnePreMult + 0.5*([(OneValues(UOI-1))^2,OneValues(UOI-1),1;(OneValues(UOI))^2,
            OneValues(UOI),1;(OneValues(UOI+1))^2,OneValues(UOI+1),1]^-1) * [0,1,0,0;0,0,1,0;0,0,0,1];
        TwoPreMult = 0.5*([(TwoValues(LTI-1))^2,TwoValues(LTI-1),1;(TwoValues(LTI))^2,TwoValues(LTI),1;(
            TwoValues(LTI+1))^2,TwoValues(LTI+1),1]^-1) * [1,0,0,0;0,1,0,0;0,0,1,0];
        TwoPreMult = TwoPreMult + 0.5*([(TwoValues(UTI-1))^2,TwoValues(UTI-1),1;(TwoValues(UTI))^2,
            TwoValues(UTI),1;(TwoValues(UTI+1))^2,TwoValues(UTI+1),1]^-1) * [0,1,0,0;0,0,1,0;0,0,0,1];
        %
        CallSubMatrix = [NewCallMatrix(LOI-1,LTI-1),NewCallMatrix(LOI-1,LTI),NewCallMatrix(LOI-1,UTI),
            NewCallMatrix(LOI-1,UTI+1);NewCallMatrix(LOI,LTI-1),NewCallMatrix(LOI,LTI),NewCallMatrix(
            LOI,UTI),NewCallMatrix(LOI,UTI+1);NewCallMatrix(UOI,LTI-1),NewCallMatrix(UOI,LTI),
            NewCallMatrix(UOI,UTI),NewCallMatrix(UOI,UTI+1);NewCallMatrix(UOI+1,LTI-1),NewCallMatrix(
            UOI+1,LTI),NewCallMatrix(UOI+1,UTI),NewCallMatrix(UOI+1,UTI+1)];
        %
        OneCallPrice(i+1,j+1) = [WantedOne^2,WantedOne,1]*OnePreMult*CallSubMatrix*(TwoPreMult')*[
            WantedTwo^2;WantedTwo;1];
        OneCallStockDelta(i+1,j+1) = VolRate/StocksOfInterest(i)*([2*WantedOne,1,0]*OnePreMult*CallSubMatrix
            *TwoPreMult'*[WantedTwo^2;WantedTwo;1] + [2*WantedTwo,1,0]*TwoPreMult*CallSubMatrix'*
            OnePreMult'*[WantedOne^2;WantedOne;1]);
        OneCallRateDelta(i+1,j+1) = VolStock * ([2*WantedOne,1,0]*OnePreMult*CallSubMatrix*TwoPreMult'*[
            WantedTwo^2;WantedTwo;1] - [2*WantedTwo,1,0]*TwoPreMult*CallSubMatrix'*OnePreMult'*[
            WantedOne^2;WantedOne;1]);
        %
```

```
    end
end
%
% ****************************************
%
for Month = 13 : 36
    for MonthlyStep = 1 : StepsPerMonth
        %
        for i = 2 + StepsProcessed : OneCalcNodes - 1 - StepsProcessed
            for j = 2 + StepsProcessed : TwoCalcNodes - 1 - StepsProcessed
                NewCallMatrix(i,j) = (UpLeft(i,j)*OldCallMatrix(i-1,j-1) + UpFlat(i,j)*OldCallMatrix(i-1,j) +
                    UpRight(i,j)*OldCallMatrix(i-1,j+1) + FlatLeft(i,j)*OldCallMatrix(i,j-1) + FlatFlat(i,j)*
                    OldCallMatrix(i,j) + FlatRight(i,j)*OldCallMatrix(i,j+1) + DownLeft(i,j)*OldCallMatrix(i+1,j
                    -1) + DownFlat(i,j)*OldCallMatrix(i+1,j) + DownRight(i,j)*OldCallMatrix(i+1,j+1))/(1+
                    RateMatrix(i,j)*Delta_t);
                NewCallMatrix(i,j) = max(NewCallMatrix(i,j),IntrinsicMatrix(i,j));
            end
        end
        %
        OldCallMatrix = NewCallMatrix;
        %
        StepsProcessed = StepsProcessed+1;
        TimeToExpiry = StepsProcessed * Delta_t;
        TimeNow = clock;
        Hours = num2str(TimeNow(4));
        if TimeNow(5) < 10
            Minutes = ['0',num2str(TimeNow(5))];
        else
            Minutes = num2str(TimeNow(5));
        end
        if TimeNow(6) < 10
            Seconds = ['0',num2str(floor(TimeNow(6)))];
        else
            Seconds = num2str(floor(TimeNow(6)));
        end
        disp(['Steps_Processed:__',num2str(StepsProcessed),'_of_',num2str(StepsPerMonth*Horizon*12),'_(at_',
            Hours,'h',Minutes,':',Seconds,')__TimeToExpiry_=_',num2str(TimeToExpiry),'__Horizon_=_',
            num2str(Horizon)])
    end
    %
    disp(['Locating_OEB_for_t_=_',num2str(TimeToExpiry)])
    disp('_')
    LocateVBSCallOEB
    %
end
%
%*********************************************************************
%
disp('Extracting_Values_of_Interest_at_t_=_3')
% Extract Values of Interest
%
ShortRatesOfInterest = SpotToShort(alpha,theta,VolRate,TimeToExpiry,SpotRatesOfInterest);
%
ThreeCallPrice = zeros(Stocks,SpotRates);
ThreeCallPrice = [StocksOfInterest,ThreeCallPrice];
ThreeCallPrice = [0,SpotRatesOfInterest;ThreeCallPrice];
%
ThreeCallStockDelta = ThreeCallPrice;
ThreeCallRateDelta = ThreeCallPrice;
%
%
for i = 1 : Stocks
    %
    for j = 1 : SpotRates
        %
        % ********** PRICE AND SENSITIVITY APPROXIMATIONS ***********
```

```
        %
        WantedOne = VolRate * log(StocksOfInterest(i)) + VolStock * ShortRatesOfInterest(j);
        WantedOnes(i+1,j+1) = WantedOne;
        WantedTwo = VolRate * log(StocksOfInterest(i)) - VolStock * ShortRatesOfInterest(j);
        WantedTwos(i+1,j+1) = WantedTwo;
        %
        LOI = floor((WantedOne-MinOneCalc)/DeltaOne)+1;
        UOI = LOI + 1;
        LTI = floor((WantedTwo - MinTwoCalc)/DeltaTwo)+1;
        UTI = LTI + 1;
        %
        OnePreMult = 0.5*([(OneValues(LOI-1))^2,OneValues(LOI-1),1;(OneValues(LOI))^2,OneValues(LOI),1;(
            OneValues(LOI+1))^2,OneValues(LOI+1),1]^-1) * [1,0,0,0;0,1,0,0;0,0,1,0];
        OnePreMult = OnePreMult + 0.5*([(OneValues(UOI-1))^2,OneValues(UOI-1),1;(OneValues(UOI))^2,
            OneValues(UOI),1;(OneValues(UOI+1))^2,OneValues(UOI+1),1]^-1) * [0,1,0,0;0,0,1,0;0,0,0,1];
        TwoPreMult = 0.5*([(TwoValues(LTI-1))^2,TwoValues(LTI-1),1;(TwoValues(LTI))^2,TwoValues(LTI),1;(
            TwoValues(LTI+1))^2,TwoValues(LTI+1),1]^-1) * [1,0,0,0;0,1,0,0;0,0,1,0];
        TwoPreMult = TwoPreMult + 0.5*([(TwoValues(UTI-1))^2,TwoValues(UTI-1),1;(TwoValues(UTI))^2,
            TwoValues(UTI),1;(TwoValues(UTI+1))^2,TwoValues(UTI+1),1]^-1) * [0,1,0,0;0,0,1,0;0,0,0,1];
        %
        CallSubMatrix = [NewCallMatrix(LOI-1,LTI-1),NewCallMatrix(LOI-1,LTI),NewCallMatrix(LOI-1,UTI),
            NewCallMatrix(LOI-1,UTI+1);NewCallMatrix(LOI,LTI-1),NewCallMatrix(LOI,LTI),NewCallMatrix(
            LOI,UTI),NewCallMatrix(LOI,UTI+1);NewCallMatrix(UOI,LTI-1),NewCallMatrix(UOI,LTI),
            NewCallMatrix(UOI,UTI),NewCallMatrix(UOI,UTI+1);NewCallMatrix(UOI+1,LTI-1),NewCallMatrix(
            UOI+1,LTI),NewCallMatrix(UOI+1,UTI),NewCallMatrix(UOI+1,UTI+1)];
        %
        ThreeCallPrice(i+1,j+1) = [WantedOne^2,WantedOne,1]*OnePreMult*CallSubMatrix*(TwoPreMult')*[
            WantedTwo^2;WantedTwo;1];
        ThreeCallStockDelta(i+1,j+1) = VolRate/StocksOfInterest(i)*([2*WantedOne,1,0]*OnePreMult*
            CallSubMatrix*TwoPreMult'*[WantedTwo^2;WantedTwo;1] + [2*WantedTwo,1,0]*TwoPreMult*
            CallSubMatrix'*OnePreMult'*[WantedOne^2;WantedOne;1]);
        ThreeCallRateDelta(i+1,j+1) = VolStock * ([2*WantedOne,1,0]*OnePreMult*CallSubMatrix*TwoPreMult'*[
            WantedTwo^2;WantedTwo;1] - [2*WantedTwo,1,0]*TwoPreMult*CallSubMatrix'*OnePreMult'*[
            WantedOne^2;WantedOne;1]);
        %
        %
    end
end
%
```

D.3.2 LocateVBSCallOEB.m

```
for i = 1 : SpotRates
    %
    ImpliedShortRate = SpotToShort(alpha,theta,VolRate,TimeToExpiry,SpotRatesOfInterest(i));
    %
    for j = 1 : VectorNodes
        %
        WantedOne = VolRate * log(StockVector(j)) + VolStock * ImpliedShortRate;
        WantedTwo = VolRate * log(StockVector(j)) - VolStock * ImpliedShortRate;
        %
        LOI = floor((WantedOne-MinOneCalc)/DeltaOne)+1;
        UOI = LOI + 1;
        LTI = floor((WantedTwo - MinTwoCalc)/DeltaTwo)+1;
        UTI = LTI + 1;
        %
        OneProp = (WantedOne - OneValues(LOI))/DeltaOne;
        TwoProp = (WantedTwo - TwoValues(LTI))/DeltaTwo;
        %
        CallVector(j) = (1-OneProp)*( (1-TwoProp)*NewCallMatrix(LOI,LTI) + TwoProp*NewCallMatrix(LOI,
            UTI) ) + OneProp * ( (1-TwoProp)*NewCallMatrix(UOI,LTI) + TwoProp*NewCallMatrix(UOI,UTI));
        IntrinsicVector(j) = (1-OneProp)*( (1-TwoProp)*IntrinsicMatrix(LOI,LTI) + TwoProp*IntrinsicMatrix(
            LOI,UTI) ) + OneProp * ( (1-TwoProp)*IntrinsicMatrix(UOI,LTI) + TwoProp*IntrinsicMatrix(UOI,
            UTI));
        %
    end
```

```
    %
    ExIndex = 0;
    Continue = 1;
    while Continue == 1
        ExIndex = ExIndex + 1;
        if abs(CallVector(ExIndex)-IntrinsicVector(ExIndex)) > 0.001
            Continue = 0;
        elseif ExIndex == VectorNodes
            Continue = 0;
        end
    end

    Continue = 1;

    while Continue == 1
        ExIndex = ExIndex + 1;
        if (CallVector(ExIndex)-IntrinsicVector(ExIndex)) < 0.001
            Continue = 0;
        elseif ExIndex == VectorNodes
            Continue = 0;
        end
    end
    %
    if ExIndex == VectorNodes
        BoundaryVector(i) = -100;
    else
        BoundaryVector(i) = StockVector(ExIndex);
        %
        QuadCoeff = ([(StockVector(ExIndex-3))^2,StockVector(ExIndex-3),1;(StockVector(ExIndex-2))^2,
            StockVector(ExIndex-2),1;(StockVector(ExIndex-1))^2,StockVector(ExIndex-1),1]^-1)*[CallVector(
            ExIndex-3);CallVector(ExIndex-2);CallVector(ExIndex-1)];
        %
        Determinant = (QuadCoeff(2)-1)^2- 4*QuadCoeff(1)*(QuadCoeff(3)+Strike);
        %
        if Determinant > 0
            BoundaryVector(i) = min((1-QuadCoeff(2)-sqrt(Determinant))/(2*QuadCoeff(1)),BoundaryVector(i));
        end
        %
    end
    %
    %disp(['BoundaryVector(i) = ',num2str(BoundaryVector(i))])
    %disp('paused')
    %pause
    %disp('unpaused')
    %
end
%
CallOEB = [CallOEB;TimeToExpiry,BoundaryVector];
```

D.4 Code for VBS American Put $I^{\mathcal{V}}$

D.4.1 AmPutVBS.m

```
% Orthogonalised Explicit Finite Difference scheme
% for a correlated GBM stock / Vasicek short rate model.
%
% Aims:
% 1.  To price an American Put option
%     at various spot rates to expiry and
%     at various stock levels , at one and
%     three years to option expiry;
%
% 2.  To establish sensitivities of said prices
%     to short rate and stock price levels ;
%
```

```
% 3.  To establish the location of the OEB.
%
% ************************************************************************
%
disp('Beginning_Calculation')
% Clear the current workspace
%
clear
%
% Accept Model Parameters
%
Horizon = 3;
alpha = 1/15;
theta = 0.09;
VolStock = 0.2;
VolRate = 0.02;
divyield = 0.03;
chi = 0.25;
Strike = 100;
%
% Accept Domain Limits
%
Smin = 25;
Smax = 250;
rmin = 0;
rmax = 0.2;
%
% Set Grid Mesh
%
StepsPerMonth = 12;
%
% Set Estimation Intervals
%
StockBoundaryEstimationStep = 0.125;
StockBoundaryMaximumMargin = 0.05;
%
% Points at which to extract values of interest
%
SpotRatesOfInterest    = [0.03,0.04,0.05,0.06,0.07,0.08,0.09,0.10,0.11,0.12,0.13,0.14,0.15];
StocksOfInterest  = [50,60,70,80,90,100,110,120,130,140,150,160,170,180,190,200]';
%
SpotRates = length(SpotRatesOfInterest);
Stocks = length(StocksOfInterest);
%
%************************************************************************
%
disp('Calculating_Working_Parameters')
% Calculate Corresponding Volatilities , Drifts and and StepSizes
%
VolOne = VolStock * VolRate * sqrt(2*(1+chi));
VolTwo = VolStock * VolRate * sqrt(2*(1-chi));
%
DriftConstOne = VolStock*alpha*theta - VolRate*divyield - VolRate*VolStock*VolStock/2;
DriftConstTwo = - VolStock*alpha*theta - VolRate*divyield  - VolRate*VolStock*VolStock/2;
%
DriftCoeffOne = VolRate - VolStock*alpha;
DriftCoeffTwo = VolRate + VolStock*alpha;
%
TimeSteps = ceil(Horizon*12)*StepsPerMonth;
Delta_t = Horizon / TimeSteps;
%
DeltaOne = VolOne*sqrt(3*Delta_t);
DeltaTwo = VolTwo*sqrt(3*Delta_t);
%
%************************************************************************
%
```

```
% Determine Limits of Orthogonal Vectors, Number of Orthogonal Steps,
%       and initialise  vectors of Orthogonal Variables
%
ymin = log(Smin);
ymax = log(Smax);
%
MinOneConcern = VolRate*ymin + VolStock*rmin;
OneConcernSteps = ceil((VolRate*ymax + VolStock*rmax - MinOneConcern)/DeltaOne);
MaxOneConcern = MinOneConcern + OneConcernSteps*DeltaOne;
%
MinTwoConcern = VolRate*ymin - VolStock*rmax;
TwoConcernSteps = ceil((VolRate*ymax - VolStock*rmin - MinTwoConcern)/DeltaTwo);
MaxTwoConcern = MinTwoConcern + TwoConcernSteps*DeltaTwo;
%
MinOneCalc = MinOneConcern - TimeSteps * DeltaOne;
MaxOneCalc = MaxOneConcern + TimeSteps * DeltaOne;
MinTwoCalc = MinTwoConcern - TimeSteps * DeltaTwo;
MaxTwoCalc = MaxTwoConcern + TimeSteps * DeltaTwo;
%
OneCalcSteps = OneConcernSteps + 2 * TimeSteps;
TwoCalcSteps = TwoConcernSteps + 2 * TimeSteps;
%
OneConcernNodes = OneConcernSteps + 1;
TwoConcernNodes = TwoConcernSteps + 1;
OneCalcNodes = OneCalcSteps + 1;
TwoCalcNodes = TwoCalcSteps + 1;
%
OneValues = zeros(OneCalcNodes,1);
TwoValues = zeros(TwoCalcNodes,1);
%
for i = 1 : OneCalcNodes
    OneValues(i) = MinOneCalc + (i-1) * DeltaOne;
end
for i = 1 : TwoCalcNodes
    TwoValues(i) = MinTwoCalc + (i-1) * DeltaTwo;
end
%
% ************************************************************
%
% Populate Matrices containing Stock, Intrinsic , Short Rate and Put Values.
%
RateMatrix = zeros(OneCalcNodes,TwoCalcNodes);
StockMatrix = zeros(OneCalcNodes,TwoCalcNodes);
IntrinsicMatrix = zeros(OneCalcNodes,TwoCalcNodes);
%
for i = 1 : OneCalcNodes
    for j = 1 : TwoCalcNodes
        StockMatrix(i,j) = exp((OneValues(i)+TwoValues(j))/2/VolRate);
        RateMatrix(i,j)  = (OneValues(i)-TwoValues(j))/2/VolStock;
        IntrinsicMatrix(i,j) = max(Strike-StockMatrix(i,j),0);
    end
end
%
OldPutMatrix = IntrinsicMatrix;
NewPutMatrix = IntrinsicMatrix;
%
% ************************************************************
%
% Create and populate vectors and values used in OEB estimation
%
VectorNodes = ceil((Strike-Smin*(1+StockBoundaryMaximumMargin))/StockBoundaryEstimationStep)+1;
StockVector = ones(VectorNodes,1);
IntrinsicVector = StockVector;
PutVector = StockVector;
%
for i = 1 : VectorNodes
```

```
    StockVector(VectorNodes+1-i) = Strike - (i-1) * StockBoundaryEstimationStep;
end
%
BoundaryVector = zeros(1,SpotRates);
%
PutOEB = [0,SpotRatesOfInterest];
PutOEB = [PutOEB;PutOEB];
for i = 1 : SpotRates
    PutOEB(2,i+1) = min( SpotRatesOfInterest(i)/divyield , 1) * Strike;
end
%
% ****************************************************************
%
disp('Calculating Probabilities')
% Populate Matrices of Conditional Movement Probabilities.
%
UpLeft = zeros(OneCalcNodes,TwoCalcNodes);
UpFlat = zeros(OneCalcNodes,TwoCalcNodes);
UpRight = zeros(OneCalcNodes,TwoCalcNodes);
FlatLeft = zeros(OneCalcNodes,TwoCalcNodes);
FlatFlat = zeros(OneCalcNodes,TwoCalcNodes);
FlatRight = zeros(OneCalcNodes,TwoCalcNodes);
DownLeft = zeros(OneCalcNodes,TwoCalcNodes);
DownFlat = zeros(OneCalcNodes,TwoCalcNodes);
DownRight = zeros(OneCalcNodes,TwoCalcNodes);
%

%
for i = 1 : OneCalcNodes
    for j = 1 : TwoCalcNodes
        %
        OneExpChange = (DriftConstOne + DriftCoeffOne * RateMatrix(i,j))*Delta_t/DeltaOne;
        TwoExpChange = (DriftConstTwo + DriftCoeffTwo * RateMatrix(i,j))*Delta_t/DeltaTwo;
        %
        OEC = OneExpChange;
        TEC = TwoExpChange;
        %
        UpProb = 0.5*(1/3 - OEC + OEC^2);
        FlatProb = 2/3 - OEC^2;
        DownProb = 0.5*(1/3 + OEC + OEC^2);
        %
        ProbLeft = 0.5*(1/3 - TEC + TEC^2);
        ProbFlat = 2/3 - TEC^2;
        ProbRight = 0.5*(1/3 + TEC + TEC^2);
        %
        UpLeft(i,j) = UpProb * ProbLeft;
        UpFlat(i,j) = UpProb * ProbFlat;
        UpRight(i,j) = UpProb * ProbRight;
        FlatLeft(i,j) = FlatProb * ProbLeft;
        FlatFlat(i,j) = FlatProb * ProbFlat;
        FlatRight(i,j) = FlatProb * ProbRight;
        DownLeft(i,j) = DownProb * ProbLeft;
        DownFlat(i,j) = DownProb * ProbFlat;
        DownRight(i,j) = DownProb * ProbRight;
        %
    end
end
%
% ****************************************************************
disp('Beginning Stepping Process...')
disp(' ')
%
StepsProcessed = 0;
for Month = 1 : 12
    for MonthlyStep = 1 : StepsPerMonth
        %
```

```
        for i = 2 + StepsProcessed : OneCalcNodes - 1 - StepsProcessed
            for j = 2 + StepsProcessed : TwoCalcNodes - 1 - StepsProcessed
                NewPutMatrix(i,j) = (UpLeft(i,j)*OldPutMatrix(i-1,j-1) + UpFlat(i,j)*OldPutMatrix(i-1,j) +
                    UpRight(i,j)*OldPutMatrix(i-1,j+1) + FlatLeft(i,j)*OldPutMatrix(i,j-1) + FlatFlat(i,j)*
                    OldPutMatrix(i,j) + FlatRight(i,j)*OldPutMatrix(i,j+1) + DownLeft(i,j)*OldPutMatrix(i+1,j
                    -1) + DownFlat(i,j)*OldPutMatrix(i+1,j) + DownRight(i,j)*OldPutMatrix(i+1,j+1))/(1+
                    RateMatrix(i,j)*Delta_t);
                NewPutMatrix(i,j) = max(NewPutMatrix(i,j),IntrinsicMatrix(i,j));
            end
        end
        %
        OldPutMatrix = NewPutMatrix;
        %
        StepsProcessed = StepsProcessed+1;
        TimeToExpiry = StepsProcessed * Delta_t;
        TimeNow = clock;
        Hours = num2str(TimeNow(4));
        if TimeNow(5) < 10
            Minutes = ['0',num2str(TimeNow(5))];
        else
            Minutes = num2str(TimeNow(5));
        end
        if TimeNow(6) < 10
            Seconds = ['0',num2str(floor(TimeNow(6)))];
        else
            Seconds = num2str(floor(TimeNow(6)));
        end
        disp(['Steps_Processed:__',num2str(StepsProcessed),'_of_',num2str(StepsPerMonth*Horizon*12),'_(at_',
            Hours,'h',Minutes,':',Seconds,')._TimeToExpiry_=_',num2str(TimeToExpiry),'._Horizon_=_',
            num2str(Horizon)])
    end
    %
    disp(['Locating_OEB_for_t_=_',num2str(TimeToExpiry)])
    disp('_')
    LocateVBSPutOEB
    %
end
%
%*************************************************************************
%
disp('Extracting_Values_of_Interest_at_t_=_1')
% Extract Values of Interest
%
ShortRatesOfInterest = SpotToShort(alpha,theta,VolRate,TimeToExpiry,SpotRatesOfInterest);
%
OnePutPrice = zeros(Stocks,SpotRates);
OnePutPrice = [StocksOfInterest,OnePutPrice];
OnePutPrice = [0,SpotRatesOfInterest;OnePutPrice];
%
OnePutStockDelta = OnePutPrice;
OnePutRateDelta = OnePutPrice;
%
PutNodesOfInterest = zeros(4,4);
%
for i = 1 : Stocks
    %
    for j = 1 : SpotRates
        %
        % ********** PRICE AND SENSITIVITY APPROXIMATIONS **********
        %
        WantedOne = VolRate * log(StocksOfInterest(i)) + VolStock * ShortRatesOfInterest(j);
        WantedOnes(i+1,j+1) = WantedOne;
        WantedTwo = VolRate * log(StocksOfInterest(i)) - VolStock * ShortRatesOfInterest(j);
        WantedTwos(i+1,j+1) = WantedTwo;
        %
        LOI = floor((WantedOne-MinOneCalc)/DeltaOne)+1;
```

```
        UOI = LOI + 1;
        LTI = floor((WantedTwo - MinTwoCalc)/DeltaTwo)+1;
        UTI = LTI + 1;
        %
        OnePreMult = 0.5*([(OneValues(LOI-1))^2,OneValues(LOI-1),1;(OneValues(LOI))^2,OneValues(LOI),1;(
            OneValues(LOI+1))^2,OneValues(LOI+1),1]^-1) * [1,0,0,0;0,1,0,0;0,0,1,0];
        OnePreMult = OnePreMult + 0.5*([(OneValues(UOI-1))^2,OneValues(UOI-1),1;(OneValues(UOI))^2,
            OneValues(UOI),1;(OneValues(UOI+1))^2,OneValues(UOI+1),1]^-1) * [0,1,0,0;0,0,1,0;0,0,0,1];
        TwoPreMult = 0.5*([(TwoValues(LTI-1))^2,TwoValues(LTI-1),1;(TwoValues(LTI))^2,TwoValues(LTI),1;(
            TwoValues(LTI+1))^2,TwoValues(LTI+1),1]^-1) * [1,0,0,0;0,1,0,0;0,0,1,0];
        TwoPreMult = TwoPreMult + 0.5*([(TwoValues(UTI-1))^2,TwoValues(UTI-1),1;(TwoValues(UTI))^2,
            TwoValues(UTI),1;(TwoValues(UTI+1))^2,TwoValues(UTI+1),1]^-1) * [0,1,0,0;0,0,1,0;0,0,0,1];
        %
        PutSubMatrix = [NewPutMatrix(LOI-1,LTI-1),NewPutMatrix(LOI-1,LTI),NewPutMatrix(LOI-1,UTI),
            NewPutMatrix(LOI-1,UTI+1);NewPutMatrix(LOI,LTI-1),NewPutMatrix(LOI,LTI),NewPutMatrix(
            LOI,UTI),NewPutMatrix(LOI,UTI+1);NewPutMatrix(UOI,LTI-1),NewPutMatrix(UOI,LTI),
            NewPutMatrix(UOI,UTI),NewPutMatrix(UOI,UTI+1);NewPutMatrix(UOI+1,LTI-1),NewPutMatrix(
            UOI+1,LTI),NewPutMatrix(UOI+1,UTI),NewPutMatrix(UOI+1,UTI+1)];
        %
        OnePutPrice(i+1,j+1) = [WantedOne^2,WantedOne,1]*OnePreMult*PutSubMatrix*(TwoPreMult')*[
            WantedTwo^2;WantedTwo;1];
        OnePutStockDelta(i+1,j+1) = VolRate/StocksOfInterest(i)*([2*WantedOne,1,0]*OnePreMult*PutSubMatrix
            *TwoPreMult'*[WantedTwo^2;WantedTwo;1] + [2*WantedTwo,1,0]*TwoPreMult*PutSubMatrix'*
            OnePreMult'*[WantedOne^2;WantedOne;1]);
        OnePutRateDelta(i+1,j+1) = VolStock * ([2*WantedOne,1,0]*OnePreMult*PutSubMatrix*TwoPreMult'*[
            WantedTwo^2;WantedTwo;1] - [2*WantedTwo,1,0]*TwoPreMult*PutSubMatrix'*OnePreMult'*[
            WantedOne^2;WantedOne;1]);
        %
    end
end
%
% ****************************************
%
for Month = 13 : 36
    for MonthlyStep = 1 : StepsPerMonth
        %
        for i = 2 + StepsProcessed : OneCalcNodes - 1 - StepsProcessed
            for j = 2 + StepsProcessed : TwoCalcNodes - 1 - StepsProcessed
                NewPutMatrix(i,j) = (UpLeft(i,j)*OldPutMatrix(i-1,j-1) + UpFlat(i,j)*OldPutMatrix(i-1,j) +
                    UpRight(i,j)*OldPutMatrix(i-1,j+1) + FlatLeft(i,j)*OldPutMatrix(i,j-1) + FlatFlat(i,j)*
                    OldPutMatrix(i,j) + FlatRight(i,j)*OldPutMatrix(i,j+1) + DownLeft(i,j)*OldPutMatrix(i+1,j
                    -1) + DownFlat(i,j)*OldPutMatrix(i+1,j) + DownRight(i,j)*OldPutMatrix(i+1,j+1))/(1+
                    RateMatrix(i,j)*Delta_t);
                NewPutMatrix(i,j) = max(NewPutMatrix(i,j),IntrinsicMatrix(i,j));
            end
        end
        %
        OldPutMatrix = NewPutMatrix;
        %
        StepsProcessed = StepsProcessed+1;
        TimeToExpiry = StepsProcessed * Delta_t;
        TimeNow = clock;
        Hours = num2str(TimeNow(4));
        if TimeNow(5) < 10
            Minutes = ['0',num2str(TimeNow(5))];
        else
            Minutes = num2str(TimeNow(5));
        end
        if TimeNow(6) < 10
            Seconds = ['0',num2str(floor(TimeNow(6)))];
        else
            Seconds = num2str(floor(TimeNow(6)));
        end
        disp(['Steps_Processed:__',num2str(StepsProcessed),'_of_',num2str(StepsPerMonth*Horizon*12),'_(at_',
            Hours,'h',Minutes,':',Seconds,')__TimeToExpiry_=_',num2str(TimeToExpiry),'__Horizon_=_',
            num2str(Horizon)])
```

```
    end
    %
    disp(['Locating_OEB_for_t_=_',num2str(TimeToExpiry)])
    disp('_')
    LocateVBSPutOEB
    %
end
%
%*************************************************************************
%
disp('Extracting_Values_of_Interest_at_t_=_3')
% Extract Values of Interest
%
ShortRatesOfInterest = SpotToShort(alpha,theta,VolRate,TimeToExpiry,SpotRatesOfInterest);
%
ThreePutPrice = zeros(Stocks,SpotRates);
ThreePutPrice = [StocksOfInterest,ThreePutPrice];
ThreePutPrice = [0,SpotRatesOfInterest;ThreePutPrice];
%
ThreePutStockDelta = ThreePutPrice;
ThreePutRateDelta = ThreePutPrice;
%
%
for i = 1 : Stocks
    %
    for j = 1 : SpotRates
        %
        % ********** PRICE AND SENSITIVITY APPROXIMATIONS ************
        %
        WantedOne = VolRate * log(StocksOfInterest(i)) + VolStock * ShortRatesOfInterest(j);
        WantedOnes(i+1,j+1) = WantedOne;
        WantedTwo = VolRate * log(StocksOfInterest(i)) - VolStock * ShortRatesOfInterest(j);
        WantedTwos(i+1,j+1) = WantedTwo;
        %
        LOI = floor((WantedOne-MinOneCalc)/DeltaOne)+1;
        UOI = LOI + 1;
        LTI = floor((WantedTwo - MinTwoCalc)/DeltaTwo)+1;
        UTI = LTI + 1;
        %
        OnePreMult = 0.5*([(OneValues(LOI-1))^2,OneValues(LOI-1),1;(OneValues(LOI))^2,OneValues(LOI),1;(
            OneValues(LOI+1))^2,OneValues(LOI+1),1]^-1) * [1,0,0,0;0,1,0,0;0,0,1,0];
        OnePreMult = OnePreMult + 0.5*([(OneValues(UOI-1))^2,OneValues(UOI-1),1;(OneValues(UOI))^2,
            OneValues(UOI),1;(OneValues(UOI+1))^2,OneValues(UOI+1),1]^-1) * [0,1,0,0;0,0,1,0;0,0,0,1];
        TwoPreMult = 0.5*([(TwoValues(LTI-1))^2,TwoValues(LTI-1),1;(TwoValues(LTI))^2,TwoValues(LTI),1;(
            TwoValues(LTI+1))^2,TwoValues(LTI+1),1]^-1) * [1,0,0,0;0,1,0,0;0,0,1,0];
        TwoPreMult = TwoPreMult + 0.5*([(TwoValues(UTI-1))^2,TwoValues(UTI-1),1;(TwoValues(UTI))^2,
            TwoValues(UTI),1;(TwoValues(UTI+1))^2,TwoValues(UTI+1),1]^-1) * [0,1,0,0;0,0,1,0;0,0,0,1];
        %
        PutSubMatrix = [NewPutMatrix(LOI-1,LTI-1),NewPutMatrix(LOI-1,LTI),NewPutMatrix(LOI-1,UTI),
            NewPutMatrix(LOI-1,UTI+1);NewPutMatrix(LOI,LTI-1),NewPutMatrix(LOI,LTI),NewPutMatrix(
            LOI,UTI),NewPutMatrix(LOI,UTI+1);NewPutMatrix(UOI,LTI-1),NewPutMatrix(UOI,LTI),
            NewPutMatrix(UOI,UTI),NewPutMatrix(UOI,UTI+1);NewPutMatrix(UOI+1,LTI-1),NewPutMatrix(
            UOI+1,LTI),NewPutMatrix(UOI+1,UTI),NewPutMatrix(UOI+1,UTI+1)];
        %
        ThreePutPrice(i+1,j+1) = [WantedOne^2,WantedOne,1]*OnePreMult*PutSubMatrix*(TwoPreMult')*[
            WantedTwo^2;WantedTwo;1];
        ThreePutStockDelta(i+1,j+1) = VolRate/StocksOfInterest(i)*([2*WantedOne,1,0]*OnePreMult*
            PutSubMatrix*TwoPreMult'*[WantedTwo^2;WantedTwo;1] + [2*WantedTwo,1,0]*TwoPreMult*
            PutSubMatrix'*OnePreMult'*[WantedOne^2;WantedOne;1]);
        ThreePutRateDelta(i+1,j+1) = VolStock * ([2*WantedOne,1,0]*OnePreMult*PutSubMatrix*TwoPreMult'*[
            WantedTwo^2;WantedTwo;1] - [2*WantedTwo,1,0]*TwoPreMult*PutSubMatrix'*OnePreMult'*[
            WantedOne^2;WantedOne;1]);
        %
        %
    end
end
```

%

D.4.2 LocateVBSPutOEB.m

```
for i = 1 : SpotRates
    %
    ImpliedShortRate = SpotToShort(alpha,theta,VolRate,TimeToExpiry,SpotRatesOfInterest(i));
    %
    for j = 1 : VectorNodes
        %
        WantedOne = VolRate * log(StockVector(j)) + VolStock * ImpliedShortRate;
        WantedTwo = VolRate * log(StockVector(j)) - VolStock * ImpliedShortRate;
        %
        LOI = floor((WantedOne-MinOneCalc)/DeltaOne)+1;
        UOI = LOI + 1;
        LTI = floor((WantedTwo - MinTwoCalc)/DeltaTwo)+1;
        UTI = LTI + 1;
        %
        OneProp = (WantedOne - OneValues(LOI))/DeltaOne;
        TwoProp = (WantedTwo - TwoValues(LTI))/DeltaTwo;
        %
        PutVector(j) = (1-OneProp)*( (1-TwoProp)*NewPutMatrix(LOI,LTI) + TwoProp*NewPutMatrix(LOI,
            UTI) )+ OneProp * ( (1-TwoProp)*NewPutMatrix(UOI,LTI) + TwoProp*NewPutMatrix(UOI,UTI));
        IntrinsicVector(j) = (1-OneProp)*( (1-TwoProp)*IntrinsicMatrix(LOI,LTI) + TwoProp*IntrinsicMatrix(
            LOI,UTI) )+ OneProp * ( (1-TwoProp)*IntrinsicMatrix(UOI,LTI) + TwoProp*IntrinsicMatrix(UOI,
            UTI));
        %
    end
    %
    ExIndex = VectorNodes;
    Continue = 1;
    while Continue == 1
        ExIndex = ExIndex -1;
        if abs(PutVector(ExIndex)-IntrinsicVector(ExIndex)) > 0.001
            Continue = 0;
        elseif ExIndex == VectorNodes
            Continue = 0;
        end
    end

    Continue = 1;

    while Continue == 1
        ExIndex = ExIndex - 1;
        if (PutVector(ExIndex)-IntrinsicVector(ExIndex)) < 0.001
            Continue = 0;
        elseif ExIndex == 1
            Continue = 0;
        end
    end
    %
    if ExIndex == 1
        BoundaryVector(i) = -100;
    else
        BoundaryVector(i) = StockVector(ExIndex);
        %
        QuadCoeff = ([(StockVector(ExIndex+3))^2,StockVector(ExIndex+3),1;(StockVector(ExIndex+2))^2,
            StockVector(ExIndex+2),1;(StockVector(ExIndex+1))^2,StockVector(ExIndex+1),1]^-1)*[PutVector(
            ExIndex+3);PutVector(ExIndex+2);PutVector(ExIndex+1)];
        %
        Determinant = (QuadCoeff(2)+1)^2-4*QuadCoeff(1)*(QuadCoeff(3)-Strike);
        %
        if Determinant > 0
            BoundaryVector(i) = max((-1-QuadCoeff(2)+sqrt(Determinant))/(2*QuadCoeff(1)),BoundaryVector(i)
                );
        end
```

```
        %
    end
    %
    %disp(['BoundaryVector(i) = ',num2str(BoundaryVector(:))])
    %disp('paused')
    %pause
    %disp('unpaused')
    %
end
%
PutOEB = [PutOEB;TimeToExpiry,BoundaryVector];
```

Bibliography

[1] AMIN, K.I. & R.A. JARROW (1992) Pricing Options on Risky Assets in a Stochastic Interest Rate Economy. *Mathematical Finance* **2**(4), 217-237.

[2] ANDREASEN, J., B. JENSEN & R. POULSEN (1998) Eight Valuation Methods in Financial Mathematics: The Black-Scholes Formula as an Example. *Mathematical Scientist* **23**, 18-40.

[3] BACHELIER, L. (1900) Theory of Speculation (translation of 1900 French edition), in Cootner (1964).

[4] BALL, C.A. & W.N. TOROUS (1983) Bond Price Dynamics and Options. *Journal of Financial and Quantitative Analysis* **18**(4), 517-531.

[5] BENSOUSSAN, A. (1988) On the Theory of Option Pricing. *Acta Applicandae Mathematica* **2**, 139-158. Reprinted as Chapter 3 in Hughston (1996).

[6] BJÖRK, T. (1998) *Arbitrage Theory in Continuous Time*. Oxford, U.K.: Oxford University Press.

[7] BLACK, F. (1989) How We Came Up With The Option Formula. *Journal of Portfolio Management*, Winter, 4-8.

[8] BLACK, F., E. DERMAN & W. TOY (1990) A One-Factor Model of Interest Rates and Its Application to Treasury Bonds. *Financial Analysts' Journal*. January/February, 33-39.

[9] BLACK, F. & P. KARASINSKI (1992) Bond and Option Pricing When Rates Are Lognormal. *Financial Analysts' Journal*, July/August, 52-59.

[10] BLACK, F. & M. SCHOLES (1972) The Valuation of Option Contracts and a Test of Market Efficiency. *Journal of Finance* **27**(2), 399-417.

[11] BLACK, F. & M. SCHOLES (1973) The Pricing of Options and Corporate Liabilities. *Journal of Political Economy* **81**(3) 637-659.

[12] BOYLE, P.P. (1986) Option Valuation Using Three-Jump Processes. *International Options Journal* **3**, 7-12.

[13] BOYLE, P.P. (1988) A Lattice Framework for Option Pricing with Two State Variables. *Journal of Financial and Quantitative Analysis* **23**(1), 1-12.

[14] BRACE, A., D. GATAREK & M. MUSIELA (1997) The Market Model of Interest Rate Dynamics. *Mathematical Finance* **7**(2), 127-147.

[15] BRENNAN, M.J. & E.S. SCHWARTZ (1978) Finite Difference Methods and Jump Processes Arising in the Pricing of Contingent Claims: A Synthesis. *Journal of Financial and Quantitative Analysis* **13**(3), 461-478.

[16] BRENNAN, M.J. & E. S. SCHWARTZ (1979) A Continuous Time Approach to the Pricing of Bonds. *Journal of Banking and Finance* **3**, 133-155.

[17] BRENNAN, M.J. & E. S. SCHWARTZ (1982) An Equilibrium Model of Bond Pricing and a Test of Market Efficiency. *Journal of Financial and Quantitative Analysis* **17**(3), 301-329.

[18] BRIGO, D. & F. MERCURICO (2001) *Interest Rate Models: Theory and Practice*. Berlin, Germany: Springer.

[19] BROWN, A. (2001). Post in General Forum at www.wilmott.com, threadid 208. Accessed 26 September 2004.

[20] BURDEN, R.L. & J.D. FAIRES (1997) *Numerical Analysis*, Sixth edition. California, U.S.A.: Brooks/Cole.

[21] CARR, P., R. JARROW & R. MYNENI (1992) Alternative Characterisations of American Put Options. *Mathematical Finance* **2**(2), 87-106.

[22] CHESNEY, M., R.J. ELLIOTT & R. GIBSON (1993) Analytical Solutions for the Pricing of American Bond and Yield Options. *Mathematical Finance* **3**(3), 277-294.

[23] CLEWLOW, L. & C. STRICKLAND (1998) *Implementing Derivative Models*. Chichester, Enland: John Wiley & Sons Ltd.

[24] COOTNER, P.H. (ED.) (1964) *The Random Character of Stock Market Prices*, Second Edition. Massachusetts, U.S.A.: M.I.T. Press.

[25] COURTADON, G. (1982) A More Accurate Finite Difference Approximation for the Valuation of Options. *Journal of Financial and Quantitative Analysis* **17**(5), 697-703.

[26] COX, J.C., J.E. INGERSOLL & S.A. ROSS (1985A) An Intertemporal General Equilibrium Model of Asset Prices. *Econometrica* **53**(2), 363-384.

[27] COX, J.C., J.E. INGERSOLL & S.A. ROSS (1985B) A Theory of the Term Structure of Interest Rates. *Econometrica* **53**(2), 385-408.

[28] COX, J., S. ROSS & M. RUBINSTEIN (1979) Option Pricing: A Simplified Approach. *Journal of Financial Economics* **7**, 229-263.

[29] CRYER, C.W. (1971) The Solution of a Quadratic Programming Problem Using Systematic Overrelaxation. *SIAM Journal of Control* **9**. 385-392. In Wilmott, Dewynne and Howison (1993).

[30] DELBAEN, F. & W. SCHACHERMAYER (1994A) A General Version of the Fundamental Theorem of Asset Pricing. *Mathematische Annalen* **300**, 463-520.

[31] DELBAEN, F. & W. SCHACHERMAYER (1994B) Arbitrage and Free Lunch With Bounded Risk For Unbounded Continuous Processes. *Mathematical Finance* **4**, 343-348.

[32] DOTHAN, L.U. (1978) On the Term Structure of Interest Rates. *Journal of Financial Economics* **6**, 59-69.

[33] DU TOIT, J. (2003) The Binomial Tree and American Options. Honours project submitted to the School of Computational and Applied Mathematics, University of the Witwatersrand.

[34] DUFFIE, D. (1996) *Dynamic Asset Pricing Theory*, Second Edition. Pennsylvania, U.S.A.: Princeton University Press.

[35] FAKEEV, A.G. (1970) Optimal Stopping Rules for Stochastic Processes with Continuous Parameter. *Theory of Probability and its Applications*, **15**(2), 324-331.

[36] FAKEEV, A.G. (1971) Optimal Stopping of a Markov Process. *Theory of Probability and its Applications*, **16**(4), 694-696.

[37] FONG, H.G. & O.A. VASICEK (1991) Fixed-income Volatility Management. *Journal of Portfolio Management*, Summer, 41-46.

[38] GAMEROV, S. (1995) An Investigation into the Use of the Black-Scholes Model for Pricing Long Term Options, for the Purpose of Costing Maturity Guarantees. M.Bus.Sc dissertation, Department of Business Science, University of Cape Town.

[39] GEMAN, H., N. EL KAROUI & J.C. ROCHET (1995) Changes of numéraire, changes of probability measure and option pricing. *Journal of Applied Probability* **32**, 443-458.

[40] GIBSON, R., F.S. L'HABITANT & D. TALAY (1998) Modeling the Term Structure of Interest Rates: A Review of the Literature. Universite de Lausanne, Institute of Banking and Financial Management, Working Paper 9801.

[41] HABERMANN, R. (1998) *Elementary Applied Partial Differential Equations*. New Jersey, U.S.A.: Prentice-Hall.

[42] HARRISON, J.M. & D. KREPPS (1979) Martingale and arbitrage in multiperiod securities markets. *Journal of Economic Theory* **20**, 381-408.

[43] HARRISON, J.M. & S.R. PLISKA (1981) Martingales and stochastic integrals in the theory of continuous trading. *Stochastic Processes and their Applications* **11**, 215-260.

[44] HEATH, D., R. JARROW & A. MORTON (1992) Bond Pricing and the Term Structure of Interest Rates: A New Methodology for Contingent Claims Valuation. *Econometrica* **60**(1), 77-105.

[45] HO, T.S.Y. & S.B. LEE (1986) Term Structure Movements and Pricing Interest Rate Contingent Claims. *Journal of Finance* **41**(5), 1011-1029.

[46] HO, T.S., R.C. STAPLETON & M.G. SUBRAHMANYAM (1994) A Simple Technique for the Valuation and Hedging of American Options. *Journal of Derivatives*, Fall, 52-66.

[47] HO, T.S., R.C. STAPLETON & M.G. SUBRAHMANYAM (1995) Multivariate Binomial Approximations for Asset Prices with Nonstationary Variance and Covariance Characteristics. *Review of Financial Studies* **8**(4), 1125-1152.

[48] HO, T.S., R.C. STAPLETON & M.G. SUBRAHMANYAM (1997A) The Valuation of American Options with Stochastic Interest Rates: A Generalisation of the Geske-Johnson Technique. *Journal of Finance* **52**(2), 827-840.

[49] HUANG, J., M.G. SUBRAHMANYAM & G.G. YU (1996) Pricing and Hedging American Options: A Recursive Integration Method. *Review of Finaicial Studies* **9**(1), 277-300.

[50] HUGHSTON, L. (1996) *Vasicek and Beyond*. London, U.K.: Risk Publications.

[51] HULL, J.C. (2000) *Options, Futures and Other Derivatives (International Edition)* Fourth Edition. New Jersey, U.S.A. : Prentice-Hall Inc.

[52] HULL, J.C. & A. WHITE (1990A) Valuing Derivative Securities Using the Explicit Finite Difference Method. *Journal of Financial and Quantitative Analysis* **25**(1), 87-100.

[53] HULL, J.C. & A. WHITE (1990B) Pricing Interest-Rate Derivative Securities. *Review of Financial Studies* **3**(4), 573-592.

[54] HULL, J.C. & A. WHITE (1993) One-Factor Interest-Rate Models and the Valuation of Interest-Rate Derivative Securities. *Journal of Financial and Quantitative Analysis* **28**(2), 235-254.

[55] HULL, J.C. & A. WHITE (1994A) Numerical Procedures for Implementing Term Structure Models I: Single-Factor Models. *Journal of Derivatives*, Fall, 7-16.

[56] HULL, J.C. & A. WHITE (1994B) Numerical Procedures for Implementing Term Structure Models II: Two-Factor Models. *Journal of Derivatives*, Winter, 37-48.

[57] JACKA, S.D. (1991) Optimal Stopping and the American Put. *Mathematical Finance* **1**(2), 1-14.

[58] JAILLET, P., D. LAMBERTON & B. LAPEYRE (1990) Variational inequalities and the pricing of American Options. *Acta Applicandae Mathematica* **21**, 263-289. In Myneni (1992).

[59] JAMES, J. & N. WEBBER (2000) *Interest Rate Modeling*. Chichester, U.K.: John Wiley & Sons.

[60] JAMSHIDIAN, F. (1987) Pricing of Contingent Claims in the One-Factor Term Structure Model. Working Paper, Merrill Lynch Capital Markets. Reprinted as Chapter 7 in Hughston (1996).

[61] JAMSHIDIAN, F. (1989) An Exact Bond Option Formula. *Journal of Finance* **44**(1) 205-209.

[62] JAMSHIDIAN, F. (1991) Bond and Option Evaluation in the Gaussian Interest Rate Model. *Research in Finance* **9**, 131-170.

[63] JAMSHIDIAN, F. (1993) An Analysis of American Options. *Review of Futures Markets* **11**(1), 72-80.

[64] JAMSHIDIAN, F. (1997) LIBOR and Swap Market Models and Measures. *Finance and Stochastics* **1**, 293-330.

[65] JARROW, R.A. & S.M. TURNBULL (2000) *Derivative Securities*, Second Edition. Ohio, U.S.A.: South-Western College Publishing.

[66] JØRGENSEN, P.L. (1996) American Bond Option Pricing in One-Factor Dynamic Term Structure Models. *Review of Derivatives Research* **1**. 245-267.

[67] KAMRAD, B. & P. RITCHKEN (1991) Multimonial Approximating Models for Options with k State Variables. *Management Science* **37**(12). 1640-1652.

[68] KARATZAS, I. (1988) On the Pricing of American Options. *Applied Mathematics and Optimisation* **17**, 37-60.

[69] KARATZAS, I. & S.E. SHREVE (1991) *Brownian Motion and Stochastic Calculus*, Second edition. Berlin, Germany: Springer.

[70] KARATZAS, I. & S.E. SHREVE (1998) *Methods of Mathematical Finance*, Third edition, Berlin, Germany: Springer.

[71] KIM, I.J. (1990) The analytic Valuation of American Options. *Review of Financial Studies* **3**(4), 547-572.

[72] KWOK, Y.K. (1998) *Mathematical Models of Financial Derivatives.* Singapore: Springer-Verlag.

[73] LANGETIEG, T.C. (1980) A Multivariate Model of the Term Structure. *Journal of Finance* **35**(1), 71-97.

[74] LI, A., P. RITCHKEN & L. SANKARASUBRAMANIAN (1995) Lattice Models for Pricing American Interest Rate Claims. *Journal of Finance* **50**(2), 719-737.

[75] LONGSTAFF, F.A. & E.S. SCHWARTZ (1992A) Interest Rate Volatility and the Term Structure: A Two-Factor General Equilibrium Model. *Journal of Finance* **47**(4), 1259-1282.

[76] LONGSTAFF, F.A. & E.S. SCHWARTZ (1992B) A Two-Factor Interest Rate Model and Contingent Claims Valuation. *Journal of Fixed Income* **3**, 16-23.

[77] MCCUTCHEON, J.J. & W.F. SCOTT (1986) *An Introduction to the Mathematics of Finance*, Oxford, U.K.: Butterworth-Heinemann.

[78] MCKEAN, H.P. (1965) A Free Boundary Problem for the Heat Equation Arising From a Problem in Mathematical Sciences. *Industrial Management Review* **6**(2) 32-39. Appendix to Samuelson(1965).

[79] MENKVELD, A.J. & T. VORST (2000) A Pricing Model for American Options with Gaussian Interest Rates. *Annals of Operations Research* **100**(1), 211-266.

[80] MERTON, R.C. (1973) Theory of Rational Option Pricing. *Bell Journal of Economics and Management Science* **4**(2), 141-183.

[81] MILTERSEN, K.R., K. SANDMANN & D. SONDERMANN (1997) Closed Form Solutions for Term Structure Derivatives with Log-Normal Interest Rates. *Journal of Finance* **52**(1), 409-430.

[82] MUSIELA, M. & M. RUTKOWSKI (1998) *Martingale Methods in Financial Modelling*, Berlin, Germany: Springer.

[83] MYNENI, R. (1992) The Pricing of the American Option. *The Annals of Applied Probability* **2**(1), 1-23.

[84] ØKSENDAL, B. (1998) *Stochastic Differential Equations*, Fifth Edition. Berlin: Springer.

[85] PESKIR, G. (2002) On The American Option Problem. *Research Report* No. 431 *Department of Theoretical Statistics, University of Aarhus* (13 pp).

[86] RABINOVITCH, R. (1989) Pricing stock and bond options when the default-free rate is stochastic. *Journal of Financial and Quantitative Analysis* **4**. 447-457.

[87] RICE, J.A. (1995) *Mathematical Statistics and Data Analysis* Second Edition. California, U.S.A.: Wadsworth.

[88] RITCHKEN, P. & L. SANKARASUBRAMANIAN Volatility Structure of Forward Rates and the Dynamics of the Term Structure. *Mathematical Finance* **5**(1), 55-72.

[89] ROGERS, L.C.G. (1996) Gaussian errors. *RISK* **9**, 42-45.

[90] SAMUELSON, P.A. (1965) Rational Theory of Warrant Pricing. *Industrial Management Review* **6**(2), 13-32.

[91] SCHAEFER, S.M. & E.S. SCHWARTZ (1984) A Two-Factor Model of the Term Structure: An Approximate Analytical Solution. *Journal of Financial and Quantitative Analysis* **19**(4), 413-424.

[92] SCHWARTZ, E.S. (1977) The Valuation of Warrants: Implementing a New Aproach. *Journal of Financial Economics* **4**, 79-94.

[93] UYS, N. (2005) Optimal Stopping Problems and American Options. Masters dissertation submitted to the School of Computational and Applied Mathematics, University of the Witwatersrand.

[94] VASICEK, O.A. (1977) An Equilibrium Characterisation of the Term Structure. *Journal of Financial Economics* **5**, 177-188.

[95] VETZAL, K.R. (1998) An Improved Finite Difference Approach to Fitting the Initial Term Structure. *Journal of Fixed Income* **7**(4), 62-81.

[96] VAN MOERBEKE, P.L.J. (1976) On Optimal Stopping and Free Boundary Problems. *Archives of Rational Mechanical Analysis* **60**, 101-148.

[97] WILMOTT, P. (2000) *Paul Wilmott on Quantitatice Finance.* Chichester, U.K.: John Wiley & Sons.

[98] WILMOTT, P., J. DEWYNNE & S. HOWISON (1993) *Option Pricing: Mathematical Models and Computation.* Oxford, U.K.: Oxford Financial Press.

[99] WILMOTT, P., S. HOWISON & J. DEWYNNE (1995) *The Mathematics of Financial Derivatives: A Student Introducion.* New York, U.S.A.: Press Syndicate of the University of Cambridge.